THE GENERATION AND APPLICATION OF METALLURGICAL THERMODYNAMIC DATA

by

A.T. Dinsdale

Division of Materials Applications

National Physical Laboratory

Submitted for the degree of Doctor of Philosophy

at Brunel University, August 1984

ABSTRACT

The power of thermodynamics in the calculation of complex chemical and metallurgical equilibria of importance to industry has, over the last 15 years, been considerably enhanced by the availability of computers. It has resulted in the storage of data in databanks, the use of physical but complex models to represent thermodynamic data, the vast effort spent in the generation of critically assessed data and the development of sophisticated software for their application in equilibrium calculations.

This thesis is concerned with the generation and application of metallurgical thermodynamic data in which the computer plays a central and essential role. A very wide range of topics have been covered from the generation of data by experiment and critical assessment through to the application of these data in calculations of importance to industry. Particular emphasis is placed on the need for reliable models and expressions which can represent the molar Gibbs energy as a function of temperature and composition. In addition a new computer program is described and used for the automatic calculation of phase diagrams for binary systems. Measurements of the enthalpies of formation of alloys in the Fe-Ti system are reported. All data for this system have been critically assessed to provide a dataset consistent with the published phase diagram. Critically assessed data for a number of binary alloy systems have been combined in order to perform quantitative calculations in two types of steel system. Firstly data for the Cr-Fe-Ni-Si-Ti system have been used to provide information about the long term stability of alloys used in fast breeder nuclear reactors. Secondly very complex calculations involving nine elements have been made to predict the distribution of carbon and various impurities between competing phases in low alloy steels on the addition of Mischmetall. Finally a new model is developed to represent the thermodynamic data for sulphide liquids and is used in the critical assessment and calculation of data for the Cu-Fe-Ni-S system. The phase diagram and thermodynamic data calculated from the assessed data are in excellent agreement with those observed experimentally.

The work reported in this thesis, whilst successful, has also indicated areas which will benefit from further study particularly the development of reliable data and models for pure elements, ordered solid phases and liquid phases for high affinity systems.

CONTENTS

CHAPTER 1

Introduction

Any stranger to the field of thermodynamics must think it rather odd that its application to industrial problems is still in a state of hectic development. It is certainly true that the basic principles of the subject are well established following the pioneering work of Gibbs and others (1-6) towards the end of the last century. It is also true, however, that in many fields of research considerable time may elapse between the conception of a theory and its development to the stage where it can be used to solve complex problems of practical interest. In the case of thermodynamics, the initial definition of the principles led to rapid growth in the amount of experimental work being performed. This experimental work with its generation of vast quantities of data led people to develop convenient mathematical expressions to link the data together. This need for convenient but reliable mathematical formalisms in turn led to greater emphasis being placed on a detailed understanding of the underlying physics and consequently the development of more fundamental theories.

As I hope to demonstrate in this thesis, thermodynamics is still at a stage where it demands a high level of intellectual application in order to provide the basis for the solution of important practical problems. However with the birth of the age of computers a dramatic change is now occurring which will allow a non-expert to solve complex problems involving thermodynamics with very little effort. This is particularly true of the area of metallurgical thermodynamics. The aim of this thesis is to show how thermodynamic data for metallurgical systems can be generated and used in conjunction with a computer to solve problems of practical interest.

The importance and the use of thermodynamics are well known and this

is reflected in the growing number of conferences and journals devoted to the subject. At NPL, there is a great tradition for conferences devoted to thermodynamics (7-10). The latest of these conferences "The Industrial Use of Thermochemical Data" (10) showed that, just within the areas of metallurgy and inorganic chemistry, thermodynamics is being used successfully in a wide range of industries for topics as diverse as the development of materials for nuclear reactors (11-13), the prediction of superalloys suitable for use in turbine blades (14,15), the hydrometallurgical and pyrometallurgical extraction of metals from minerals (14,16), the growth of crystals by vapour transport (17), pollution control (18), steelmaking (19-23) and the development of materials for lamp technology (24,25). It is probably true that even in these areas, thermodynamics is not being used to its full potential.

One other aspect that stood out from this conference was the breakdown of the delegates between government organisations, universities and private industry. It was rather encouraging to note the large representation of industry which may indicate that the scepticism or even fear on the part of the industrial scientist in the use and power of thermodynamics is disappearing.

There are many reasons for this sceptical attitude. The last time a typical industrial scientist would have thought in detail about thermodynamics would have been during his undergraduate days at university. There he would have been confronted with an array of partial differential equations, strange concepts such as reversible and irreversible reactions, adiabatic and isothermal changes and the escalation of entropy. All this might have seemed a long way from solving a practical chemical or metallurgical problem. It is small wonder that after a break of a few years he would view the prospect of returning to thermodynamics with some trepidation. Even for those bold enough to get past this stage, the problems have only just begun. The

non-expert must first find the data he needs for his calculations, perhaps from the literature or standard compilations. However, can he be sure that these data are reliable, sufficiently accurate and consistent with each other and with the most recent experimental results? He may also need to estimate some data which are not available or to interpolate or extrapolate them well outside the range of their measurement. Furthermore when all the data have been found or estimated, the problems of interest are often so complex that they are impossible to solve without resorting to a powerful computer. He may then need to develop software so sophisticated that even the best intentioned industrial scientist will feel thwarted in his attempts to use thermodynamics to solve his problem.

However the application of thermodynamics is fast becoming painless because of the expanding series of data compilations and computer databanks, and the development of extremely general computer programs for the calculations of complex equilibria. The problem therefore now becomes one of making industry aware of what is available, and competent and confident in its ability to use such tools. In the long run, much of the responsibilty lies with the universities. They must provide undergraduate teaching courses which are both relevant, showing just what can be achieved by the use of thermodynamics, and up-to-date by demonstrating the most recent techniques and facilities for solving these problems painlessly, reliably and cost effectively.

There are a number of aspects of the application of thermodynamics which must be covered in order to solve a particular problem and these will be discussed in some detail in the next three chapters of this thesis. In chapter 2, the question is considered of where it is possible to find the data required for the calculations. Generally data for the most important materials can be found in tabular form in books although the opportunities offered by the computer now allow the storage and

retrieval of data as coefficients to an expression relating the variation of the thermodynamic properties to the composition and temperature. This is especially important for the more complex equilibrium calculations which may require interpolation or extrapolation of tabulated data. The formalisms commonly used are described in Chapter 3.

Thermodynamic data are very versatile and can be used for the calculation of equilibria for a wide range of systems and industrial applications. Several different types of computer programs have been developed and these have been reviewed in chapter 4 along with the other applications of computers to the world of thermodynamics. As these calculations become more and more important, so the need for reliable and efficient procedures grows. Moreover as the power of computers increases and their price drops these calculations fall well within the scope of any interested individual. It now becomes important to develop programs specifically for microcomputers. In chapter 5 the mathematics and the strategy used for one particular computer program is described. This program is used at NPL for the automatic calculation of binary alloy phase diagrams. The techniques used for this program are very reliable and so compact that they allow the calculation of phase equilibria even on a hand held microcomputer.

Ultimately the basis of all the calculations of phase equilibria is experimental work. In chapter 6 a series of measurements are described for the enthalpies of formation of alloys in the iron rich side of the Fe-Ti system. This work involved the use of a high temperature adiabatic calorimeter designed by Dench (26) but with experimental procedures modified to allow measurements in highly exothermic systems such as the Fe-Ti system. These experimental data, with thermodynamic and phase diagram data from other sources were critically assessed in order to provide a representation of the thermodynamic data over a wide range of

temperatures and compositions but consistent with the accepted phase diagram.

In chapter 7 two sets of phase equilibrium calculations for steel systems are described. The first set of calculations, which used a database including the critically assessed data for the iron-titanium system, was undertaken to provide reliable phase diagrams for multicomponent stainless steels to help understand the phenomenon of neutron induced void swelling of cladding materials used in fast breeder nuclear reactors. These calculations are more reliable than could be obtained from direct experiment because phase transformations in the temperature range of interest are very sluggish in these systems. They therefore give information about the long term stability of these cladding alloys. The second set of calculations was designed to provide quantitative information about the levels of Mischmetall which could be added to certain low alloy steels to remove harmful impurities such as phosphorus, tin and copper and yet would not cause a disruption of the carbide structure of the steel.

In chapter 8 the assessment of thermodynamic and phase diagram data for certain sulphide systems is described. These systems are characterised by dramatic changes in the thermodynamic properties of the liquid phase close to the compositions of known stoichiometric compounds. A new model has been derived to represent the thermodynamic data for the liquid phase as a function of temperature and composition. In particular data have been derived for the Cu-S and Ni-S systems which were then used to calculate the phase diagram and thermodynamic data for the Cu-Fe-S, Cu-Ni-S, Fe-Ni-S and Cu-Fe-Ni-S system. These calculations are in good agreement with available experimental information.

The final chapter, chapter 9, is a summary of the work carried out for this thesis. Although the work has been successful a number of aspects require further study and these have been highlighted.

CHAPTER 2

Sources of Data

One of the most difficult and important problems facing a potential user of thermodynamics is to find the basic data needed to solve his problem. This might involve the daunting task of searching through the literature for thermodynamic data, equilibrium data and potentially related measurements such as spectroscopic data. Even after a comprehensive search and after the collection of the available data there is no guarantee that he will have found all the data he requires. He might then try to estimate those data that aren't available. The estimation of data is a complex and time consuming task in its own right and often requires many years of experience. Moreover he will have to make some judgement about the validity of all the data he has collected and ensure that they are all interconsistent. For many practical problems he will also need to express the dependence of these thermodynamic data on the temperature or composition. The choice of expression is often far from simple especially for condensed solution phases as described in Chapter 3.

Fortunately in response to the need for accurate and consistent thermodynamic and phase diagram data, many governments and industries have sponsored the preparation of various data compilations. In the past this has included programmes to measure key unknown thermodynamic data. Unfortunately these are generally labour intensive and recently they have suffered greatly from the world recession and economic crisis. Traditionally the compilations of thermodynamic and phase diagram data have been in the form of hard copy publications and have been of immense benefit to industry. For thermodynamic data the most useful general publications have been the JANAF tables (27-31), those of Barin and Knacke (32,33) and the IVTAN group (34-37), the NBS 270 series (38,39),

Medved'ev (40), and the CODATA publications (41,42), all of which have been concerned primarily with data for pure substances or species. Other publications such as Hultgren (43,44), Kubaschewski and Alcock (45), Kaufman and Bernstein (46) and the CALPHAD journal (47) have covered data for both pure substances and for solution phases. Data for dilute solution in metals and alloys have also been tabulated (48-52). There are also many comprehensive sources of phase diagrams and equilibrium measurements of which the best known are undoubtedly Hansen and Anderko and its supplements (53-55), Moffatt (56), Prince (57,58), Ageev (59), Wisniak (60), the Pourbaix atlasses (61), 'The Phase Diagrams for Ceramicists' (62), the Metals Handbook (63) and more recently the Bulletin of Alloy Phase Diagrams (64).

These publications are generally easy to use and contain their information in a form which can often be applied directly to the problem of interest. Indeed so useful have they become that in many quarters they are regarded as a sort of Bible. This dependence on individual publications is also their main drawback. For example, many of the phase diagrams presented in Hansen are now out of date many times over and yet the phase diagrams it contains are used, often without any regard to whether a more recent phase diagram is available. A more acute problem can occur because of inconsistency between the tabulated thermodynamic data obtained from different sources. Different compilations often refer to different reference states and this can lead the unaware to obtain completely incorrect results. Despite their undoubted use such compilations should therefore be used with some caution.

Moreover many of the published phase diagrams can be improved by applying some simple knowledge of thermodynamics even without the use of a computer. A good example of this has been demonstrated by Hillert (65). In the phase diagram for the Fe-Cu system published in the Metals Handbook (63) and reproduced in Fig 2.1, the phase boundary between the

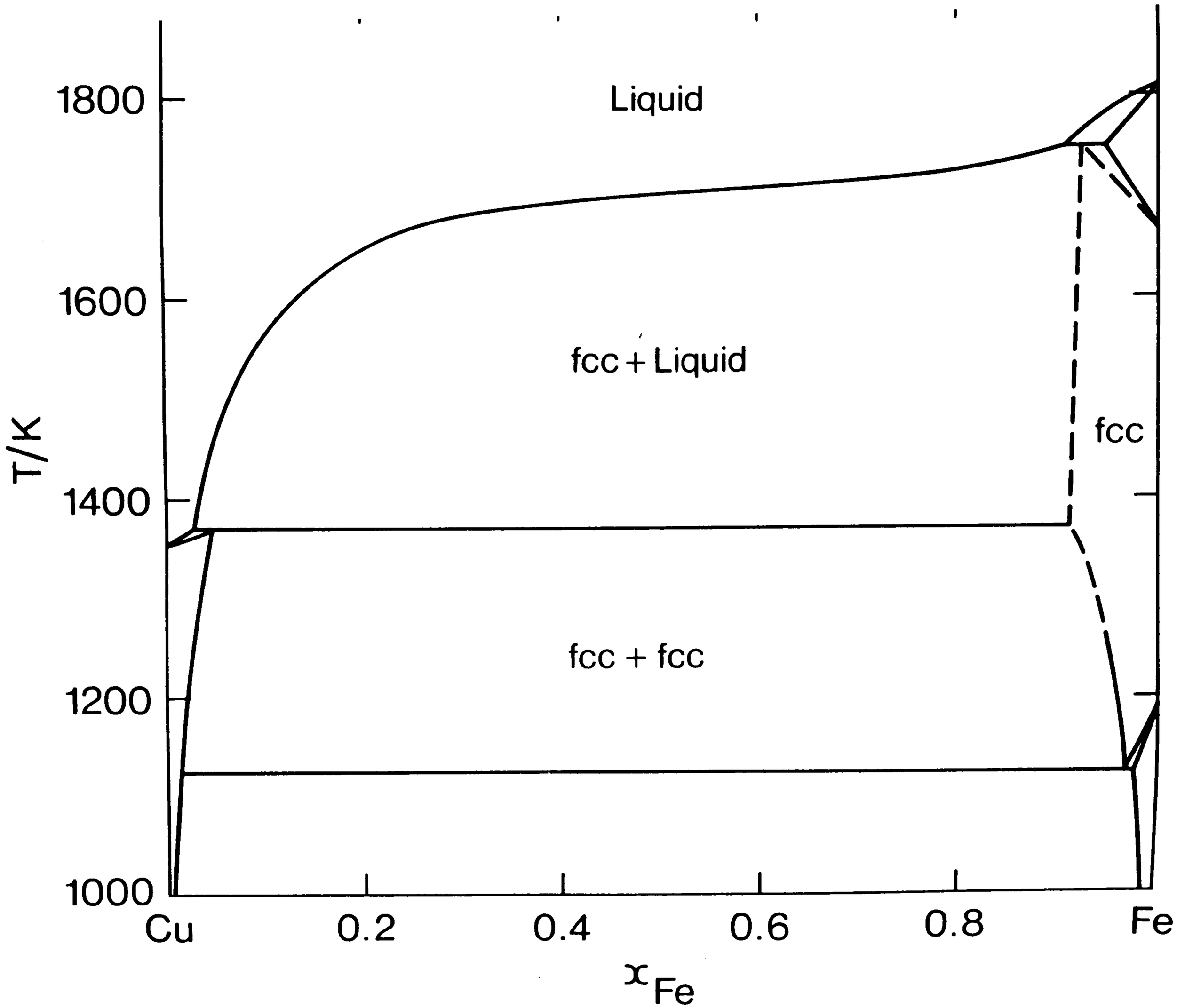

Fig 2.1 The phase diagram for the Fe-Cu system published in the Metals Handbook (63) showing an interpolated solidus curve (dashed line).

Cu rich liquidus and the Fe rich fcc phase is represented by a dotted line to indicate an editorial interpolation in the absence of specific experimental results. Hillert (65) pointed out that the editor could have defined this phase boundary more precisely. Firstly the two ends of the dotted line indicate experimental compositions for which the fcc phase is in equilibrium with the liquid phase. Also however the melting point of metastable fcc Fe is known accurately from studies of a variety of binary systems involving Fe where the fcc phase is stabilised (eg. Fe-Ni). Hillert argued that the two ends of the dotted line and the hypothetical melting point of fcc Fe, since they pertain to equilibrium between the same two phases, should lie on a smooth curve as shown in Fig 2.2. This has since been demonstrated experimentally.

In a similar way thermodynamics can be used very simply to examine experimental liquidus and solidus curves in dilute solutions (66) and to derive rules for the geometry of the intersections of phase boundaries (67). Use of such knowledge in conjunction with experimental equilibrium data can lead to more reliable phase diagrams.

Most of the compilations listed above are concerned with pure substances or binary systems for perhaps alloys, aqueous solutions etc. The number of tables or diagrams required for these systems is sufficiently small that they can be stored in a few volumes. Unfortunately, in practice, alloys or other materials of use to industry rarely consist of only two elements and a source or compilation of phase diagrams for complex materials is therefore sorely needed. Ageev (59) to a certain extent fulfils this need for alloys. Recently The Metals Society, in conjunction with SERC, has supported a project of work to provide in hard copy form reviews of ternary phase diagrams for iron based systems (68-72). Similarly Chang (73,74) has recently reviewed selected ternary phase diagrams involving copper. However it is clearly impossible to store phase diagrams for all multicomponent systems of

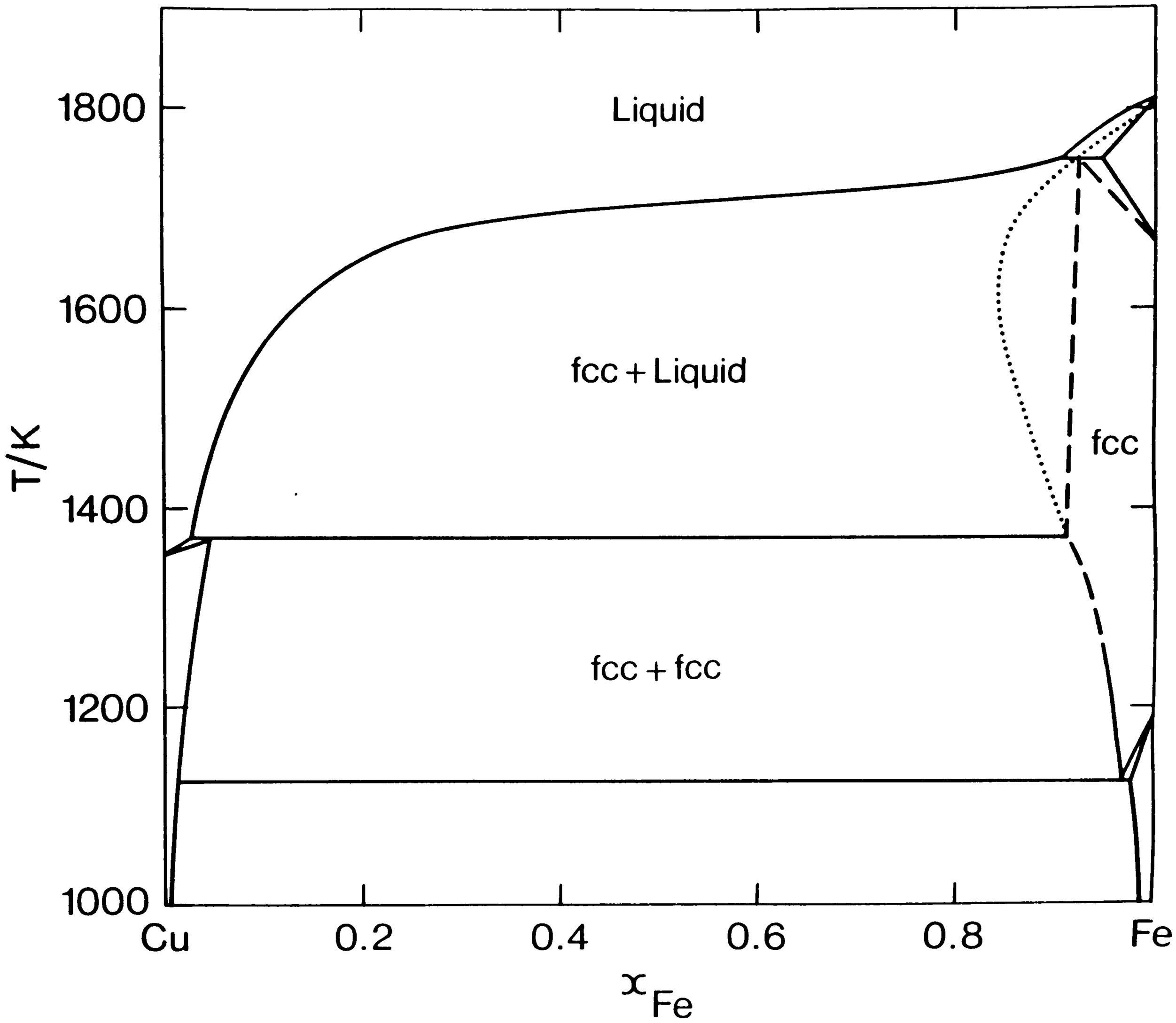

Fig 2.2 The phase diagram for the Fe-Cu system as in Fig 2.1 but showing the dotted solidus curve deduced by Hillert through

interest in hard copy form.

Fortunately there is a very close link between phase diagrams and thermodynamic data. In fact it is correct to say that a phase diagram is merely one of a number of different ways to represent the thermodynamic data for a given system in a diagrammatic form. As the speed of computers increases and reliable packages become available to calculate phase diagrams from thermodynamic data (as described in Chapter 4) it becomes tempting to replace hard copy data compilations by computer databanks where the thermodynamic data are stored on computers in the form of coefficients to some mathematical expression or expressions. The quantity of data necessary to reproduce these hard copy compilations is sufficiently small for them to be stored easily on a magnetic tape or disc. Furthermore they will be self consistent, can be updated frequently and accessed by people all over the world via a telephone system or packet switching network. Perhaps more important the computer will allow the calculation and presentation of results in any form particularly appropriate to the user eg. a diagram could be plotted in terms of weight percent rather than mole fraction.

Rather than produce hard copy data compilations the task now facing professional thermodynamicists is to provide reliable, accurate and consistent data for a wide variety of materials as a function of temperature, composition and pressure. This in turn recognises the need for reliable expressions to the represent the data and computer programs both to assist in the generation of data and to calculate complex equilibria.

This work is beyond the ability of one person or even one group of people and has led to increased collaboration between different centres throughout the world. One particularly effective forum for collaboration is the CALPHAD organisation (CALculation of PHAse Diagrams) which encourages free exchange of thermodynamic data. CALPHAD hosts a

conference every year at various centres throughout the world and a journal, published quarterly, which acts as a focus for the development of ideas, methods and data.

Within Europe a smaller organisation, SGTE (Scientific Group Thermodata Europe), has been set up to provide European industries with a source of reliable thermodynamic data and facilities for their use in equilibrium calculations. A number of major European organisations concerned with chemical and metallurgical data actively participate including NPL, Harwell, RWTH Aachen, The Royal Institute of Technology Stockholm, LTPCM and THERMODATA based in Grenoble and IRSID. One of its main projects, which is sponsored in part by the EEC, is to set up a computer based databank containing data for gases, alloys, oxide systems, aqueous solutions, sulphides etc. and be capable of a wide range of phase equilibrium calculations. It is planned to make this databank available on-line to industry throughout the world from January 1986.

As will be described in chapter 4 similar databanks are being developed in other parts of the world.

CHAPTER 3

Representation of Thermodynamic Data

Molar Gibbs Energy

Of all the various types of data for materials, thermodynamic data are probably the best suited for storage on a computer. One of the main reasons for this is that a single function G, the molar Gibbs energy, when expressed as a function of various system variables such as temperature, pressure or composition, can be used to generate an expression for any other thermodynamic property.

For example

Molar Volume	$V = (\partial G/\partial P)_T$
Molar entropy	$S = -(\partial G/\partial T)_P$
Molar enthalpy	$H = G - T(\partial G/\partial T)_P$
Internal energy	$U = G - T(\partial G/\partial T)_P - P(\partial G/\partial P)_T$
Helmholtz energy	$A = G - P(\partial G/\partial P)_T$
Specific heat at constant pressure	$C_p = -T(\partial^2 G/\partial T^2)_P$
Specific heat at constant volume	$C_v = -T(\partial^2 G/\partial T^2)_P - T(\partial^2 G/\partial T \partial P)^2/(\partial^2 G/\partial P^2)_T$
Partial Gibbs energy	$\bar{G}_A = G - \frac{1}{(1-x_A)}(\partial G/\partial x_A)_{y_i}$ where $y_i = \frac{x_i}{1-x_A}$ and $i \neq A$

Equally important from the point of view of the calculation of chemical and metallurgical equilibria is that for a system to be in thermodynamic equilibrium the Gibbs energy is at a minimum provided that the system is homogeneous in temperature and pressure. Therefore for a multiphase system the calculation of equilibria becomes a mathematical

problem of determining the phases and their compositions which, for a given overall temperature and composition, give the lowest Gibbs energy. For this it is essential that the Gibbs energies of all the competing phases are represented as a single valued function of temperature, pressure, composition and other appropriate variables. For practically all problems of metallurgical interest this will be possible although occasionally difficult. However for studies of critical phenomena involving a liquid phase and a gas phase the Gibbs energy will no longer be single valued. In this case it is more appropriate to use the Helmholtz energy.

One handicap to the use of Gibbs energy is that it has no absolute value - one can only discuss differences or changes in Gibbs energy. Fortunately this is all that is necessary for the calculation of equilibria.

Temperature dependence

For reliable calculations of phase equilibria it is very important to use a good representation of the thermodynamic data as a function of temperature even in regions where the phase is metastable. For most materials where contributions to the thermodynamic properties arise from electronic, vibrational and translational degrees of freedom the Gibbs energy above 298.15 K can be conveniently and accurately represented by an expression of the form:

$$G = a + b\,T + c\,T\,\ln(T) + d\,T^{2} + e\,T^{3} + f\,T^{-1}$$

and this is equivalent to the four term expression for Cp often used in conjunction with some enthalpy and entropy values. Sometimes it is not possible to represent data over a very wide temperature range using just

6 coefficients and in these conditions it is convenient to split the temperature range into two or more intervals, each with a set of these 6 coefficients. The coefficients would normally be chosen such that there was no discontinuity in the Gibbs energy, its first derivative or its second derivative at the change from one temperature range to another.

There are however contributions to the thermodynamic properties which for some substances can complicate the above treatment. The first occurs for magnetic materials especially below and just above the Néel or Curie temperature. Consider the case of Nickel which below 631 K is a ferromagnet. We could choose to represent the thermodynamic data for Nickel in two parts - firstly that for the paramagnetic form, hypothetical at lower temperatures, which could be represented by the conventional 6 term expression, and secondly a term for the magnetic ordering. According to Inden (75,76) and Hillert and Jarl (77) this magnetic contribution to the Gibbs energy will be given by:

$$G^{mag} = - RT \ln (\beta + 1) \phi$$

where β is the magnetic moment expressed as the number of Bohr magnetons per atom, equivalent to twice the number of unpaired spins. The function ϕ is different above and below the Curie temperature.

Above the Curie temperature

$$\phi = \{ \frac{\tau^{-5}}{2} + \frac{\tau^{-15}}{63} + \frac{\tau^{-25}}{300} \} / 5 \text{ K}$$

Below the Curie temperature

$$\phi = -1 + \frac{79}{7 \text{ K}} [\frac{\tau^{-1}}{20 \text{ p}} + \frac{2}{71} \{ \frac{\tau^{3}}{2} + \frac{\tau^{9}}{45} + \frac{\tau^{15}}{200} \} \{ \frac{1}{\text{p}} - 1 \}]$$

where

$$K = \frac{518}{1125} + \frac{11692}{15975}\left\{\frac{1}{p} - 1\right\}$$

and $\tau = T/T_c$ where T_c is the Curie temperature and p is the fraction of the total magnetic enthalpy absorbed above the Curie temperature. It was suggested by Inden that $p = 0.28$ for fcc metals and 0.40 for bcc metals. Fig 3.1 shows the two contributions to the Gibbs energy for fcc Ni.

A second phenomenon is responsible for the so-called glass transition through which a liquid gradually transforms as it is cooled especially below the melting point. At present the thermodynamic properties of liquids are not well understood. It is generally believed that for most elements, the heat capacity of the liquid phase on cooling down will rise corresponding to the liquid assuming greater glassy character. This behaviour is expected to continue through the melting point into the region where the liquid is metastable. Eventually at a temperature, about 2/3 of the melting temperature, the glass transition occurs where the heat capacity falls dramatically to roughly the value of the heat capacity of the stable solid phase. This phenomenon is summarised in Fig 3.2 which is a plot of the heat capacity of typical liquid and solid phases as a function of temperature. Fig 3.3 shows the typical difference in Gibbs energy between a solid and a liquid/glass. It shows that at the glass transition the curvature of the Gibbs energy curve for the liquid phase changes. Extrapolation of the curve from above the glass transition temperature towards 0 K could lead to the liquid phase becoming apparently stable again at low temperatures. The glass transition prevents this from happening.

Unfortunately the lack of a detailed understanding of the thermodynamics of the glassy phase impairs our accuracy in the prediction of multicomponent data for a liquid phase and consequently the calculation of eutectic behaviour. Theoretical advances for this and

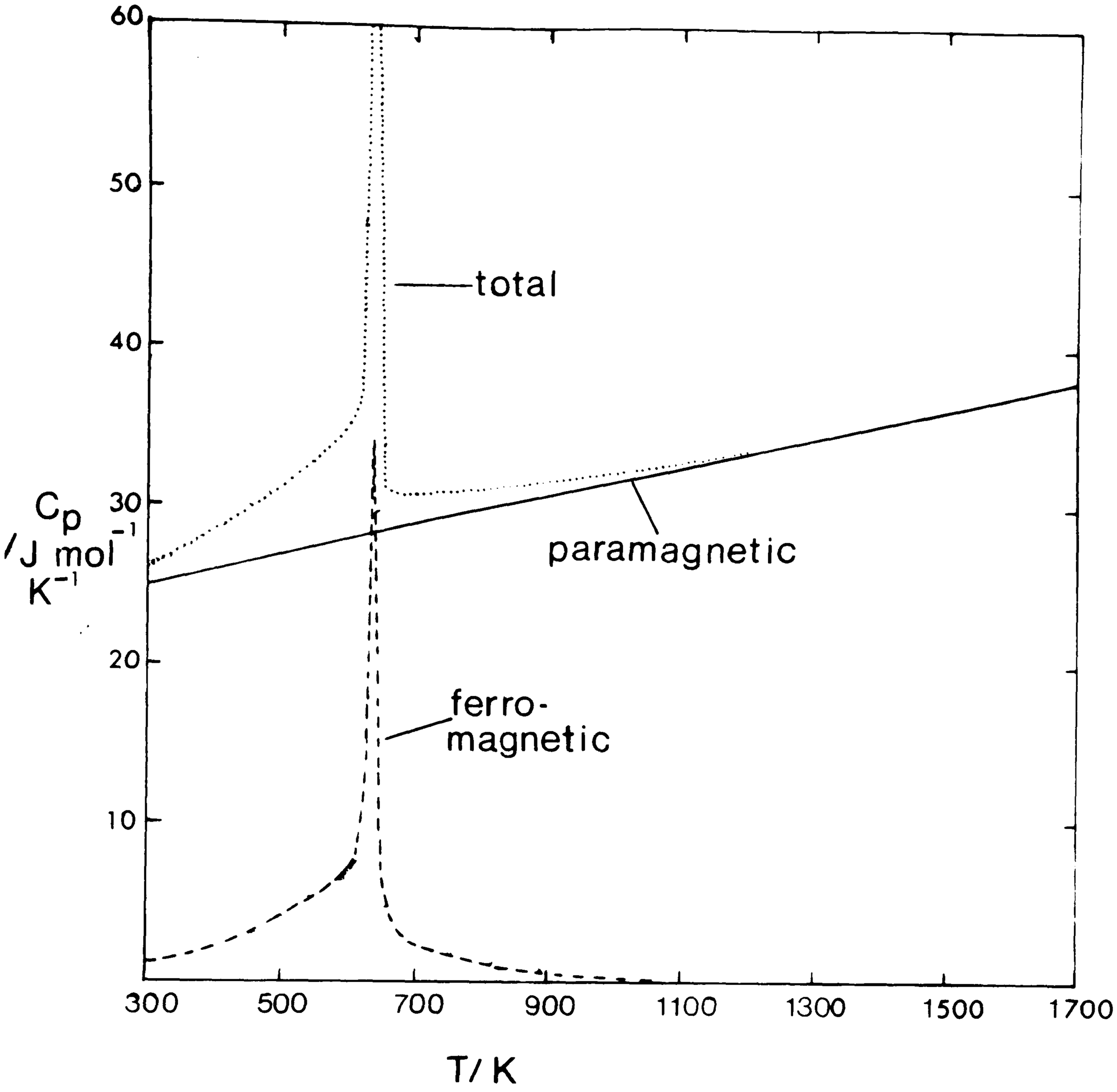

Fig 3.1 The heat capacity of nickel in the region of the Neel temperature showing the ferromagnetic and paramagnetic contributions.

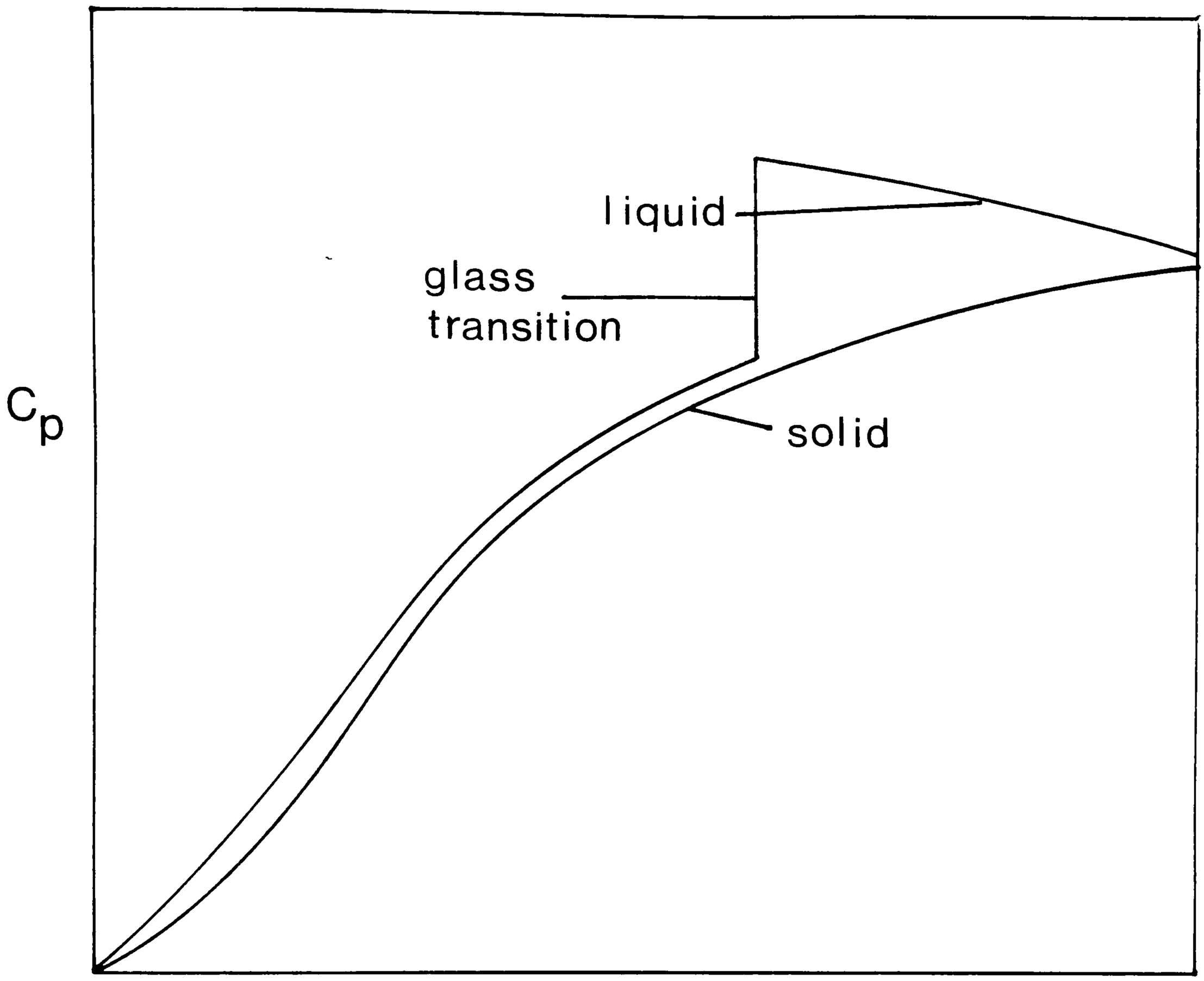

Fig 3.2 The heat capacity of typical solid and liquid phases as a function of temperature. This shows the glass transition where the heat capacity of the metastable liquid phase drops abruptly to approximately that of the stable solid phase.

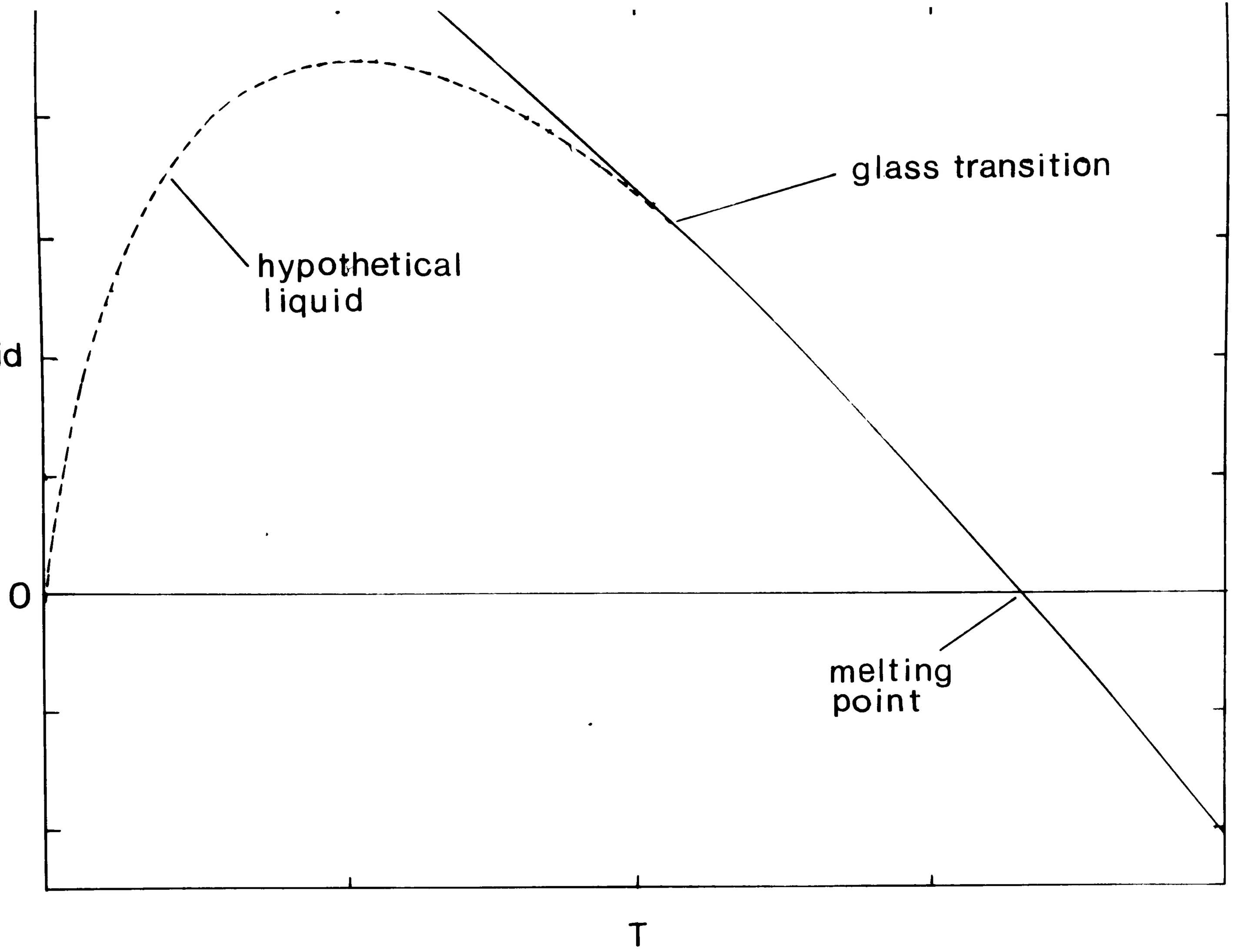

Fig 3.3 The difference in Gibbs energy between typical liquid and solid phases. This shows that without the glass transition the liquid phase could become stable again at low temperatures.

other phases of pure elements would be most welcome.

Concentration dependence

A great deal of work has been carried out into the development of models and expressions to represent thermodynamic data for condensed solution phases in binary systems and to extrapolate them into multicomponent systems. Three general approaches have been adopted. The most rigorous approach usually develops from the use of statistical mechanics and an expression of the partition function from knowledge of the various energy states available to the material. This in turn can be related directly to the various thermodynamic functions.

An equivalent approach is to express the Gibbs energy in terms of some internal variables of the system and then to find the conditions, perhaps by numerical methods, which will give the lowest Gibbs energy of the system.

The third approach, a more empirical one, is to adapt an essentially theoretical model and use some power series expression to obtain good agreement between the real behaviour and that predicted by the model. This is the approach that is normally most useful and productive.

a) Ideal Solution Model

The most simple model is for a system where the elements involved have very similar properties. Consider for example the liquid phase in a system of two metals such as Co and Ni which are very similar in size, are surrounded by the same number of nearest neighbour atoms and mix together without any appreciable volume change or expulsion or absorption of heat. Here it could be assumed that the metals would mix together randomly and therefore form what is called an ideal solution.

In this case the thermodynamic properties of the solution can be described fairly simply. Let us consider the Gibbs energy of formation from the pure liquid elements of a composition in this liquid phase where the mole fractions of Co and Ni are x_{Co} and x_{Ni} respectively. For an ideal solution, by definition, there is no enthalpy change on mixing. However, there is an entropy contribution to the Gibbs energy because the mixture has acquired some disorder. From the Boltzmann relationship

$$S = k \ln(\Omega)$$

where Ω is the number of ways of arranging the system and k is the Boltzmann constant. If the number of atoms per mole of the material is N then kN = R. Therefore

$$S = k \ln \left\{ \frac{N!}{(Nx_{Co}!)(Nx_{Ni})!} \right\}$$

Applying Stirling's approximation

$$\ln(z!) = z \ln(z) - z$$

$$S = - R \{ x_{Co} \ln(x_{Co}) + x_{Ni} \ln(x_{Ni}) \}$$

The contribution of ideal mixing to the Gibbs energy therefore

$$= RT [x_{Co} \ln(x_{Co}) + x_{Ni} \ln(x_{Ni})]$$

Suppose now that the reference phases for pure nickel and cobalt are not the liquid phase. In this case we must consider the transformation of the pure metals from their reference phases to the liquid phase which we can label by G_{Co} and G_{Ni} respectively. The contribution from these terms to the Gibbs energy of formation will be $x_{Co}G_{Co} + x_{Ni}G_{Ni}$. Therefore the general expression for the Gibbs energy of formation for

such an ideal solution is given by:

$$\Delta_f G = x_{Co} G_{Co} + x_{Ni} G_{Ni} + RT \left[x_{Co} \ln(x_{Co}) + x_{Ni} \ln(x_{Ni}) \right]$$

and this expression could equally apply to any other phase such as fcc or bcc.

In Fig 3.4 we see a plot of the Gibbs energy for the liquid and fcc phases at a temperature 1750 K as a function of composition. As is shown in Chapter 4 the phase boundaries are given by the points of common tangency to the two curves. If this procedure is performed for a number of temperatures the phase diagram in Fig 3.5 is built up. This shows a very simple lens type phase diagram in very good agreement with that found from experiment.

Therefore for some materials a simple ideal solution model is able to represent known thermodynamic and phase diagram data accurately. It can easily be extended to any number of components in the solution to give the equation

$$\Delta_f G = \sum_{i=1}^{n} x_i G_i + R T \sum_{i=1}^{n} x_i \ln x_i$$

where n is the number of components and x_i their concentrations. G_i is the Gibbs energy of transformation from the pure component i in its reference state to the phase in question at the temperature T.

b) Regular Solution Model

Solutions which exhibit ideal behaviour are rare and it is the norm for components to show some kind of net interaction manifested either in the form of a positive or negative enthalpy of mixing. This deviation from ideality is called the excess Gibbs energy G^E and it is the expression of this as a function of composition that is the main focus

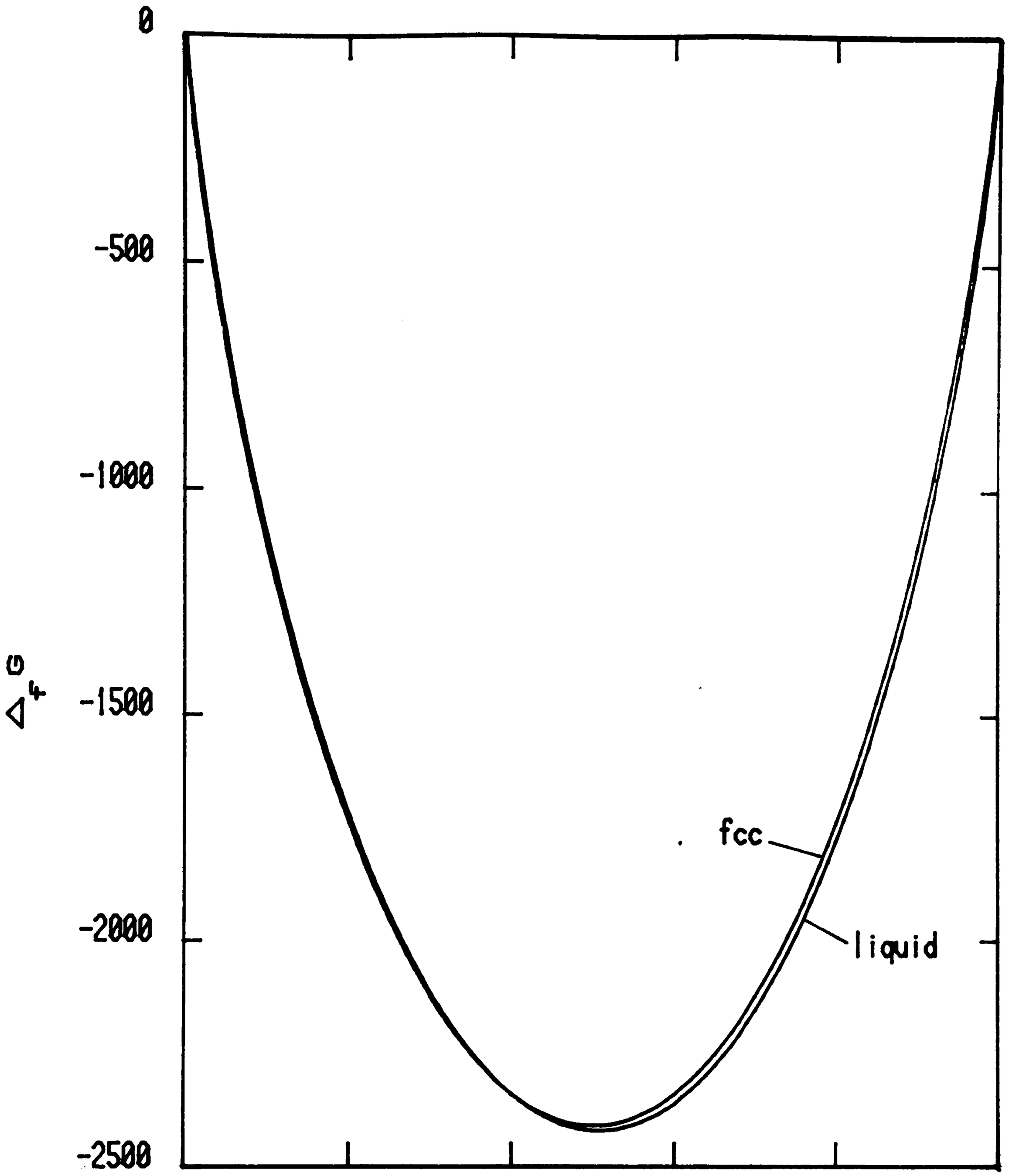

Fig 3.4 The Gibbs energies of formation for 1750 K of the liquid and fcc phases in the Co-Ni system modelled as ideal solutions

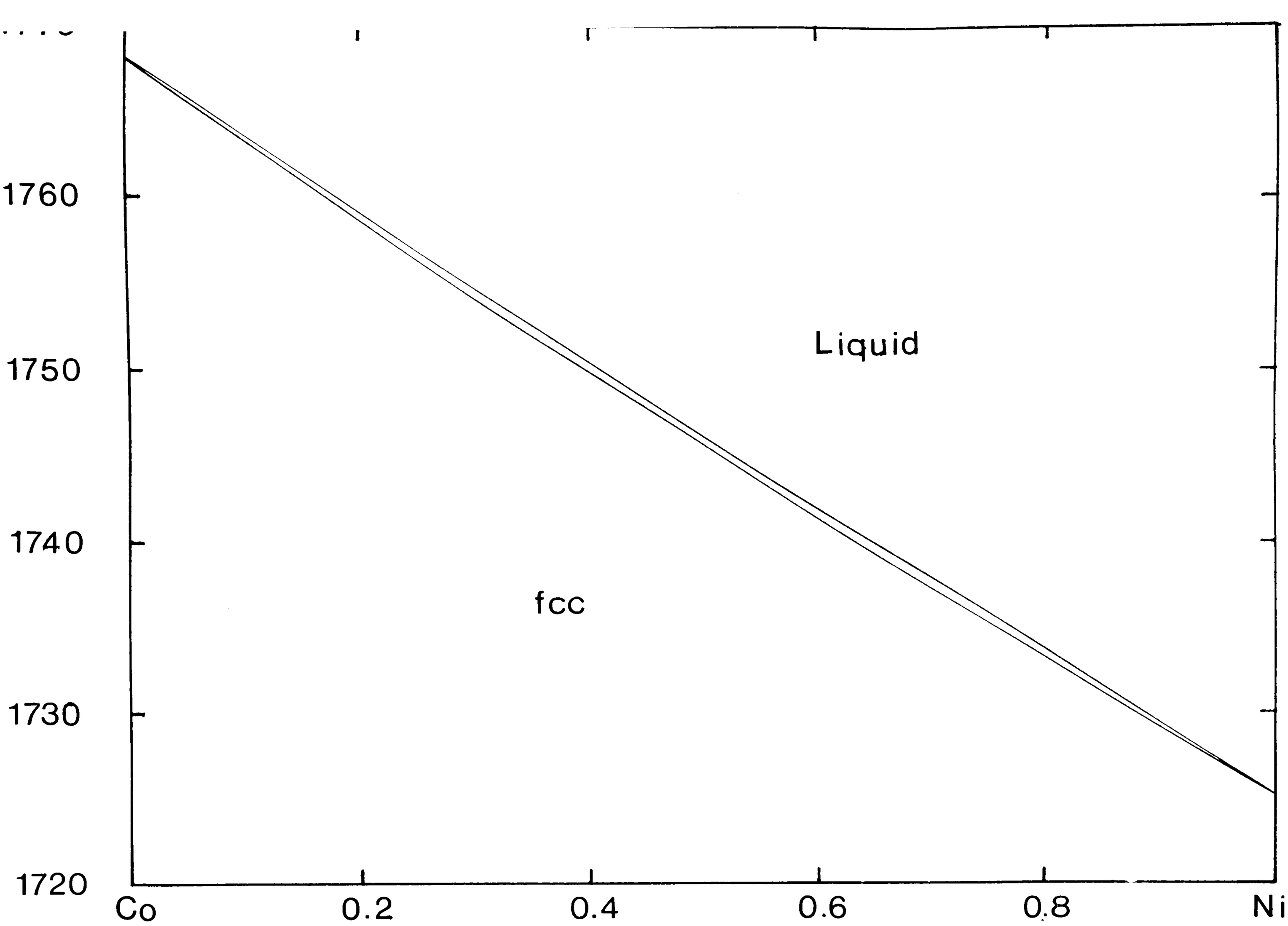

Fig 3.5 Calculated phase diagram for the Co-Ni system with the liquid and fcc phases modelled as ideal solutions.

of theoretical and practical interest. The subject has been reviewed by a number of authors, in particular by Oriani and Alcock (78), Ansara (79,80) and Kapoor (81). The most basic approximation to represent the excess Gibbs energy is the regular solution model.

The concept of regular solutions was introduced by Hildebrand (82-84) from a study of the deviations of solubility curves from Raoult's law. He found that "particularly among substances of low polarity, there exist families of solubility curves which bespeak a marked regularity". He called systems which were members of these families 'regular solutions'. In order to explain this behaviour he adopted an approach of Heitler (85,86) which considered a solution as a lattice and predicted that the partial enthalpy of mixing should vary in an approximately parabolic way. This formalism fitted Hildebrand's solubility data very well.

The theory of regular solutions as developed by Hildebrand (82-84) and Bragg and Williams (87) is such an important concept that it is worth considering in some detail the theoretical background to the model. Consider a mole of binary solution between two elements A and B. As with the ideal solution model we can assume that the elements A and B are of approximately the same size, are surrounded by the same number of nearest neighbours, and mix together without any change in volume. Here however we are considering a solution where there is an enthalpy change on mixing arising from a net interaction between the elements. The bond energy between two atoms should be short range and independent of the other atoms they are bonded to. The total potential energy is then assumed to be equal to the sum of contributions only from pairs of atoms in direct contact. The most important assumption is that this interaction between the atoms has no effect on the order of the solution ie. the entropy of mixing is that for an ideal solution.

The total lattice energy of a solution having composition in mole

fraction terms (x_A,x_B) can be written as:

$$E = n_{AA}E_{AA} + n_{AB}E_{AB} + n_{BB}E_{BB}$$

where n_{AA}, n_{AB} and n_{BB} are the number of bonds of the type A-A, A-B and B-B respectively and E_{AA}, E_{AB} and E_{BB} are their respective energies. The probability of finding an A atom and a B atom on a given site will be x_A and x_B respectively. Therefore the probability of finding two chosen adjacent sites occupied by two A atoms, two B atoms or one A atom and one B atom will be x_A^2, x_B^2 and $2x_Ax_B$ respectively.

If we assume that all atoms in the solution have z nearest neighbours the total number of bonds will be zN/2 where N is the number of atoms per mole. We can now define the number of bonds of each type as its probability of occurring multiplied by zN/2.

ie. $n_{AA} = \frac{z\,N}{2} x_A^2$ $\quad n_{BB} = \frac{z\,N}{2} x_B^2$ $\quad n_{AB} = z\,N\,x_Ax_B$

This leads us to the expression:

$$E = \frac{zN}{2}\,[x_A^2E_{AA} + x_B^2E_{BB} + 2x_Ax_BE_{AB}]$$

The change in energy on alloying will be this quantity E minus lattice energies for the pure elements which will be $zNx_AE_{AA}/2$ and $zNx_BE_{BB}/2$ respectively.

ie $\Delta E = \frac{zN}{2}\,[-x_A(1-x_A)E_{AA}-x_B(1-x_B)E_{BB} + 2x_Ax_BE_{AB}]$

or, since $x_A + x_B = 1$,

$$\Delta E = \frac{zN}{2}\,x_Ax_B\,[2E_{AB}-E_{AA}-E_{BB}] = N\,x_A\,x_B\,w$$

$$= x_Ax_BL$$

where 2w/z is the energy required to change one AA pair and one BB pair into two AB pairs, and L = N w.

This quantity ΔE is equal to the enthalpy of mixing and therefore the excess Gibbs energy since according to our initial assumptions the volume change is zero and the mixing has been accompanied by no ordering within the solution.

The expression for the excess Gibbs energy in the binary alloy case can also be generalised for a multicomponent system through the same procedure outlined above. Here one obtains

$$G^E = \sum_{i=1}^{n-1} \sum_{j=i+1}^{n} x_i x_j L_{ij}$$

Consequently for systems obeying the regular solution assumptions the thermodynamic data can be represented by one coefficient for each binary system. Strictly this coefficient should be independent of temperature although it has been the custom to relax this condition. Many binary and ternary alloy systems have been represented successfully using the regular solution model (88-90).

It is worth considering at this stage some of the implications of the regular solution approximation for binary systems. Fig 3.6 shows typical curves for the Gibbs energy of formation with different values of the interaction parameter L. If L = 0 we have an ideal solution as in curve (a). If L is negative ie. there is a negative enthalpy of formation as in curve (b), this is manifested by a Gibbs energy curve more negative over all the composition range than for an ideal solution. If L is positive, however, the ideal entropy term and the enthalpy of formation term oppose one another and at certain temperatures will result in a curve such as (c) with two distinct minima leading to a region where two phases of the same structure are immiscible. For a regular solution a positive interaction term will always lead to a miscibility gap for

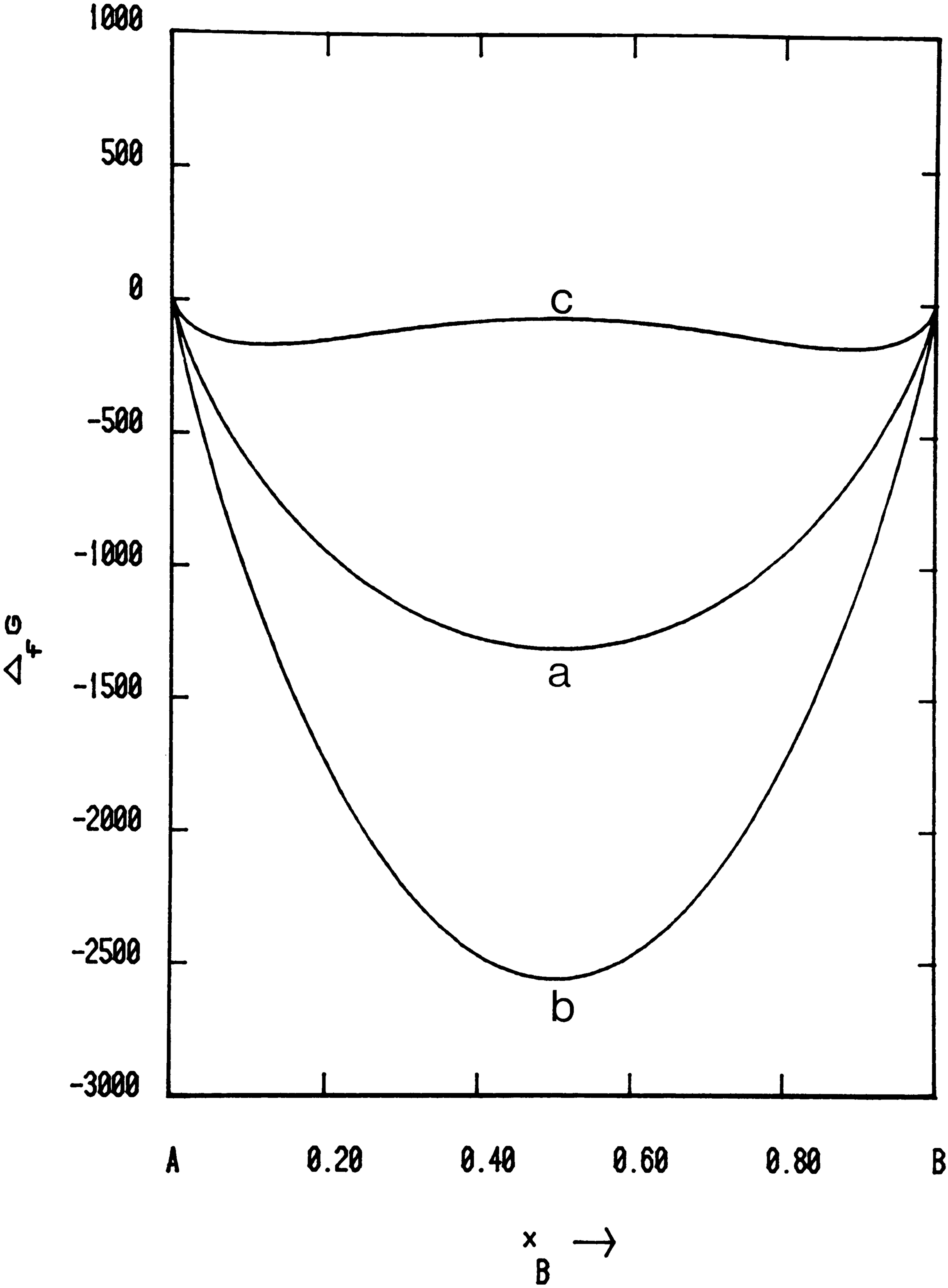

Fig 3.6 Curves for the Gibbs energies of formation of a phase modelled as a regular solution according to whether the interaction parameter is 0 (ie. ideal solution, curve a), negative (curve b) or positive (curve c with two distinct minima leading to a region of immiscibility).

temperatures less than L/2R providing the phase is itself stable.

c) Quasi-Chemical Theory

The regular solution model has been criticised from a theoretical point of view by Guggenheim (91) and Rushbrooke (92) because of its assumption that even in systems with non-zero heats of mixing the atoms will distribute themselves randomly among the lattice sites. In reality the atoms will distribute themselves in order to reach the state with the lowest Gibbs energy.

For the regular solution model, as shown earlier, the number of AB bonds will be given by:

$$n_{AB} = z\ N\ x_A\ x_B$$

If we let the number of A atoms be n_A (= N x_A) and the number of B atoms be n_B (= N x_B) and rearrange we obtain

$$n_{AB}^2 = (z\ n_A - n_{AB})(z\ n_B - n_{AB})$$

Guggenheim and Rushbrooke (91-93) developed the Quasi-Chemical theory to take into account the preferential distribution of various components of the solution and these ideas were developed by Fowler (94,95) and Bethe (96). From a rigorous treatment using statistical mechanics they showed that:

$$n_{AB}^2 = (z\ n_A - n_{AB})(z\ n_B - n_{AB})\ e^{-2w/zkT}$$

From this equation one can see that if w = 0 ie. for an ideal solution we obtain the expression required for random mixing. If however, w>0 ie. an endothermic system, the formation of AB bonds will be discouraged and there will be a tendency to form AA and BB bonds and

for phase separation. If however w<0 there will be a tendency for AB pairs to form and ordering to occur.

The quantity $zn_A - n_{AB}$ is equal to $2n_{AA}$, twice the number of A-A bonds in the mixture and similarly $zn_B - n_{AB}$ is equal to $2n_{BB}$, twice the number of BB bonds in the mixture. Therefore for the quasi-chemical theory:

$$\frac{n_{AB}^2}{n_{AA}n_{BB}} = 4\, e^{-2w/zkT}$$

The similarity of this expression to the mass action law for chemical reactions led to the adoption of the name 'quasi-chemical theory'.

The above expression can be solved for n_{AB} or more appropriately $\bar{x} = n_{AB}/N$ given values for the other parameters.

ie. $$\bar{x} = \frac{\{1 + 4\, x_A\, x_B\, \eta\}^{1/2} - 1}{2\eta}$$

where $$\eta = e^{2w/zkT} - 1$$

This expression can then be introduced into the statistical expression for the excess Gibbs energy to give:

$$G^E = \frac{R\,T\,z}{2}\left[x_A \ln\frac{(x_A - \bar{x})}{x_A^2} + x_B \ln\frac{(x_B - \bar{x})}{x_B^2}\right]$$

This approach has been extended by Bonnier et al. (97) and Jena (98) into ternary systems by solving iteratively equations of the form

$$\bar{x}_{ij}^2 = (z\, x_i - \bar{x}_{ij})(z\, x_j - \bar{x}_{ij})\, \alpha_{ij}$$

where $i \neq j$ and α_{ij} is given by:

$$\alpha_{ij} = e^{-2w_{ij}/kT}$$

and incorporating into the expression

$$G^E = \frac{R\ T\ z}{2} \sum_{i=1}^{n} x_i \ln\left(\frac{x_i - \sum_{j=1}^{n} \bar{x}_{ij}}{x_i^2}\right)$$

where $j \neq i$.

Bonnier et al. applied this method to the Cd-Sn-Bi, Cd-Pb-Sn and Cd-Pb-Bi systems. A numerical approach was also adopted by Stringfellow and Greene (99,100) for the calculation of the phase diagrams for the In-Ga-As, In-As-Sb, Ge-Si-Sn and Ge-Si-Pb systems.

For cases where the net interactions between atoms or molecules are small an alternative approach can be adopted. As an example, for binary systems the expression for $\bar{x}$ can be expanded as a power series in $x_A x_B \eta$ and then expanded again by expressing η as a power series in terms of $2w/zkT$ which on omitting the higher order terms gives

$$G^E = x_A\ x_B\ L\ [\ 1 - x_A\ x_B\ \frac{2\ L}{z\ R\ T}\ ]$$

which was been adopted by Kleppa (101) in his study of the Sn-Au system.

Hagemark (102,103) and Wagner (104) have derived analytical expressions for the thermodynamic properties of multicomponent systems using the quasi-chemical approximation.

d) Cluster Variation Method

The regular solution model discussed earlier takes its basic building block to be lattice points which interact with their neighbours. The quasi-chemical theory discussed in the last section is based around pairs of atoms but as shown by Guggenheim (93) this is still an approximation. In a generalisation of Bethe's procedure he showed that

even better approximations could be obtained by considering triangular triplets or tetrahedral quadruplets and this was used by Li (105) to explain ordering phenomena in fcc binary alloys. Unfortunately larger clusters lead to greater numerical problems.

Takagi (106) adopted a different procedure from the quasi chemical theory but still using pairs of atoms as the basic building block and derived essentially the same expression. From a generalisation of Takagi's approach Kikuchi, in a series of papers (107-115) developed the Cluster Variation method. According to this method the Gibbs energy is described in terms of a set of variables derived from a predefined cluster of atoms. Instead of forming the partition function as used for the quasi-chemical theory, the Gibbs energy is minimised with respect to these variables in order to find the most stable atomic arrangement. The smallest cluster possible is a lattice point from the Bragg-Williams' approximation and the cluster variation method reproduces the regular solution model. The next most complicated cluster is a pair of atoms, and as demonstrated by Takagi, this gives results identical to the quasi-chemical theory. For higher order clusters, represented in the Cluster Variation model as extensions of these smaller clusters, the method gives more accurate results than the quasi-chemical model. For example a tetrahedon cluster variation approximation has been applied by van Baal to fcc binary alloys (116) giving different and more accurate results than those of Li (105).

To date the cluster variation method has been used mainly with considerable success for the study of ordering reactions in alloy systems using one parameter for the pairwise interaction between two elements. Recently Kikuchi has used the method to calculate the phase diagrams of the In-Ga-As and In-Sb-As systems, previously studied by Stringfellow and Greene using the quasi-chemical approximation. He obtained good agreement with their calculations and with experimental

data.

More recently Kikuchi (115) has attempted to derive data for the Hg-Te and Cd-Te systems to be consistent with the observed liquidus measurements. He used essentially an associated solution model (see later) with species of HgTe and CdTe with their interactions represented by a pair approximation of the cluster variation model.

e) Asymmetric Models

Unfortunately all the models discussed so far suffer from the same basic drawback in that one parameter is rarely sufficient to represent the thermodynamic data for typical binary alloy systems. This is not surprising since one would expect that the bond energy between say an A atom and a B atom might be dependent on their environments. Similarly other factors such as the relative sizes of A and B and electronic effects cannot usually be represented by just one parameter (46,117-119).

A number of different attempts have been made to solve this problem. Hardy (120) introduced a so-called subregular solution model when he assumed that the interaction coefficient L could be represented as a function of composition

ie. $G^E = x_A x_B (L_1 x_A + L_2 x_B)$

Kaufman has also used the subregular model but as an extension he represented the coefficients L_1 and L_2 as functions of temperature (46).

Sharkey et al. (121) derived an expression based upon the quasi-chemical theory which incorporates composition dependence in the form:

$$H^m = \alpha_1 x_A^2 x_B + \alpha_2 x_A x_B^2 - \alpha_3 x_A^2 x_B^2$$

and applied this to a large number of binary alloy systems. They also proposed an extrapolation into ternary systems using a ternary interaction term and applied their formalism with some success to the Bi-Cd-Pb, Cd-Pb-Sn and Cd-Pb-Sb systems.

Another model which allows the interpretation of asymmetric data for binary systems is the Central or Surrounded Atom model. This model was suggested simultaneously by Lupis and Elliott (122) and Mathieu et al. (123-125). Rather than concentrating on bonds, this model considers the effect on individual atoms in the field of force of its nearest neighbours.

Here the bonding energy between two atoms is no longer assumed to be independent of its surroundings. Furthermore vibrational contributions to the thermodynamic properties of mixing, neglected in previous models were introduced. Normally an empirical function was used to represent the changes in bond energy or vibrational parameters with changes in the composition of the nearest neighbour environment although a linear or parabolic function has generally been used.

The surrounded atom model has been extended into ternary system by Brion et al. (126,127). For simplicity the Bragg-Williams' statistics are usually applied giving a quasi-regular solution model. According to Ansara (79) the application of the Bethe statistics as used for the quasi-chemical theory requires unreasonable computing time.

f) Empirical Representations

The theoretical approach adopted hitherto has had great success in describing complex phenomena such as ordering. However in most binary alloy systems, the physical interactions are too complicated to be represented simply by one or two parameters. It is then necessary to use

an empirical extension of the theoretical approach. The most widely used representation is a power series expression.

There is nothing new about the use of power series expressions - one form was used by Margules (128,129) in the last century. However the advent of digital computers and data fitting techniques have made the use of power series expressions practicable. A number of expressions have been suggested eg. by Guggenheim (130), Wohl (131), Carlson and Colburn (132), Benedict et al. (133) and Bale and Pelton (134) who also advocated the use of Legendre polynomials (135). Other formalisms have been suggested by Krupkowski (136), Esdaile (137) and Wilson (138). However the most useful form was suggested by Redlich and Kister (139,140).

$$G^E = x_A x_B(L_0 + L_1(x_A-x_B) + L_2(x_A-x_B)^2 + L_3(x_A-x_B)^3 .....)$$

g) Extrapolation of binary data into Multicomponent Systems

The extension of the regular solution model into a multicomponent system is straightforward as was shown earlier. For binary data represented by more complex expressions there is no longer a unique way of carrying out this extrapolation. Several different approaches have been suggested for use usually in terms of some geometrical model where the multicomponent excess Gibbs energy is calculated as a weighted sum of excess Gibbs energies of certain defined binary compositions. These are shown in Fig 3.7 and will now be discussed in turn.

Bonnier equation

According to the Bonnier equation (141) the excess Gibbs energy derived from the composition path shown in Fig 3.7a is given by

$$G^E = \frac{x_B}{1-x_A} G_{AB}(x_A, 1-x_A) + \frac{x_C}{1-x_A} G_{AC}(x_A, 1-x_A)$$

$$+ (1-x_A)\, G_{BC}\left(\frac{x_B}{x_B+x_C}, \frac{x_C}{x_B+x_C}\right)$$

where for example the term $G_{AB}(x_A, 1-x_A)$ refers to the excess Gibbs energy of a composition in the binary system AB with the composition of element A equal to x_A and that of B equal to $1-x_A$.

Spencer et al. (142) showed that this equation orginates from the summation of three terms, the formation of the two binary compositions in the AB and AC binaries weighted according to the overall composition followed by a mixing of the two binary compositions using the data for the binary system BC.

Toop equation

According the Toop equation (143) the excess Gibbs energy for a ternary composition is given by:

$$G^E = \frac{x_B}{1-x_A} G_{AB}(x_A, 1-x_A) + \frac{x_C}{1-x_A} G_{AC}(x_A, 1-x_A)$$

$$+ (1-x_A)^2\, G_{BC}\left(\frac{x_B}{x_B+x_C}, \frac{x_C}{x_B+x_C}\right)$$

The composition path also corresponds to Fig 3.7a, the same as that used for the Bonnier equation. However the Toop equation is different from the Bonnier equation since the final term is multiplied by $(1-x_A)^2$ rather than $(1-x_A)$. This model was used by Toop to make calculations in the Cd-Pb-Bi, Pb-Sn-Cd and $CaO-FeO-SiO_2$ systems and by Ajersch et al. (144) to calculate an isothermal section of the Cd-Bi-Sb phase diagram.

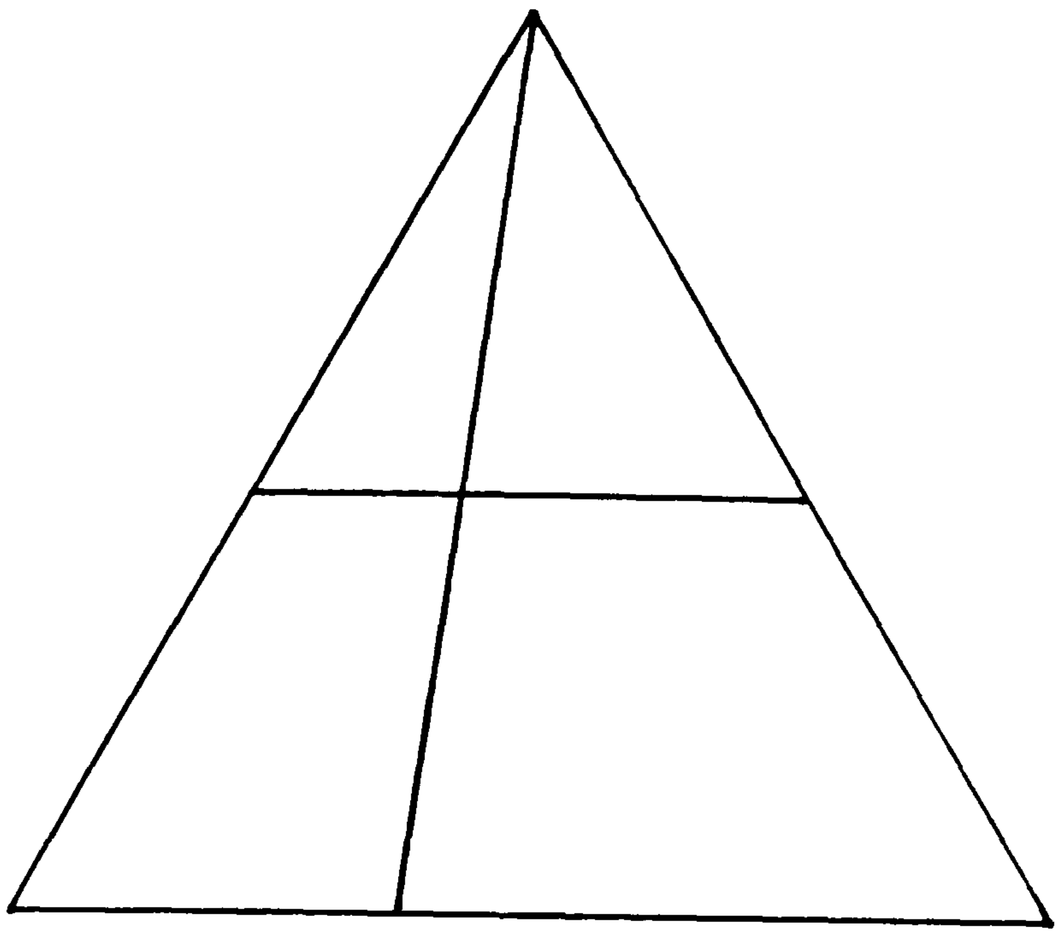

a

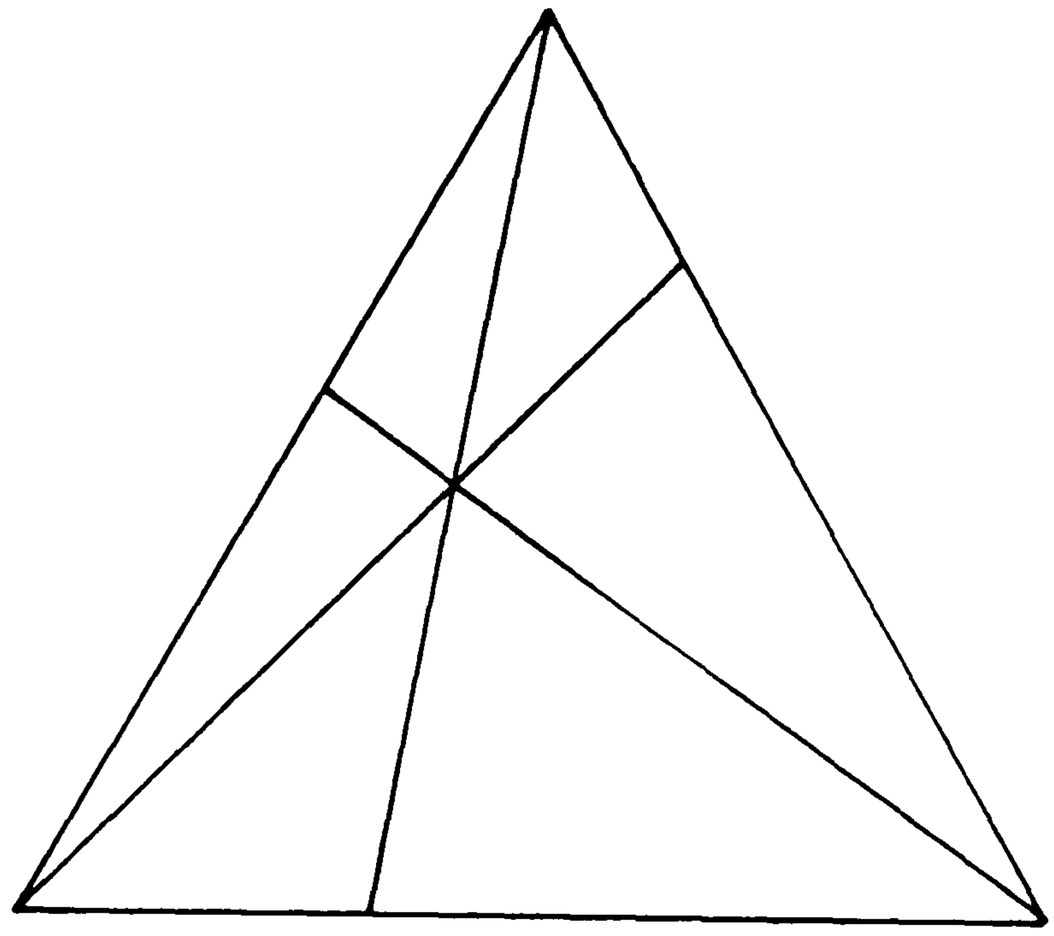

b

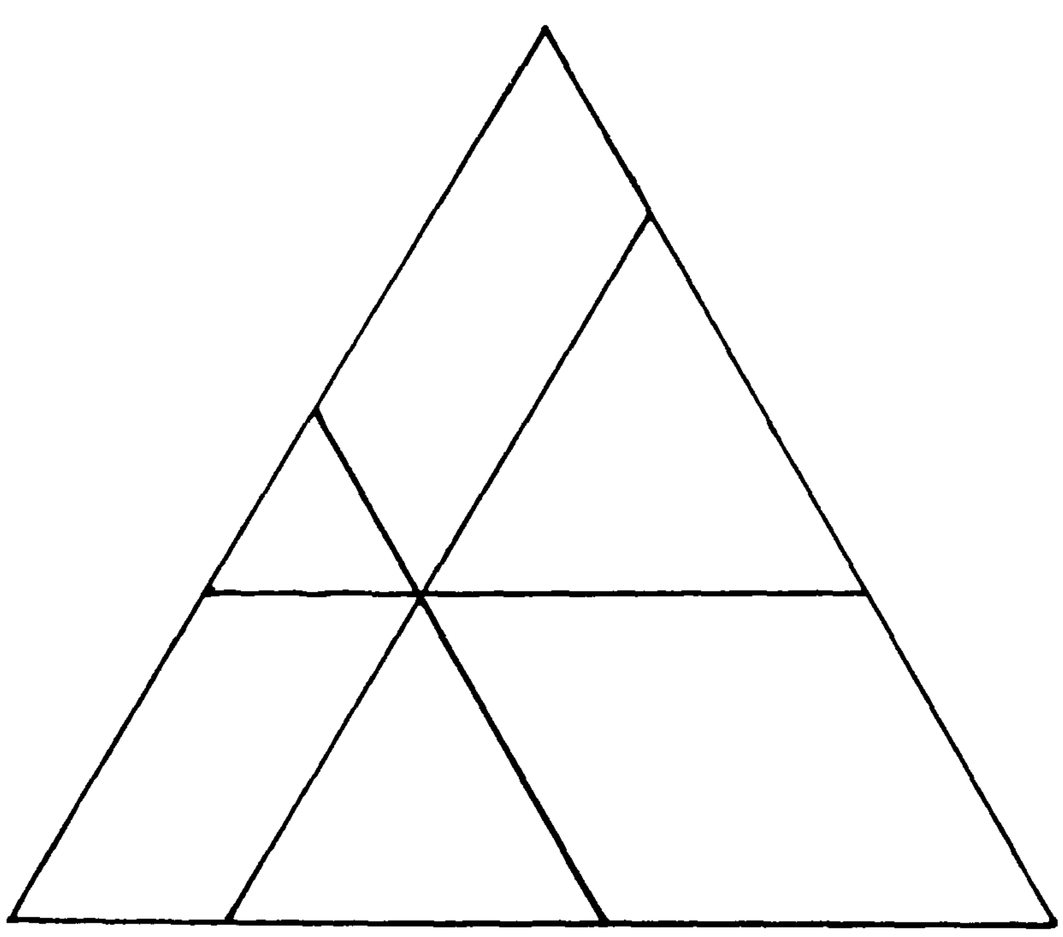

c

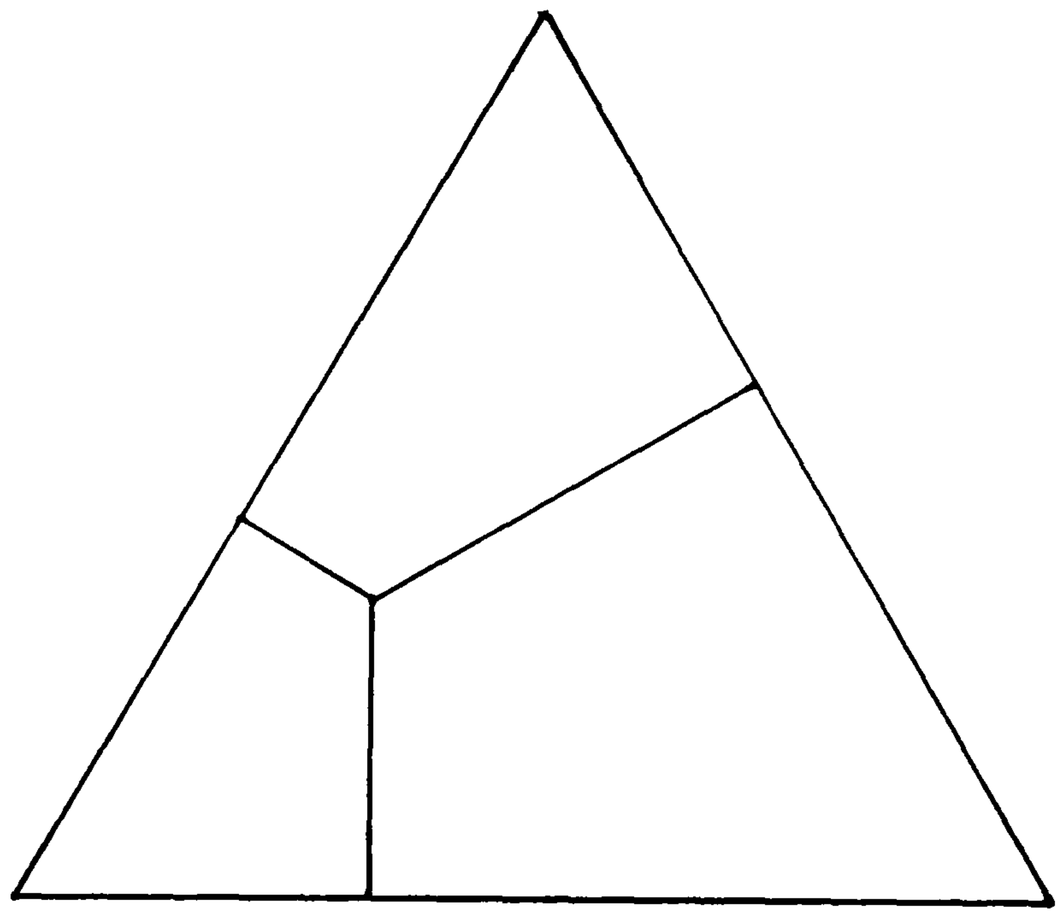

d

Fig 3.7 Geometrical models for the extrapolation of binary thermodynamic data into a multicomponent system a) Bonnier and Toop equations b) Kohler equation c) Colinet equation d) Muggianu equation.

Kohler equation

Kohler (145) and Olson and Toop (146) derived the following equation independently.

$$G^E = (x_A + x_B)^2 G_{AB} \left(\frac{x_A}{x_A+x_B}, \frac{x_B}{x_A+x_B} \right)$$

$$+ (x_A + x_C)^2 G_{AC} \left(\frac{x_A}{x_A+x_C}, \frac{x_C}{x_A+x_C} \right)$$

$$+ (x_B + x_C)^2 G_{BC} \left(\frac{x_B}{x_B+x_C}, \frac{x_C}{x_B+x_C} \right)$$

which is shown as the composition path in Fig 3.7b. The Kohler equation has been extended into a generalised multicomponent system by Kehiaian (147) and has been used extensively by Kaufman (148-159) and others (160,161).

Both the Kohler equation and the Toop equation have their base in a completely rigorous treatment of Darken (162) in which he showed that for a ternary system A-B-C the excess free energy may be calculated from true binary terms for the A-B and A-C systems and a term for a pseudo binary section along a line of constant B/C ratio.

Colinet equation

For the Colinet equation (163) the excess Gibbs energy is given by:

$$G^E = 1/2 \left[\frac{x_A}{1-x_B} G_{AB} (1-x_B, x_B) + \frac{x_B}{1-x_A} G_{AB} (x_A, 1-x_A) \right.$$

$$+ \frac{x_A}{1-x_C} G_{AC} (1-x_C, x_C) + \frac{x_C}{1-x_A} G_{AC} (x_A, 1-x_A)$$

$$\left. + \frac{x_B}{1-x_C} G_{BC} (1-x_C, x_C) + \frac{x_C}{1-x_B} G_{BC} (x_B, 1-x_B) \right]$$

as shown in the composition path Fig 3.7c. The Colinet equation is rarely used.

Muggianu equation

The composition path used by the Muggianu equation (164) was called by Jacobs and Fitzner (165) 'the shortest composition path' as in Fig 3.7d.

The excess Gibbs energy is given by:

$$G^E = \frac{4x_Ax_B}{(2x_A+x_C)(2x_B+x_C)} G_{AB}\,(x_A+x_C/2,\ x_B+x_C/2)$$

$$+ \frac{4x_Ax_C}{(2x_A+x_B)(2x_C+x_B)} G_{AC}\,(x_A+x_B/2,\ x_C+x_B/2)$$

$$+ \frac{4x_Bx_C}{(2x_B+x_A)(2x_C+x_A)} G_{BC}\,(x_B+x_A/2,\ x_C+x_A/2)$$

This expression may seem complex but, as shown by Jacobs and Fitzner and Hillert (166), if the binary systems are represented by the Redlich-Kister expression the expression simplifies to

$$G^E = x_Ax_B\,(L^0_{AB} + L^1_{AB}(x_A-x_B) + L^2_{AB}(x_A-x_B)^2 \ldots..)$$

$$+ x_Ax_C\,(L^0_{AC} + L^1_{AC}\,(x_A-x_C) + L^2_{AC}\,(x_A-x_C)^2 \ldots.)$$

$$+ x_Bx_C\,(L^0_{BC} + L^1_{BC}\,(x_B-x_C) + L^2_{BC}\,(x_B-x_C)^2 \ldots.)$$

This is simply the ternary Redlich-Kister expression (139) and has been used at NPL for many years (167-169).

h) Comparison between geometrical equations

These equations have been compared in a number of papers (79,80,142,143,165,166,170,171). From the theoretical point of view none of the models can be considered to be anything other than an approximation. Nevertheless the models can be tested for certain desirable features such as compatibility with the regular solution model, symmetric behaviour with respect to the pure components and correct limiting behaviour when the amount of one of the components becomes zero or when two elements have very similar properties.

Of the five models both the Bonnier and the Toop models are unsymmetrical with respect to the pure components. The Bonnier model is little used now since it is not consistent with the regular solution model. The Toop model is used for systems only where one component is very different from the others. The other three models are all symmetrical and consistent with the regular solution model. Unfortunately none of them transform to a binary data set when two of the elements become very similar. Hillert (166) compared the Kohler, Colinet and Muggianu models in detail by deriving expressions for the ternary excess Gibbs energy representing the three component binary systems by the subregular model. He showed that, despite the different composition paths, the Colinet and Muggianu methods give identical results. Furthermore the difference between these models and the Kohler model will always be very small.

In the other papers the predictions of the models were compared with available experimental information. They found essentially that all these models represent the data reasonably well and that there is no overriding reason why one model should be chosen in preference to another. The model used at NPL and in this thesis for metallic systems is the full ternary Redlich-Kister expression with a ternary interaction

term given by:

$$\Delta_f G = \sum_{i=1}^{n} x_i G_i + R\,T \sum_{i=1}^{n} x_i \ln x_i$$

$$+ \sum_{i=1}^{n-1} \sum_{j=i+1}^{n} x_i x_j \left(L_{ij}^{0} + L_{ij}^{1} (x_i - x_j) + L_{ij}^{2} (x_i - x_j)^2 \ldots\ldots\right)$$

$$+ \sum_{i=1}^{n-2} \sum_{j=i+1}^{n-1} \sum_{k=j+1}^{n} x_i x_j x_k K_{ijk}$$

i) Models for solid 'compound' phases

In many systems of practical interest the interatomic forces have sufficient strength to favour phases for certain ranges of composition where different types of atom occupy preferentially different types of lattice site. Such phases are often loosely described as compounds. These 'compound' phases often coexist within the same system as the so-called substitutional phases discussed earlier. Often within a binary system these compound phases have a very narrow range of homogeneity and it is common to treat such phases as having a fixed stoichiometry.

In a ternary system it is common for a third element, say C, again to enter into one particular type of site eg. the type occupied by B in the compound A_pB_q and to substitute for element B. If the compound A_pC_q were stable in this particular structure we might have a line representing the phase from A_pB_q to A_pC_q in the phase diagram as in Fig 3.8. These so-called 'line-compounds' are very common in systems of practical interest. Often the compound A_pC_q with this structure is not actually stable in the A-C binary system, but it is still convenient to think of the hypothetical form, obviously with a higher Gibbs energy than the stable phase assemblage for that composition.

The thermodynamic data for such a 'line-compound' phase are naturally related back to the data for the pure compounds. A number of equivalent

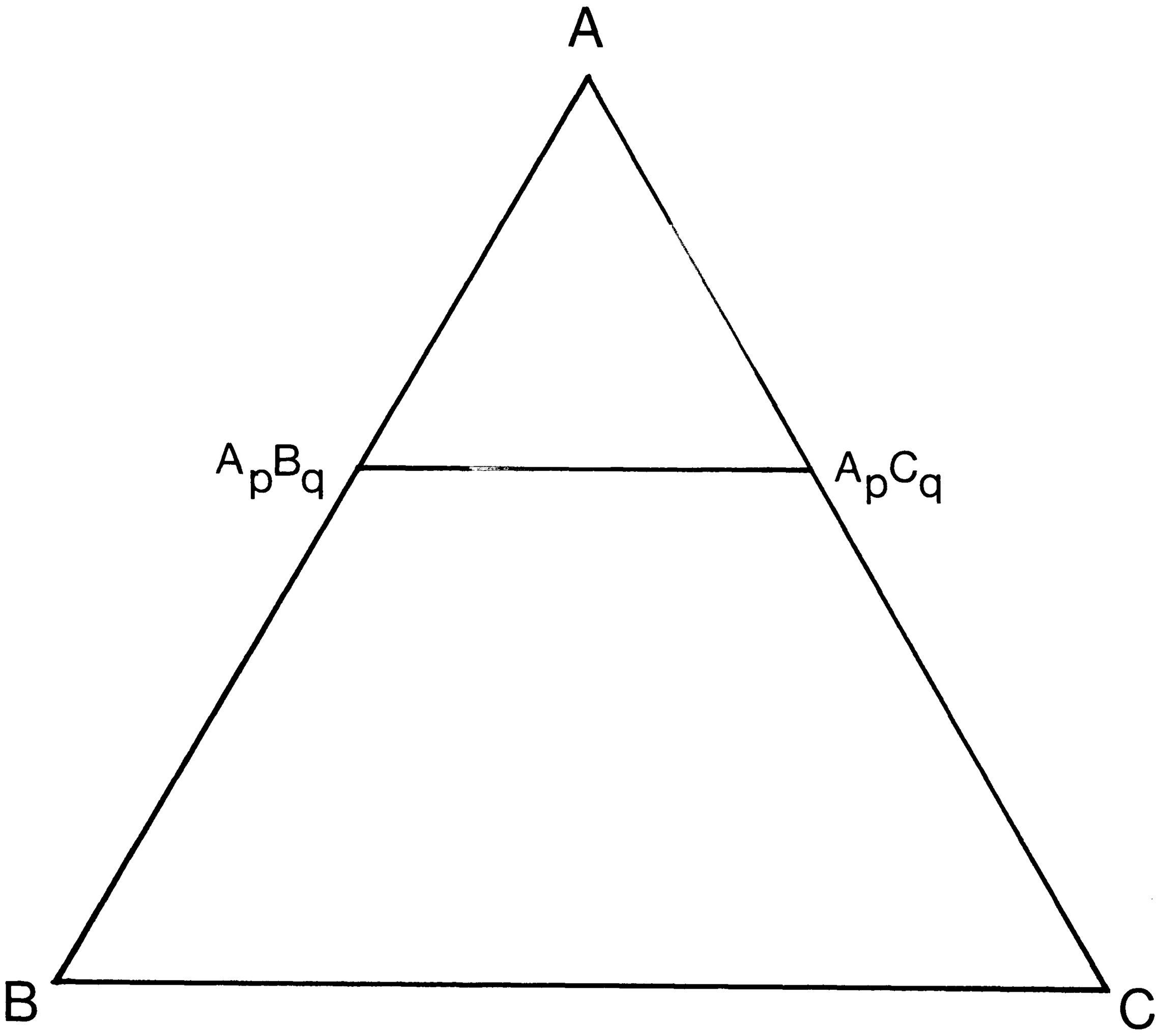

Fig 3.8 Ternary 'line-compound' phase between binary stoichiometric compounds A_pB_q and A_pC_q.

approaches have been adopted (46,172-174) based on the assumption of ideal mixing between the atoms on the same type of site or sublattice with a superimposed interaction expressed in a way analogous to the regular solution model or power series expansion.

This gives an expression of the form:

$$\Delta_f G = \frac{x_B}{q} \Delta_f G_{A_pB_q} + \frac{x_C}{q} \Delta_f G_{A_pC_q}$$

$$+ R T [x_B \ln(x_B) + x_C \ln(x_C) - (1-x_A) \ln(1-x_A)]$$

$$+ x_B x_C L$$

where the Gibbs energy of formation of the line-compound refers to one mole of material while the Gibbs energies of the binary stoichiometric compounds refer to one mole of formula unit.

This approach was generalised by Sundman and Agren (175), incorporating work of Hillert and Staffansson (176) and Harvig (177), into a form suitable for computer application for phases with any number of components and sublattices. A key feature of their approach is the use of site fractions ie. the fraction of one sublattice occupied by one particular type of atom.

Some classes of phases exhibit appreciable ranges of homogeneity within binary systems and it is no longer always possible to treat these phases as stoichiometric. The effect of non-stoichiometry on the thermodynamic properties was first studied in detail by Wagner and Schottky (178) and their work has been extended by Libowitz (179,180) and Brebrick (181). Any deviations from stoichiometry are due to some imperfections in the lattice. By assigning energies to each of the possible point defects it is possible to account for the variation of the Gibbs energy with composition.

The systematic sublattice approach of Sundman and Agren (175) has also been used to describe the thermodynamic data for these non-stoichiometric compounds. Here however the data are not energies for each point defect but interactions between atoms or vacancies within the same sublattice together with data for hypothetical pure compounds. This approach has been used with success for the sigma phase (182,183)

j) Molten Salt Solutions

One area of particular interest for modelling thermodynamic data is in molten halide solutions. As with alloy systems the simplest model, the so-called Temkin model (184), is one for ideal mixing although here the mixing of cations and anions is assumed to take place independently. Nearest neighbour interactions have been allowed for in the model of Flood et al. (185) and in Forland's extension (186).

The similarity between these models and those used for alloy systems has led various groups to apply power series expressions such as the Redlich-Kister model to these molten salts. For example Chart (187) has derived data for the component binary systems of the $KCl-CaCl_2-ZnCl_2$ system and calculated ternary phase equilibria which are in excellent agreement with experimental measurements. Similarly Oonk et al. (188-190) have derived data for a wide range of alkali halide binary systems.

A completely new model has been introduced by Saboungi and Blander (191-193) called the Conformal Ionic Solution (CIS) theory which they describe as a statistical mechanical perturbation theory. The model has been used by Pelton et al. (194,195) for a number of molten salt systems including carbonates, hydroxides and sulphates.

A problem arises where the mixing occurs between ions of different charge eg. in the $KCl-CaCl_2$ system. In the work discussed so far

components were chosen such that one mole of solution contains one mole of the ions that are mixing and this is identical to the approach recommended by Hillert et al. in their generalised lattice model of the liquid phase (196).

Molten oxide systems are particularly important types of molten salt system. Kaufman (152,155) has chosen a different model from those described above derived from a substitutional model with oxygen as a component but where the composition has been constrained to lie between binary stoichiometric oxides. These oxides were expressed in terms of a mole of atoms rather than moles of metal ions and he derived data for a wide range of systems between Cr_2O_3, MgO, Al_2O_3, Fe_2O_3, Fe_3O_4, FeO, SiO_2, and CaO using a temperature dependent two coefficient expression. For some of these pseudo binary systems e.g. CaO-SiO_2, he found that it was necessary to split the systems into two ranges of composition.

Howald et al. (197-201) have also derived data for some oxide systems. The data were represented by Redlich-Kister polynomials in terms of the proportions of the metal ions e.g. proportions of the $NaO_{0.5}$ in the system $NaO_{0.5}$-SiO_2. They also found that the CaO-SiO_2 system was too complex to fit with one expression. The CaO-SiO_2 system has also been represented with power series expressions by Kaestle and Koch (202) and Lumsden (203).

The problems found in representing the data for some of these oxide systems implies the need for a closer examination of the structure of these phases. Attempts to do this will be described later.

k) Metal-Salt Systems

The liquid phase for metal-salt systems eg. in sulphide systems is especially difficult to model thermodynamically. Attempts have been made to represent the data with power series or equivalent expressions (161)

but the large number of coefficients required makes this approach of little use.

The two most useful approaches to understanding the data for these systems have been the associated species model (204-228) and a sublattice model with vacancies (229-235). Measured data for these liquid phases are often characterised by an abrupt change in the activity of one of the components and a sharp minimum in the Gibbs energy function such as is shown in Fig. 3.9. The compositions of these abrupt changes often seem to correspond to the composition of a solid phase which itself exhibits a range of homogeneity.

The associated solution model, has been much used over the last few years. It postulates that the phase consists of distinct molecular aggregates rather like the gas phase which shows similar dramatic changes in thermodynamic properties at certain compositions. In the case of the liquid phase the various species would interact with one another.

As an example, Sharma and Chang (204) for the Cu-S system proposed the existence of Cu_2S species in addition to the elemental species of copper and sulphur. Species of Cu_2S were chosen because the thermodynamic properties of the liquid phase changed abruptly at about this composition. For an overall composition x_{Cu} and x_S the model postulates that some of the copper and sulphur atoms combine to form species of Cu_2S. If the fractions of the species are y_{Cu_2S}, y_S and y_{Cu}, it can be shown that:

$$y_{Cu} = x_{Cu} - 2\, y_{Cu_2S}\, x_S \qquad \text{and} \qquad y_S = x_S - y_{Cu_2S}\,(1-2x_S)$$

For this overall composition the relative amounts of the various species are not defined directly but depend upon the affinity of the elements for forming the associated species. These relative amounts must be calculated by some iterative procedure in order to find the

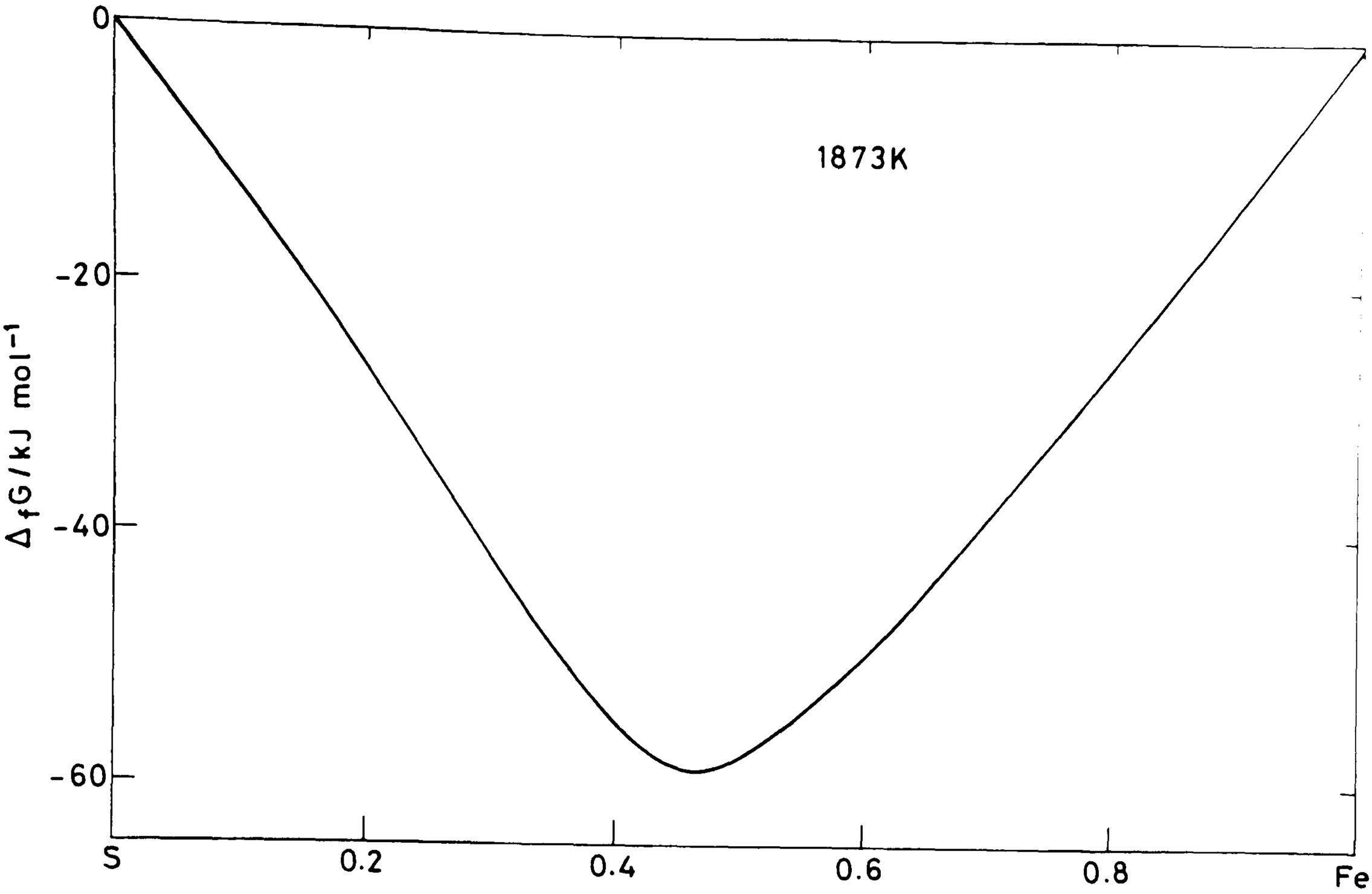

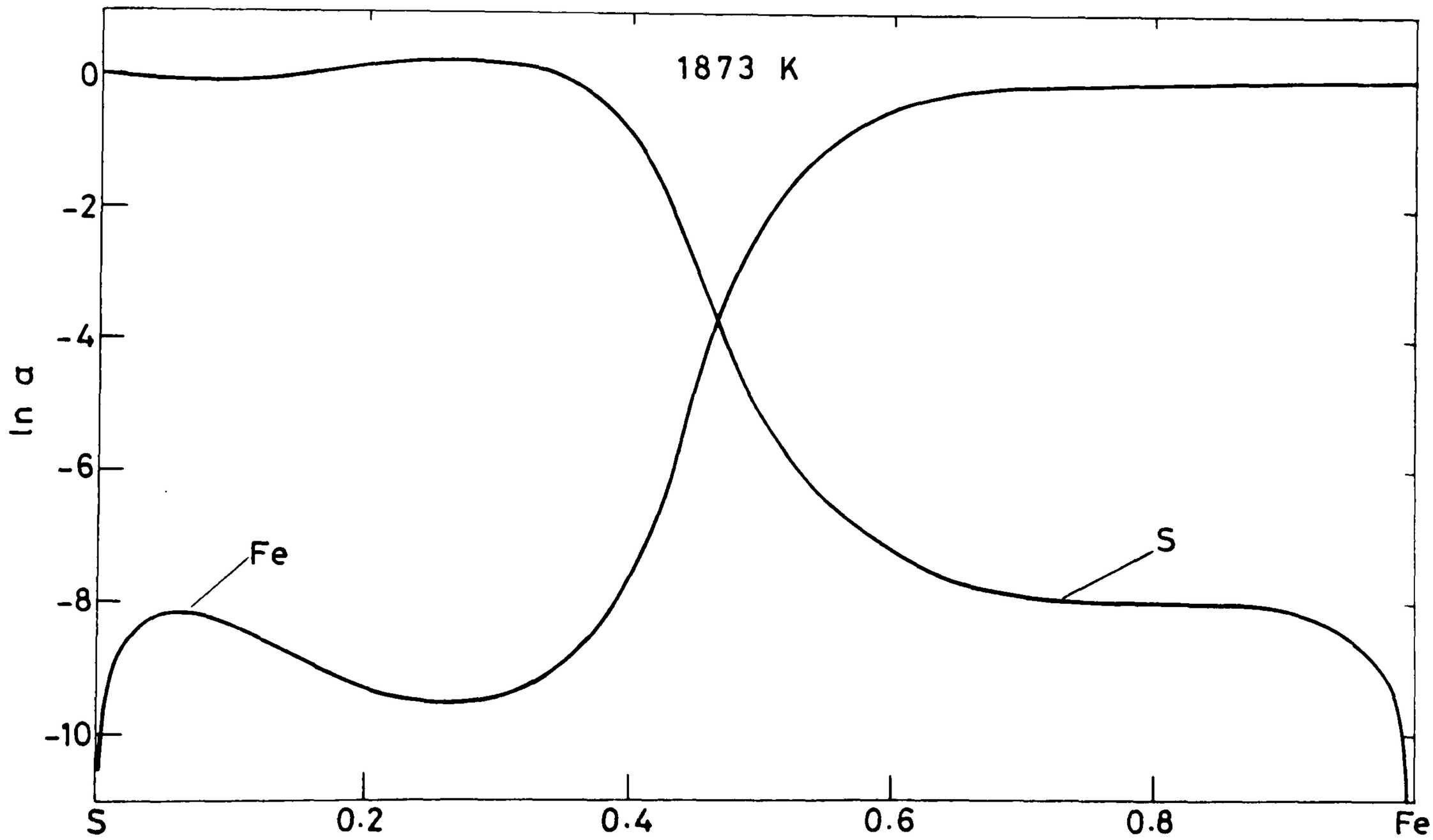

Fig 3.9 Curve for Gibbs energies of formation and logarithm of the activity for 1873 K for compositions in the Fe-S system calculated from data of Sharma and Chang.

conditions which give the minimum Gibbs energy of formation. This can be calculated as the sum of terms for the formation of the associated species and the normal expression for a ternary system with random mixing and interactions between the species, the latter being expressed by a Redlich-Kister power series.

The concept of postulating associate species in condensed solution phases was introduced and developed a number of years ago (205-208) but it was Jordan (209-211) who first used this for metallic systems. The model, which has been reviewed by Gerling et al. (212) has been very successful for representing the thermodynamic data for the liquid phase in a number of systems (204-227). It has also been used to represent the thermodynamic data for solid phases (218,228) including those traditionally represented by a substitutional model.

The application of a sublattice model to high affinity liquids was suggested by Hillert et al. (176,196,229-233) and Brebrick (234) and extended in this present work (see chapter 8 and ref. 235). Here the approach is directly analogous to the models used for condensed compound phases which exhibit wide ranges of homogeneity and abrupt changes in the thermodynamic properties similar to those observed for the liquid phase. The use of this model implies that for these systems some aspects of the solid lattice structure are retained on fusion.

The sublattice model was first tested by Hillert and Staffansson for the liquid phase in the metal rich portion of the Fe-S (229) and Mn-S (230) systems and to calculate the metal rich part of the Fe-Mn-S system (231). Here they assumed that the liquid phase consisted of two sublattices with an equal number of sites. The first sublattice was completely filled with metal atoms while the second sublattice consisted of sulphur atoms and vacancies.

Recently the model was extended by Fernandez Guillermet et al. (232,233) to represent the liquid phase for the whole of the Fe-S

system. For this, vacancies were introduced into the metal sublattice in addition to the sulphur sublattice. The Gibbs energy for a composition in the phase is expressed as the sum of three terms - the first for the Gibbs energies of formation of pure compounds formed by filling each of the sublattices with its constituents. Hence there are four compounds FeVa, FeS, VaS and VaVa. The second term is in two parts to represent the ideal mixing of the constituents in each of the two sublattices. The third term represents the interactions between the different constituents on the sublattices. The details of this expression will be shown in a chapter 8. Also it will be demonstrated how this approach has been used and extended to extrapolate data into the Fe-Cu-Ni-S liquid phase. For a given composition the vacancy concentration is not defined and a process of iteration must be used to find the condition which gives the lowest Gibbs energy.

Recently Hillert et al. (196) have suggested a new model for representing the data for the liquid phase. For the Fe-S system for example there would no longer be the same number of sites in the two sublattices. Instead the ratio of the number of sites would be determined by a condition of electroneutrality between the ionic constituents of the sublattices. In addition the new model excludes vacancies from the metal sublattice which now consists simply of Fe^{2+} ions but introduces sulphur atoms on the sulphur sublattice in addition to S^{2-} and negatively charged vacancies.

This new model has two particularly interesting features. Firstly it was shown that as the system develops lower affinity the expression for the Gibbs energy approaches that for a substitutional solution. Secondly for a binary system the expression for the Gibbs energy is identical to that derived for an associated solution provided that the associate species contain one atom only of the electronegative element.

1) Silicate Systems

It was pointed out earlier that for certain oxide systems, in particular silicates, the power series approach derived for an essentially substitutional solution is not well suited to representing the thermodynamic data adequately. For these complex systems certainly, the use of an incorrect model cannot allow us to extrapolate binary data into multicomponent systems with any confidence. The success of the associated solution model and the multiple sublattice model in representing data for sulphides and other systems has implied that they could be used for molten silicate systems. As yet the multiple sublattice model has not been tested. Attempts to use the new model for the liquid phase derived by Hillert et al. (196) would be of great interest.

The associated solution model has been used with some success by Bottinga and Richet (236) and by Goel et al. (228) for the Fe-O-SiO_2 system. Goel et al. introduced species of Fe, FeO, $FeO_{1.5}$ and SiO_2 and the data for these species and the interaction between them gave remarkably good agreement over the whole system. However a large number of parameters is required for this model and it should not be thought of as an assessment but rather as a very good correlation of the observed properties.

Many other models have been developed to represent the thermodynamic data through a close examination of the structure of silicates. In these models it is a generally accepted principle that every silicon atom is tetrahedrally surrounded by oxygen atoms. Two basic mechanisms can be considered as limiting cases. In very basic slags ie. slags with low silica content, the structure can be thought of in terms of M^{2+}, O^{2-} and SiO_4^{4-} (orthosilicate) ions. This is the approach introduced by Flood and

Knapp (237) and the thermodynamic data can be thought of in terms of the formation of the orthosilicate ion and the random distribution of the O^{2-} and SiO_4^{4-} anions. The addition of more silica leads to the formation of more complex silicates. At the silica rich side of the system ie. for acidic slags one could expect the mechanism of Fincham and Richardson (238) to operate whereby one oxide anion breaks down a bridge formed by another oxygen atom joined to two silicon atoms.

In a number of these silicate systems there is immiscibility between basic and acidic slags e.g. in the $FeO-SiO_2$ and $CaO-SiO_2$ systems where the metal oxide typically dissolves in the silica up to about 5%. In general there is always considerably higher solubility of silica in the metal oxide. In some systems, e.g. $Al_2O_3-SiO_2$ there is complete miscibility between basic and acidic slags where it is believed the aluminium atom can substitute directly for silicon atoms.

Flood and Knapp (237) extended the description of very basic slags which consists of M^{2+}, O^{2-} and SiO_4^{4-} ions by including other polymeric anions. From a study of the $PbO-SiO_2$ system they concluded that the addition of $Si_3O_9^{6-}$ and $Si_6O_{15}^{6-}$ anions mixing ideally resulted in a good representation of the thermodynamic data for compositions up to 60 mole % SiO_2. This approach was adopted recently by Bjorkman et al. (239,240) for the $PbO-SiO_2$ and $Fe-O-SiO_2$ systems using more complexes than suggested by Flood and Knapp. The description of Bjorkman et al. is limited to basic slags.

Other models for liquid silicates have been reviewed by Gaskell (241) and Bottinga et al. (242) which take their basis from the work of Toop and Samis (243). This is in itself an extension of the work of Fincham and Richardson (238) mentioned earlier. The breakdown of an oxygen bridge by an oxide ion can be written in terms of:

$$2\,O^- = O^0 + O^{2-}$$

where O^0, O^- and O^{2-} represent bridging oxygen atoms, singly bonded oxygen atoms and free oxide ions. According to Toop and Samis an equilibrium constant can be written for this reaction:

$$k = \frac{[O^0]\,[O^{2-}]}{[O^-]^2}$$

where k is a constant for a given temperature and a given metal ion ie. independent of composition of the melt and the complex ions involved. The Gibbs energy of formation from pure liquid components would be written by:

$$\Delta_f G = \frac{1}{2}\,[O^-]\,R\,T\,\ln(k)$$

which implies ideal mixing between the three types of oxygen atom. This simple model gave good quantitative agreement with experimental information and led Toop and Samis to perform calculations in the $CaO-FeO-SiO_2$ system at $1600^{\circ}C$.

This approach was extended by Masson (244-246) who applied polymer theory to the breakdown of the silicon-oxygen-silicon chains. Kapoor (247-249) developed the polymerisation approach using statistical thermodynamics and used an approach of Guggenheim (93) for the configurational entropy of mixing rather than the Temkin expression.

A completely new approach was adopted by Yokokawa and Niwa (250) who considered a silicate melt in terms of a basic sublattice of oxygen atoms or ions with silicon atoms occupying a proportion of the tetrahedrally coordinated sites, the rest remaining vacant. This model was adopted by Borgianni and Granati (251,252) for use in Monte Carlo calculations.

A more empirical approach was adopted by Lin and Pelton (253) who also considered the melt as a lattice. According to this treatment polymeric anions are not considered directly since the configurational

entropy is calculated simply from the distribution of the different types of 'structural units' (silica tetrahedra, O^{2-} ions and oxygen bridges) throughout the melt. Furthermore the enthalpy change for the breakage of oxygen bridges was considered to be independent of the composition of the melt. The results they obtained were in excellent agreement with those determined experimentally. This model has two great strengths. Firstly the polymeric ions, although not treated explicitly, can be examined for each calculation through analysis of the probabilities of various ionic configurations. Secondly unlike all the other structural models discussed, the approach of Lin and Pelton is applicable to the whole composition range from basic to acidic slags.

More recently Blander and Pelton (254) have devised a new empirical model for slags as an attempt to devise a method for analysing data for multicomponent systems. The model, an 'ad-hoc modification of the quasi-chemical theory' appears to have been very successful.

Summary

A number of different approaches have been used to model thermodynamic data for metallurgical systems. Some of these have been described in this chapter. This area of work is assuming greater industrial importance and can be expected to develop significantly over the next few years as industry becomes more demanding in its needs for data.

CHAPTER 4

The Role of the Computer in Thermodynamics

Introduction

The principles involved in the use of thermodynamics for the calculation of phase equilibria and many of the models which can be used to represent thermodynamic data for various phases are now well established. However the calculations themselves, except for the simplest cases are quite complex and generally require the use of a computer in order to search for the compositions and amounts of the competing phases which give the lowest Gibbs energy. Many different types of computer program have been developed for the calculation of phase equilibria as will be described below. Computers are now also becoming essential for the reverse process when, during the critical assessment of thermodynamic data, parameters for the thermodynamic models are derived from known equilibrium properties. Large data files are often required for both the critical assessment of data and the calculation of complex equilibria and this has led to a third use for computers ie. that in the storage of data in computer based databanks which ultimately leads to greater reliability and efficiency.

Calculation of Equilibria

One of the first computer databanks developed for the storage of thermodynamic data was the NPL MTDATA system (255-258) which has been offered on-line within the UK for a number of years over the telephone or a packet switching network, and now forms part of the CSIRO system within Australia (259). Until 1980 it also formed part of the MANLABS system within the USA (260). It contains data for pure condensed

substances, gaseous species and dilute solutions, and in the on-line service is used to tabulate, for various temperatures, the thermodynamic properties of pure substances or the change in these properties during a chemical reaction. Originally the databank was designed for a mainframe computer but it has now been modified at NPL for implementation on microcomputers (261).

Since then similar databanks have been developed elsewhere. In Canada, Pelton, Bale and Thompson (262,263) in Montreal have constructed the FACT databank service, which is available on-line throughout North America, and offers rather more extensive facilities than that developed by Alcock and Goetze (264) in Toronto. In Moscow the IVTAN group have been augmenting their data compilations with a computerised databank while within Western Europe, equivalent databanks have also been developed in Uppsala (265), Grenoble (266), Aachen (267-269) and Harwell. These last three groups are now working with NPL and others within Europe to construct a joint database and on-line databank system through the organisation SGTE.

Although tables or plots of the change in thermodynamic properties for chemical reactions are useful in predicting simple types of equilibria more sophisticated software must be used for complex equilibria. One such type of calculation for multicomponent equilibria between gaseous and condensed phases is to produce a so-called Predominance Area or Pourbaix diagram such as is shown in Fig 4.1 where the partial pressure of one of the gaseous species is plotted against the temperature or the partial pressure of another species. A number of programs have been developed to calculated these diagrams, many of them linked to databank systems eg. those of Barry (270,271), Pelton and Bale (262) and Barin et al. (267,268).

More sophisticated still are the programs used to calculate equilibria, for a given overall composition, between various gaseous

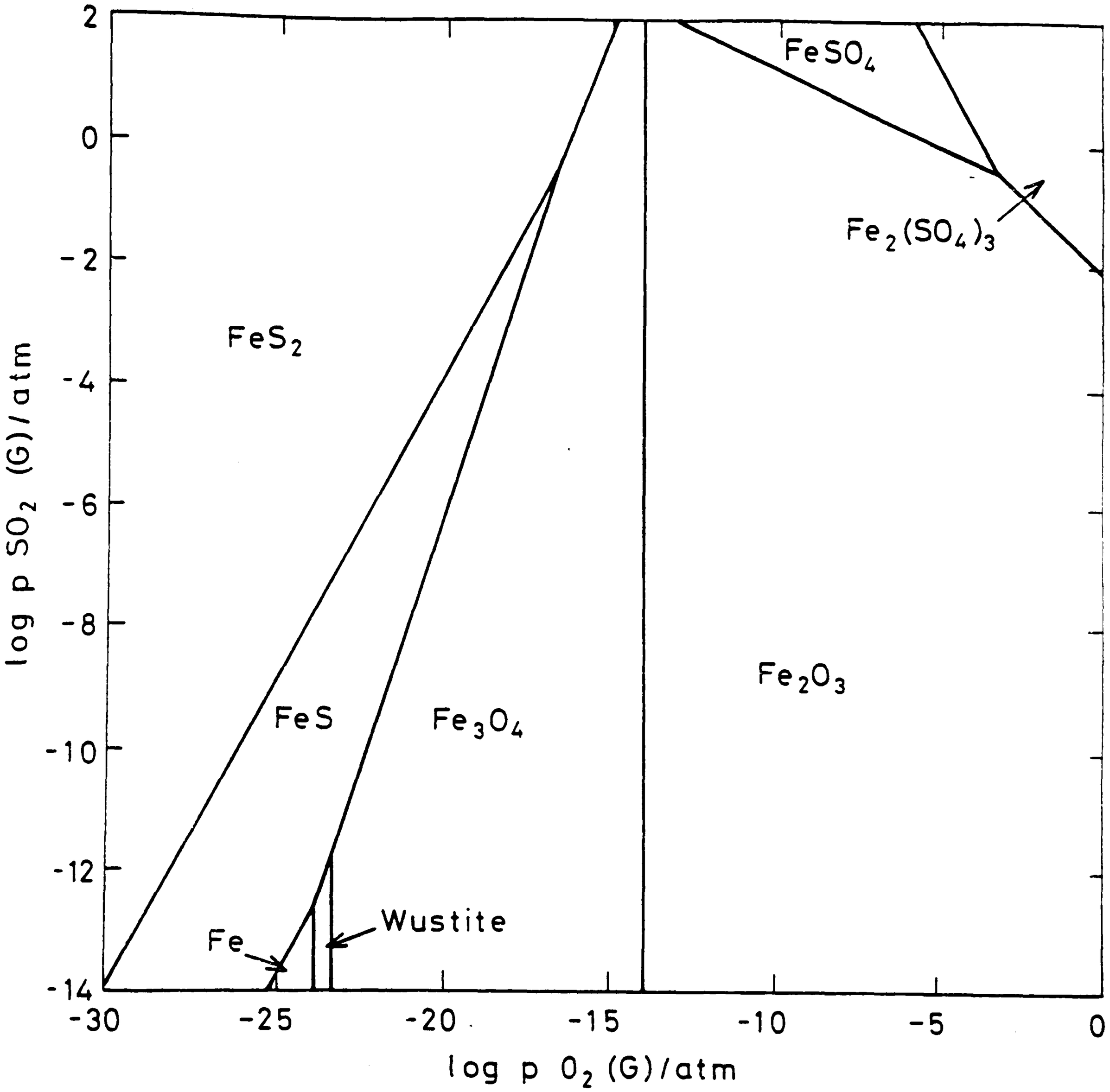

Fig 4.1 Predominance Area diagram for the Fe-S-O system calculated by Barry showing regions of stability for the various condensed phases as a function of the partial pressures of SO_2 and O_2.

species and condensed phases. This problem is often known as Gibbs energy minimisation although the mathematical formalism can be expressed in other equivalent ways. The search for reliable and efficient programs has attracted many groups of scientists and mathematicians and many of these programs have been reviewed by Smith (272,273) and van Zeggeren and Storey (274).

Perhaps the most widely used program and certainly one of the most versatile is Eriksson's SOLGASMIX. This program was originally designed for equilibria between a gaseous phase and condensed stoichiometric phases (275,276) but it has been extended to include condensed solution phases (277). It has also now been linked to many substance databanks eg. by Gallagher (269), Turnbull (278), Thompson (279) and by Dinsdale to allow these calculations to be performed quickly and in a routine fashion. SOLGASMIX has also been adapted for speciation calculations within dilute aqueous solutions and their equilibria with a gas and stoichiometric solid phases. In this program, SOLGASWATER (280), water is assumed to be at unit activity. The versatility of SOLGASMIX is perhaps best shown in its use in the program SOLGASMIX-REACTOR (281) when predicting, in detail, the behaviour of an industrial process. SOLGASMIX-REACTOR in many respects reflects the ultimate aim for these types of calculation. By breaking down a complex industrial process into a number of levels and linking the thermodynamic data to details of the process SOLGASMIX-REACTOR can be used to predict conditions to obtain the maximum yield or the minimum consumption of energy.

Another example of where these types of calculations can be linked directly to an industrial process is in the prediction of the optimum conditions for Chemical Vapour Deposition and the growth of crystals. One such program for these calculations has been developed by Nolang and Richardson (282-287) in Uppsala consisting of a database with packages for the calculation of predominance area diagrams, transport flux and

chemical equilibria. It has been used, for example, to improve growth of crystals of yttrium iron garnet. Similar calculations have been performed by Bernard et al. (17).

At the same time as programs were being developed to calculate the equilibria between gas phase species and stoichiometric compound phases, interest was also being focussed on routines and programs for the calculation of multicomponent phase diagrams for condensed solution phases especially alloys. Much of the early work in this field was done by Kaufman and his colleagues (46) who developed computer programs and also many of the datasets commonly used.

Other early work has been carried out by Ansara et al. (79,288) and Counsell et al. (289). The work of Counsell et al. was extended by Dinsdale (15,173) who developed an on-line databank system, ALLOYDATA, containing critically assessed binary and ternary thermodynamic data linked to software for the calculation of multicomponent phase diagrams. Lukas (290) has also made significant contributions towards routines for the calculation of phase equilibria.

More recently great advances have been made at the Royal Institute of Technology in Stockholm under the direction of Hillert. Sundman (291) has developed a sophisticated subroutine package, Gibbs Energy System, for calculating the Gibbs energy and its derivatives for a very general representation of thermodynamic data involving multiple sublattices. This subroutine package is used in particular by the program POLY developed by Jansson (292) for the calculation of binary and multicomponent phase equilibria for alloys. POLY is undoubtedly the most sophisticated program of its type available at present. Both the Gibbs Energy System and POLY are in turn used as subroutine packages to a third program developed by Agren (293-295) for the prediction of phase transformations and diffusion related equilibria.

The division between the two types of programs, one designed to

calculate essentially the distribution of species within the gas phase or aqueous solution and the other to calculate the equilibrium between different condensed solution phases is somewhat arbitrary although the two problems make different demands in terms of the numerical analysis routines. Furthermore under certain circumstances it is important to solve both kinds of problem simultaneously e.g. corrosion of superalloys by gaseous environments, and consequently programs have now been written to perform these more complex calculations. Of particular note is the program of Eriksson, SOLGASMIX, which has recently been used for calculations of multicomponent alloy phase diagrams (296). Eriksson himself has recently reported most ambitious calculations, carried out using SOLGASMIX in conjunction with Saxena, of equilibrium mineral assemblages on cooling down a gas of solar composition (297,298). The aim was to further understanding of the formation of planets and meteorites. Here the phases involved included a gas phase, liquid and solid alloy phases, various solid oxide phases of variable composition, a carbide solution phase and various stoichiometric phases such as sulphides, nitrides and hydrides. They included 14 elements in their calculations. SOLGASMIX has been used here to calculate equilibria in a nine component alloy system as will be shown in chapter 7.

Jansson (299,300) has now developed a new and extremely general program POLY-II based upon the ideas of Hillert (301,302) and linked to the Gibbs Energy System. This program has been designed to include speciation calculations for the gas phase in addition to the multicomponent phase equilibrium calculations involving alloys. Present tests seem to indicate that performance for speciation calculations is inferior to that of SOLGASMIX. More recently Hodson (303) at NPL has developed a program MULTIPHASE to allow simultaneous calculations involving the gas phase, aqueous phase and various condensed non ideal solution phases. The program is extremely reliable and efficient.

To date none of these sophisticated types of programs have been linked to an extensive database comprising, for example, data for alloys, aqueous solutions, gases and other phases of importance. This is one of the major aims of the organisation SGTE and it is planned to have such a databank available on-line throughout the world by early 1986. Although it is recognised that the major users of such a service would be the member organisations of SGTE the databank is being designed to encourage industries and universities to use extensively. To this end, SGTE has made major efforts to design the outer appearance of the databank so that the user finds it easy and convenient to use and can find his way through the system with a minimum of tuition.

Critical Assessment of Data

The computer is also rapidly becoming completely indispensible for the critical assessment of thermodynamic data. For pure substances, the computer has been used mainly for the calculation of the thermodynamic properties of gas phase species from statistical mechanics and subsequently fitting the heat capacity data to a convenient power series expression. More recently, work has begun, pioneered by Pedley et al. (304) to optimise enthalpies of formation from measurements of the thermodynamic data (e.g. partial pressures, equilibrium constants, formation measurements) for the various reaction networks that relate substances to one another. As an example a consistent set of the enthalpies of formation at 298.15 K and thermal functions (energy and heat capacity data) of gaseous metal oxides have been obtained. Ambitious plans are now under consideration to incorporate all such experimental data for pure substances into a computer database. By linking this database to Pedley's program any new experimental measurements can immediately result in a revised set of thermodynamic

data.

For condensed solution phases eg. in alloy systems, the role of the computer in the critical assessment of data is even more important than for pure substances. Firstly the data for condensed solution phases are normally more complicated than data for gases requiring the use of a variety of different models for representation as shown in the last chapter. The computer is ideal for repetitive calculations of the thermodynamic properties for these phases. Secondly the types of experimental data are more diverse including many types of measurements of thermodynamic properties and phase equilibria in addition to intuitive information that the assessor may need to provide. The computer would normally be used to calculate the agreement between the measured values and those calculated from a set of parameters often involving quite complex calculations of equilibria. The computer can then minimise these errors and find automatically the best set of parameters.

Normally this type of program is used for the assessment of data for binary systems. However it is important to realise that data are required for phases not just in the regions where they are stable but generally across the whole of the system as shown in the last chapter. An optimisation type of assessment program is ideal for this where, for example, the experimental extension of a phase, stable in only one binary system, into a ternary system can be used to derive data for this phase for the other two binary systems.

The assessment of thermodynamic data direct from phase diagram information was first suggested by Hiskes and Tiller (305-307), Rao et al. (308) and Chiotti et al. (309). Since then others, in particular Lukas et al. (310-312), Boyle et al. (313), Jansson (314,315), Sundman (316), Pelton and Bale (317) and Oonk et al. (188,318-321) have developed computer procedures to carry out such calculations. The work

of Lukas is particularly important since the programs are very portable, widely used and allow choice of a number of models to represent the data. Versions of the program are now available for binary, ternary and quaternary systems.

It is also worth noting the program of Jansson, PARROT (314,315), which is connected to the suite of programs referred to earlier including POLY, Gibbs Energy System and POLY-II. These provide a highly flexible framework for all assessment work.

Conclusions

The role of the computer in thermodynamics is now so well established that it is difficult to contemplate a time when computers were not available. In the future this role can only increase as large databases are constructed containing not just critically assessed data but also the raw experimental data. The computer also has enormous potential as a teaching aid. If all the tiresome and errorprone arithmetic were collected within a reliable computer program, a student would be able to concentrate on the basic principles of the subject and their application to industrial processes. It has even been suggested (302) that in the future little thermodynamics as such need be taught other than the general principles and how databanks could be interrogated to solve particular equilibrium calculations. Certainly we can look forward to the most complicated equilibrium calculations being carried out with great reliability and ease. Furthermore the work of Agren (293-295), Eriksson (281) and Nolang and Richardson (283-287) points the way to the use of the computer and thermodynamic data for modelling problems occurring in practical chemical and metallurgical industry. Certainly the incorporation of databank packages in expert systems (322) will be of utmost importance.

CHAPTER 5

Development of Computational Procedures for the Calculation of Binary Phase Diagrams

Introduction

Over the last few years the computer aided calculation of phase diagrams from thermodynamic data has become widely accepted as a most useful tool to assist in the solution of industrial problems. This has led to the search for reliable and efficient procedures to facilitate these calculations. Many of the programs developed so far have been designed for use on main-frame computers. With the advent of desk top or even hand held microcomputers it is also important to develop compact programs.

Discussed in this chapter is the mathematical basis for a program used to calculate binary phase diagrams automatically. It is hoped that these techniques will be of benefit in the critical assessment of thermodynamic data and also highlight some major problems to be overcome for the automatic calculation of multicomponent phase diagrams. In particular a very compact and reliable method has been developed to calculate efficiently binary phase equilibria for a fixed temperature. It is shown how this method can be extended to predict the changes in the phase boundaries with variation of temperature. Finally a generalised procedure is described which can be used to calculate all the stable phase boundaries in a binary system for a given temperature. Through use of this procedure binary phase diagrams can be calculated automatically.

Often in the past direct calculation of phase equilibria in binary

systems was avoided and instead the Gibbs energies of formation for the different phases involved in the alloy system were plotted out and the phase boundaries determined manually by using the well known common tangent construction (45) shown in Fig 5.1. The phase diagram could be built up by following this procedure for a number of temperatures. In order for a computer to calculate phase diagrams automatically, it would need to search for conditions either giving these common tangents or the minimum Gibbs energy of formation of a composition within the two phase region. Of course, these two methods are equivalent as will be shown later.

A number of methods for calculating equilibria in binary alloy systems have been reported. The basic principles have been described by Ansara (79), Hillert (323,324), Oonk (318,325) and Kaufman and Bernstein (46). Hillert (324) also suggested use of a particular method based upon the partition function and the partial molar Gibbs energies. Gale and Davis (326) used a steepest descent algorithm to solve a pair of non-linear equations and calculate the composition of the alloy phases in equilibrium. Kaufman and Bernstein (46), Gaye and Lupis (327,328), Tomiska et al. (329) and Henig et al. (330) have solved similar equations based on the partial molar Gibbs energies by using the Newton-Raphson procedure (page 56). Gaye and Lupis moreover developed their technique to facilitate calculations over a range of temperatures. Pelton et al. (331) have developed a stepwise iteration procedure to calculate common tangents, a method which they have extended to calculate multicomponent equilibria. Nussler (332) has used the simplex Nelder and Mead procedure (333) programmed by Counsell et al. (289) while Jansson (292) has included the facility for the calculation of binary phase diagrams within his sophisticated program POLY.

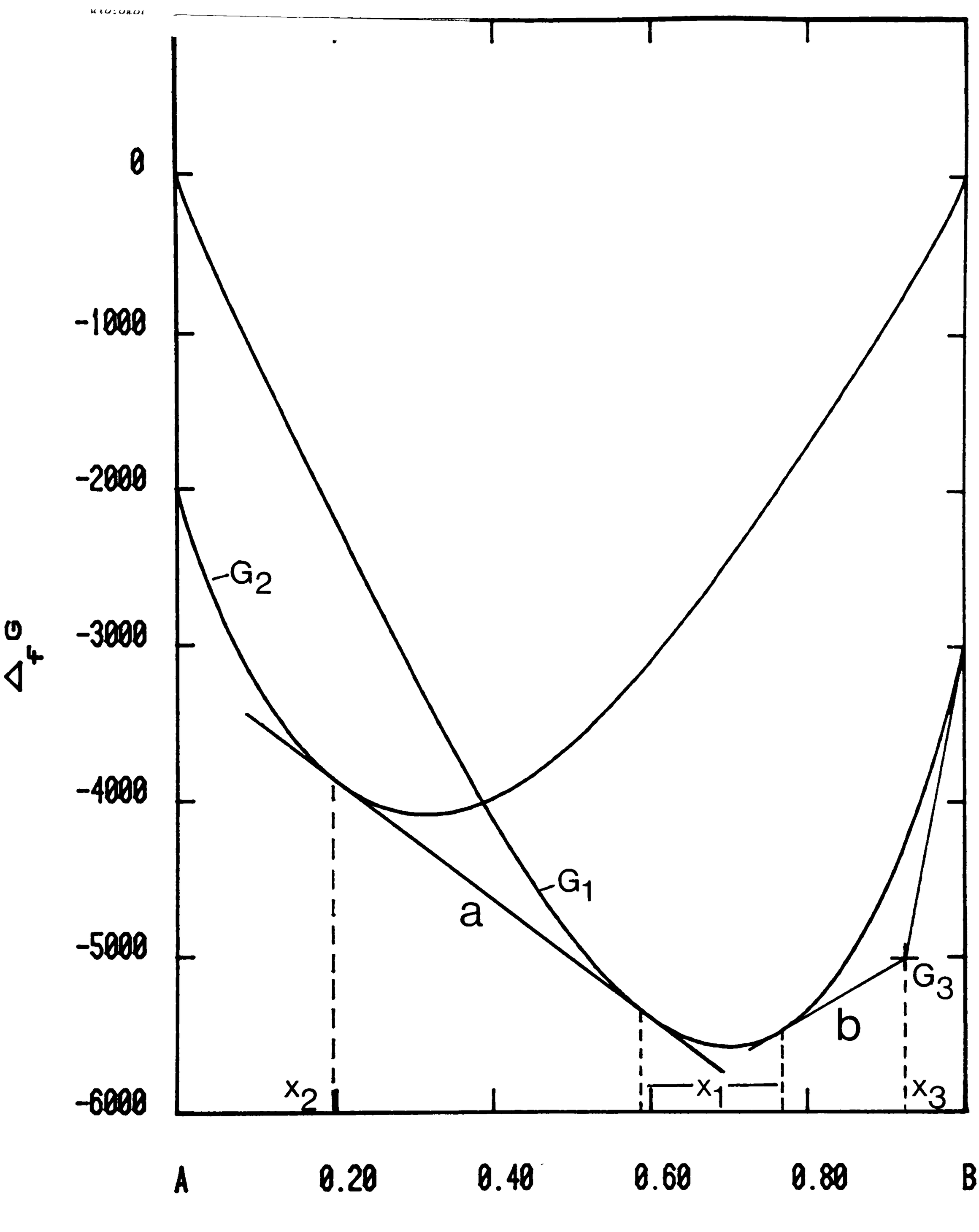

Fig 5.1 Determination of phase boundaries by common tangent construction a) between two intersecting solution phases and b) between a solution phase and a stoichiometric compound phase (Gibbs energy represented by a cross).

Recent developments in computer technology have made it possible to perform these types of calculation on microcomputers or even on hand calculators. Consequently it is tempting to develop very efficient computational methods which also require relatively small amounts of software. This present work is carried out in the light of this need.

Calculation of two phase equilibria

a) Common tangent construction

The basic condition for an alloy to be in chemical equilibrium is for its Gibbs energy to be at a minimum. Consequently if an alloy is chosen which, at equilibrium, lies in a two phase region, the most stable state will be that one which gives rise to the lowest Gibbs energy taking into account all possible states that could be formed by varying the compositions of the coexisting phases.

Consider first the example of a hypothetical alloy system A-B. Fig 5.1 shows the variation of the Gibbs energies of formation G_1 and G_2 of two intersecting solution phases as a function of their compositions of element B, x_1 and x_2 at a temperature T. Consider an overall alloy composition shown by x on the figure and assume that at equilibrium the alloy consists of a mixture of the two solution phases.

Let the proportion of the first solution phase in the mixture be α. The proportion of the second solution phase will therefore be $1-\alpha$. By equating the overall composition x with the total quantities of element B in the two phases one obtains the well know lever-rule.

$$x = \alpha x_1 + (1-\alpha)\, x_2$$

which on rearrangement gives:

$$\alpha = \frac{x - x_2}{x_1 - x_2}$$

In a similar way, the Gibbs energy of formation G of this composition x is given by

$$G = \alpha G_1 + (1-\alpha)G_2 \qquad (1)$$

or

$$G = \frac{(x - x_2)}{(x_1 - x_2)} G_1 + \frac{(x_1 - x)}{(x_1 - x_2)} G_2$$

$$= \frac{(x - x_2)}{(x_1 - x_2)} (G_1 - G_2) + G_2$$

This shows that, diagrammatically, the value of G corresponding to the composition x will lie on a straight line between G_1 and G_2.

For the system to be in equilibrium the Gibbs energy of formation, which is a function of both x_1 and x_2, must be at a minimum. Therefore

$$\left(\frac{\partial G}{\partial x_1}\right)_{x_2} = \left(\frac{\partial G}{\partial x_2}\right)_{x_1} = 0$$

Differentiating equation (1)

$$\left(\frac{\partial G}{\partial x_1}\right)_{x_2} = \alpha \frac{dG_1}{dx_1} + G_1\left(\frac{\partial \alpha}{\partial x_1}\right)_{x_2} + (1-\alpha)\frac{dG_2}{dx_1} - G_2\left(\frac{\partial \alpha}{\partial x_1}\right)_{x_2}$$

$$\therefore \left(\frac{\partial G}{\partial x_1}\right)_{x_2} = \alpha \frac{dG_1}{dx_1} + (G_1-G_2)\left(\frac{\partial \alpha}{\partial x_1}\right)_{x_2}$$

since G_2 is independent of x_1.

But $$\alpha = \frac{x - x_2}{x_1 - x_2}$$

$$\left(\frac{\partial \alpha}{\partial x_1}\right)_{x_2} = -\frac{(x - x_2)}{(x_1 - x_2)^2} = -\frac{\alpha}{(x_1 - x_2)}$$

$$\therefore \left(\frac{\partial G}{\partial x_1}\right)_{x_2} = \alpha \frac{dG_1}{dx_1} - \frac{\alpha (G_1 - G_2)}{(x_1 - x_2)}$$

ie. since for equilibrium $$\left(\frac{\partial G}{\partial x_1}\right)_{x_2} = 0$$

$$\frac{dG_1}{dx_1} = \frac{(G_1 - G_2)}{(x_1 - x_2)} \qquad (2)$$

Similarly

$$\frac{dG_2}{dx_2} = \frac{(G_1 - G_2)}{(x_1 - x_2)} \qquad (3)$$

These two conditions indicate that the gradients of the two Gibbs energy curves at x_1 and x_2 respectively should not just be equal but also equal to the gradient of the line joining the two Gibbs energy curves. This is also the condition that there should be a common tangent between the two curves as indicated by line a in Fig 5.1.

Consider now the equilibrium between the first solution phase, whose Gibbs energy, G_1, is shown as a function of the composition of element B, x_1, and the stoichiometric compound of composition x_3 and Gibbs energy G_3. In this case x_3 and G_3 cannot vary and so that, while the equivalent of equation (2) still is valid, equation (3) is not relevant. Again therefore the condition for equilibrium is that the line joining the Gibbs energy of the solution phase at x_1 to that of the compound should be a tangent to the solution phase curve at x_1 as shown by the line b in Fig 5.1.

Therefore the conditions for equilibria both between a solution phase and a stoichiometric compound and between two solution phases can be expressed diagrammatically in terms of tangents and this is a very simple way for determining phase boundaries. The method does however have certain disadvantages. The Gibbs energy curves have to be calculated and plotted for all the phases involved in the system which requires a certain amount of computation. Furthermore the point of common tangency cannot be measured accurately to within perhaps 1 atomic per cent in a typical case. Moreover while the common tangent construction can be very useful for binary systems, there is no simple analogous method for multicomponent systems. A more reliable method for calculating phase boundaries would be to calculate the conditions for the minimum Gibbs energy of formation directly.

b) Calculation of common tangents by Newton-Raphson Method

The method has its basis in Newton's law of successive approximations. Consider Fig 5.2 which shows a function F of a variable z and we need to find a value of z for which F becomes zero.

An initial guess z_0 is made for which the function $F(z_0)$ and its derivative $F'(z_0)$ are evaluated. As shown in Fig 5.2, by using $F(z_0)$ and $F'(z_0)$ a new estimate of the required value z_1 can be made as the point where the tangent at z_0 crosses the axis F = 0.

since $$F'(z_0) = \frac{F(z_0)}{(z_0 - z_1)}$$

$$z_1 = z_0 - \frac{F(z_0)}{F'(z_0)} \qquad (4)$$

In the same way a new value of z can be derived from z_1

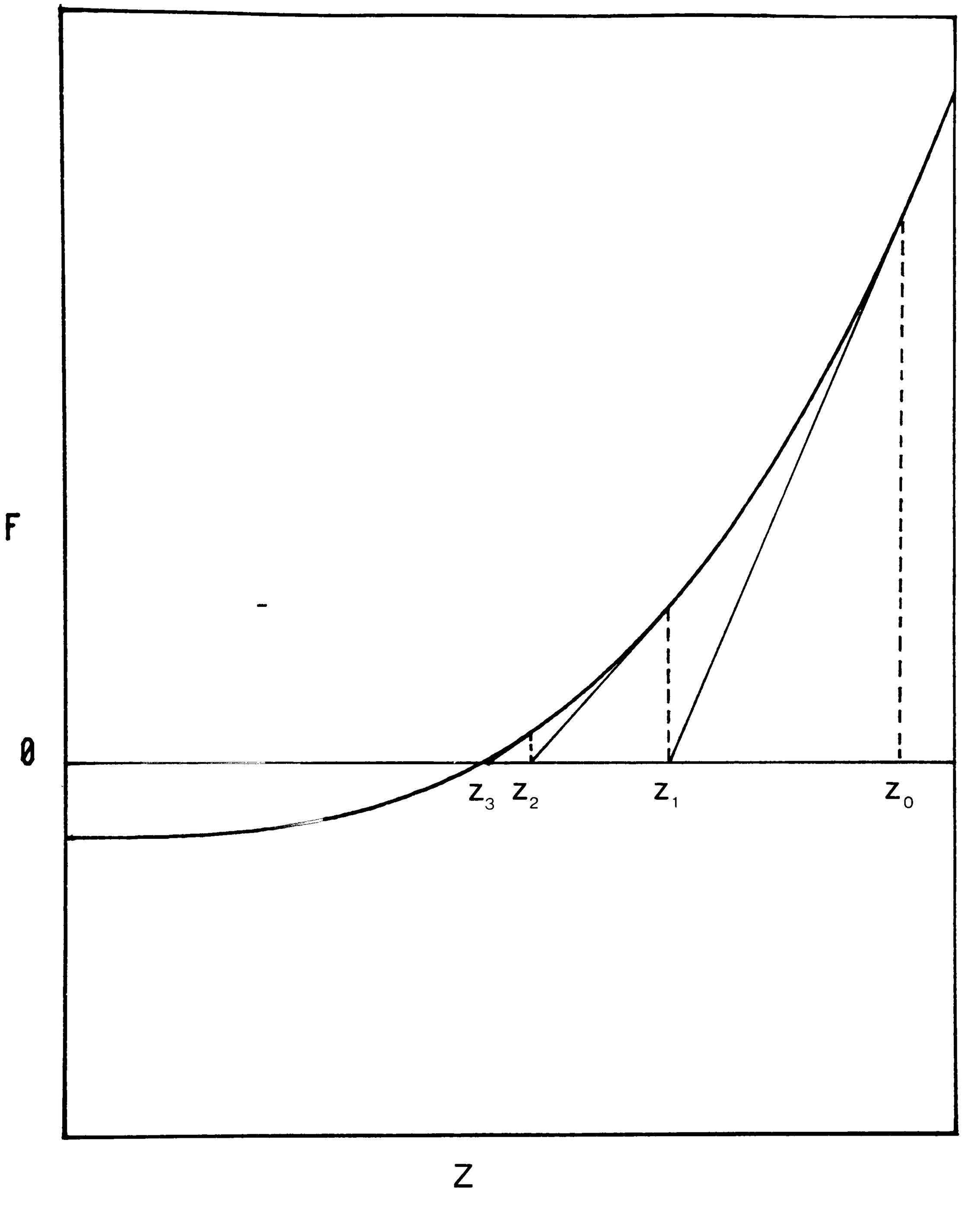

Fig 5.2 Newton's law of successive approximations where a value of z is determined for which the function F is zero.

$$z_2 = z_1 - \frac{F(z_1)}{F'(z_1)}$$

and so on until the required accuracy has been obtained.

The equilibrium between a solution phase and a stoichiometric compound can be treated in precisely this way. Here the function F can be chosen as:

$$F = \frac{dG_1}{dx_1} - \frac{(G_1 - G_2)}{(x_1 - x_2)} \qquad (5)$$

and we require the value of x_1 for which F = 0. Differentiating equation (5)

$$F' = \frac{dF}{dx_1} = \frac{d^2G_1}{dx_1^2} - \frac{1}{(x_1-x_2)}\frac{dG_1}{dx_1} + \frac{(G_1-G_2)}{(x_1-x_2)^2} = \frac{d^2G_1}{dx_1^2} - \frac{F}{(x_1-x_2)} \qquad (6)$$

Equations (4), (5) and (6) provide a method for evaluating the equilibrium between a compound and a solution phase.

For the equilibrium between two solution phases there are two variables and two functions to set to zero (ie. to satisfy equations 2 and 3). However these variables are not linked to one other by any constraints and it is possible to solve this problem in a completely analogous way to that used above.

Suppose that the problem involves two independent variables y and z. These two compositions are varied in turn rather than simultaneously, as shown in Fig 5.3. The line A-B represents the initial guess for the equilibrium between the two phases, composition A for the first solution phase and composition B for the second solution phase. Firstly the composition of the first Gibbs energy curve G_1 is varied from A using the first function resulting in a new composition C. Then the second function is used to vary the

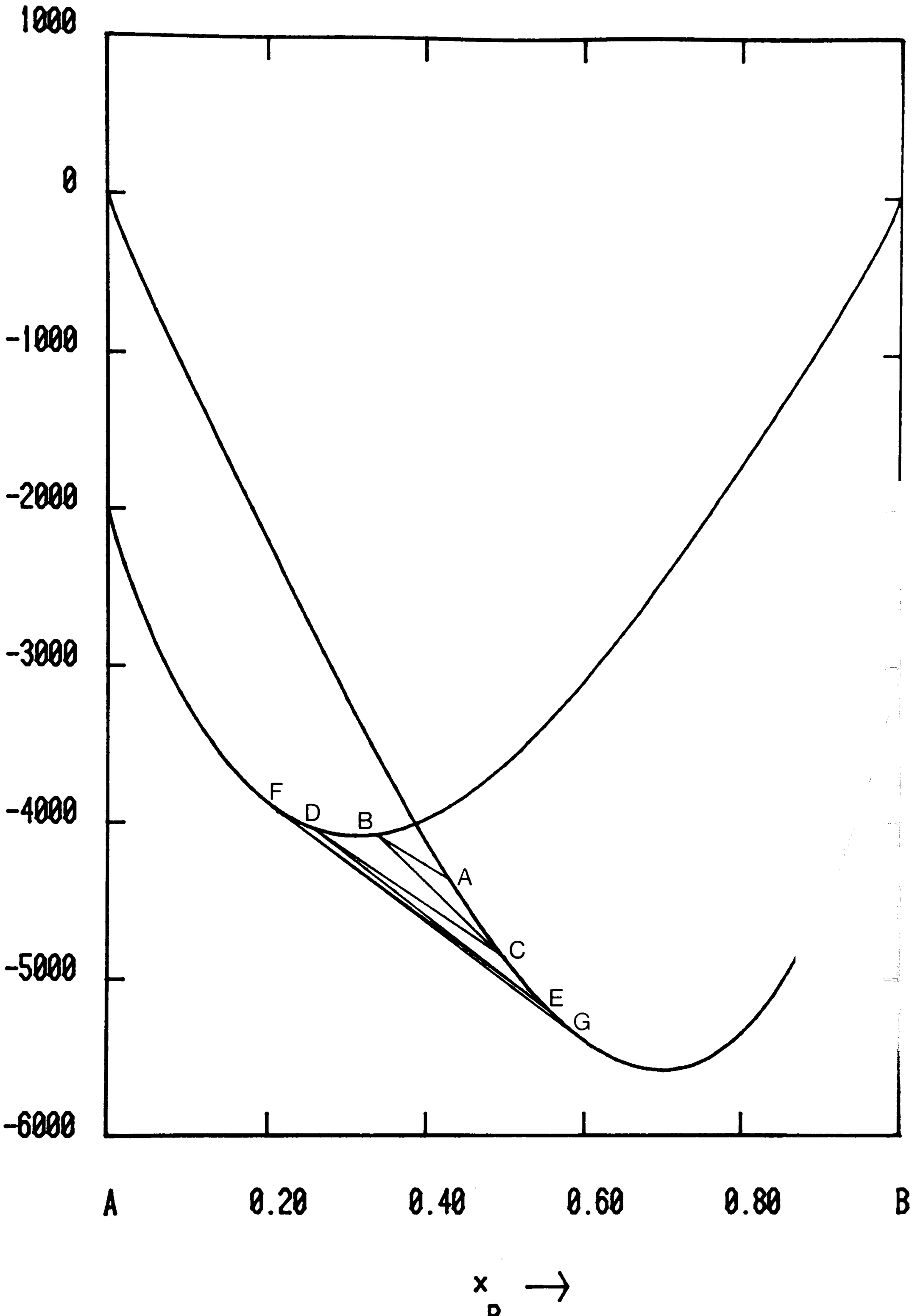

Fig 5.3 Application of Newton's law of successive approximations to the equilibrium between two solution phases where each composition variable is varied in turn.

composition of the second Gibbs energy curve G_2 from B to result in a new composition D. These two steps are repeated until the required accuracy has been obtained.

Suppose that the conditions for equilibrium are

$$F_1(y,z) = 0 \qquad \text{and} \qquad F_2(y,z) = 0$$

The derivative of F_1 with respect to y at constant z for the compositions (y_0,z_0) can be designated by $[F_1'(y_0,z_0)]_z$. Similarly the derivative of F_2 with respect to z at constant y for the compositions (y_0,z_0) will be $[F_2'(y_0,z_0)]_y$.

The Newton-Raphson procedure of equation (4) can be represented by:

$$y_1 = y_0 - \frac{F_1(y_0,z_0)}{[F_1'(y_0,z_0)]_z} \qquad z_1 = z_0 - \frac{F_2(y_1,z_0)}{[F_2'(y_1,z_0)]_y} \qquad (7)$$

$$y_2 = y_1 - \frac{F_1(y_1,z_1)}{[F_1'(y_1,z_1)]_z} \qquad \text{etc}$$

As for equations (5) and (6)

$$F_1 = \frac{dG_1}{dx_1} - \frac{(G_1 - G_2)}{(x_1 - x_2)} \qquad (8)$$

and

$$F_1' = \frac{d^2G_1}{dx_1^2} - \frac{F_1}{(x_1-x_2)} \qquad (9)$$

Similarly

$$F_2 = \frac{dG_2}{dx_2} - \frac{(G_1 - G_2)}{(x_1 - x_2)} \qquad (10)$$

and

$$F_2' = \frac{d^2G_2}{dx_2^2} - \frac{F_2}{(x_2-x_1)} \qquad (11)$$

These equations can be used in the procedure in (7) to evaluate the equilibrium.

The methods just described were tested by translating into a computer program. They were found to be extremely reliable, very efficient and compact. Indeed the programs were so compact that they

fitted comfortably onto a SHARP PC1251 hand held microcomputer.

Calculation of the change in phase boundaries with temperature

It is common for these phase diagram calculations to be carried out over a range of temperatures and clearly it is more efficient from the computational aspect if results from a given temperature can be used to generate a good starting point for the calculations for the next temperature. One possibility would, for example, be to take the results of the calculation as they stand. However very little extra information is needed to derive a value for the slope of the phase boundary with change in temperature and this can lead to a much better starting value. This is similar to the procedures outlined by Gaye and Lupis (327,328) and Henig et al. (330).

Consider for example the equilibrium between a stoichiometric compound phase and a solution phase. As shown before the condition for equilibrium at a fixed temperature T is given by:

$$F = \frac{dG_1}{dx_1} - \frac{(G_1 - G_2)}{(x_1 - x_2)} = 0$$

Now this function F is both a function of composition and temperature and for small changes Δx_1 and ΔT we can write:

$$F = \frac{dF}{dT}\Delta T + \frac{dF}{dx_1}\Delta x_1$$

But since for the temperature T, F = 0

$$\Delta x_1 = -\Delta T \frac{dF}{dT} \Big/ \frac{dF}{dx_1}$$

The value of dF/dx_1 has already been determined during the calculation

of the equilibrium whilst dF/dT can easily be obtained from knowledge of the variation of the thermodynamic data with temperature.

In a similar way, for the equilibrium between two solution phases we have two equilibrium conditions both of which are functions of x_1, x_2 and T.

ie. $$F_1 = \frac{dG_1}{dx_1} - \frac{(G_1 - G_2)}{(x_1 - x_2)} = 0$$

and $$F_2 = \frac{dG_2}{dx_2} - \frac{(G_1 - G_2)}{(x_1 - x_2)} = 0$$

For small changes in T, x_1 and x_2 we can write:

$$F_1 = \frac{dF_1}{dT}\Delta T + \frac{dF_1}{dx_1}\Delta x_1 + \frac{dF_1}{dx_2}\Delta x_2 = 0$$

$$F_2 = \frac{dF_2}{dT}\Delta T + \frac{dF_2}{dx_1}\Delta x_1 + \frac{dF_2}{dx_2}\Delta x_2 = 0$$

It can be shown that

$$\frac{dF_1}{dx_2} = \frac{F_2}{(x_1-x_2)} \quad \text{and} \quad \frac{dF_2}{dx_1} = \frac{F_1}{(x_2-x_1)}$$

which are both equal to zero since for the temperature T, F_1 and F_2 equal zero. Therefore again we obtain:

$$\Delta x_1 = -\Delta T \frac{dF_1}{dT} \Big/ \frac{dF_1}{dx_1}$$

$$\Delta x_2 = -\Delta T \frac{dF_2}{dT} \Big/ \frac{dF_2}{dx_2}$$

The quantities dF_1/dx_1 and dF_2/dx_2 are known from the equilibrium calculations while dF_1/dT and dF_2/dT can be derived from a knowledge of the temperature dependence of the thermodynamic data.

Using these expressions good initial guesses can be derived for

equilibrium calculations at a new temperature. This will speed up the overall calculation of the phase diagram.

Procedure for the calculation of stable phase boundaries at a fixed temperature

There have been three main methods used for calculating a complete binary phase diagram. Kaufman (46) has preferred to calculate all possible equilibria over a wide range of temperatures and then identify those equilibria which are stable. An alternative method used by Ansara (79) in his program BINAIRE is to calculate for each temperature all the stable two phase equilibria by determining the combinations of phases across the binary system which give the lowest Gibbs energy. Jansson (292) has developed a third method within his general program POLY whereby a given phase boundary is followed automatically until it is found to be unstable with respect to some new equilibrium or a pair of equilibria. These new equilibria are followed in turn. In this way all stable phase boundaries which are topologically linked can be determined.

For this work a similar approach has been adopted to that used by Ansara (79). The intersections between stable solution phases are calculated in order to define the lowest Gibbs energy curve against composition from the various individual solution phases as shown in Fig 5.4. At this stage each solution phase is scanned for pairs of points of inflection which indicate tendency towards immiscibility. The Gibbs energy of each of the stoichiometric compound phases is then compared with that of the stable solution phase at that composition. Then using the methods described in the last section, phase equilibria are calculated between the intersecting solution phases, and between

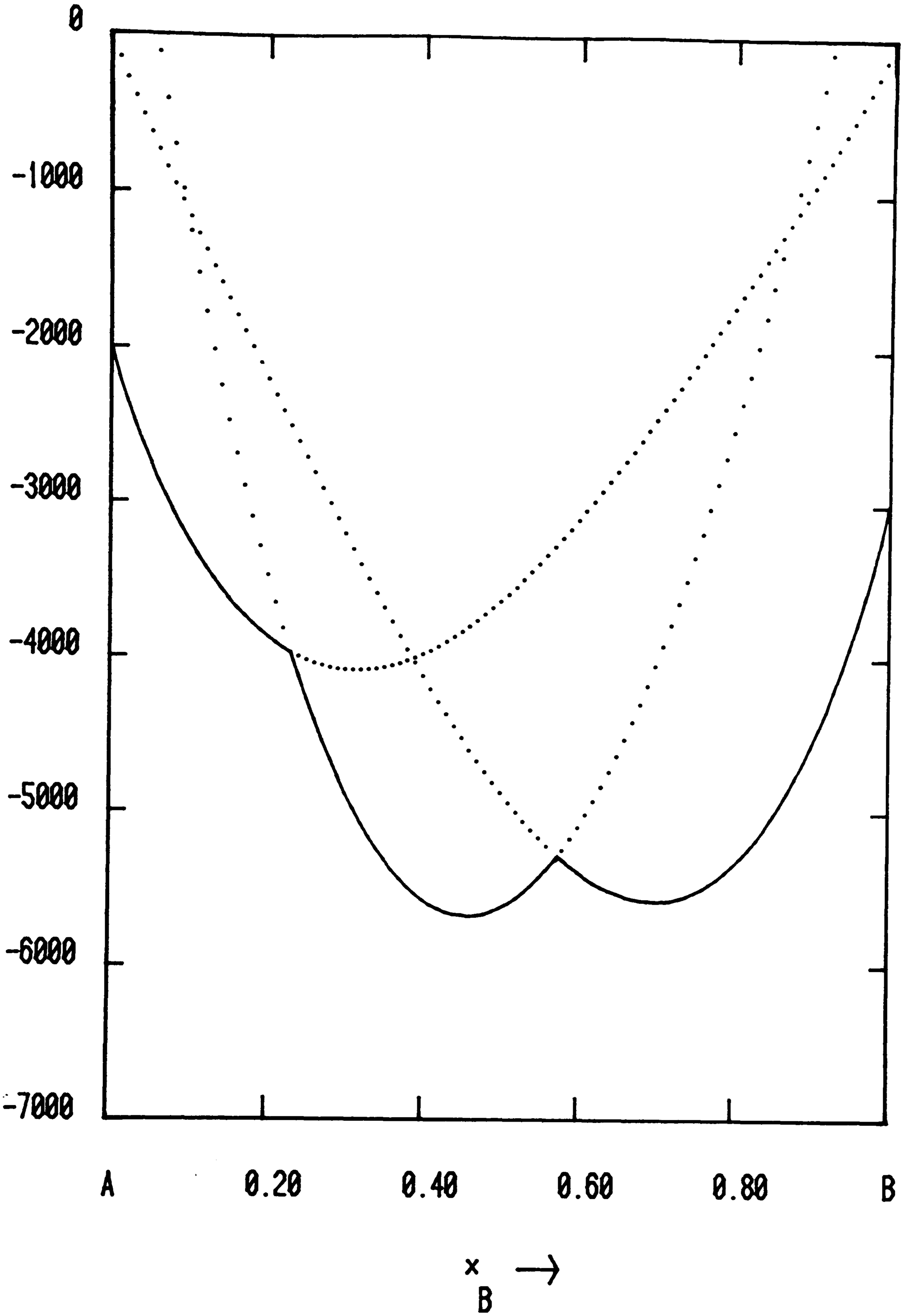

Fig 5.4 Lowest Gibbs energy profile for various intersecting solution phases.

stable compounds and the solution phase stable at that composition as shown in Fig 5.5. For each solution phase the equilibrium composition is noted. If the calculated phase boundaries for a given solution phase overlap, this phase is then unstable relative to a two phase region between the two other phases as shown in Fig 5.5. For equilibria involving stoichiometric compounds the Gibbs energy gradient is noted. If two such gradients for a given compound indicate a concave Gibbs energy envelope the compound will also be unstable as shown in Fig 5.6. New phase equilibria are then calculated and compared in turn with neighbouring equilibria until a set of consistent phase boundaries have been obtained for the whole composition range.

Any possible miscibility gaps then have to be tested against this set of equilibria. A miscibility gap is calculated for each solution phase with inflections provided that the phase had been calculated to take part in the set of stable equilibria. For each of these miscibility gaps then, the phase boundaries of this phase lying within the region of immiscibility are counted. If there are none and the phase had also been calculated to be stable within this region, the miscibility gap is stable and must be entered accordingly into the set of stable equilibria as shown in Fig 5.7. If the number of phase boundaries is found to be one the miscibility gap is metastable and furthermore, a metastable solution had previously been calculated to be stable as is shown in Fig 5.8. A new calculation of this same equilibrium is required but with the two phase region stretching across the metastable miscibility gap. Finally if two phase boundaries were found to be within the miscibility gap, the phase will no longer be stable. A new calculation of equilibrium is required between the two phases on either side of the metastable miscibility gap as shown

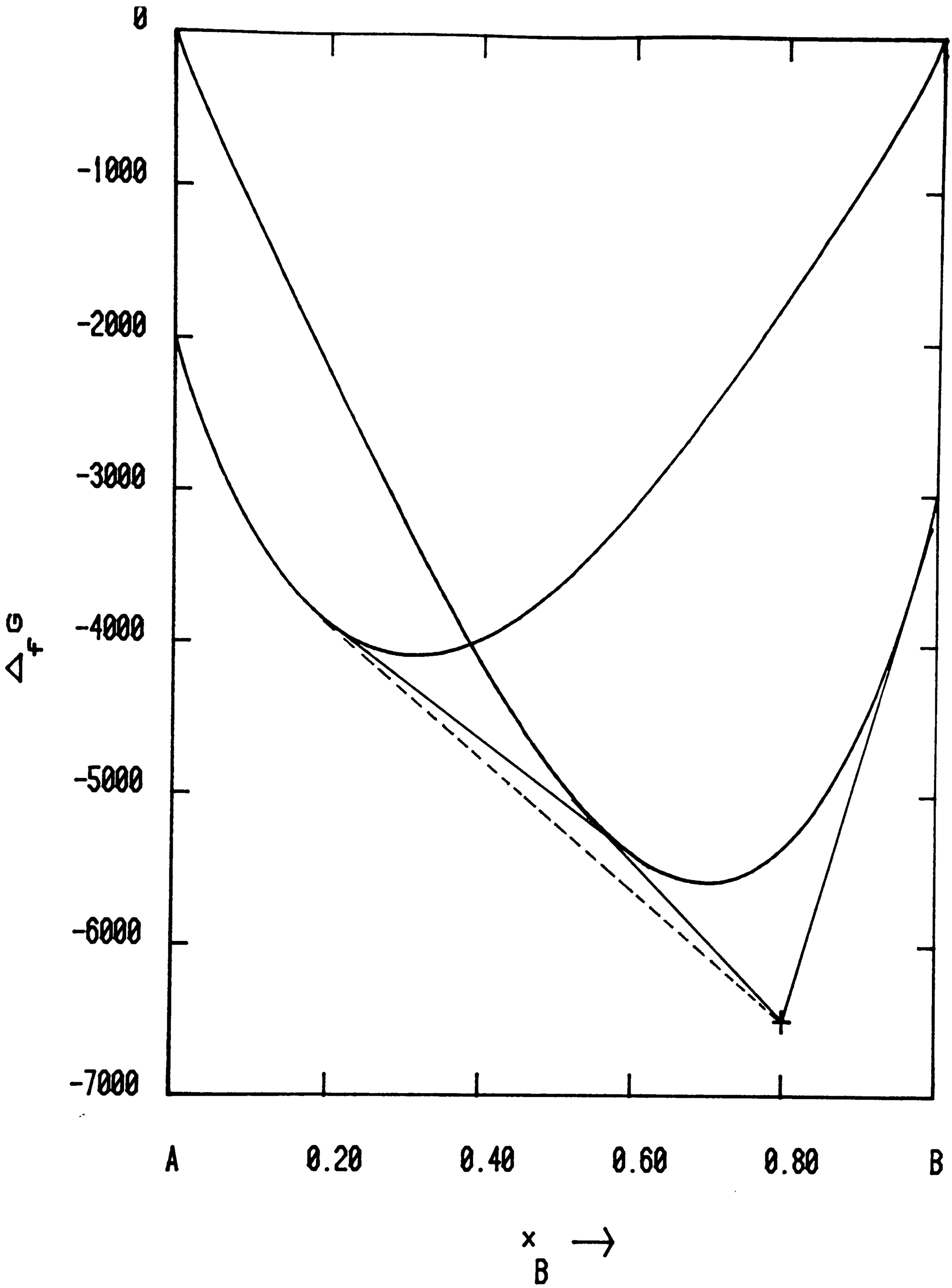

Fig 5.5 Calculation of phase equilibria between two intersecting solution phases and between a compound phase and stable solution phase. The phase boundaries for one solution phase overlap indicating that the phase is unstable relative to a two phase region.

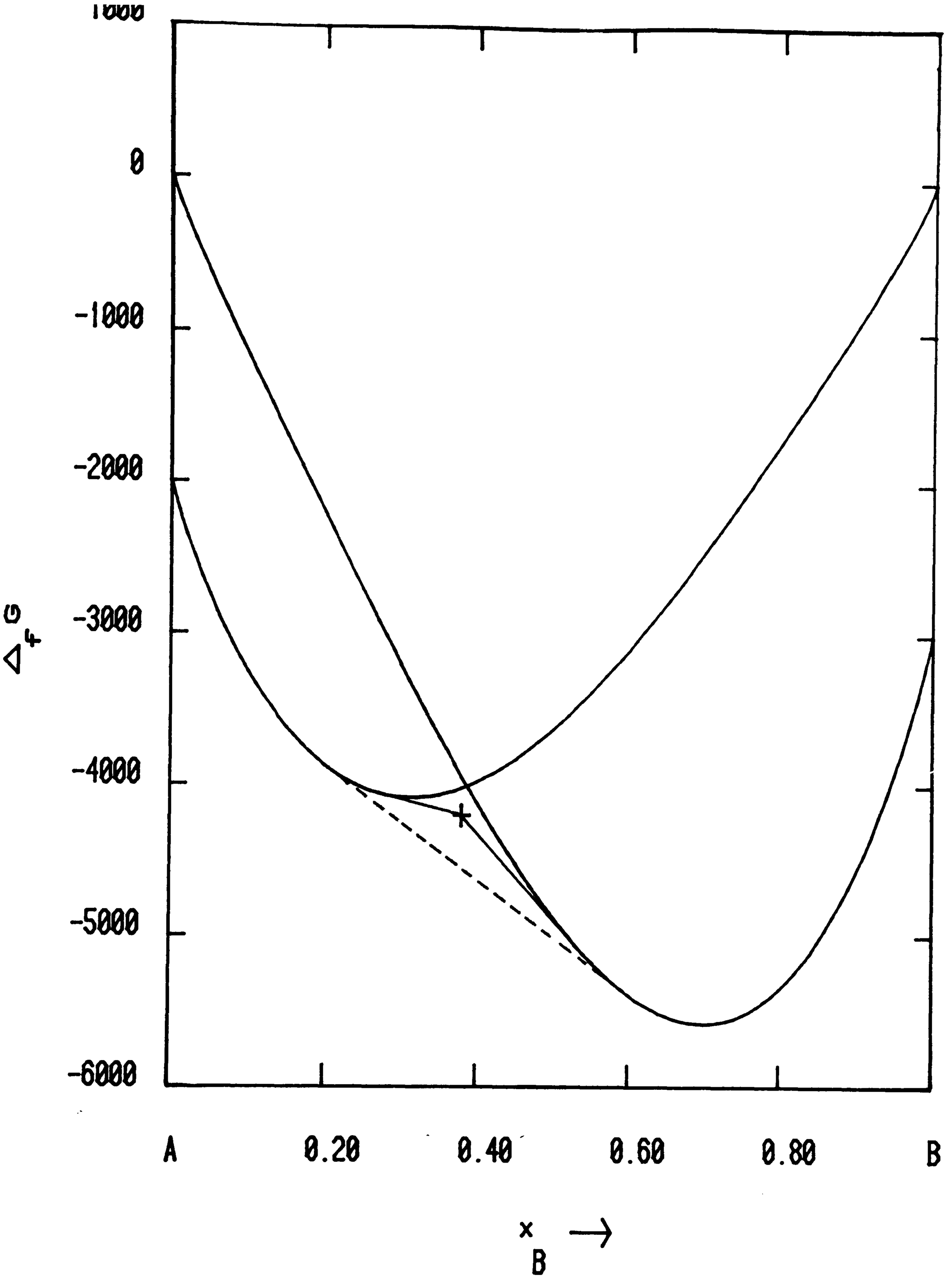

Fig 5.6 Concave Gibbs energy envelope about a stoichiometric compound phase indicating instability of the compound relative to a two phase region.

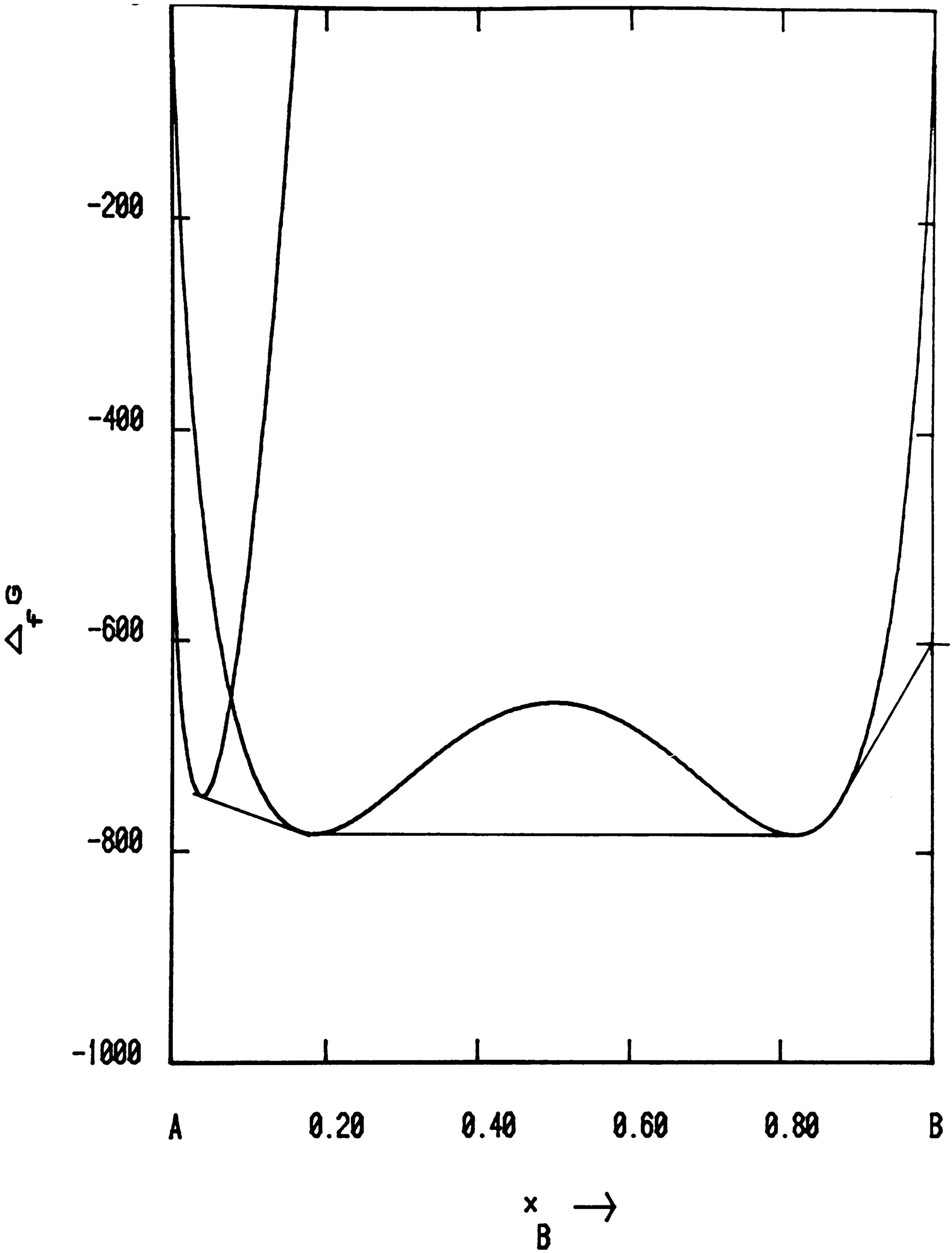

Fig 5.7 Stable miscibility gap.

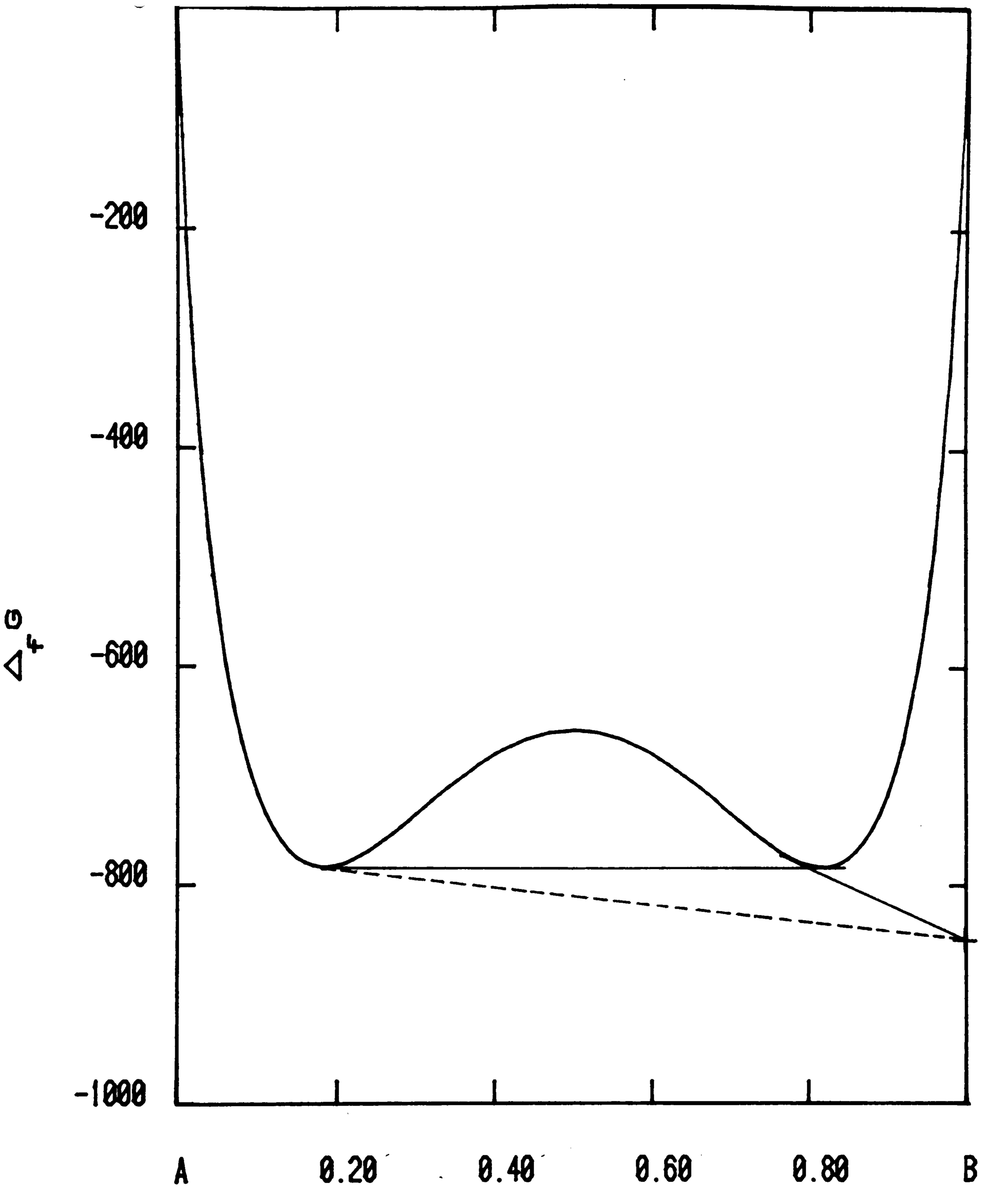

Fig 5.8 The calculated miscibility gap is metastable relative to a two phase region between this phase and another phase spanning the region of immiscibility.

in Fig 5.9. In these last two cases (Fig 5.8 and Fig 5.9) the new phase boundaries could result in an overlap of compositions for a solution phase as in Fig 5.5 or a concave Gibbs energy envelope as in Fig 5.6. This must be identified and equilibria recalculated where appropriate.

Conclusions

In principle a number of methods can be used to calculate phase equilibria in binary alloy systems. In this present work a procedure based upon the Newton-Raphson technique has been developed. The method is efficient, reliable and compact. This method has also been extended in order to predict the effect of temperature on the phase boundaries and this allows very efficient calculations of equilibria over a range of temperature. A procedure has also been developed to calculate automatically the stable phase boundaries for a binary system at a given temperature. This procedure can be repeated for a series of temperatures allowing the calculation of the whole phase diagram. Fig 5.10 and Fig 5.11 show examples of phase diagrams calculated automatically using this program.

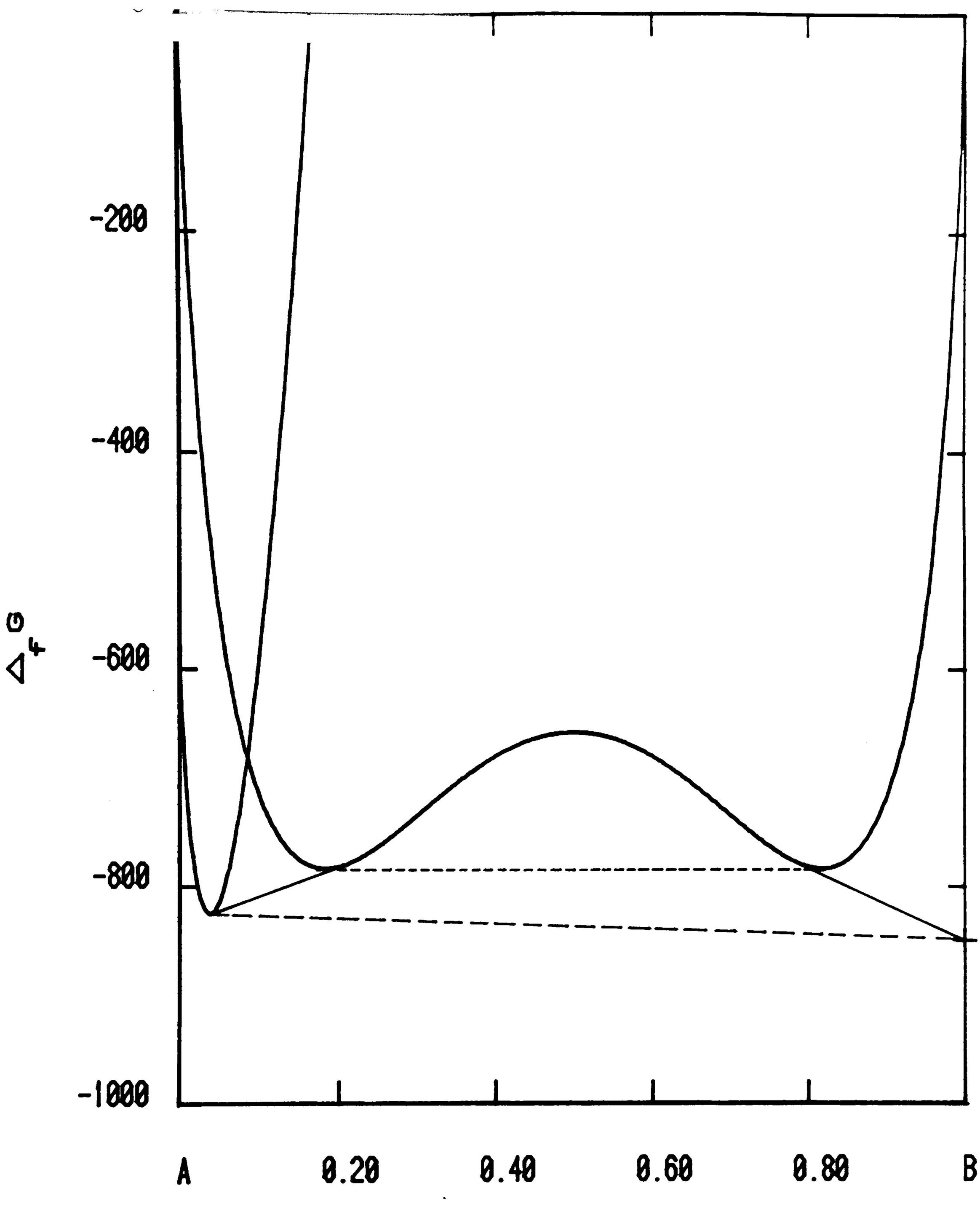

Fig 5.9 The calculated miscibility gap is metastable relative to a two phase region between two other phases spanning the region of immiscibility.

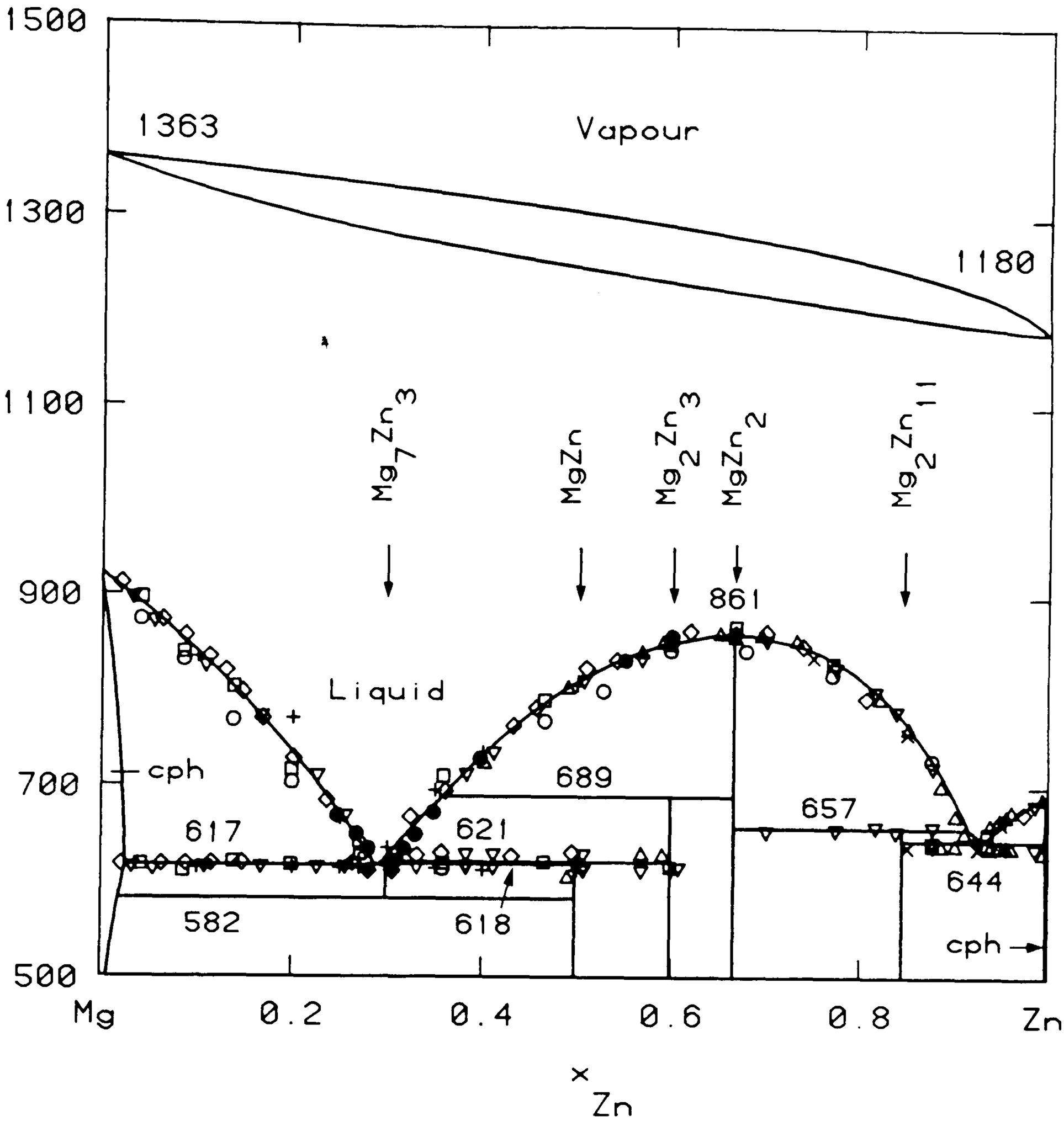

Fig 5.10 Phase diagram for the Mg-Zn system calculated automatically using the binary phase diagram program. The experimental phase equilibria have been superimposed.

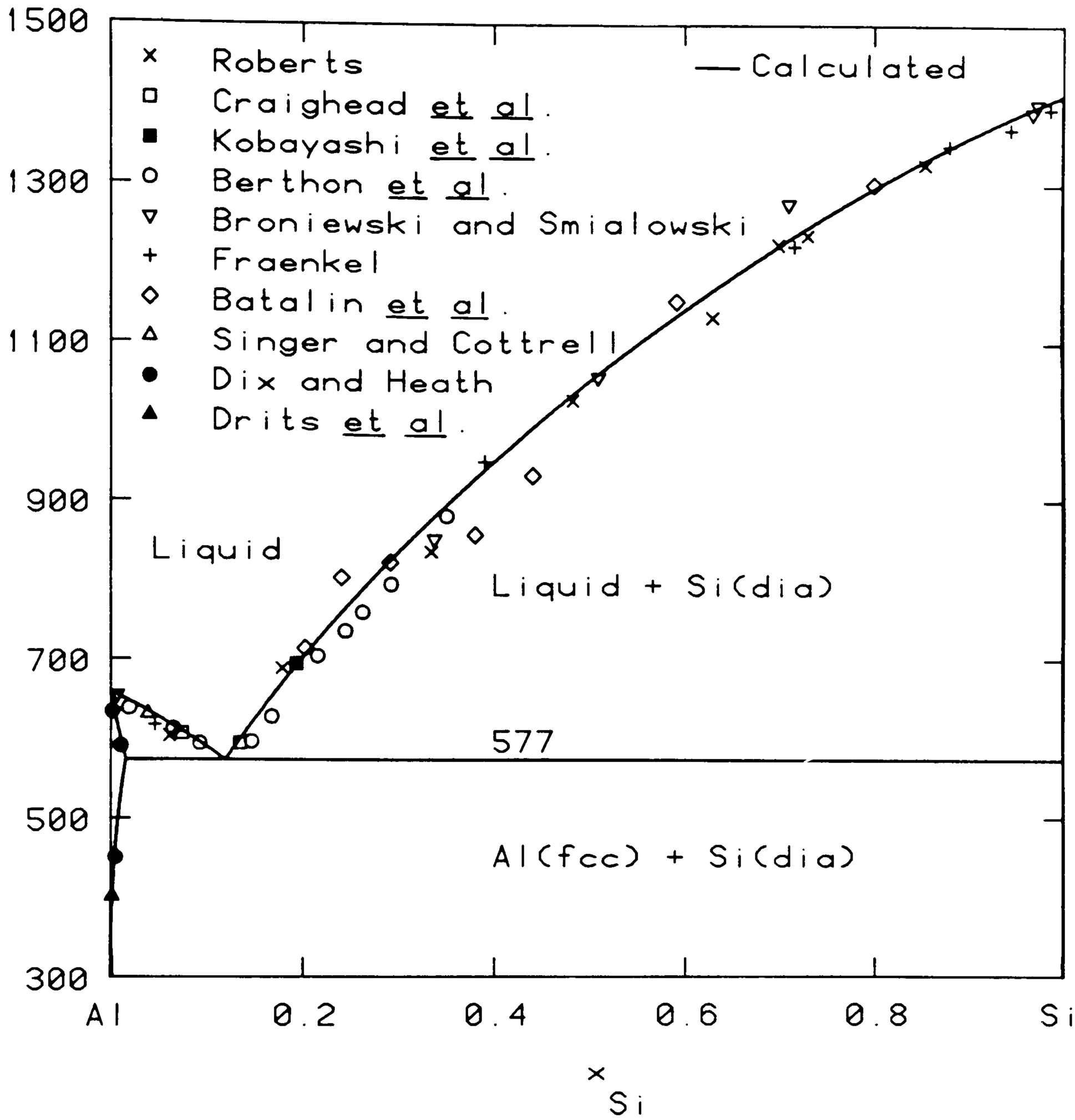

Fig 5.11 Phase diagram for the Al-Si system calculated automatically using the binary phase diagram program. The experimental phase equilibria have been superimposed.

CHAPTER 6

Thermodynamic Properties of Alloys in the Fe-Ti System

Introduction

This work was the last of a series of experimental studies on thermodynamic data for binary and ternary alloy systems of industrial importance carried out at the National Physical Laboratory. The system Fe-Ti was chosen because critically assessed thermodynamic data for this system were needed for use in the calculation of multicomponent phase diagrams (15,334). Ti is often added to stabilise stainless steels and also acts as a deoxidant. Therefore information relating to its effect on the phase diagrams of steel systems is particularly important. There had however, been very little experimental thermodynamic work done on solid alloys in this system upon which to base a critical assessment.

In addition, it was hoped to extend the range of the adiabatic calorimeter used for previous measurements (335,336) to include more exothermic alloy systems such as the Fe-Ti system. Previously the systems studied were restricted to those in which the enthalpies of formation were between about $\pm$ 8 kJ/mol.

The Fe-Ti phase diagram determined by experiment is shown in Fig 6.1 and is based on that presented in Elliott (54) but incorporates experimental work referred to in Hansen and Anderko (53) and Shunk (55), and work of Abrahamson and Lopota (337), Raub et al. (338), Nasu et al. (339), Matyka et al. (340) and Ko and Nishizawa (341).

In the work described here, the enthalpy of formation was determined for 5 different compositions: for x_{Ti}=0.05 which at high temperatures is in the bcc phase field, for x_{Ti} = 0.10 and 0.20 which lie in the two

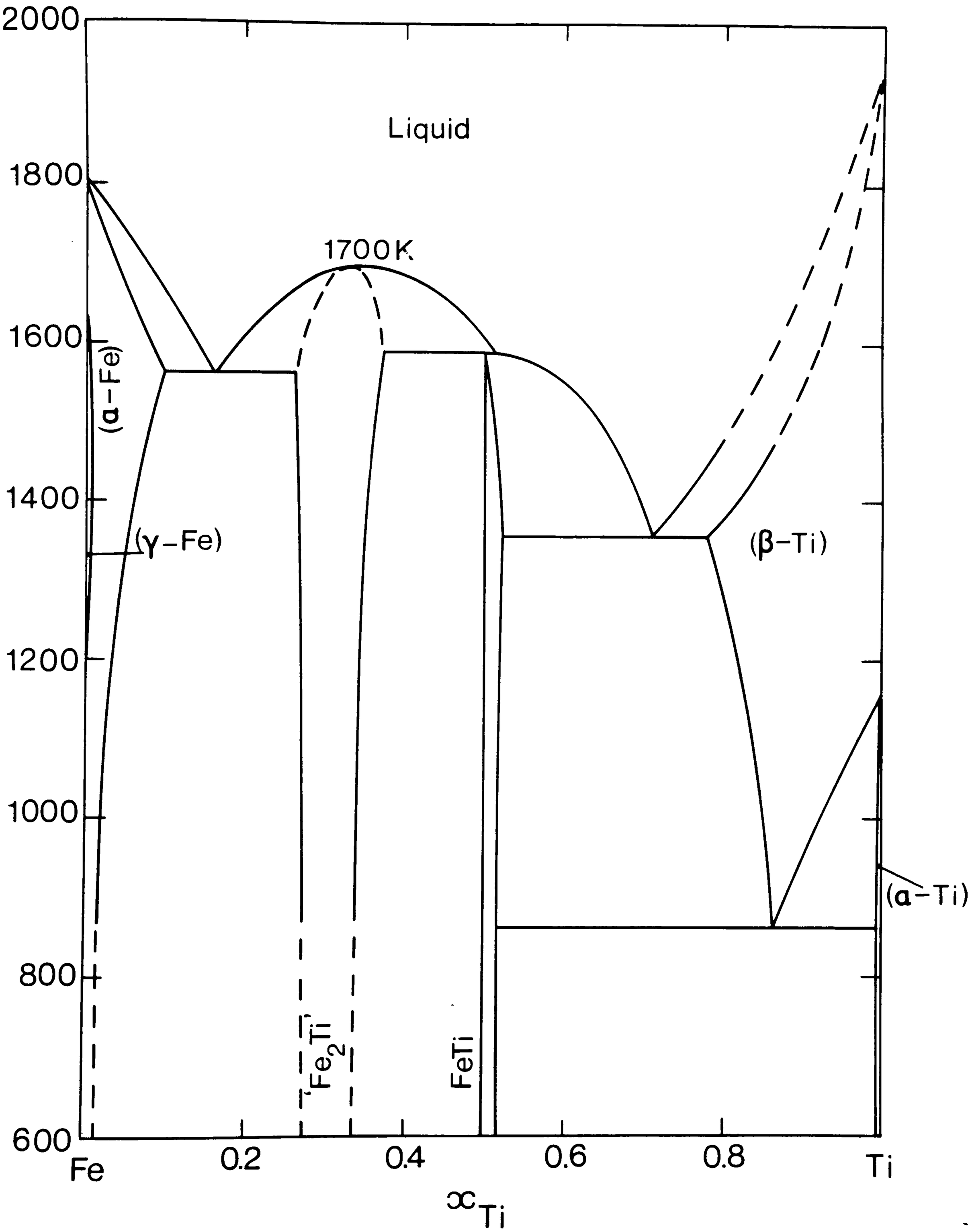

Fig. 6.1 Experimentally determined phase diagram for the Fe-Ti system.

phase region between the Fe based bcc solid solution and the Laves phase compound Fe_2Ti, and for x_{Ti} = 0.333 and 0.50 for the two compounds Fe_2Ti and FeTi respectively. Based upon these and other measurements of thermodynamic properties a critical assessment was carried out to provide data for the various phases in the system as a function of temperature and composition. These critically assessed data are now suitable for use in the calculation of multicomponent phase diagrams.

Experimental

The measurements were carried out using a high temperature adiabatic calorimeter designed by Dench (26) and shown in Fig 6.2. The details of its construction, operation, and of the preparation of specimens have been described elsewhere (26).

The materials used in the experiments were 'carbonyl' iron powder, and titanium powder supplied by ICI Mond division. The iron powder was reduced under hydrogen at 630 K, ground in an agate mortar, and sieved. The -400 mesh fraction was used in the experiments. The titanium powder was also sieved, and the -300 mesh fraction used. The gas contents of the powders, determined by the vacuum fusion method, are shown in Table 6.1.

The enthalpies of formation of the alloys were determined by measuring the energy required to heat specimens between two chosen temperatures. Two measurements were required to measure an enthalpy of formation - a) one in which complete alloying takes place and b) one where no alloying takes place. To make sure that the alloying occurred only during the experiment and was complete by the end of the experiment, preliminary tests were made to determine a 'safe' temperature where no detectable alloying occurs even when the specimens were held at this temperature for 4 hrs, and a 'final' temperature at

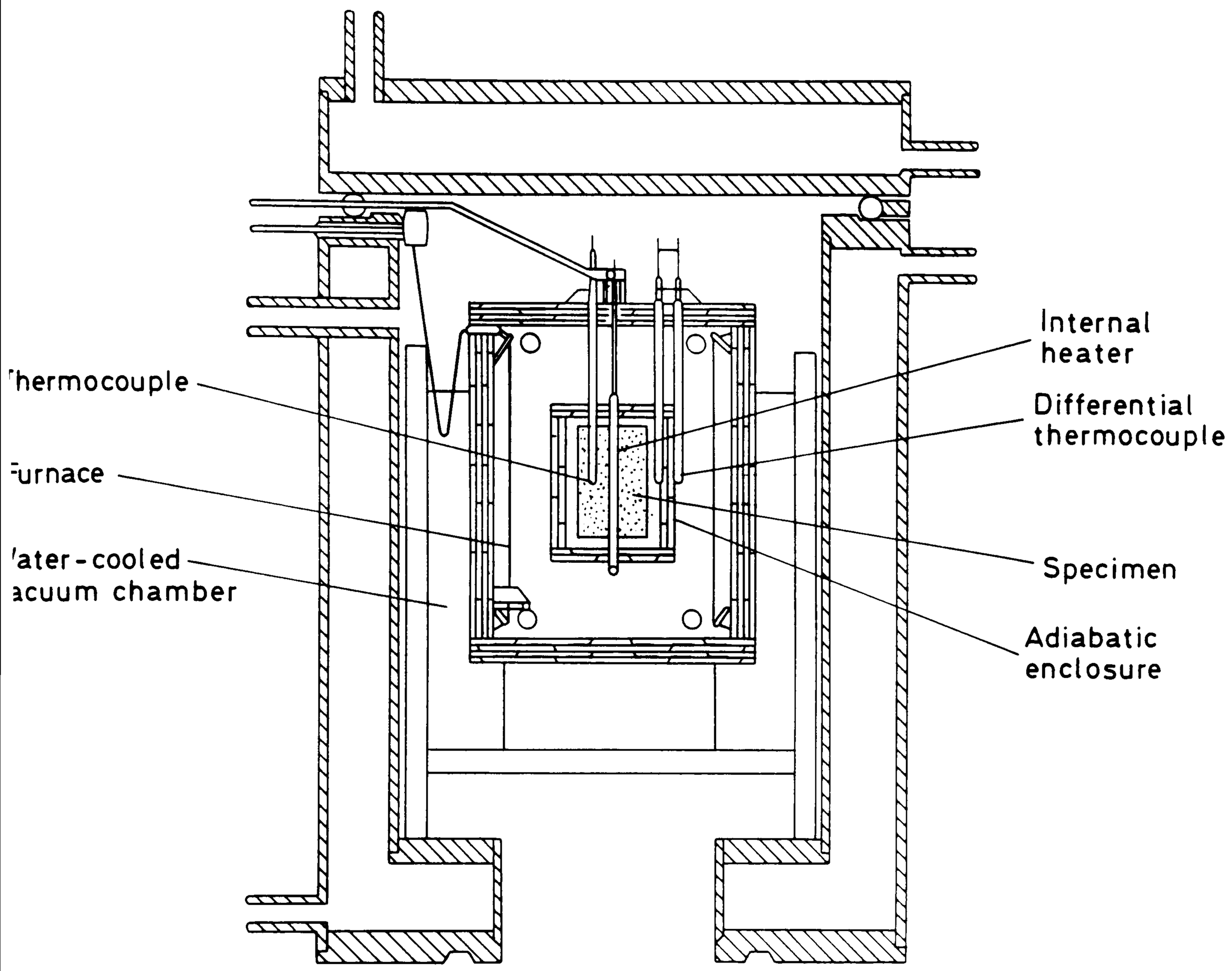

Fig. 6.2 Schematic diagram of the adiabatic calorimeter.

Table 6.1. Mole fraction of impurities in the alloying materials from gas analysis.

	x_O	x_N	x_H
Ti	0.0072	0.0044_6	0.0081
Fe	0.0010	$<3\times10^{-6}$	-

Table 6.2. Results of preliminary experiments to determine the 'safe' and 'final' temperatures.

x_{Ti}	Sintering temp / K	Sintering time / hrs	Constitution
0.04	873	4	Fe + Ti
	973	4	Fe + Ti
	1073	4	Fe + Ti + Alloy
	1273	1	Fe + Fe_2Ti
	1373	1	Bcc Alloy
	1473	1	Bcc Alloy
0.333	873	4	Fe + Ti
	973	4	Fe + Ti
	1073	4	Fe + Ti
	1273	1	Fe + Ti
	1373	1	Fe_2Ti + FeTi (trace)
	.473	1	Fe_2Ti
0.5	873	4	Fe + Ti
	973	4	Fe + Ti
	1073	4	Fe + Ti
	1273	1	FeTi + Fe_2Ti
	1373	1	FeTi
	1473	1	FeTi
0.95	873	4	Fe + Ti
	973	4	Fe + Ti
	1073	4	Fe + Ti
	1273	1	Alloy + Fe_2Ti (?)
	1373	1	Alloy + Fe_2Ti (?)
	1473	1	Alloy + Fe_2Ti (?)

which complete alloying took place in the specimens within 1 hour. The specimens from these preliminary tests were examined both metallographically and by powder x-ray diffraction and the results are summarised in Table 6.2. Suitable temperatures were found to be 973 K for the 'safe' temperature and 1473 K for the 'final' temperature.

Two different procedures were used to determine the enthalpies of formation as can be seen from the following scheme:

$$xFe(T_1) + yTi(T_1) \longrightarrow Fe_xTi_y(T_2) \qquad H_1$$

$$Fe_xTi_y(T_1) \longrightarrow Fe_xTi_y(T_2) \qquad H_2$$

$$xFe(T_1) + yTi(T_1) \longrightarrow xFe(T_2) + yTi(T_2) \qquad H_3$$

Here, T_1 refers to the 'safe' temperature and T_2 to the 'final' temperature. The mole fractions of Fe and Ti are x and y respectively.

In this scheme, H_1 refers to the energy change in the alloying measurement while H_2 and H_3 refer to energy changes when no alloying occurs. For measurements of H_2, the specimen consisted of the alloyed compacts from the previous measurement ie. for measuring H_1. This type of measurement is called a 'repeat' run. For measurements of H_3, the specimen consisted of discrete compacts of the component elements of the same weight and in the same overall composition as the alloying specimen - a so-called 'composite' specimen. The compacts of Fe in the composite specimen were separated from the Ti compacts by thin layers of Ta sheet to prevent any alloying occurring at the surfaces.

When these measurements are combined it is possible to derive the enthalpy of formation applicable to either the 'safe' temperature or the 'final' temperature.

ie. $\Delta_f H(Fe_xTi_y, T_1) = H_1 - H_2$

$\Delta_f H(Fe_xTi_y, T_2) = H_1 - H_3$

Fig 6.3 shows a typical heating curve, in this case for an alloying run. The specimen is heated up using the calorimeter furnace and stabilised approximately at the 'safe' temperature. The heater is then used to heat the specimen until the 'final' temperature is reached. During and after the heating period, adiabatic conditions are maintained by an automatic control system which responds to temperature gradients across the adiabatic enclosure detected by differential thermocouples (Fig 6.2). The final slope after the heater is switched off is extrapolated back to a time mid-way through the heating period to determine the exact final temperature. This allows for slight departures from adiabatic conditions. The energy supplied to the heater is corrected using measured heat capacity data around T_1 and T_2 to determine the energy that would have been required to heat the specimen from the precise 'safe' temperature to the precise 'final' temperature.

The sharp change in slope in the heating curve marks the onset of alloying. Figure 6.3, which refers to the formation of an alloy with x_{Ti}=0.10, shows this change in slope at about 1300 K which is approximately the eutectic temperature in the Ti rich side of the phase diagram.

Two factors make measurements difficult when alloying is very exothermic. Firstly, a large quantity of heat is evolved in a short time, too much for the automatic system of the calorimeter to control, causing the loss of adiabatic conditions. Secondly the large amount of heat evolved would produce a large temperature rise. The final temperature might then be so high that the specimen would melt or the calorimeter would be outside its safe operating range. In general, the calorimeter is restricted to temperatures below 1600 K.

In order to overcome these problems, it was necessary to reduce the quantity of heat evolved per gram of specimen.

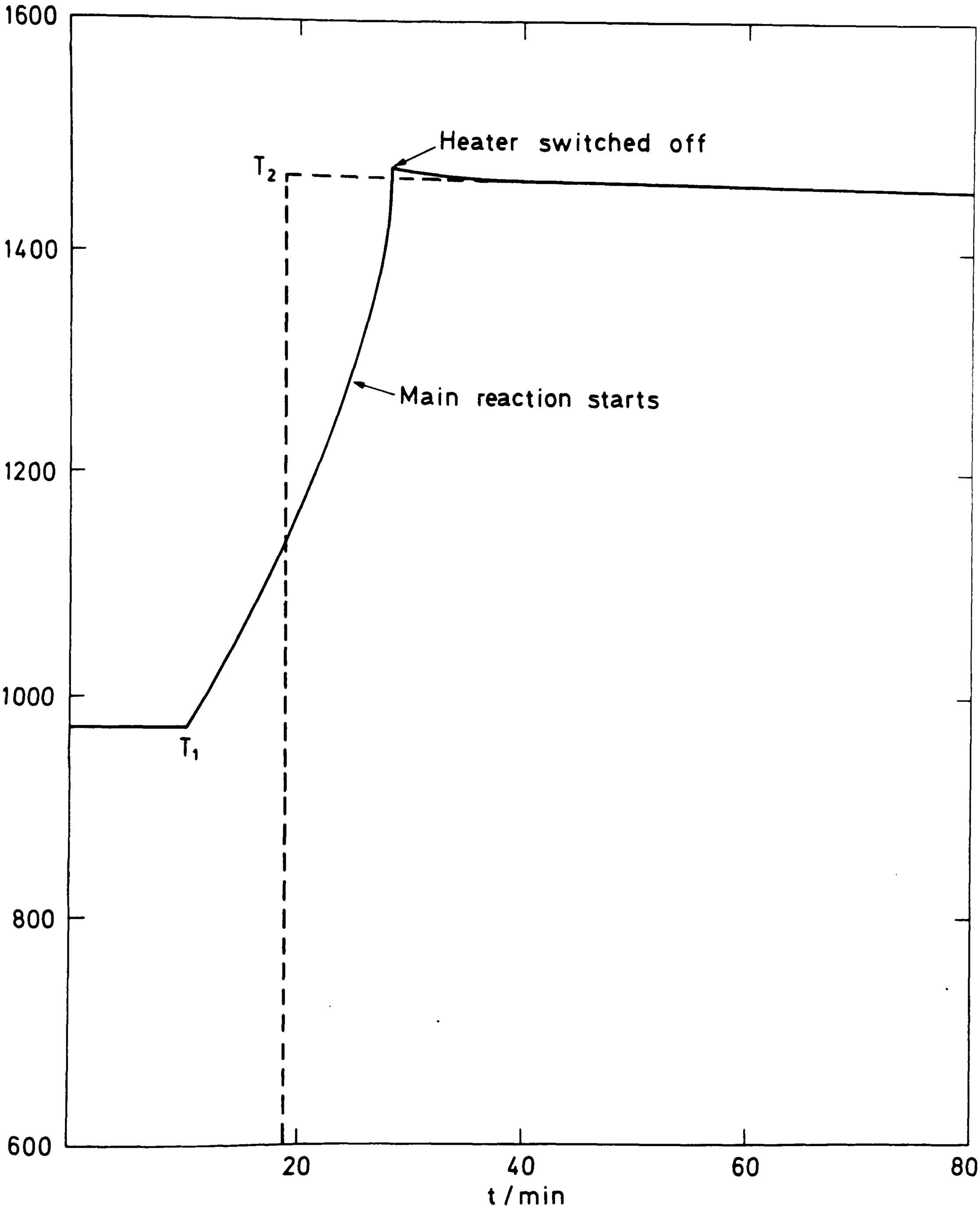

Fig. 6.3 Typical heating curve for an alloying run.

Fig 6.4 shows the method used where the alloying compacts were separated by discs of molybdenum which acted a heat sink. This method proved to be very effective. However the errors in measurement were inherently much greater than for previous sets of experiments since less alloying material was used per specimen. This showed up in the scatter of the experimental results as shown below.

Results and Discussion

Table 6.3 shows the results obtained for the Fe-Ti system for each of the compositions studied. The derived enthalpies of formation are plotted as a function of composition in Fig 6.5 for 973 K and in Fig 6.6 for 1473 K. The estimated accuracy of the $\Delta_f H$ values, which varies according to the degree of dilution, is shown as errors bars in the figures. These results clearly show the exothermic nature of these alloys. It is difficult to compare the two curves for the enthalpy of formation however since they refer to different reference phases for the pure elements and also because the bcc/(bcc+Fe_2Ti) phase boundary varies appreciably with temperature.

There have been four other sets of measurements on solid alloys in the Fe-Ti system. Kubaschewski and Dench (342) measured the enthalpies of formation of the two compounds. They obtained for FeTi a value of -20.3 $\pm$ 3 kJ/mol at 298 K. The present work shows that the enthalpy of formation for 973 K is -29.9 $\pm$ 3 kJ/mol. This is of the order of 7-9 kJ/mol more exothermic than Kubaschewski and Dench's value even if one allows for a difference of heat capacity between products and reactants of up to 4 J $mol^{-1}K^{-1}$. This discrepancy is almost certainly due to Kubaschewski and Dench's calorimetric method where considerable heat loss was likely.

Kubaschewski and Dench also attempted to measure the enthalpy of formation of Fe_2Ti. They obtained the value of -19.0 $\pm$ 2 kJ/mol but were

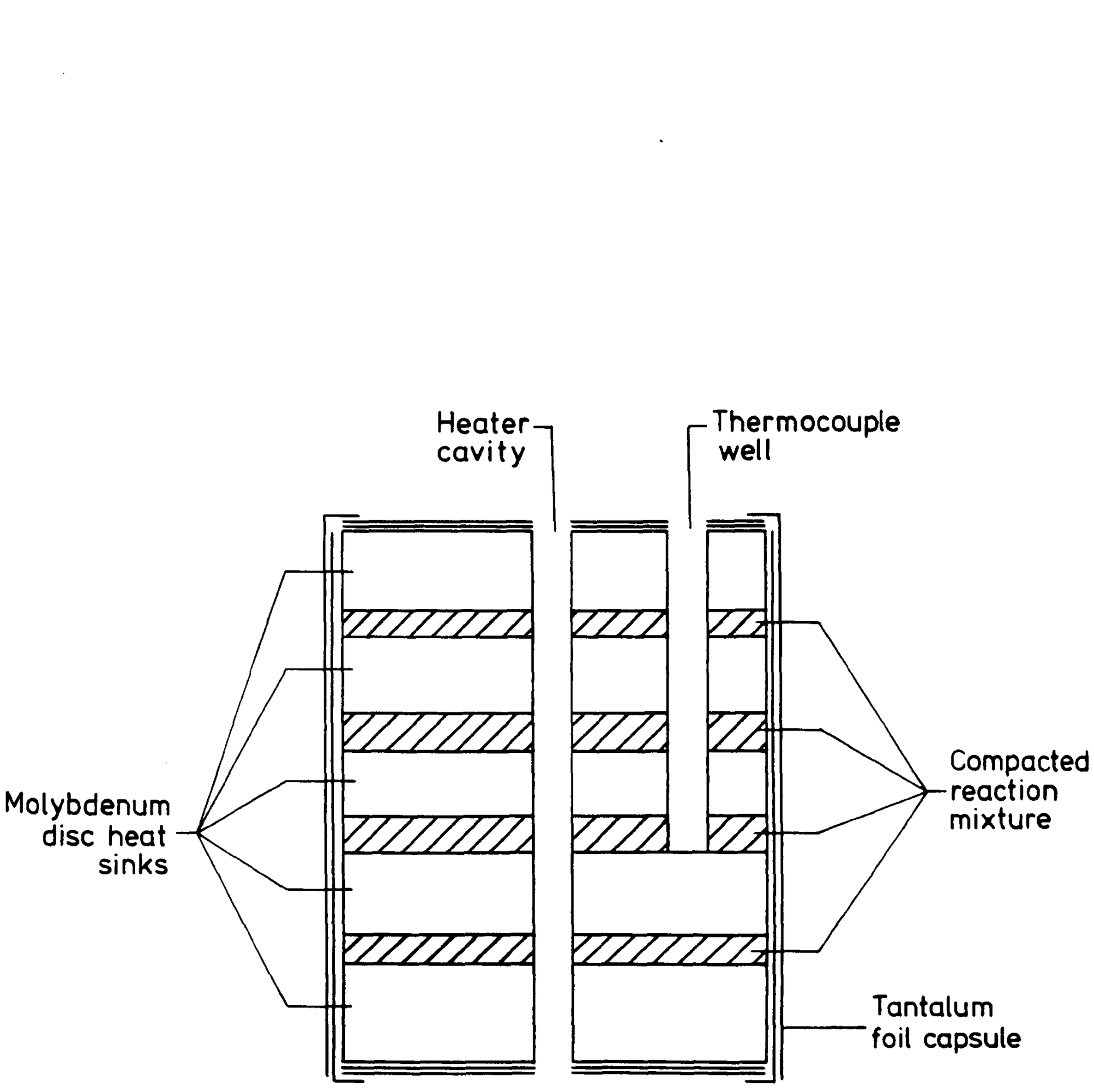

Fig. 6.4 Schematic layout of alloying specimen. Alloying compacts are separated by molybdenum discs.

y	Wt. of Alloying Compacts /g	T_1/K	T_2/K	Alloying Run Energy input /J	Repeat Run Energy input /J	$\Delta_f H(T_1)$ /J mol^{-1} bcc Fe, hcp Ti	Composite Run Energy input /J	$\Delta_f H(T_2)$ /J mol^{-1} fcc Fe, bcc Ti
0.05	56.3204	973	1473	24349.29	25454.08, 25460.18	-1090.77	24474.14, 24105.03	+58.79
	56.3204	973	1473	23291.32		-2132.42		-982.86
	55.4537	973	1473	23265.97	24735.05	-1469.04	24139.59, 23770.48	-389.45
0.10	51.3789	973	1473	20898.24	26217.78	-5700.28		-1722.30
	51.3785	973	1473	19399.12	24241.26	-5188.58	22493.18, 22517.87	-3328.71
	51.3786	973	1473	18783.23	24093.15	-5689.82		-3988.65
0.20	15.1274	973	1403	11171.28	14221.00	-10938.94		-12633.88
	15.1274	973	1403	10537.15	14080.04	-12707.85	14562.24	-14908.43
	15.1269	973	1403	10594.14	14063.97	-12446.23	14824.67	-14704.50
	15.1157	973	1403	10988.52	14184.47	-11472.32		-13298.63
0.333	8.9807	973	1413	10455.23	13743.69	-19480.20	14401.50	-24242.68
	8.9809	973	1413	10167.71	13881.59	-21999.85	14577.01, 14484.63	-25945.36
	8.9803	973	1413	9811.44	13819.96	-23746.79	14621.82, 14653.33	-28057.65
	8.9845	973	1413	10462.26	13941.84, 13953.18	-20706.28		-24215.44
	8.9805	973	1473	12364.81	15831.50	-20536.49	16393.37, 16589.10 16524.75	-24510.92
0.50	7.2261	973	1513	12382.67	17274.65, 17045.91	-34297.67	17229.63	-32633.19
	7.2258	973	1513	13116.46	16960.35	-27595.74	16932.23	-27366.87
	7.2251	973	1513	13731.34	17961.95, 17506.19	-28738.93	16684.37	-22945.47
	7.2250	973	1513	12988.85	16849.30	-27717.79	16867.42	-28283.76

Table 6.3 ENTHALPIES OF FORMATION OF ALLOYS Fe_xTi_y

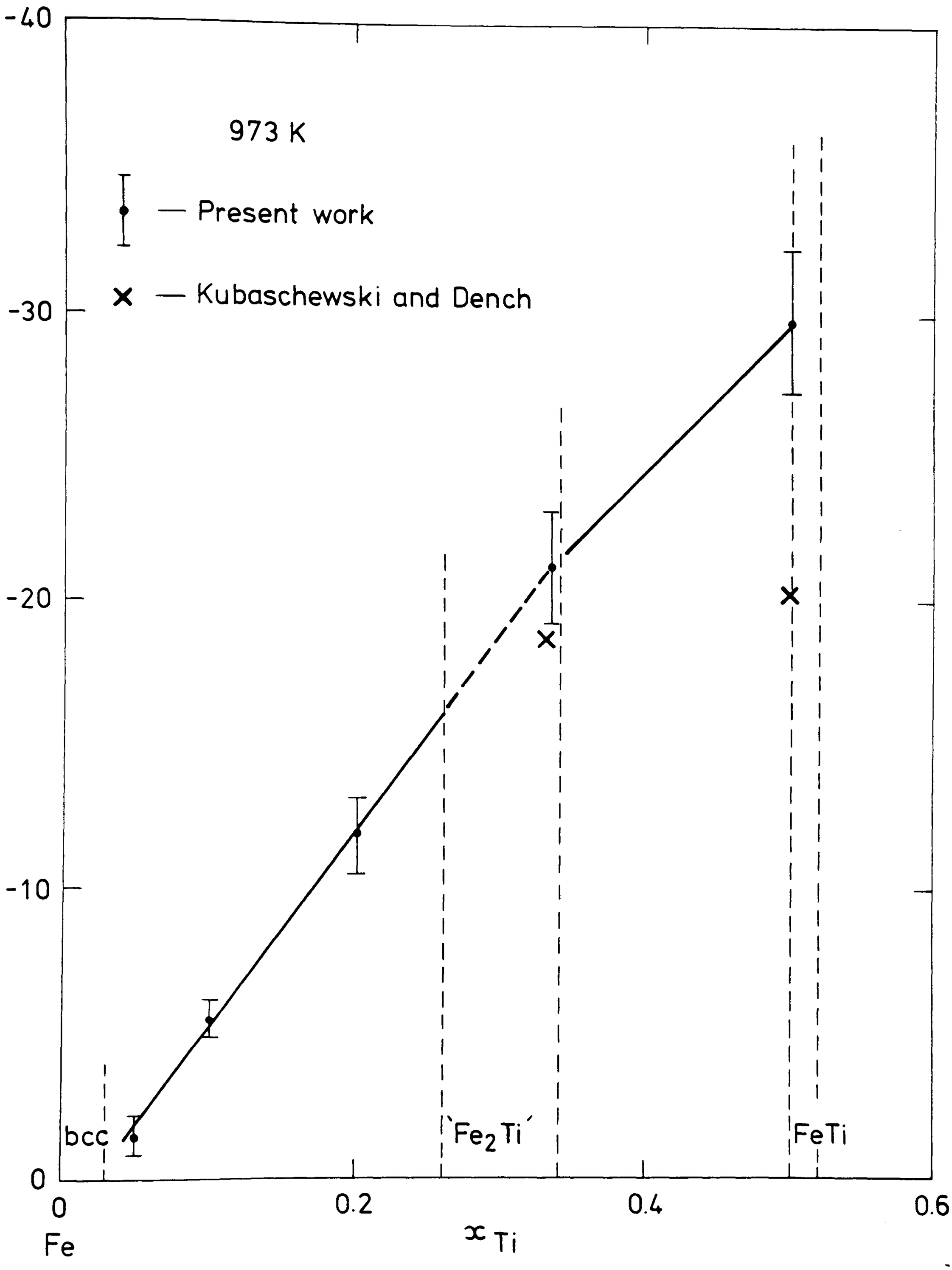

Fig. 6.5 Experimental enthalpies of formation for 973 K from bcc Fe and hcp Ti.

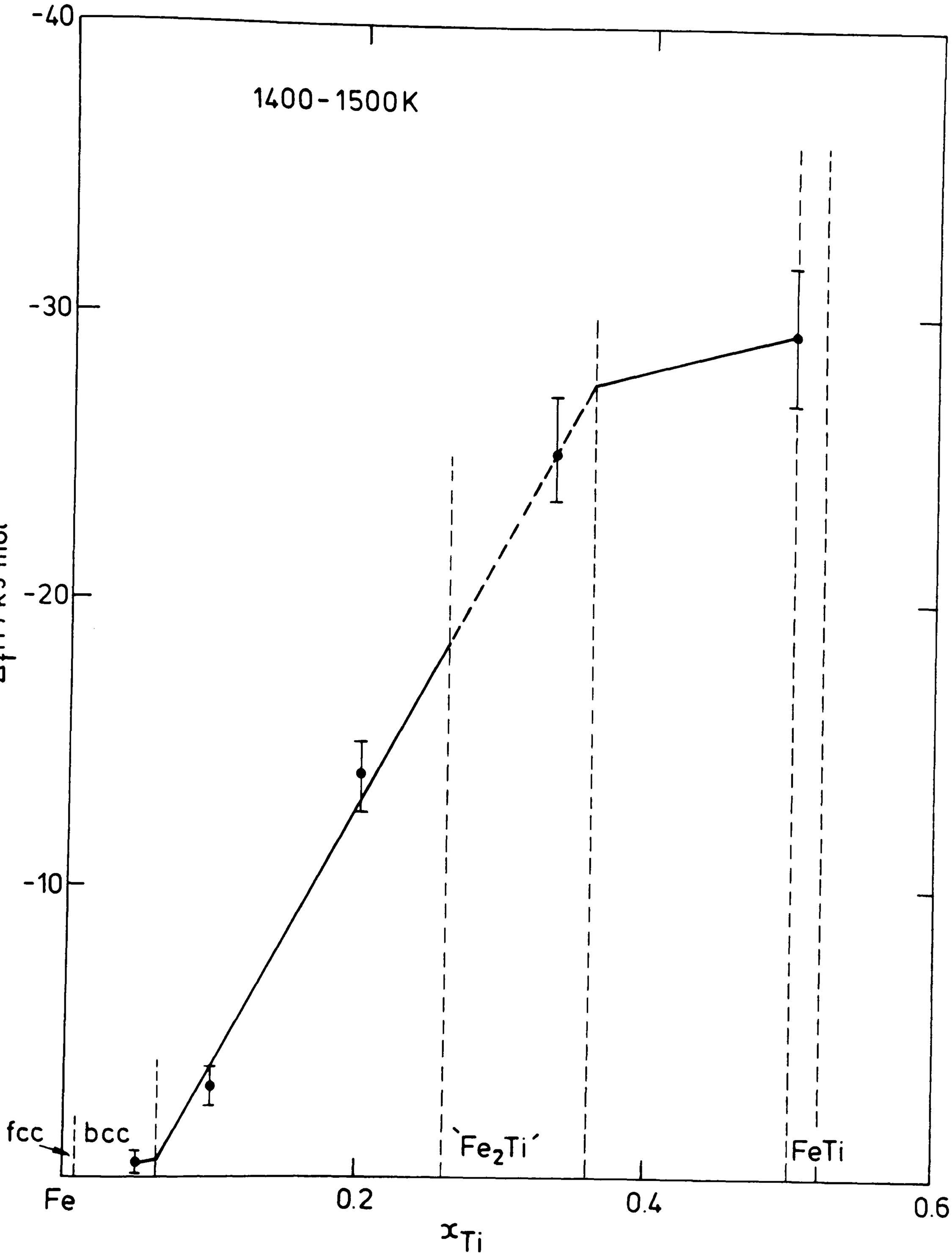

Fig. 6.6 Experimental enthalpies of formation for 1473 K from fcc Fe and bcc Ti.

suspicious because they had expected to find that $\Delta_f H(Fe_2Ti)$ would be more negative than $\Delta_f H(FeTi)$ in view of the erroneously high melting point then accepted for Fe_2Ti. On investigation they found however, that during their experiments the reaction produced a mixture of FeTi and the bcc iron based solid solution rather than the expected Fe_2Ti.

The present measurements gave -21.3 $\pm$ 2.5 kJ/mol for $\Delta_f H(Fe_2Ti)$ at 973 K, a value quite close to that obtained by Kubaschewski and Dench. From the preliminary experiments described earlier, and summarised in Table 6.2, it was found that Fe_2Ti forms completely when the specimens are held at 1473 K for one hour, and with a small quantity of FeTi only, when they are held at 1373 K for one hour. Furthermore, an X-ray examination of an alloying specimen revealed that Fe_2Ti had been formed completely. The fact that Kubaschewski and Dench formed only a mixture of FeTi and bcc may be attributed to the much larger particle size of the material they used which would have caused much slower alloying.

The enthalpies of formation of the two compounds have also been studied by Gachon et al. (343-345) subsequent to the present measurements. They obtained values of -31.0$\pm$1.3 kJ/mol for FeTi at 1440 K, and -27.6$\pm$1.0 kJ/mol for Fe_2Ti at 1514 K. Their results imply even more exothermic behaviour than implied by the results obtained during the present work and they also confirm that the enthalpy of formation of FeTi is more negative than that of Fe_2Ti.

The enthalpies of formation for both of these compounds have been calculated by Miedema and Niessen (346) using their semi-empirical electronic model, and for FeTi by Watson and Bennett (347). Both sets of predictions give results in remarkable agreement with the present experimental results (within 1 kJ/mol).

Palma and Schroder (348) reported high temperature heat capacity measurements of iron-rich alloys between 600 and 1150 K in the region of

the magnetic transformation. They found that the heat capacity and the Curie temperature were effectively independent of the amount of titanium for compositions up to $x_{Ti} = 0.048$.

Robinson and Argent (349) used Knudsen cell mass spectrometry to determine the partial enthalpies, excess partial Gibbs energies and excess partial entropies of solution at about 1600 K. Their values for the partial enthalpies of mixing agree well with the enthalpies of formation reported here. It should however be pointed out that their enthalpies were derived from the temperature dependence of vapour pressure measurements, a method subject to large errors.

A number of thermodynamic studies on the iron-titanium system have been concerned with the liquid phase. The results of Wagner and St. Pierre (350) for 1818 K and Furukawa and Kato (351) for 1823 K and 1873 K from Knudsen cell mass spectrometry show that the liquid phase can be represented approximately as a regular solution. However there is significant disagreement between the Gibbs energies of formation derived from the two sets of experimental ion intensities - the results of Furukawa and Kato (351) implying more negative Gibbs energies of formation.

A number of workers have studied the deoxidation equilibrium of iron at low titanium concentrations and derived the titanium activity coefficient at infinite dilution (352-357). Their results are summarised in Table 6.4 and compared with the γ^{o}_{Ti} values obtained from the results of Wagner and St. Pierre (350) and Furukawa and Kato (351). The results reported by Fruehan (356) and by Smellie and Bell (357) refer to a reference state of pure solid titanium. The titanium activity coefficient at infinite dilution was derived by Fruehan from extrapolation of activities at various titanium concentrations.

The ion current ratios reported by Wagner and St. Pierre (350) and Furukawa and Kato (351), have been used to derive activities and

Table 6.4. Experimental values for the Activity coefficient, γ°_{Ti} at infinite dilution.

Authors	Method	Temperature / K	γ°_{Ti}
Chipman (352) from results of Hadley and Derge (353)	Deoxidation	1900	0.011
Chino et al. (354)	Deoxidation	1823	0.020
		1873	0.033
		1923	0.060
Suzuki and Sanbongi (355)	Deoxidation	1873	0.016
Fruehan (356) *	EMF	1873	0.038
Smellie and Bell (357) *	Deoxidation	1973	0.059
Wagner and St. Pierre (350)	Mass Spec.	1818	0.056
Furukawa and Kato (351)	Mass Spec.	1823	0.022
		1873	0.024

* Refers to reference state of bcc Titanium

activity coefficients for the whole composition range. Fig 6.7 shows a plot of the activity coefficient of titanium (referenced to liquid Ti) converted to 1873 K for all the results on this liquid phase. The figure shows a marked difference between the two sets of mass spectrometric results and this is emphasised in Fig 6.8 where the integral excess Gibbs energies at 1823 K derived from these activity coefficients are plotted. Fig 6.7 also shows that the deoxidation data agree better with Furukawa and Kato's results than with those of Wagner and St. Pierre. For this reason and because they also agree well with the present enthalpy measurements, the results of Furukawa and Kato were preferred for use in the critical assessment.

Dyubanov et al. (358) measured calorimetrically the partial enthalpy of solution of Ti in liquid iron as -52.0 $\pm$ 3 kJ/mol at 1823 K.

Critical Assessment

The thermodynamic data for this system have been assessed previously by Kaufman and Nesor (359) using a subregular solution model for the liquid, bcc and fcc solution phases and assuming that the compounds Fe_2Ti and FeTi were stoichiometric. Because of the new measurements this assessment is now superseded.

Since this present work was completed the phase diagram and the thermodynamic data for the Fe-Ti system have been critically assessed by Murray (360). In her assessment she preferred the data of Wagner and St.Pierre to those of Furukawa and Kato and also had no access to the recent experimental measurements of the enthalpies of formation of solid alloys. The liquid, fcc, bcc and hcp phases were represented by regular or subregular solution models with no temperature dependence for the parameters. However she used different descriptions for the Fe rich bcc phase and the Ti rich bcc phase. The two compounds were represented as

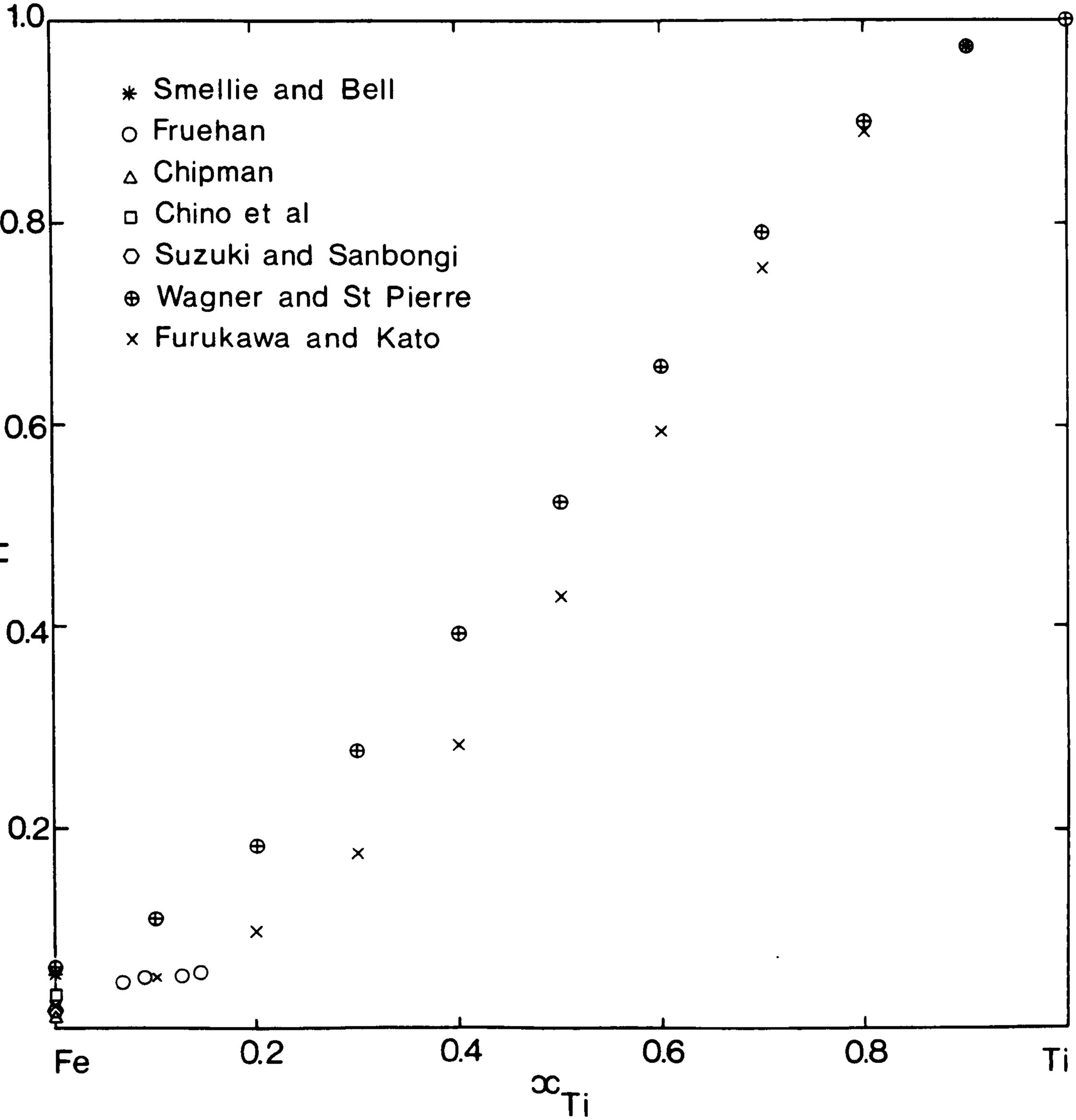

Fig. 6.7 The variation of activity coefficient of titanium for 1873 K derived from experimental measurements.

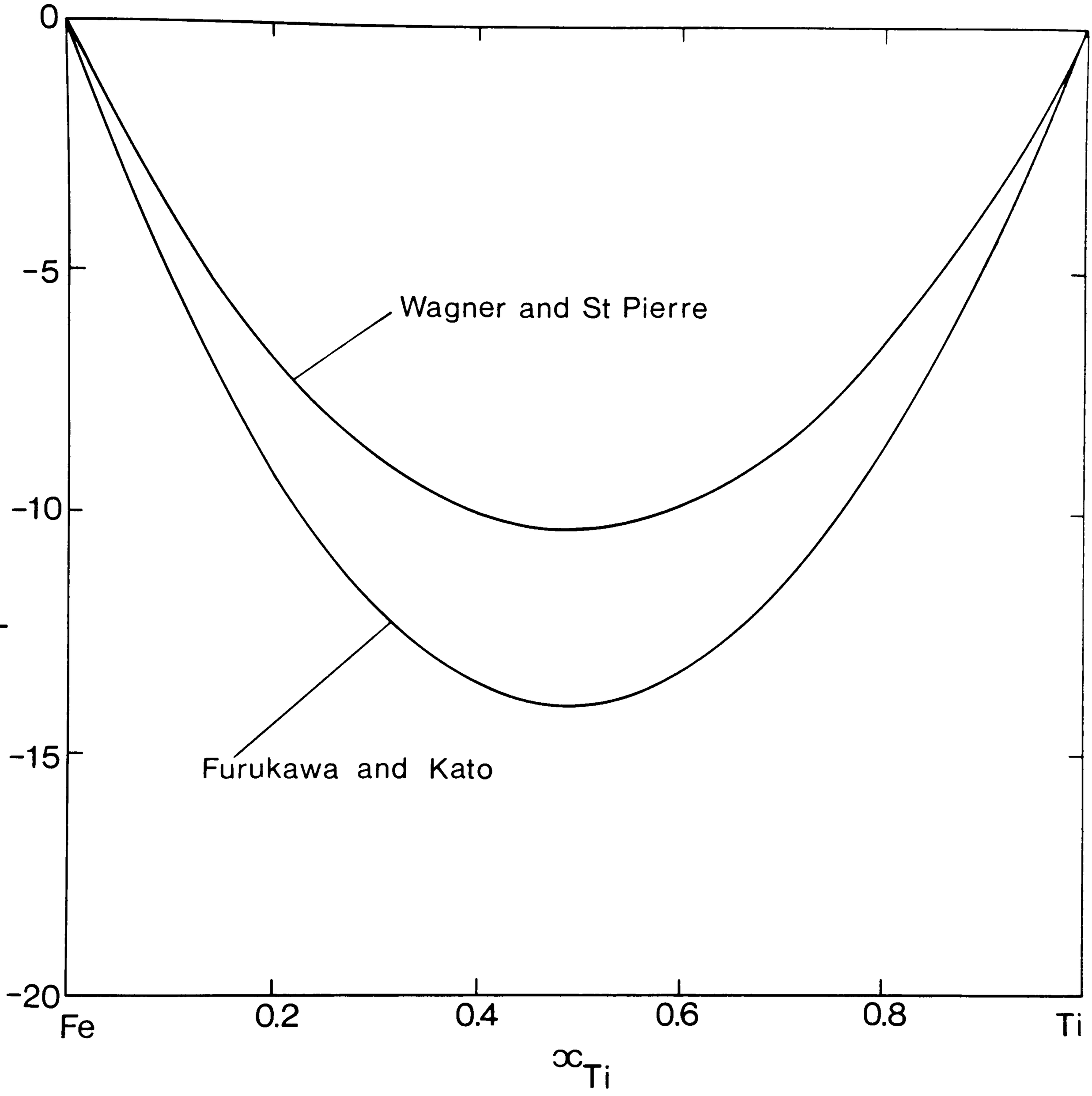

Fig. 6.8 Integral Gibbs energies of formation for 1823 K derived from experimental results of Wagner and St. Pierre (350) and Furukawa and Kato (351).

Wagner Schottky phases with iron and titanium sublattices. Vacancies were introduced onto the titanium sublattice while titanium atoms were assumed to substitute onto the iron sublattice. Very good agreement was obtained between the calculated and experimental phase diagram except that she failed to reproduce the peritectic fusion of FeTi.

For the present critical assessment it was decided that the liquid, bcc and fcc phases should be represented by Redlich-Kister power series. The solubility of Fe in the hcp phase, which is known from experiment to be very low (338-340), was neglected and the phase was treated as stoichiometric. In a similar way the compound FeTi, which exists over a narrow range of homogeneity was treated as a stoichiometric phase. The Laves phase compound Fe_2Ti exists over a fairly wide range of homogeneity. For this assessment its data were represented by a Redlich-Kister power series. This approach had already been used with some success for the Laves phase compounds Co_2Zr and Cr_2Zr (361) and with the treatment of sigma phases (167,362).

For this assessment all data were referred to pure bcc Fe and pure bcc Ti at the temperature of interest. The fusion data for Fe (bcc to liquid) were taken from Hultgren et al. (43) and for Ti (also bcc to liquid) from the experimental work referred to in Hultgren et al. (43), and the work of Berezin et al. (363). Data for the Gibbs energies of transformation for the pure elements from the bcc phase to the fcc and hcp phases were taken from Kaufman (364). It was also necessary to estimate data for the hypothetical transition bcc to Laves for both of the elements. These Gibbs energies of transition were taken to be temperature independent in the absence of any other information.

Using the measured enthalpy of formation for the Laves phase at $x_{Ti} = 0.333$ for 1473 K, the Gibbs energies of formation of the liquid phase at 1873 K derived from the experimental measurements of Furukawa and Kato (351) and the congruent melting temperature of the Laves phase

compound at 1700 K, the entropy of formation for the liquid and the Laves phases at x_{Ti} = 0.333 were estimated. This was subject to the constraint that the entropy of formation be compatible with the known empirical relationship between enthalpies and excess entropies of formation (365) and, in addition, that the entropy of fusion of the compound is less than that for an order to disorder transformation. The data now derived for the liquid phase were found to be in good agreement with the partial enthalpy of titanium at infinite dilution in liquid Fe measured by Dyubanov et al. (358).

From these assessed data, data for the Laves phase as a function of temperature and composition were derived to reproduce as closely as possible the experimental phase boundaries between the Laves phase and the liquid phase. The calculated phase width is, in terms of mol fraction, about 0.04 greater than that determined experimentally.

The compound FeTi melts peritectically at about 1590 K. Using the enthalpy of formation data reported here, an entropy of formation was derived to reproduce the known fusion behaviour.

Data for the bcc phase were derived in order to reproduce the experimentally determined eutectics at x_{Ti} = 0.16 and at x_{Ti} = 0.71 (see Fig 6.1.) using the activity data of Robinson and Argent (349) but keeping approximately the same excess entropy curve as for the liquid phase. The agreement with the experimental phase diagram is good at high temperatures as shown in Fig 6.9. At low temperatures, however, the agreement is less satisfactory and the calculated eutectoid between the bcc, hcp and FeTi phases at high titanium concentrations is about 230 K lower than experimentally determined. This is probably due to the use of an inappropriate model for the Laves phase resulting in its calculated homogeneity range being too large, linked with the absence of heat capacity data for FeTi which could introduce significant errors over, say, 1000 K. The experimental and selected enthalpies of formation are

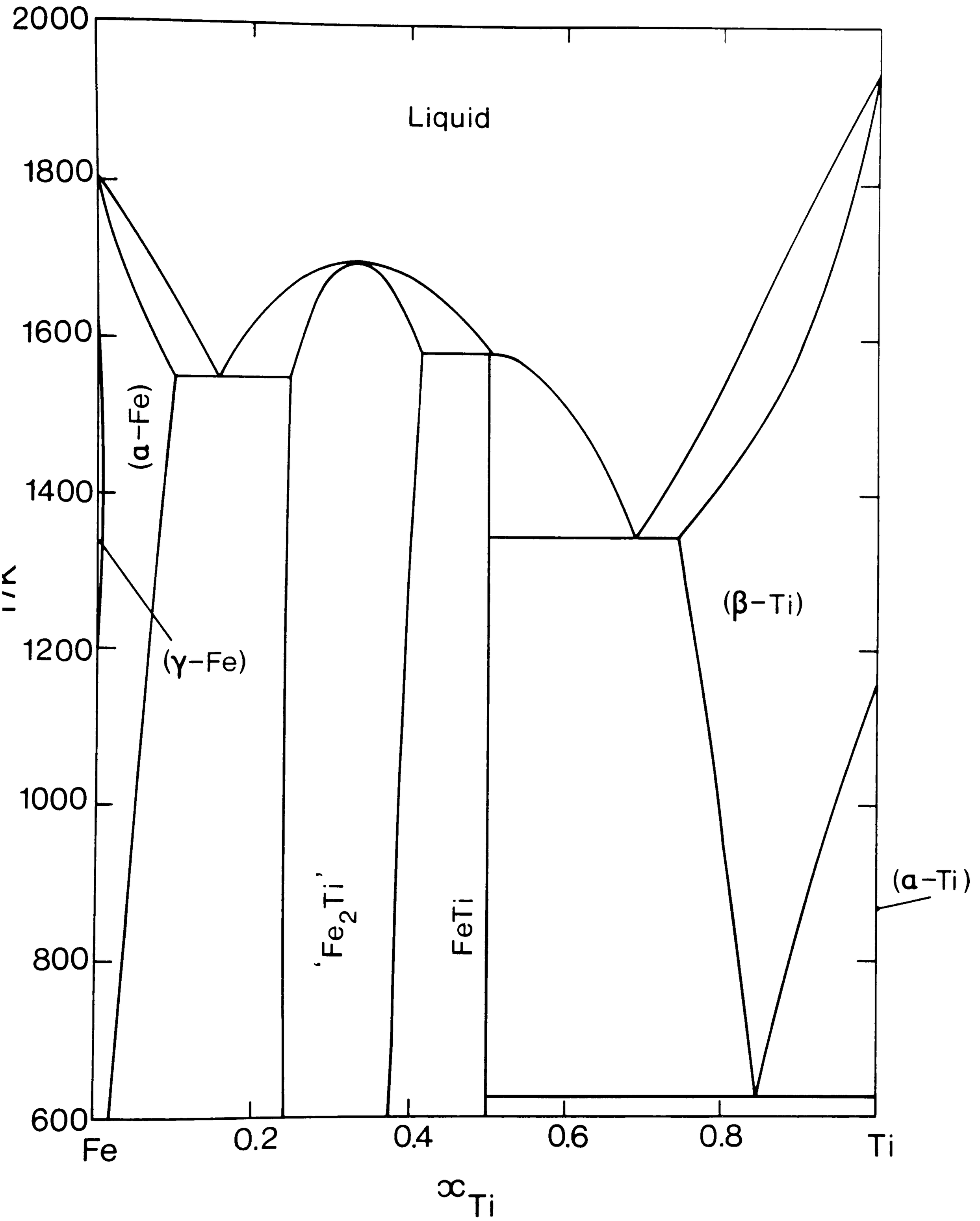

Fig. 6.9 Phase diagram for the Fe-Ti system calculated from the critically assessed thermodynamic data.

compared in Fig 6.10.

There seems to be some confusion concerning the equilibrium between the fcc and bcc phases at high Fe concentrations. A number of measurements have been reported. Roe and Fishel (366) interpreted their results from dilatrometry studies to show that the bcc/(bcc+fcc) phase boundary extended in to a maximum of x_{Ti}=0.0085 and that the maximum width of the two phase region was 0.001 in terms of mol fraction. Roe and Fishel's results also suggested that there is a minimum in the γ (fcc)-loop phase boundary similar to that found for the Fe-Cr system. No phase boundaries were found for compositions higher in titanium than x_{Ti}=0.0085.

No evidence for this minimum was found from Wada's experiments (367) also by dilatrometry. The maximum of the γ-loop was determined to be at about x_{Ti}=0.008, in good agreement with Roe and Fishel's results. However it is not clear whether Wada's results refer to the fcc/(fcc+bcc) or the bcc/(fcc+bcc) phase boundary. Wada also suggested that the two phase region between fcc and bcc should be about 0.006 wide rather than 0.001 measured by Roe and Fishel.

Moll and Ogilvie (368), from solid state diffusion studies, determined that the maximum solubility of titanium in the fcc phase was 0.0075. Hellawell and Hume-Rothery (369) used thermal analysis techniques to investigate the fcc/bcc phase boundaries. Their measurements on an alloy with x_{Ti}=0.0128, however, showed no detectable phase transformation.

The γ-loop was also studied by Fischer et al. (370) by measurement of the magnetic susceptibility although their work was not available for this assessment. Their results show that the maximum solubility of Ti in the fcc phase was 0.008 and that the maximum width of the two phase field bcc+fcc was 0.006.

Shunk (55) in his assessment of the phase diagram did not consider

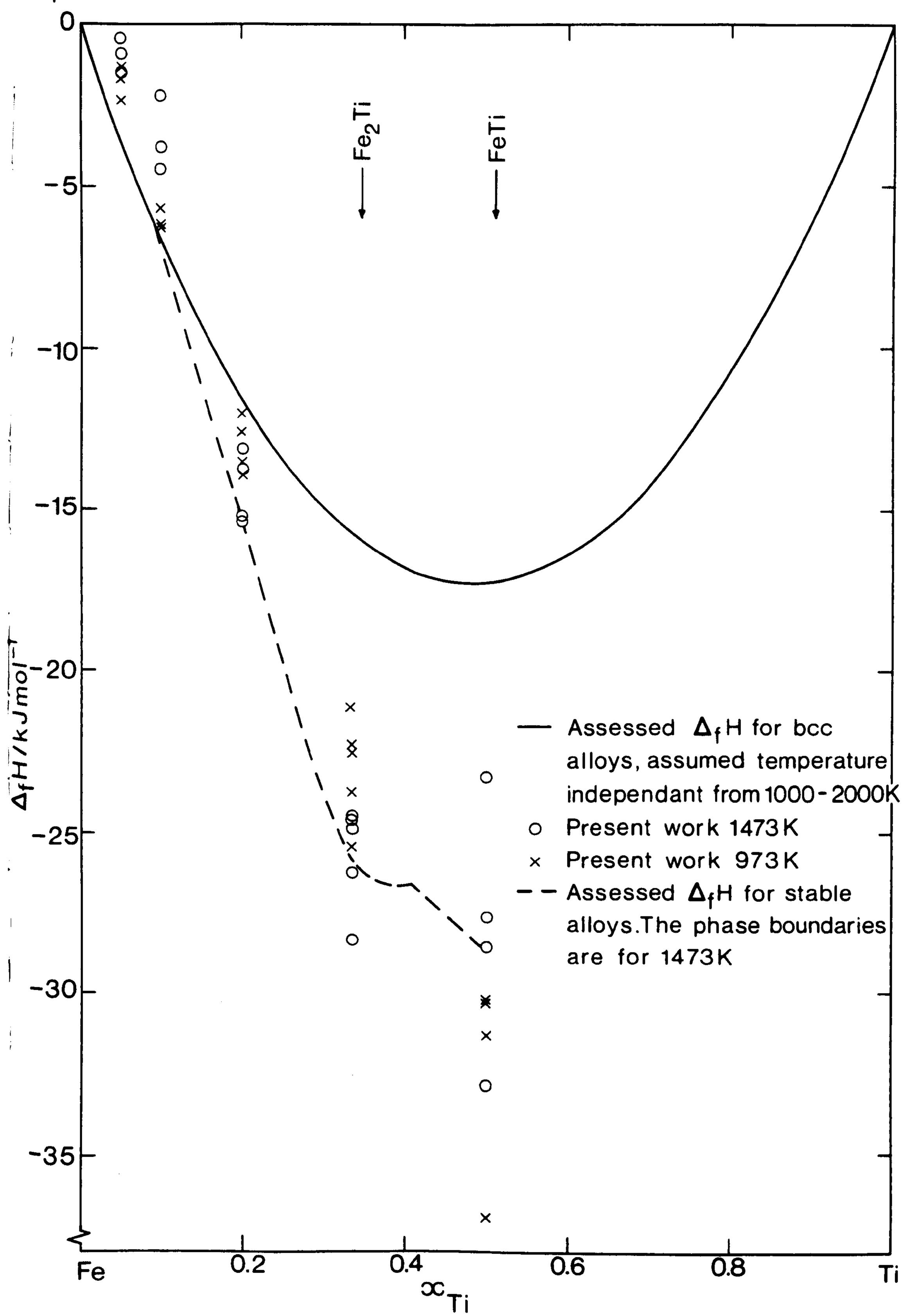

Fig. 6.10 Comparison of the experimental and selected enthalpies of formation for 1473 K.

the work of Fischer et al. and suggested that the maximum solubility of Ti in the fcc phase should be 0.002. For this work the phase diagram implied by Shunk has been adopted and data were derived for the fcc phase to reproduce this diagram. It was also assumed that the temperature dependence and asymmetry of the excess Gibbs energy curve for the fcc phase is similar to that for the bcc phase. Fig 6.11 shows the calculated δ-loop phase boundaries with some of the experimental data superimposed. In the more recent assessment, Murray (360) adopted the data of Fischer et al. for her assessment of the γ-loop equilibria.

Table 6.5 shows the critically assessed data for the Fe-Ti system. Fig 6.12 shows a plot of the Gibbs energy of formation for each phase at 1600 K.

Summary and Suggestions for Future Work

The thermodynamic data for the Fe-Ti system have been critically assessed to be as consistent as possible with the accepted phase diagram. The assessed data are now suitable for use in the calculation of multicomponent alloy phase diagrams. This assessment, which was carried out without the use of optimisation programs such as the one developed by Lukas et al. (290,310), has one or two minor inconsistencies compared with the diagram now accepted, notably the extension of the δ-loop into the binary system, the homogeneity range of the Laves phase and the eutectoid temperature at high titanium compositions.

The more recent critical assessment of Murray (360) is in rather better agreement with the accepted phase diagram although it is based on experimental thermodynamic data which have now been superseded and which differ significantly from values considered now to be correct. Murray also used two different descriptions for the thermodynamic data for the

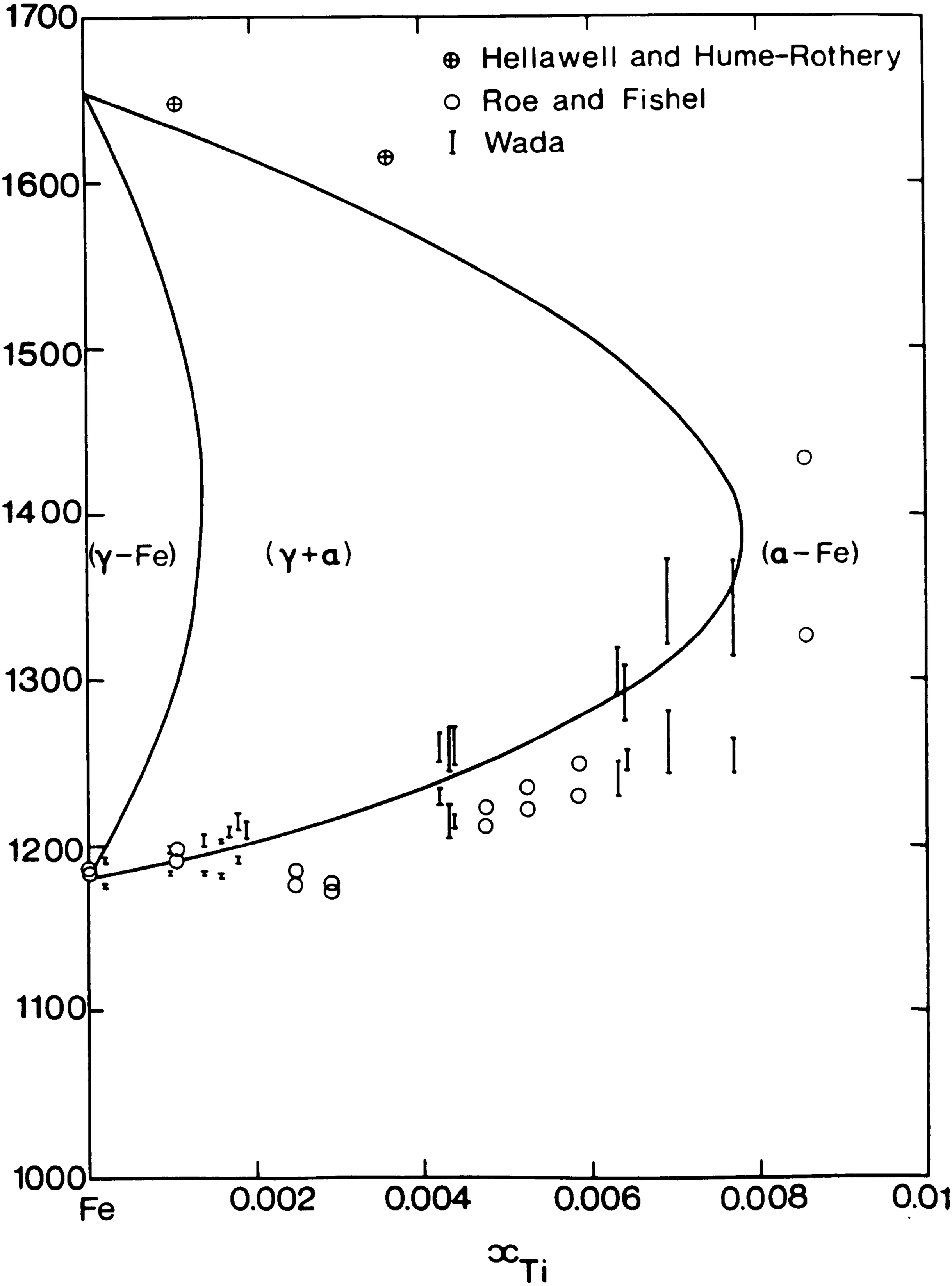

Fig. 6.11 The γ-loop for the Fe-Ti system calculated from the critically assessed thermodynamic data and compared with the experimental results.

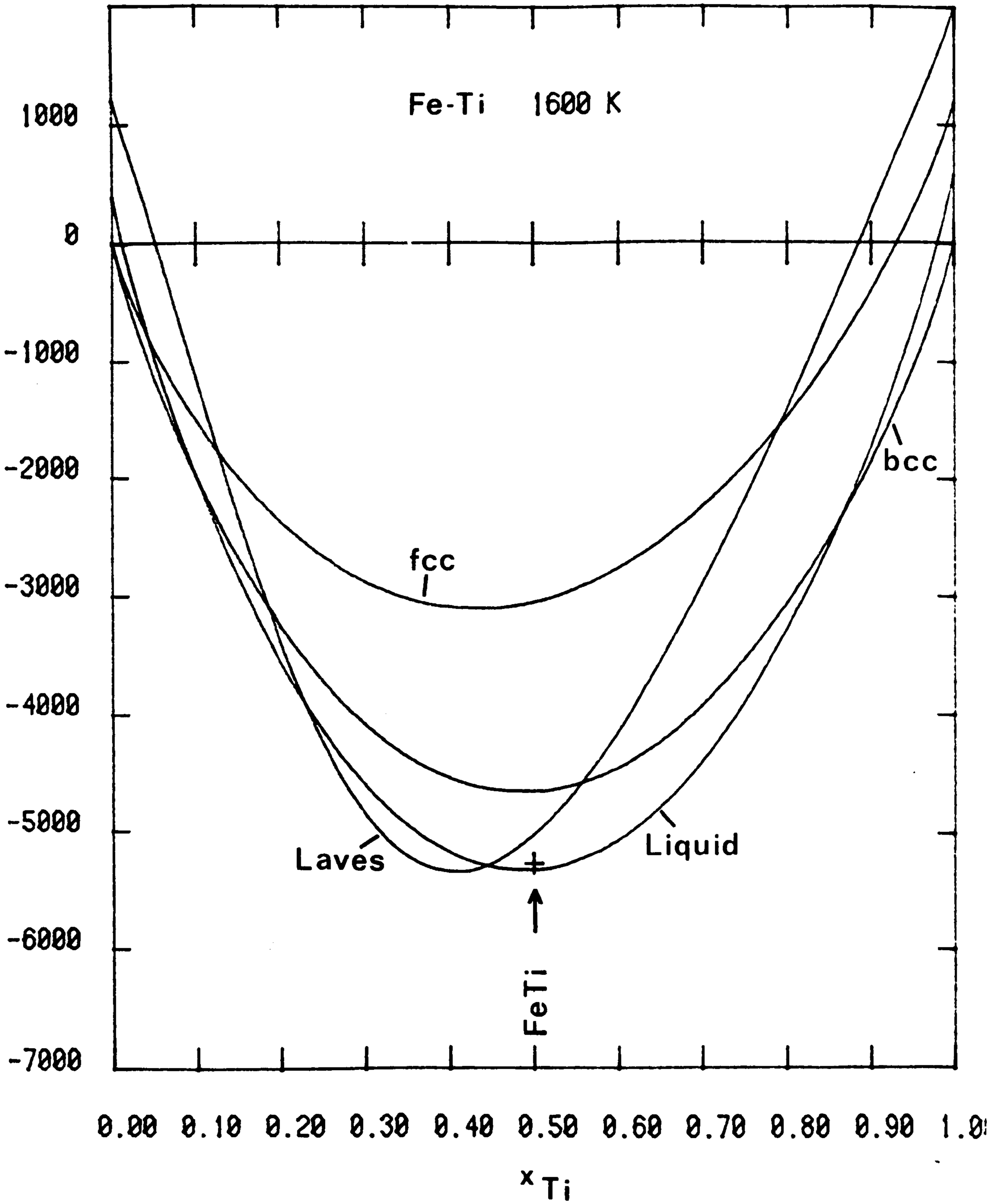

Fig. 6.12 Gibbs energy of formation as a function of composition for the different phases of the Fe-Ti system for 1600 K calculated using the critically assessed data.

bcc phase - one for iron rich compositions and one for titanium rich compositions. Her assessment is therefore difficult to use in multicomponent phase diagram calculations. In addition her data do not reproduce the peritectic fusion of FeTi.

The model used by Murray to represent the composition dependence of the Laves phase is more realistic than the Redlich-Kister expression used in the present calculations. She represented the non-stoichiometry of Fe_2Ti in terms of a Wagner Schottky model with vacancies introduced onto the titanium sublattice to explain deviations to iron rich compositions, and titanium atoms substituting into the iron sublattice to explain deviations to titanium rich compositions. In practice, of the six types of point defects allowed, only the introduction of interstitials will not take place to any appreciable extent in these highly ordered Laves phases. The other four point defects - substitution on each of the sublattices and the introduction of vacancies on each of the sublattices should occur to some degree. In the case of the Fe_2Ti Laves phase, the homogeneity range is large to compositions iron rich of Fe_2Ti while it is fairly small except at high temperatures to titanium rich compositions. In view of the slightly larger size of titanium atoms the most important defects could be expected to be substitution of iron atoms onto the titanium sublattice and the intoduction of vacancies on the iron sublattice. This is different description from that adopted by Murray.

It is recommended that the thermodynamic and the phase diagram data be reassessed at some stage using an optimisation program. Such an assessment should also include new data for the pure elements, a treatment of the magnetic contribution to the thermodynamic properties, data to represent the solubility of Fe in hcp Ti and the use of more realistic models to represent the composition dependence of the thermodynamic data for the Laves phase and FeTi.

Table 6.5

ASSESSED DATA FOR THE IRON-TITANIUM SYSTEM

1 Solution Phases

The Gibbs energy of formation of a binary alloy from its component elements in their reference phase is given by the following expression

$$\Delta_f G = \Delta_t G + G^E + \Delta G_{ideal}$$

where $\Delta_t G$ is the Gibbs energies of transformation of the elements from their reference phases to the phase in question, G^E is the 'so-called' excess Gibbs energy and ΔG_{ideal} is the ideal contribution to the Gibbs energy of formation given by the expression:

$$\Delta G_{ideal} = RT\,(x \ln x + y \ln y)$$

where R is the gas constant, T the temperature and the alloy is of composition A_xB_y .

a) Gibbs energies of transformation for elements in J mol^{-1}

Element	Transformation	$\Delta_t G = a + bT + cT^2 + dT^3$			
		a	b	c	d
Fe	bcc ⟶ Liquid	13807.2	-7.6316	0	0
	bcc ⟶ Laves	5020.8	0	0	0
	bcc ⟶ bcc	0	0	0	0
	bcc ⟶ fcc	5235.02	-9.4006	5.2949×10^{-3}	-9.2215×10^{-7}
Ti	bcc ⟶ Liquid	13807.2	-7.1128	0	0
	bcc ⟶ Laves	8368.0	0	0	0
	bcc ⟶ bcc	0	0	0	0
	bcc ⟶ fcc	-1004.16	3.7656	0	0

b) Coefficients for excess Gibbs energy of formation for the Fe-Ti system

The excess Gibbs energy of formation in J mol^{-1} is given by:

$$G^E = x_{Fe}x_{Ti}\,[a + bT + (x_{Fe} - x_{Ti})(a_1 + b_1T) + (x_{Fe} - x_{Ti})^2(a_2 + b_2T) + (x_{Fe} - x_{Ti})^3(a_3 + b_3T) + (x_{Fe} - x_{Ti})^4(a_4 + b_4T)]$$

	a	b
Liquid	-88453.76 -3364.64 0 0 0	17.5529 0 0 0 0
Laves	-123498.31 -78573.89 27913.70 65733.98 66038.13	30.9428 19.6870 -6.9940 -16.4699 -16.5460
bcc	-69036.00 -4184.00 0 0 0	17.5529 0 0 0 0
fcc	-52300.00 -4184.00 0 0 0	17.5728 0 0 0 0

2 Compound Phases

For compounds the Gibbs energy of formation from the elements in their reference phases is given by:

$$\Delta_f G = a + bT + cT \ln T$$

Compound	x_{Fe}	x_{Ti}	a	b	c
FeTi	0.50	0.50	-28660.40	4.1112	0

CHAPTER 7

Quantitative Equilibrium Calculations for Steel Systems

It was shown in chapter 6 how thermodynamic data for the iron-titanium system were measured and used in a critical assessment to provide data for the various phases of the system which could be used in the calculation of multicomponent phase diagrams. In chapter 4 a variety of computer programs were discussed which were developed for the calculation of phase equilibria. In this chapter data and programs are linked in order to provide quantitative calculations of phase equilibria of importance to industry for steel systems.

The first set of calculations were undertaken to throw light on the relationship between neutron induced void swelling and alloy constitution. It had been postulated by Watkin and Gittus (371,372) that the degree of void swelling is related to the number and types of phases present in the stainless steel cladding alloy before irradiation, and in particular to the presence of the embrittling sigma phase (373). This work is, in fact, a good example of the application of phase diagram calculations since experimental measurements for stainless steels at temperatures of interest ie. 700 - 800 K are difficult, costly and unreliable because of the sluggishness of phase transformations. Moreover phase diagram information for commercial alloys containing perhaps 9 elements are just not available. There are however fairly reliable experimental phase diagram data for the solid phases in the base system, Cr-Fe-Ni, above 1000 K and these can be used together with critically assessed thermodynamic data for the binary systems to calculate the phase diagram for lower temperatures. These calculated phase diagrams are more reliable than could be determined at present by

experiment. Fig 7.1 shows, as an example, the phase diagram for the Cr-Fe-Ni system for 800 K calculated from the critically assessed data from Chart et al. (167) and Kaufman and Nesor (374) using the NPL ALLOYDATA system (15,173).

While calculations of the Cr-Fe-Ni system are of importance, the stainless steels used as cladding alloys also contain other elements such as silicon, titanium and carbon. Therefore calculations showing the effect of these minor additions on the phase diagram are of great importance. To this end the data for the stable phases in the binary systems Cr-Si, Fe-Si and Ni-Si were critically assessed by Chart et al. (167) and, in addition, data were derived for the sigma phase for these systems in order to reproduce experimental ternary phase equilibria. It is interesting to note that the data derived predict the existence of the sigma phase in the Cr-Ni-Si system even though the phase is not stable in any of the component binary systems. Phase diagram calculations were performed for the Cr-Fe-Ni-Si system using the ALLOYDATA system. Unfortunately whereas in ternary systems these calculations can be represented in terms of an isothermal section, in a quaternary system the equivalent representation is a pyramid which is difficult to display quantitatively. A schematic representation of the calculated diagram for 800 K is shown in Fig 7.2 for alloys containing up to 0.08 mole fraction Si. This shows the dramatic stabilising effect of silicon on the sigma phase which consequently has ramifications for the use of these alloys as cladding materials.

The representation of the quaternary phase diagram for the Cr-Fe-Ni-Si system is possible only schematically. Even this is not possible for systems of 5 or more elements. Nevertheless calculations can be made and tabulated as shown in Fig 7.3 for the Cr-Fe-Ni-Si-Ti system in this case using the program MULTIPHASE developed by Hodson (303). Here the compositions and type of the phases in equilibrium are

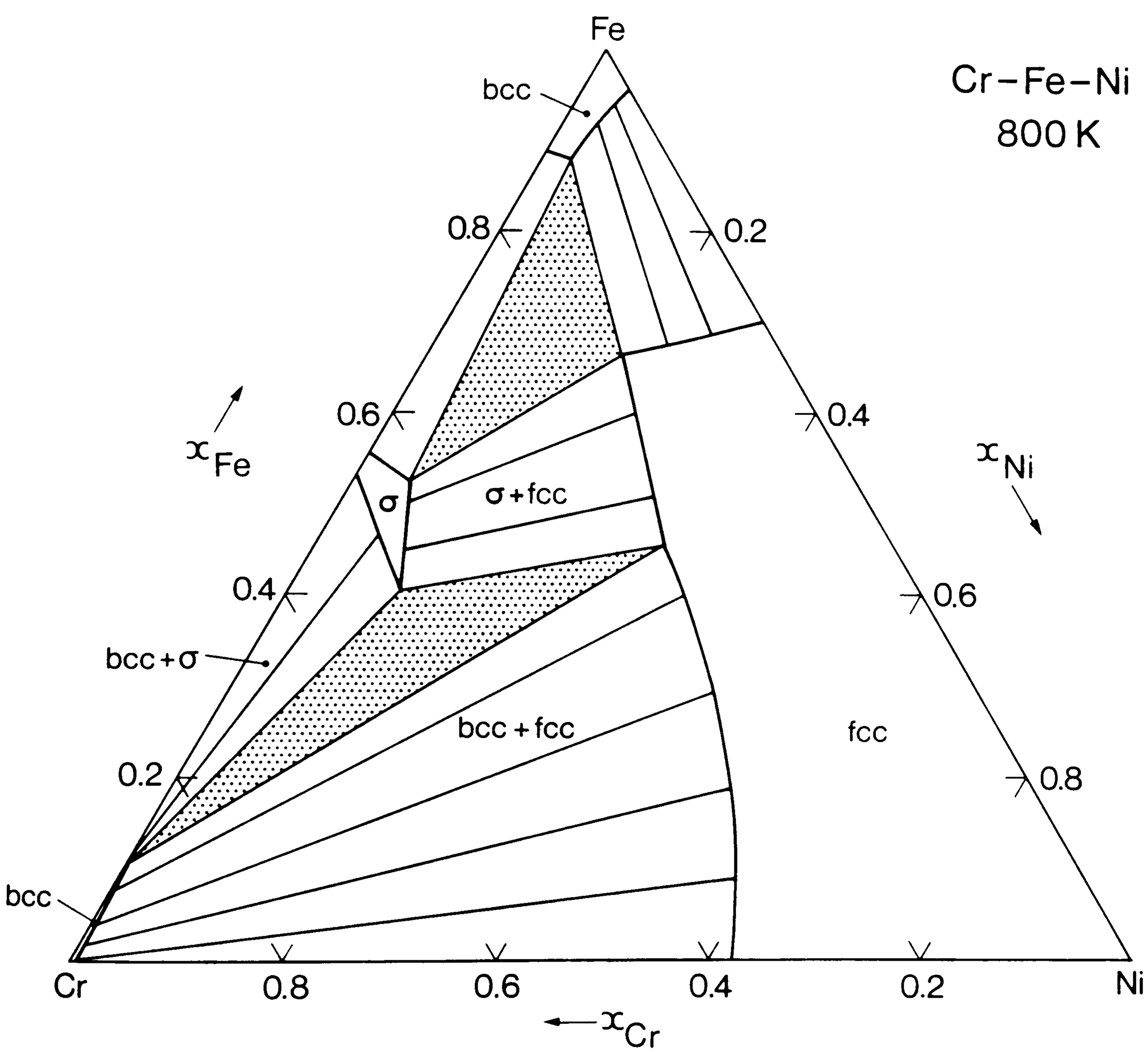

Fig 7.1 Calculated phase diagram for the Cr-Fe-Ni system for 800 K.

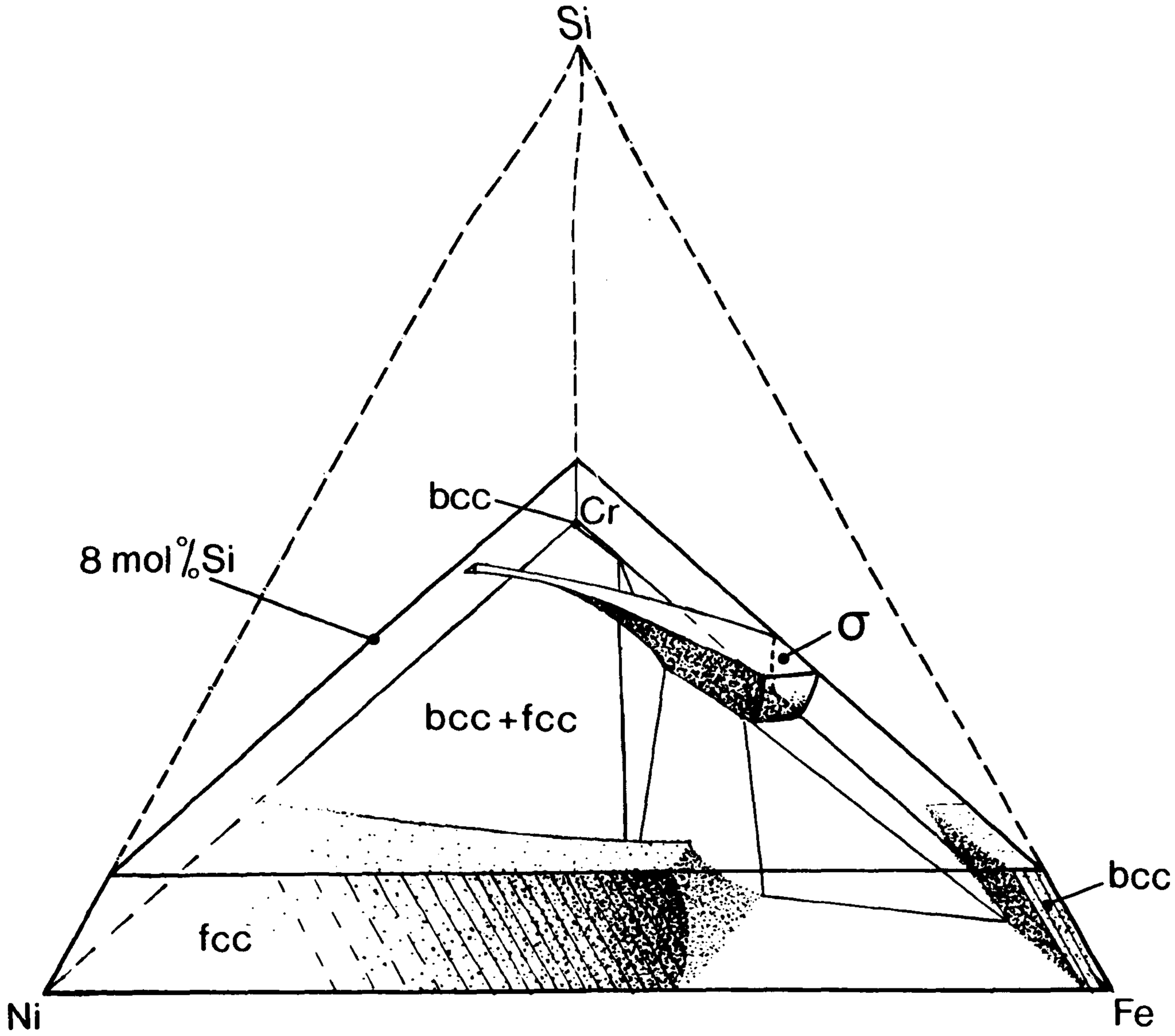

Fig 7.2 Schematic representation of calculated phase diagram for the Cr-Fe-Ni-Si system for 800 K for alloys containing up to 0.08 mole fraction Si.

Fig 7.3 Output from MULTIPHASE for the calculation of the compositions and types of phases in equilibrium for the Cr-Fe-Ni-Si-Ti system at 900 K for a given overall composition.

```
TEMPERATURE  900.000

COMPONENT QUANTITIES
 CR              1.400000D-01
 FE              7.400000D-01
 NI              8.000000D-02
 SI              3.000000D-02
 TI              1.000000D-02

SUM OF COMPONENTS =  1.000000D 00
INITIAL POINT SET BY PROGRAM

 ERROR IN AMOUNT IS LESS THAN 1.5D-05
```

PHASE	SPEC PHASE -IES PRESENT	AMOUNT(N)	MOLE FRACTION		CHEMICAL POTENTIAL
STOICHIOMETRIC PHASES					
CR3SI	1	1	0		
CR5SI3	2	1	0		
FE5SI3	3	1	0		
FESI	4	1	0		
NI5SI2	5	1	0		
NI3TI	6	1	0		
SI3TI5	7	1	0		
CRFETI	8	1	0		
FCC PHASE					
CR(FCC)	9	1	1	5.379778D-02	1.268670D-01 -4.102883D 03
FE(FCC)	9	2	1	2.935041D-01	6.921474D-01 -1.257559D 03
NI(FCC)	9	3	1	6.083208D-02	1.434555D-01 -2.392371D 04
SI(FCC)	9	4	1	1.421155D-02	3.351397D-02 -1.211684D 05
TI(FCC)	9	5	1	1.703040D-03	4.016144D-03 -8.050750D 04
PHASE TOTAL IS				4.240486D-01	
BCC PHASE					
CR(BCC)	10	1	1	5.359688D-02	1.085184D-01 -4.102883D 03
FE(BCC)	10	2	1	4.041430D-01	8.182741D-01 -1.257559D 03
NI(BCC)	10	3	1	1.515611D-02	3.068679D-02 -2.392371D 04
SI(BCC)	10	4	1	1.270697D-02	2.572798D-02 -1.211684D 05
TI(BCC)	10	5	1	8.293910D-03	1.679280D-02 -8.050750D 04
PHASE TOTAL IS				4.938969D-01	
SIGMA PHASE					
CR(SIGMA)	11	1	1	3.260506D-02	3.973872D-01 -4.102883D 03
FE(SIGMA)	11	2	1	4.235062D-02	5.161650D-01 -1.257559D 03
NI(SIGMA)	11	3	1	4.009348D-03	4.886552D-02 -2.392371D 04
SI(SIGMA)	11	4	1	3.081402D-03	3.755581D-02 -1.211684D 05
TI(SIGMA)	11	5	1	2.169456D-06	2.644110D-05 -8.050756D 04
PHASE TOTAL IS				8.204860D-02	
XNI3 PHASE					
FENI3FCC	12	1	0		
NI3SIFCC	12	2	0		
HEX PHASE					
CR2TIHEX	13	1	0		
FE2TIHEX	13	2	0		
CUB PHASE					
CR2TICUB	14	1	0		
FE2TICUB	14	2	0		

```
GIBBS FREE ENERGY = -7.858971D 03
```

calculated for a given temperature and set of element mole fractions.

The second series of calculations were carried out on some low alloy steels to test a procedure suggested for the removal of certain unwanted impurities by precipitation. It is thought that most common low alloy steels manufactured in Europe have sufficiently high levels of impurities such that all intergranular failures are caused by segregation. The obvious procedure, that of using purer materials in the steelmaking process is expensive and may also lead to other desirable properties being affected. Moreover these impurities tend to accumulate as a result of recycling (375). An alternative and potentially cheaper process would be to add some material to the steel which would 'lock up' these unwanted impurities by forming stable intermetallic compounds.

For these low alloy steels the harmful impurities are phosphorus, copper and tin which appear to segregate to the grain boundaries and cause intergranular stress corrosion as shown by Lea and Hondros (376). Rare earth elements and in particular lanthanum were suggested as suitable additions to 'lock up' these impurities. Early calculations of Seah et al. (377) showed that such an approach should be successful and this was confirmed by experimental work. However their calculations were essentially qualitative, did not consider the effect on the carbide structure of the steel and used thermochemical models, data and computer programs which, for these types of calculation, have now been superseded. New calculations were performed which were quantitative and made use of the latest data and techniques.

For this work four low alloy steels, about 96% Fe, were studied including a basically 2.25Cr-1Mo steel and one with rather lower Cr and Mo content. For simplicity the steel was assumed to consist of 7 elements - Fe, Cr, Mo and C with the harmful impurities P, Cu and Sn. For these calculations the rare earth additions were assumed to be in the form of Mischmetall which is rather cheaper than pure lanthanum. It

was taken to consist of equal proportions of La and Ce. Any oxygen or sulphur impurities in the steel which had not been removed by manganese, aluminium or titanium added were predicted to react with the Mischmetall in preference to the other impurities forming stable oxysulphides (e.g. La_2O_2S). Thermodynamic data were derived or taken from the ALLOYDATA database for the bcc phase in the 36 component binary systems of the nine component system and 35 selected stoichiometric binary compounds in order to calculate the equilibria for certain ranges of composition between temperatures of 800 K and 1200 K. Cementite, Fe_3C, was included in the calculations in spite of the fact that it is known to be metastable relative to ferrite and graphite. In practice it is known that the kinetics favour its formation and that it is stabilised by small quantities of other elements.

Calculations were performed using Eriksson's SOLGASMIX computer program (276,277) suitably modified to allow the representation of a multicomponent bcc solution phase in terms of a Redlich-Kister polynomial (296). The equilibrium assemblage was calculated for various additions of Mischmetall to the steels. Fig 7.4 shows the output for a typical calculation. These calculations represented a considerable advance over earlier calculations involving the precipitation of compounds in steels (255,377). In these previous calculations the interactions between different solute atoms were neglected and no account was taken of the relative amounts of the minor constituents. Consequently the calculations could not predict accurately the distribution of the minor elements between the various competing phases. The dataset and computer program used for these calculations do not suffer from such limitations and can in principle be used for a wide range of compositions and temperatures.

Fig 7.5 and Fig 7.6 show the distribution of C and the harmful impurities P, Sn and Cu between the bcc phase and the competing

Fig 7.4 Output from SOLGASMIX for the calculation of the distribution of carbon and the harmful impurities P, Cu and Sn between the various competing phases in a low alloy steel following the addition of Mischmetall.

T = 1000.00 K
P = 1.000E+00 ATM

	INPUT AMOUNT MOL	EQUIL AMOUNT MOL	MOLE FRACTION	ACTIVITY
FE(BCC)	0.96128E+00	0.96128E+00	0.97808E+00	0.97895E+00
CE(BCC)	0.10000E-02	0.10000E-02	0.10175E-02	0.54417E-07
LA(BCC)	0.10000E-02	0.58880E-07	0.59909E-07	0.92097E-04
CU(BCC)	0.11000E-02	0.64531E-03	0.65659E-03	0.86374E-01
SN(BCC)	0.60000E-04	0.15726E-05	0.16001E-05	0.31136E-05
C(BCC)	0.56000E-02	0.19858E-03	0.20205E-03	0.25936E-07
CR(BCC)	0.23100E-01	0.15778E-01	0.16053E-01	0.88276E-01
P(BCC)	0.22000E-03	0.27904E-09	0.28392E-09	0.18416E-14
MO(BCC)	0.61000E-02	0.39219E-02	0.39905E-02	0.10951E+00
FE17CE2	0.00000E+00	0.00000E+00		0.96204E+00
FE2CE	0.00000E+00	0.00000E+00		0.19278E-01
FE3SN	0.00000E+00	0.00000E+00		0.59943E-01
FE3SN2	0.00000E+00	0.00000E+00		0.10857E-01
FESN	0.00000E+00	0.00000E+00		0.32117E-02
FE3C	0.00000E+00	0.00000E+00		0.60417E+00
FE3P	0.00000E+00	0.00000E+00		0.11421E-01
FE3MO2	0.00000E+00	0.00000E+00		0.51101E+00
CECU	0.00000E+00	0.00000E+00		0.15747E-02
CECU2	0.00000E+00	0.00000E+00		0.40140E-01
CECU4	0.00000E+00	0.00000E+00		0.18689E+00
CECU5	0.00000E+00	0.00000E+00		0.27088E+00
CECU6	0.00000E+00	0.00000E+00		0.33304E+00
CE2SN	0.00000E+00	0.00000E+00		0.68186E-02
CE2SN3	0.00000E+00	0.00000E+00		0.31549E-02
CESN3	0.00000E+00	0.00000E+00		0.12258E-02
CEC2	0.00000E+00	0.00000E+00		0.11762E+00
CEP	0.00000E+00	0.00000E+00		0.23773E-01
LACU	0.00000E+00	0.00000E+00		0.66237E-01
LACU2	0.00000E+00	0.00000E+00		0.48429E+00
LACU5	0.00000E+00	0.00000E+00		0.93737E+00
LACU6	0.00000E+00	0.53056E-03		0.10000E+01
LA2SN	0.00000E+00	0.17546E-03		0.10000E+01
LA2SN3	0.00000E+00	0.00000E+00		0.62822E-01
LASN3	0.00000E+00	0.00000E+00		0.79501E-02
LAC2	0.00000E+00	0.17629E-02		0.10000E+01
LAP	0.00000E+00	0.44000E-03		0.10000E+01
CU31SN8	0.00000E+00	0.00000E+00		0.31464E-01
CU3SN	0.00000E+00	0.00000E+00		0.20246E-01
CU3P	0.00000E+00	0.00000E+00		0.27312E-02
CUP2	0.00000E+00	0.00000E+00		0.11524E-07
C2CR3	0.00000E+00	0.00000E+00		0.98823E+00
C3CR7	0.00000E+00	0.10461E-01		0.10000E+01
C6CR23	0.00000E+00	0.00000E+00		0.52446E+00
CMO2	0.00000E+00	0.32654E-02		0.10000E+01

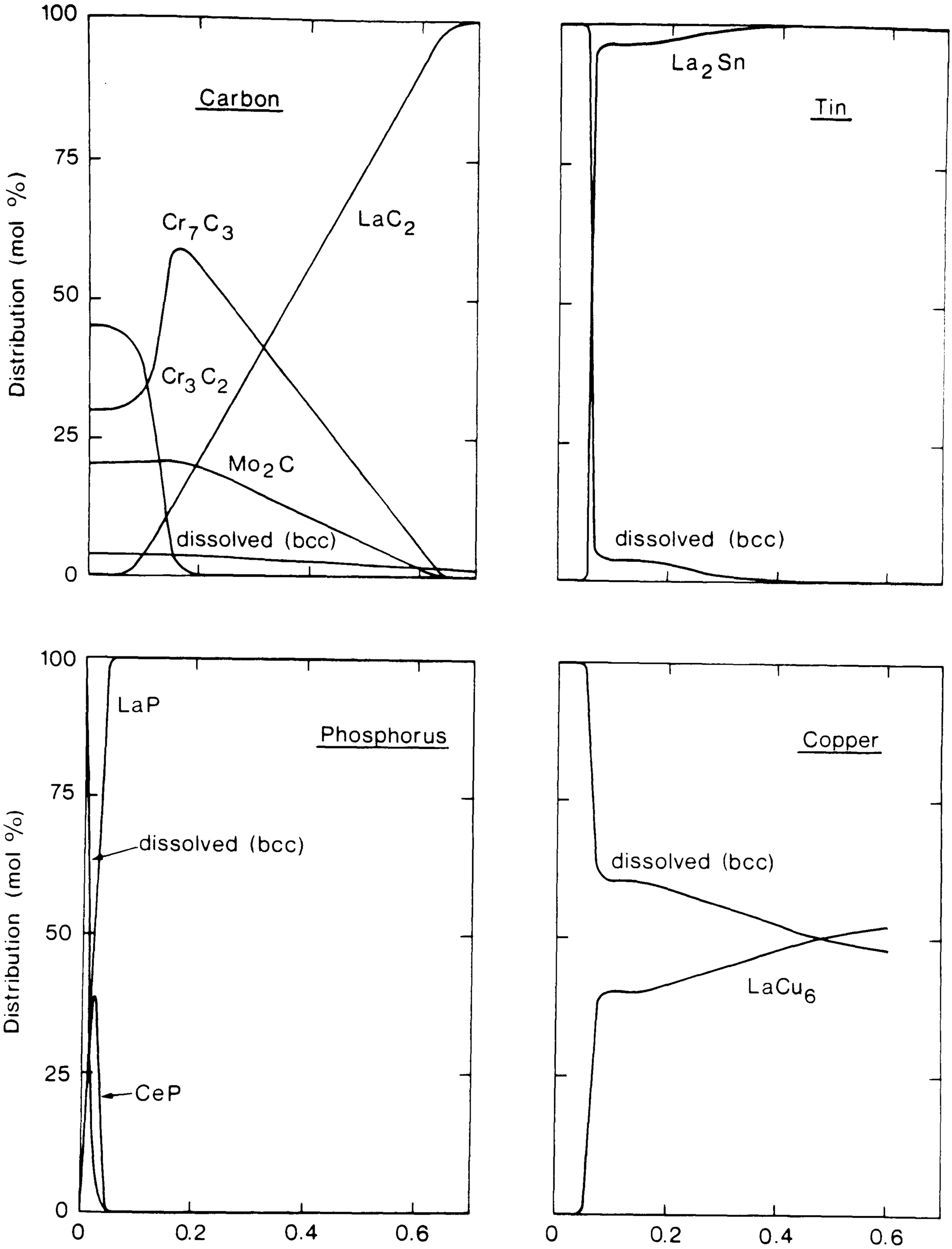

Fig 7.5 Distribution of carbon and the harmful impurities P, Cu and Sn between the various competing phases for a 2.25Cr-1Mo steel as a function of the amount of added Mischmetall at 1000 K.

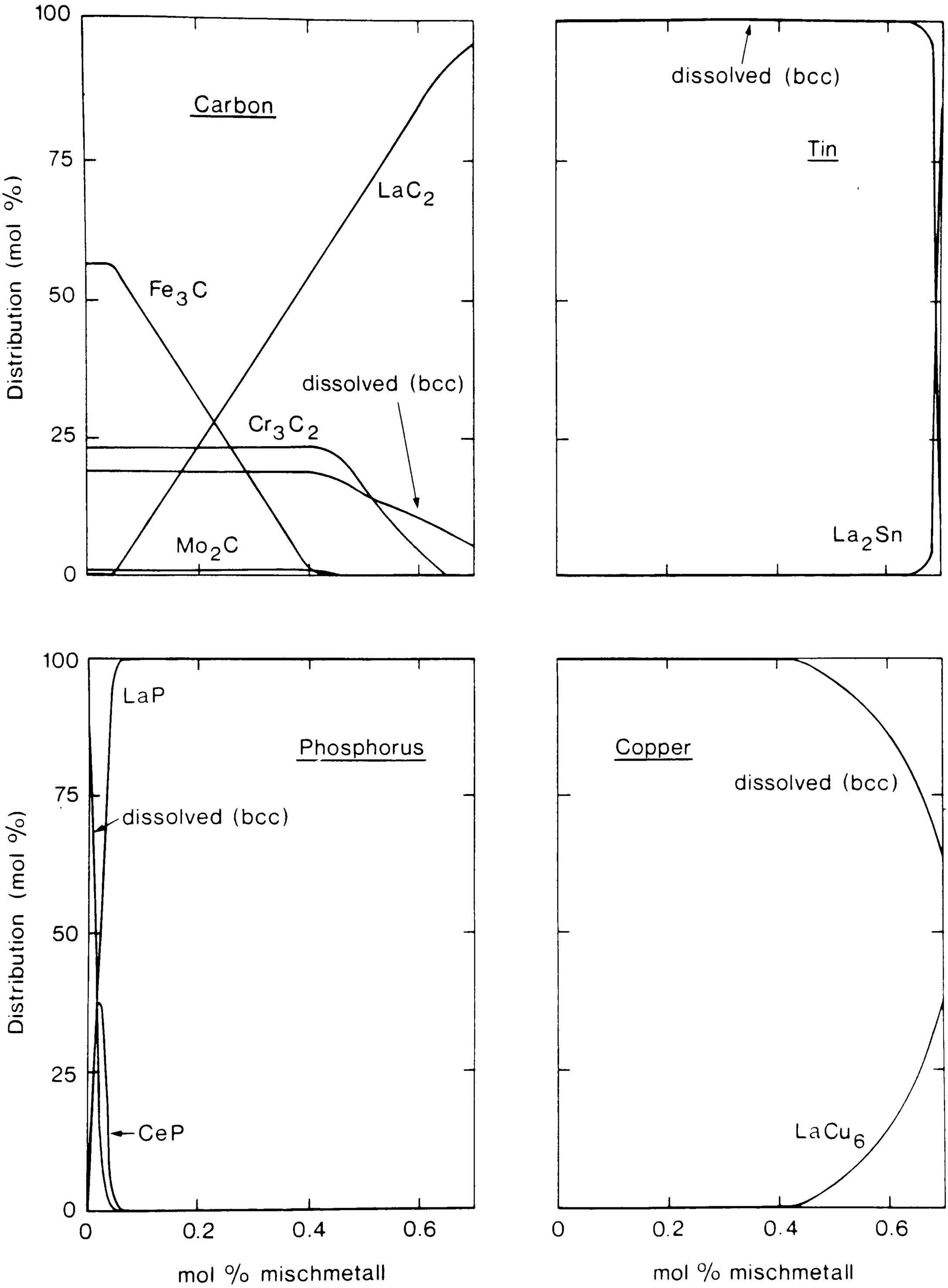

Fig 7.6 Distribution of carbon and the harmful impurities P, Cu and Sn between the various competing phases for a low alloy steel as a function of the amount of added Mischmetall at 1000 K.

intermetallic compounds for two of the steels under study at 1000 K. It can be seen from these calculations that lanthanum is a far more effective additive than cerium. Fig 7.5, for a 2.25Cr-1Mo steel shows that relatively small amounts of Mischmetall need be added in order to obtain essentially complete removal of phosphorus and tin as LaP and La_2Sn respectively and removal of 40% of Cu in the form of $LaCu_6$. It should be mentioned that this work predicts the removal of phosphorus before tin in contrast to that predicted by Seah et al. (377). This is due largely to the more reliable thermodynamic data available now. The removal of phosphorus is most important since phosphorus is known to be very embrittling in a 2.25Cr-Mo steel. Seah et al. were unable to gauge the effect of the addition of the Mischmetall on the carbide structure of the steel. Fig 7.5 shows this to be unaffected for relatively modest additions of Mischmetall.

Fig 7.6, on the other hand, which represents the effect of Mischmetall on a steel with rather less Cr and Mo, shows that while relatively small amounts of Mischmetall are required to remove phosphorus, large amounts are required to have any effect on the levels of dissolved tin and copper. By that stage the Mischmetall additions would have affected the carbide structure of the steel to the extent that its physical properties would no longer be within the specification.

The difference between the two steels can be attributed to the lower Cr and Mo content in the steel represented by Fig 7.6. For the 2.25Cr-1Mo steel (Fig 7.5) the activity of carbon in the bcc phase is effectively lowered by the formation of the stable carbides Cr_3C_2, Cr_7C_3 and Mo_2C. This allows Mischmetall to react with the tramp elements. For Fig 7.6 the carbon activity is higher promoting reaction with the Mischmetall before the Mischmetall can react with the tin or copper.

This work was able to define successfully a range of Mischmetall

additions to various steels to provide, in theory, immunity to stress corrosion cracking. The results are based on thermodynamic data and do not take into account the kinetics of phase transformation which can also be expected to be important. However the results can be applied with confidence when predicting the long term stability of materials.

Conclusions

Presented in this chapter is a brief description of two sets of calculations from thermodynamic data which have been performed to elucidate the long term stability of certain steels. The work has utilised the latest techniques for the calculation of phase equilibria and representation of thermodynamic data. More calculations of importance to industry can be performed readily, especially when the thermodynamic database has been expanded to cover more elements.

CHAPTER 8

Phase Diagrams and Thermodynamic data for Cu-Fe-Ni-S system

Introduction

The aim of this work was to gain greater understanding of the phase equilibria in the metal rich part of the Cu-Fe-Ni-S system in order to help improve the pyrometallurgical extraction of copper and other valuable metals from sulphide ores based on this system. Experience has shown that phase transformations in these systems occur readily at moderate temperatures and this suggests that a reliable way for understanding and predicting behaviour would be to perform calculations of the phase diagram from the thermodynamic data. The success achieved for alloy systems in the calculation of multicomponent thermodynamic data and phase diagrams from the thermodynamic data of the component binary systems has led to the adoption of this approach for sulphide systems.

Representation of Data for the Liquid Phase

The major problem associated with this work was the representation of the thermodynamic data in terms of composition for the different phases. The liquid phase is particularly difficult to represent because in all metal-sulphur systems its thermodynamic properties show marked changes at particular compositions. These compositions differ from system to system and it has been proposed that this phenomenon was due to some sort of ordering. Conventional power series expressions such as the Redlich-Kister expression are not capable of representing the data adequately although Pelton and Bale (161) have represented the liquid

data for the Cu-Fe-S system using a Fourier cosine series. Clearly any reliable method for predicting multicomponent phase diagrams must attempt to model this physical ordering phenomenon.

As discussed in chapter 3 much research has already been carried out into methods for representing the data for these sulphide liquids. In particular it is worth emphasising the work of Kellogg, Larrain and their colleagues (213,214,217,219,220,378-382) who have carried out extensive measurements of sulphur pressures above the liquid phase and modelled their data in terms of associated species. Their work should not, however, be thought of as predictive but rather as a correlation of the data in terms of a large number of coefficients and associate species. Chang and his colleagues (74,204,216,221,223,383,384) have also been interested in these systems and have also used the associated solution model for the liquid phase. Their approach has been rather more predictive and they have attempted to represent both liquid and solid phases with as few coefficients as necessary.

The other major effort on these systems to date was from Hillert and his colleagues (229,231-233) who have advocated the use of an extended two sublattice model for the liquid phase whereby metal atoms and vacancies mix on the first sublattice and sulphur atoms and vacancies mix on the other sublattice. Except for their treatment of the metal rich part of the Fe-Mn-S system (231) using a simplified description they have not reported any ternary sulphide phase diagram calculations.

An extensive analysis of the different models on the Fe-S and Cu-S system was carried out in this present work leading to the conclusion that an extended two sublattice model was best suited to represent the complex behaviour of these systems. This model was chosen because it seems in principle physically more realistic than the associated solution model for melts of substances that as crystals have extended rather than molecular bonding such as mattes. Because of this it should

offer superior prospects for the extrapolation of the binary thermodynamic data for the liquid phase into the ternary and quaternary systems without the necessity of introducing an excessive number of ternary or higher order parameters. This extrapolation is vital for the correct prediction of the phase diagram for the Fe-Cu-Ni-S system.

For the Fe-S liquid phase Fernandez Guillermet et al (232-233) assumed that there was an equal number of sites in the two sublattices which reflects the abrupt change in the thermodynamic properties at about the composition x_S=0.5. For the Cu-S system this abrupt change in behaviour occurs at about x_S=0.33 while in the Ni-S system it occurs at about x_S=0.4. A number of variations of the two sublattice model could in principle be used to represent the liquid data of the Cu-S system. However, it is important that the model, in addition to representing the Cu-S binary data accurately and extrapolating them reliably into a ternary system, is consistent with accepted descriptions for the other component systems.

One model that was tested allows the combination of the data for the Fe-S system (1:1 site ratio) with data for the Cu-S system derived assuming a 2:1 ratio of the number of sites between the sublattices. This ratio of sites for the Cu-S system is implied by the change in the thermodynamic properties at about x_S=0.33. It assumes that in the ternary system the copper atoms can occupy twice as many sites as the iron atoms even though the iron and copper atoms would mix together on the same sublattice. In effect an iron atom would occupy twice the space occupied by a copper atom. Even though trial calculations made with this model were in good agreement with available experimental data it required a non-conventional and non-physical representation of the thermodynamic data for the copper-iron binary system.

A second model, based on a suggestion of Hillert (385), does not suffer from such a drawback. It assumes that the liquid phase consists

of ions and charged vacancies. Vacancies would be considered as having a charge equal in magnitude but opposite in sign to a corresponding ion on the other sublattice. Hillert proposed that copper would be univalent while iron and sulphur would be divalent. Therefore for the Cu-S liquid phase, on the metal sublattice there would be copper ions and vacancies with a charge of +2 while on the sulphur sublattice there would be sulphur ions and vacancies with a charge of -1. The ratio of sites between the two sublattices would not be fixed but would be defined by a charge balance between the various ions and charged vacancies. There is however no suggestion that these charges are formally present.

According to the original approach suggested by Hillert, the ternary Cu-Fe-S liquid phase could be represented in terms of two sublattices with three species on each sublattice. The metal sublattice would consist of Fe^{+2} and Cu^{+} ions and vacancies with a +2 charge. The sulphur sublattice would consist of S^{-2} ions with two types of vacancy to balance the two types of metal ions on the other sublattice. This has a severe disadvantage in requiring many data that are unavailable from the component binary systems. The model was therefore modified so as to require only one type of vacancy on the sulphur sublattice where its charge would be non-integral varying according to the relative amounts of copper and iron in the phase.

This model was also tested for its capability for extrapolation into the Cu-Fe-S system and was found to give excellent agreement with the ternary experimental data. This together with its use of conventionally represented Cu-Fe data led to the adoption of this model to represent the liquid phase thermodynamic data for phase diagram calculations.

The general multicomponent model for metal-sulphides will now be described and an expression derived for the Gibbs energy of formation of compositions in that phase.

Details of liquid phase model

First of all we can consider that the phase contains m elements - ie. m-1 metallic elements plus sulphur. The metal atoms in the system can be designated by A_i and their the mole fractions by x_i while the mole fraction of sulphur will be x_S.

In the two sublattice model adopted for this work it is assumed that the metal atoms and sulphur atoms occupy different sublattices. Following Hillert's suggestion (385) each species in the phase carries a notional charge. We can define the charge of the sulphur species as -b and the charge on each metal atom as $+a_i$. Vacancies are included in each of the sublattices and they also have charges. In the case of the vacancies Va on the metal sublattice the charge will be opposite in sign but equal in magnitude to the charge on the sulphur atoms in the second sublattice ie. +b. The charge -e on the vacancies Vc in the second sublattice would vary according to the relative proportions of metal ions and their charges according to:

$$e = \frac{\sum_{i=1}^{m-1} a_i x_i}{\sum_{i=1}^{m-1} x_i} \qquad 1$$

For convenience we can designate the phase in terms of the various species on the two sublattices as:

$$[\ M_i^{+a_i}, \ldots\ldots, Va^{+b}\ ]_p\ [\ S^{-b}, Vc^{-e}\ ]_q$$

where p and q are the number of sites on the two sublattices per unit cell. It is often convenient to choose the value of q as 1. The ratio of p to q is not fixed for the whole phase but is defined by a condition that the system should be electrically neutral.

It is useful to define a variable s, the size of the system given by:

$$s = \frac{\sum_{i=1}^{m-1} x_i + x_{Va}}{p} = \frac{x_S + x_{Vc}}{q} \qquad 2$$

For simplicity it is also useful to designate x_{Va} as x_m. For each species it is necessary to define a site fraction Z_i such that:

$$Z_i = \frac{x_i}{\sum_{k=1}^{m} x_k} \qquad 3$$

where in this case the species i is on the first sublattice. The site fractions of species on the second sublattice can be defined in a similar way.

Since the phase is electrically neutral it is possible to derive a relationship between p and q.

$$\sum_{i=1}^{m-1} a_i x_i + b\, x_{Va} = b\, x_S + e\, x_{Vc} \qquad 4$$

According to equation 2

$$\sum_{i=1}^{m-1} x_i + x_{Va} = p\, s$$

and

$$x_S + x_{Vc} = q\, s$$

Substituting these into the above equation and rearranging one obtains:

$$\sum_{i=1}^{m-1} x_i \sum_{i=1}^{m-1} a_i x_i + b\, p\, s \sum_{i=1}^{m-1} x_i - b \left(\sum_{i=1}^{m-1} x_i\right)^2 =$$

$$b\, x_S \sum_{i=1}^{m-1} x_i + q\, s \sum_{i=1}^{m-1} a_i x_i - x_S \sum_{i=1}^{m-1} a_i x_i$$

which gives, on further rearrangement and through application of the

condition:

$$\sum_{i=1}^{m-1} x_i + x_S = 1$$

$$p = \frac{b \sum_{i=1}^{m-1} x_i + (q\,s - 1) \sum_{i=1}^{m-1} a_i x_i}{b\,s \sum_{i=1}^{m-1} x_i} \qquad 5$$

If we consider for example a binary system (m=2) where the charge on the the metal atoms is the same as that on the sulphur atoms ie. b = a, this expression simplifies to p = q. This is equivalent to the representation of Fernandez Guillermet et al. (232,233) for the Fe-S system. If however b = 2a as with the Cu-S system for example

$$p = \frac{1 + qs}{2s}$$

The Gibbs energy of formation can now be expressed as the sum of four terms.

a) The Gibbs energies of transformation for the pure elements from their reference phases to the liquid phase, ${}^{o}G_i$ and ${}^{o}G_S$.

b) The formation of the hypothetical materials, liquid $A_{i_w}S$ for each metal, where w represents the stoichiometry b/a_i.

c) The ideal mixing between ions and vacancies within the sublattices.

d) The interaction between species on the same sublattice. This part of the expression contains coefficients of the form $G[A_i:S,Vc]$ which in this case represents the interaction between sulphide ions and anionic vacancies in the presence of A_i ions on the metal sublattice. Similarly $G[A_i,A_k:S]$ describes the interaction between the metal ions A_i and A_k in the presence of S ions on the second sublattice.

The Gibbs energy of formation is therefore given by:

$$\Delta_f G = \sum_{i=1}^{m-1} x_i \, {}^{o}G_i + x_S \, {}^{o}G_S$$

$$+ s \{ \sum_{i=1}^{m-1} Z_i Z_S \, {}^{o}G_{A_i w S}$$

$$+ R T p [\sum_{i=1}^{m} Z_i \ln Z_i]$$

$$+ R T q [Z_S \ln Z_S + Z_{Vc} \ln Z_{Vc}]$$

$$+ \sum_{i=1}^{m} Z_i Z_S Z_{Vc} \sum_{h=0}^{r} G[A_i : S, Vc]_h \, (Z_S - Z_{Vc})^h$$

$$+ Z_S \sum_{i=1}^{m-1} \sum_{k=i+1}^{m} Z_i \, Z_k \sum_{h=0}^{r} G[A_i, A_k : S]_h \, (Z_i - Z_k)^h$$

$$+ Z_{Vc} \sum_{i=1}^{m-1} \sum_{k=i+1}^{m} Z_i \, Z_k \sum_{h=0}^{r} G[A_i, A_k : Vc]_h \, (Z_i - Z_k)^h$$

$$+ Z_S Z_{Vc} \sum_{i=1}^{m-2} Z_i \sum_{k=i+1}^{m-1} Z_k \sum_{h=0}^{r} \sum_{l=0}^{t} G[A_i, A_k : S, Vc]_{h,l}$$

$$(Z_i - Z_k)^h \, (Z_S - Z_{Vc})^l \}$$

where, for example, h defines the coefficient of the polynomial up to the maximum order r.

The Gibbs energy of formation is a function of the size of the system s which is related to the total population of the vacancies within the phase. This is not defined directly by the model and it is necessary to find the value of s which will give the lowest value for the Gibbs energy of formation. This will in turn describe the vacancy population.

It is not possible to solve this problem explicitly and it is neccessary to use some sort of numerical technique to determine the conditions for the minimum value of the Gibbs energy. A convenient

method is to use a Newton-Raphson method whereby one searches for the values of s that satisfies the condition that (dG/ds)=0. An explicit expression was derived for this first differential while the second differential (d^2G/ds^2) was evaluated numerically from the first differential evaluated for two very close values of s. For a given estimate of s the first and second derivatives can be combined to lead to a better value which can itself be used in the same way and so on until the required accuracy has been obtained.

The differential of the Gibbs energy of formation with respect to the size of the system is given by:

$$\frac{d\,\Delta_f G}{ds} = - k\, Z_S \sum_{i=1}^{m-1} Z_i\, {}^{o}G_{A_{iw}S}$$

$$+ R\,T\,p\,k\,\ln(Z_{Va}) + R\,T\,q\,\ln(Z_{Vc})$$

$$+ Z_S(Z_S - k\,Z_{Vc}) \sum_{i=1}^{m-1} Z_i \sum_{h=0}^{r} G[A_i:S,Vc]_h\,(Z_S - Z_{Vc})^h$$

$$+ Z_S(k\,Z_{Vc}(1 - Z_{Va}) + Z_{Va}Z_{Vc}) \sum_{h=0}^{r} G[Va:S,Vc]_h\,(Z_S - Z_{Vc})^h$$

$$- 2Z_S^2 Z_{Vc} \sum_{i=1}^{m} Z_i \sum_{h=1}^{r} h\,G[A_i:S,Vc]_h\,(Z_S - Z_{Vc})^{h-1}$$

$$- 2\,k\,Z_S \sum_{i=1}^{m-2} Z_i \sum_{k=1}^{m-1} Z_k \sum_{h=0}^{r} G[A_i,A_k:S]_h\,(Z_i - Z_k)^h$$

$$+ k\,Z_S\,(1 - 2\,Z_{Va}) \sum_{i=1}^{m-1} Z_i \sum_{h=0}^{r} G[A_i,Va:S]_h\,(Z_i - Z_{Va})^h$$

$$- k\,Z_S \sum_{i=1}^{m-2} \sum_{k=i+1}^{m-1} Z_i\,Z_k\,(Z_i - Z_k) \sum_{h=1}^{r} h\,G[A_i,A_k:S]_h\,(Z_i - Z_k)^{h-1}$$

$$+ (1 - 2\,k\,Vc) \sum_{i=1}^{m-2} \sum_{k=i+1}^{m-1} Z_i\,Z_k \sum_{h=0}^{r} G[A_i,A_k:Vc]_h\,(Z_i - Z_k)^h$$

$$+ (Z_{Va} + Z_{Vc}\,k\,(1 - 2\,Z_{Va}) \sum_{i=1}^{m-1} Z_i \sum_{h=0}^{r} G[A_i,Va:Vc]_h\,(Z_i - Z_{Vc})^h$$

$$- \; k \, Z_{Vc} \sum_{i=1}^{m-2} \sum_{k=i+1}^{m-1} Z_i \, Z_k \, (Z_i - Z_k) \sum_{h=1}^{r} h \, G[A_i, A_k : Vc]_h \, (Z_i - Z_k)^{h-1}$$

$$- \; k \, Z_{Vc} \, Z_{Va} \sum_{i=1}^{m-1} Z_i \, (1 + Z_i - Z_{Va}) \sum_{h=1}^{r} h \, G[A_i, Va : Vc]_h \, (Z_i - Z_{Vc})^{h-1}$$

$$- \; k \, Z_S \, Z_{Va} \sum_{i=1}^{m-1} Z_i \, (1 + Z_i - Z_{Va}) \sum_{h=1}^{r} h \, G[A_i, Va : S]_h \, (Z_i - Z_{Vc})^{h-1}$$

$$+ \; Z_S \, (Z_S - 2 \, k \, Z_{Vc}) \sum_{i=1}^{m-2} Z_i \sum_{k=i+1}^{m-1} Z_k \sum_{h=0}^{r} \sum_{l=0}^{t} G[A_i, A_k : S, Vc]_{h,s} \cdot$$

$$(Z_i - Z_k)^h \, (Z_S - Z_{Vc})^l$$

$$- \; k \, Z_S \, Z_{Vc} \sum_{i=1}^{m-2} \sum_{k=i+1}^{m-1} Z_i \, Z_k \, (Z_i - Z_k) \sum_{h=1}^{r} \sum_{l=0}^{t} h \, G[A_i, A_k : S, Vc]_{h,l}$$

$$(Z_i - Z_k)^{h-1} \, (Z_S - Z_{Vc})^l$$

$$- \; 2 \, Z_S^2 \, Z_{Vc} \sum_{i=1}^{m-2} \sum_{k=i+1}^{m-1} Z_i \, Z_k \sum_{h=0}^{r} \sum_{l=1}^{t} l \, G[A_i, A_k : S, Vc]_{h,l}$$

$$(Z_i - Z_k)^h \, (Z_S - Z_{Vc})^{l-1}$$

where $k = \dfrac{q \, e}{b \, p}$

Representation of data for the other phases

The thermodynamic data for the bcc, fcc and $L1_2$ phases of the metal-metal binary systems were represented by the widely used Redlich - Kister power series for the excess Gibbs energy of formation. It was assumed that the solubility of sulphur in these phases could be neglected. Using the binary data for the metallic systems which were combined using the Redlich-Kister ternary expression, Chart et al. (169) calculated the phase diagram for the Cu-Fe-Ni system over a range of temperatures and obtained good agreement with available experimental information. These data were therefore used for the Cu-Fe-Ni-S system.

Therefore for these phases containing m elements A_i where x_i denote their mole fractions, the Gibbs energy of formation from chosen reference phases for the pure elements is given by:

$$\Delta_f G = \sum_{i=1}^{m} x_i \, {}^{o}G_i$$

$$+ \; R\,T \sum_{i=1}^{m} x_i \ln(x_i)$$

$$+ \sum_{i=1}^{m-1} \sum_{j=i+1}^{m} x_i x_j \sum_{h=0}^{r} G[A_i,A_j]_h \, (x_i - x_j)^h$$

$$+ \sum_{i=1}^{m-2} \sum_{j=i+1}^{m-1} \sum_{k=j+1}^{m} x_i x_j x_k \, G[A_i,A_j,A_k]$$

where ${}^{o}G_i$ represents the Gibbs energies of transformation for the pure element i from its reference phase at the temperature T, $G[A_i,A_j]_h$ represents the h'th order coefficient for the binary interactions between atoms of A_i and atoms of A_j, $G[A_i,A_j,A_k]$ represents the ternary interaction between elements A_i,A_j and A_k and R represents the gas constant. All of the terms ${}^{o}G_i$, $G[A_i,A_j]_h$ and $G[A_i,A_j,A_k]$ can be expressed as a function of temperature.

For the purpose of this work where the metal rich part of the phase diagram is of interest, and in order to simplify the ternary and quaternary phase diagram calculations, sulphur solubility was also neglected in the binary phases FeS (pyrrhotite), Cu_2S (digenite) and NiS even though it is known to be appreciable. A study of ternary experimental information showed that none of the several phases of higher sulphur content than digenite and pyrrhotite has any effect on the phase equilibria in the metal rich part of the system. From experimental data it appeared that FeS and NiS are completely miscible and for convenience this whole phase has been labelled pyrrhotite for these calculations. In the literature the phase is often referred to as the monosulphide solid solution. Pyrrhotite and digenite (based about Cu_2S and sometimes labelled as bornite) are not completely miscible although both phases appear to intrude into the ternary systems in the direction of the other and this was assumed for these calculations. The model used to represent the data for these phases was a simplification of the model used to represent the data for the liquid phase but with the added assumption that no vacancies are present. The phase is assumed to contain m-1 metallic elements A_i and sulphur with mole fractions x_i (i=1...m-1) and x_S respectively. As for the liquid phase the metal and sulphur atoms are assigned notional charges : a_i for the metal atoms and b for the sulphur atoms.

The phase is restricted in composition to lie on a plane between binary stoichiometric compounds of composition $A_{iw}S$ where w represents the stoichiometry given by b/a_i. The size of the system, s, here is equal to x_S, the mole fraction of sulphur, since sulphur is the sole occupant of the anionic sublattice. We can also define site fractions for the metal sublattice Z_i, ie. the proportion on the sublattice of a given metal atom which will be given by:

$$Z_i = \frac{x_i}{ps}$$

Since the sum of the site fractions on the metal sublattice is equal to 1, the ratio of sites on the metal sublattice to those on the sulphur sublattice, p, will be given by:

$$p = \frac{1 - x_S}{x_S}$$

The Gibbs energy can therefore be expressed by:

$$\Delta_f G = x_S \{ \sum_{i=1}^{m-1} Z_i \, {}^{o}G_{A_{iw}S} + R\,T\,p \left[\sum_{i=1}^{m-1} Z_i \ln Z_i \right] + \sum_{i=1}^{m-2} \sum_{k=i+1}^{m-1} Z_i \, Z_k \sum_{h=0}^{r} G[A_i, A_k : S]_h \, (Z_i - Z_k)^h \; \}$$

where h defines the coefficient of the polynomial up to the maximum order r.

This expression contains three terms:

a) The Gibbs energies of formation of the compounds $A_{iw}S$.

b) The ideal mixing between the metal atoms.

c) The interaction between the metal atoms.

This expression requires data for the hypothetical forms of FeS and NiS in the digenite phase and Cu_2S in the pyrrhotite phase and these data must be derived from ternary thermodynamic or phase diagram information.

The beta phase based about the composition Ni_3S_2 was treated, for simplicity, in the derivation of the data for Ni-S system using a Redlich-Kister expression. This is almost certainly inappropriate and some sort of sublattice description similar to the liquid phase model may be better equipped to represent its data. Unfortunately the phase is apparently unquenchable which makes the exact choice of model difficult.

Furthermore certain evidence (383,386) suggests that in the Ni-S binary system the phase region consists of two distinct phases separated by a narrow two phase region. Both Fe and Cu are appreciably soluble in this phase and because of the obvious difficulties concerning this phase it was decided to continue to use, for simplicity, the Redlich-Kister expression which can be readily extrapolated into a multicomponent system. The expression for this model was also used for the bcc, fcc and $L1_2$ phase and was shown earlier.

The remaining solution phase of interest in the metal rich part of the Cu-Fe-Ni-S system is the pentlandite phase $(Fe,Ni)_9S_8$. It is believed that the solubility of Cu and S in this phase is small and was therefore neglected. This phase was modelled as a conventional substitutional solution between the Fe and Ni atoms on the metal sublattice with a second sublattice occupied solely by sulphur atoms. The ratio of sites between the sublattices is 9:8.

The remaining phases of interest in this system are the low temperature binary stoichiometric phases Chalcocite (Cu_2S), Millerite (NiS), Heazlewoodite (Ni_3S_2) and Ni_7S_6.

Assessment or Validation of data for the Binary Systems

The Cu-Fe system

The data for this system have been validated by Chart et al. (169). The phase diagram (Figure 8.1) is well established (44,53,55,387-391) although the Fe-based fcc solvus reported in earlier compilations, (e.g. Ref 53) has now been revised (44,387,390). The adopted thermodynamic data were taken from the assessment of Kubaschewski et al. (390). Other detailed thermodynamic assessments for this system have been carried out by Hasebe and Nishizawa (387,388) and Lindqvist and Uhrenius (389).

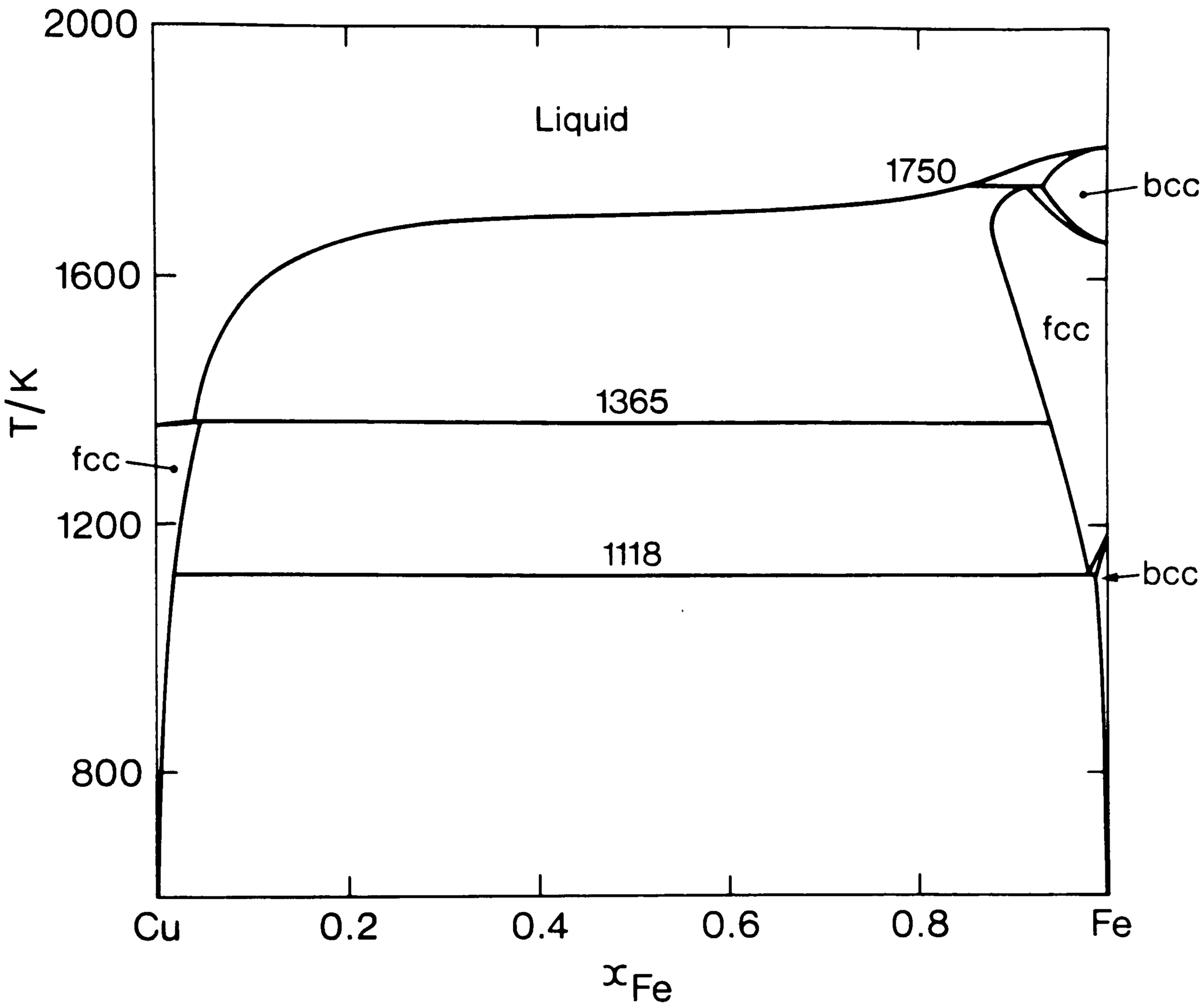

Fig 8.1 Calculated phase diagram for the Cu-Fe system.

The Cu-Ni system

The data for this system have also been validated by Chart et al (169). The phase diagram (Figure 8.2) is well established (44,53,54). Thermodynamic data have been taken from the assessment of Hasebe and Nishizawa (392). Other thermodynamic assessments for this system have been carried out by Elford et al. (393), Kaufman (394) and Larrain (395). The experimental thermodynamic data for this system (393) indicate the existence of a miscibility gap at temperatures below approximately 600 K.

The Fe-Ni system

The data for this system were also validated by Chart et al. (169). The phase diagram (Figure 8.3) is fairly well established (44,53-55). The phase relationships of reported ordered structures based on Fe_3Ni and FeNi (396-398) remain uncertain and these phases have not been considered. A detailed assessment of phase diagram data for this system has since been carried out by Xing and Chart (399). For this work the thermodynamic data have been taken from the assessment of Kaufman and Nesor (374), modified to incorporate the ordered $FeNi_3$-based phase as a solution phase. Thermodynamic assessments for this system have also been carried out by Hasebe and Nishizawa (392) and Larrain (218).

The Fe-S system

The Fe-S system has been critically assessed by Sharma and Chang (221) who used an associated solution model for the liquid phase, and by Hillert and Staffansson (229) and Fernandez Guillermet et al. (232,233) who used a two sublattice description for the liquid phase. The

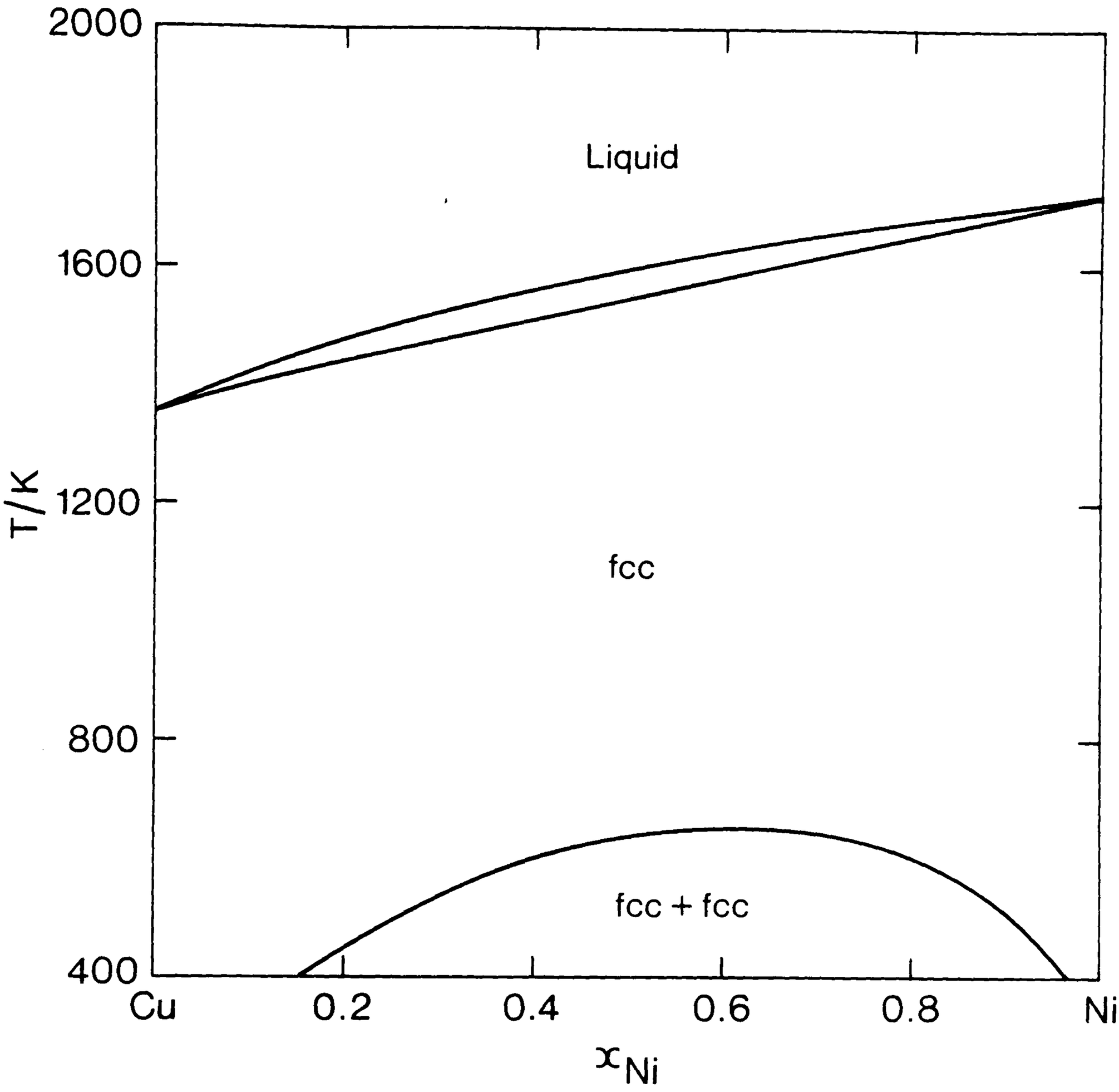

Fig 8.2 Calculated phase diagram for the Cu-Ni system.

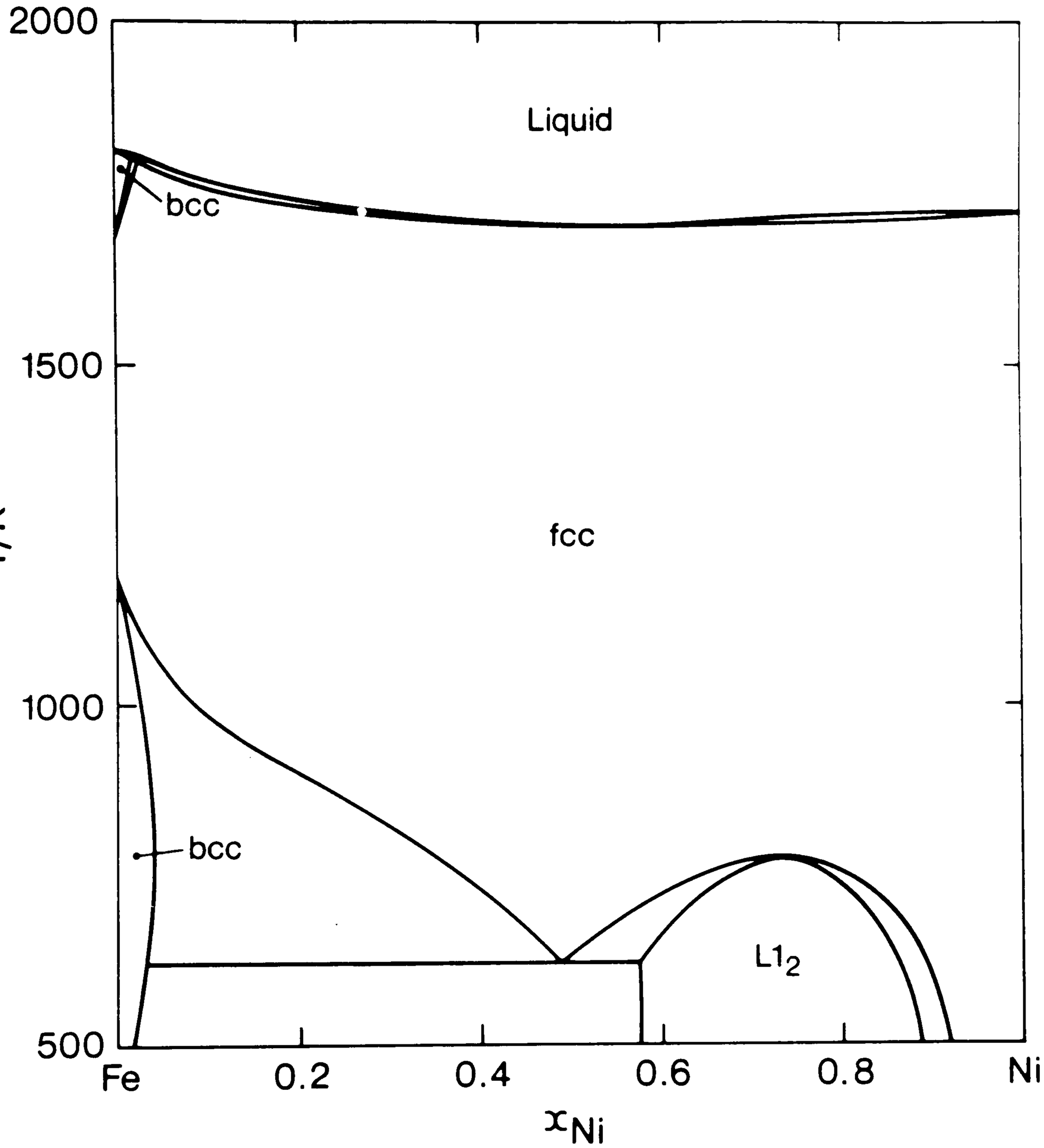

Fig 8.3 Calculated phase diagram for the Fe-Ni system.

assessment of Fernandez Guillermet et al. is fully compatible with the liquid phase model described earlier and was therefore adopted for this present work. The phase diagram calculated using their data is shown in Figure 8.4 and is in very good agreement with that determined experimentally. In the original description the pyrrhotite phase was described as a solution phase. For the reasons described earlier, for this work it was treated as a stoichiometric phase. In the same way the solubility of sulphur in solid iron which is very small has been neglected. The phase diagram calculated using these simplified data is shown in Figure 8.5. The differences from Figure 8.4 are very slight.

The Cu-S system

The selected phase diagram for the Cu-S system is shown in Fig 8.6. The diagram has been based primarily on those given in the reviews by Bale and Toguri (400), Barton (401), Craig and Scott (402), Kellogg (63,213) and Sharma and Chang (204) but incorporating additional information (53-55,403-410).

The basic features shown by this diagram are typical of a number of high affinity systems. The solubility of the solid elements in one another is very low, there is a compound digenite $Cu_{2-x}S$ which melts congruently and also exhibits non-stoichiometry to sulphur rich compositions. The liquid phase shows a pronounced tendency to immiscibility on either side of the composition corresponding to digenite and sharp changes in the thermodynamic data at about this composition. These data imply ordering of the liquid phase as confirmed by electrical conductivity measurements.

Experimental measurements in the Cu-S system are difficult especially at high sulphur concentrations where the vapour pressure of sulphur can become very high. On the copper rich side of the diagram the phase

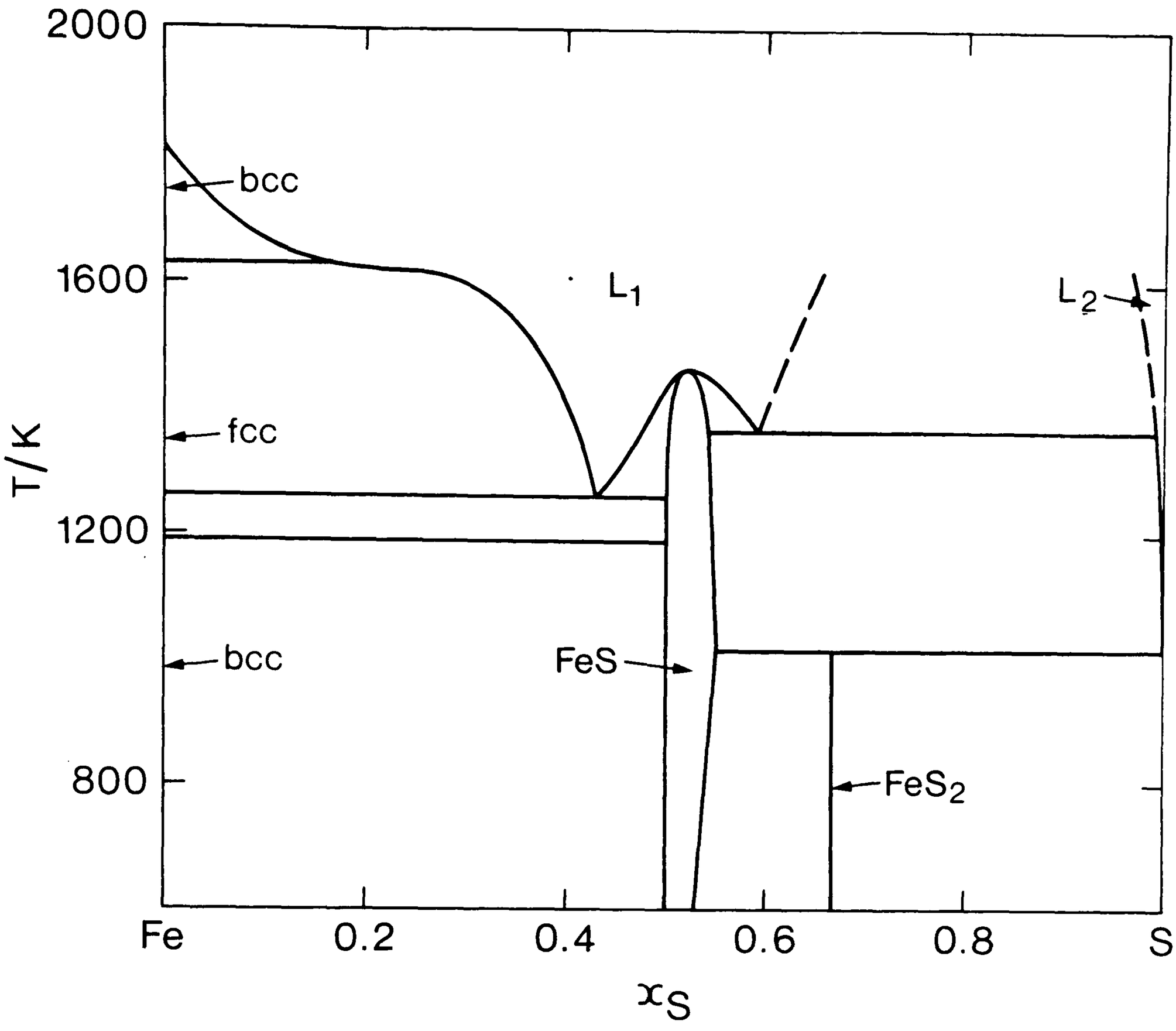

Fig 8.4 Phase diagram for the Fe-S system calculated using data derived by Fernandez Guillermet et al.

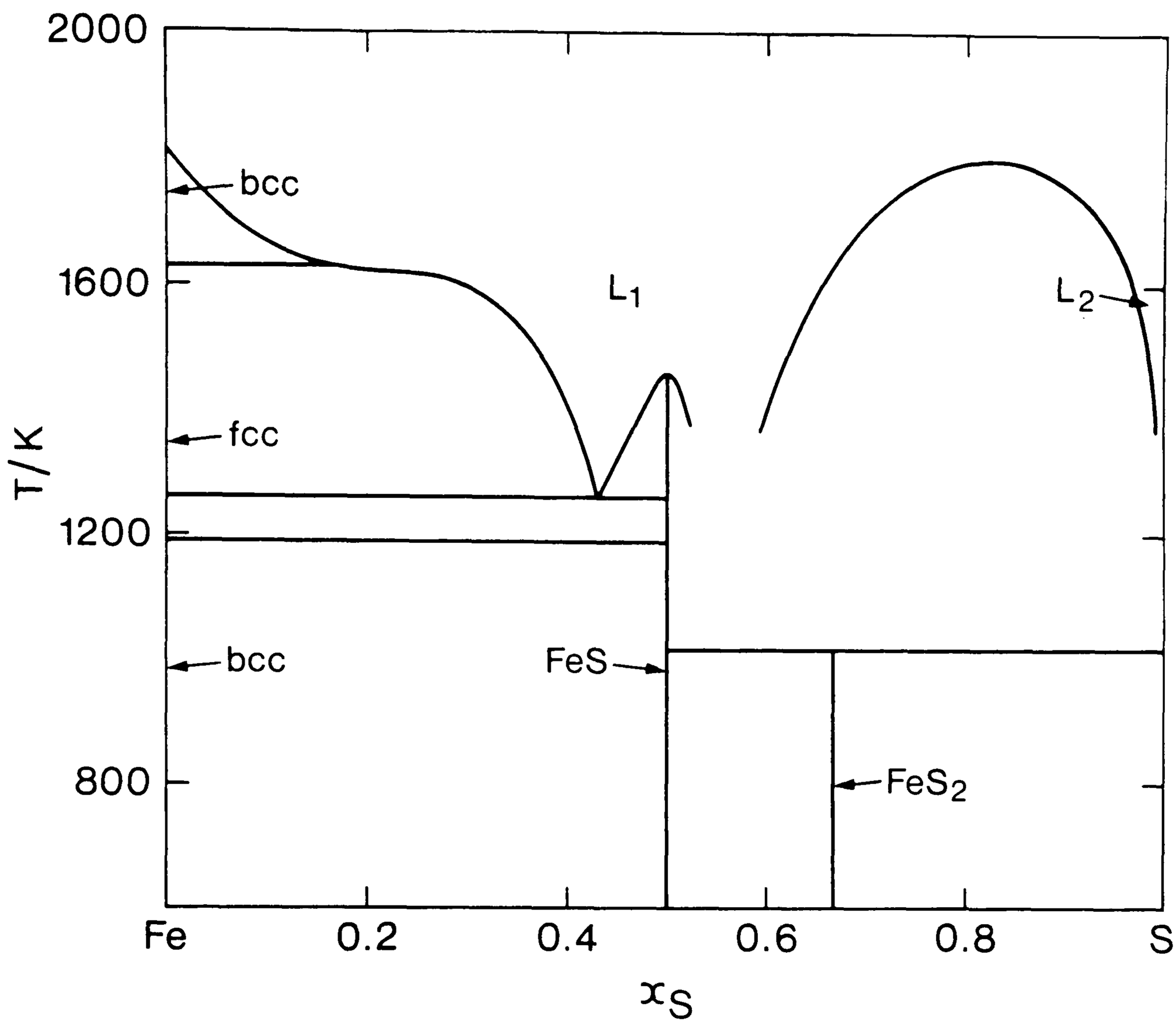

Fig 8.5 Phase diagram for the Fe-S system calculated using data derived by Fernandez Guillermet et al. modified to include pyrrhotite as a stoichiometric phase.

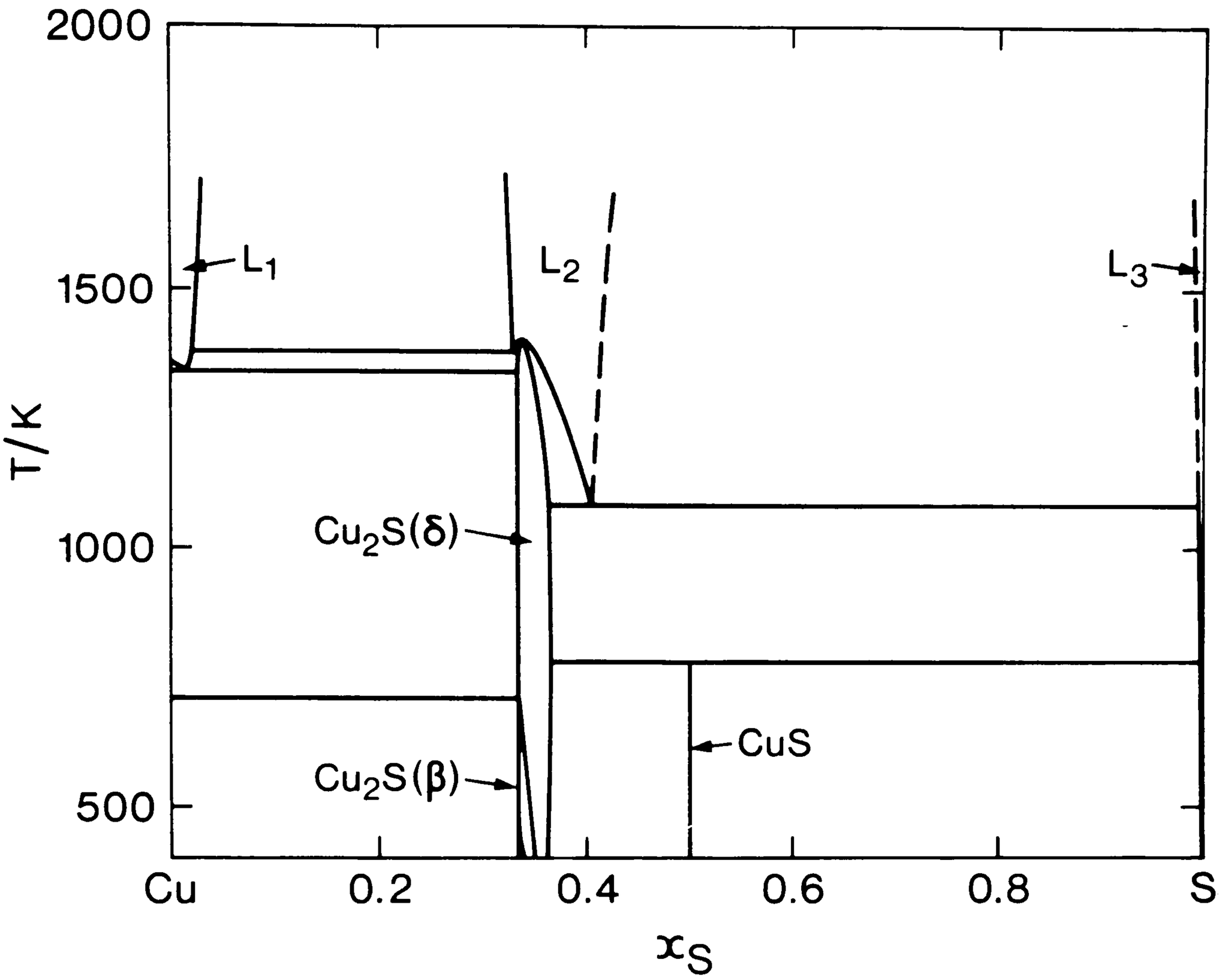

Fig 8.6 Selected phase diagram for the Cu-S system.

boundaries are fairly well known. There is an uncertainty in the metal rich boundary of the miscibility gap of about 0.02 in mole fraction. The melting behaviour and the range of homogeneity of digenite ($Cu_{2-x}S$) seem well established. The thermodynamic properties in the system have been studied extensively especially those of the liquid phase (411-415) and of the solid $Cu_{2-x}S$ phase (406-408,416-419).

Most attempts to represent these data in terms of mathematical expressions have involved only one phase in isolation. For example Rau (407,408) and Nagamori (406) have been concerned with high temperature digenite only, while Kellogg (213,214) and Larrain (219,220) have considered only the liquid phase. Only the recent work of Chang and Sharma (204,216,420) has attempted to cover all the phases in the Cu-S system over a wide range of temperatures. In this work, also described elsewhere (235), a partial assessment of the Cu-S system has been carried out and uses the two-sublattice description for the properties of the liquid phase described earlier.

The vacancy concentrations calculated from the liquid phase model are shown in Fig 8.7, which reveals that only in the region of Cu_2S are there significant concentrations of vacancies on both sublattices. Fig 8.8 shows a plot of the Gibbs energy of formation for 1423 K calculated using the data fitted to this model. The thermodynamic properties can be thought of in terms of the chemical contribution arising from the formation of the material and a physical contribution arising from the mixing of the atoms and vacancies as shown in the diagram. Fig 8.9 shows the log of the activities of Cu and S relative to the pure elements in the liquid phase also calculated using these data. It agrees well the experimental data for the system.

Fig 8.10 shows the calculated phase diagram. For simplicity in the multicomponent phase diagram calculations as described earlier, digenite was treated as stoichiometric rather than as a solution phase.

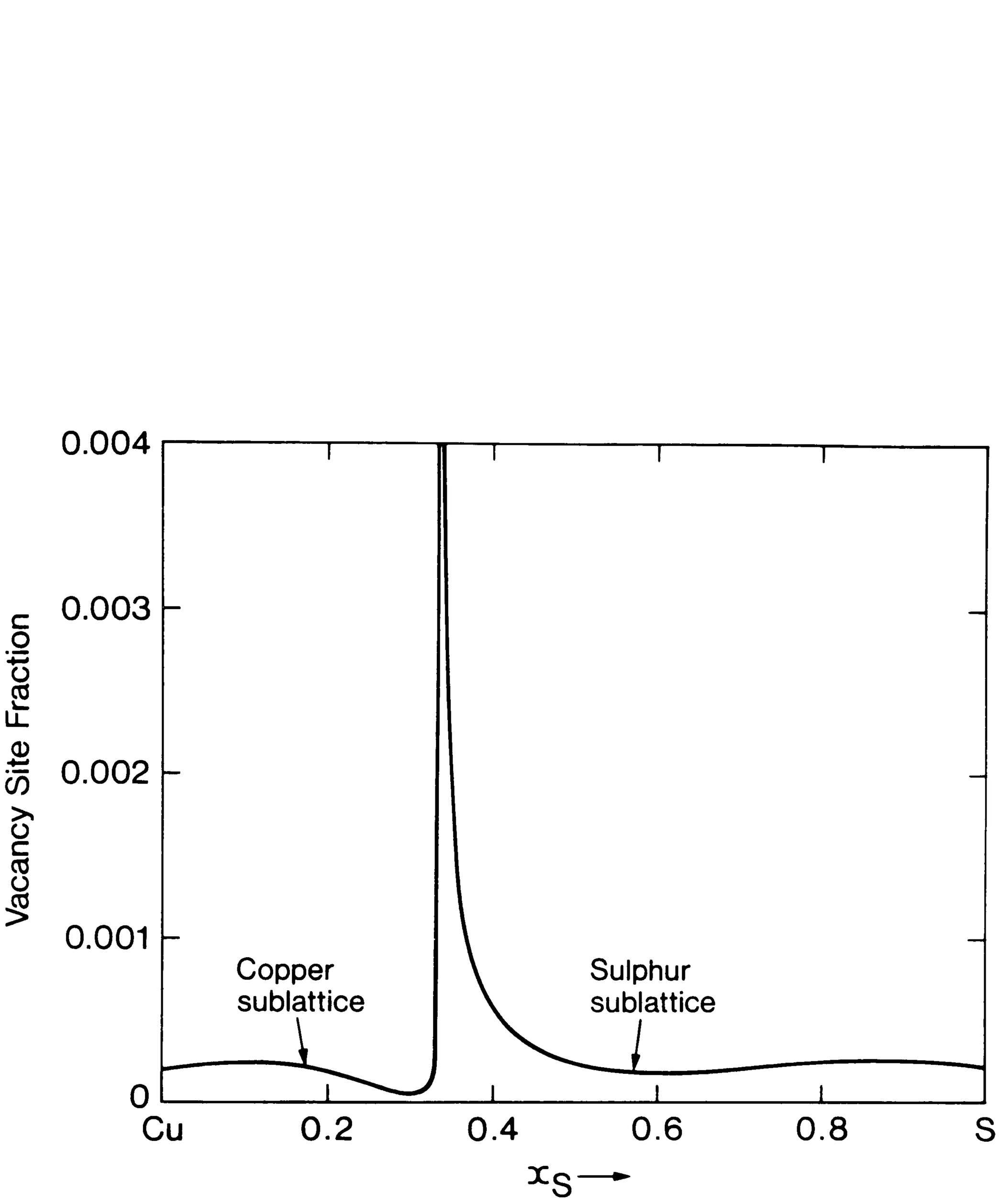

Fig 8.7 Fractions of vacancies on the copper and sulphur sublattices as a function of the overall composition calculated for 1423 K.

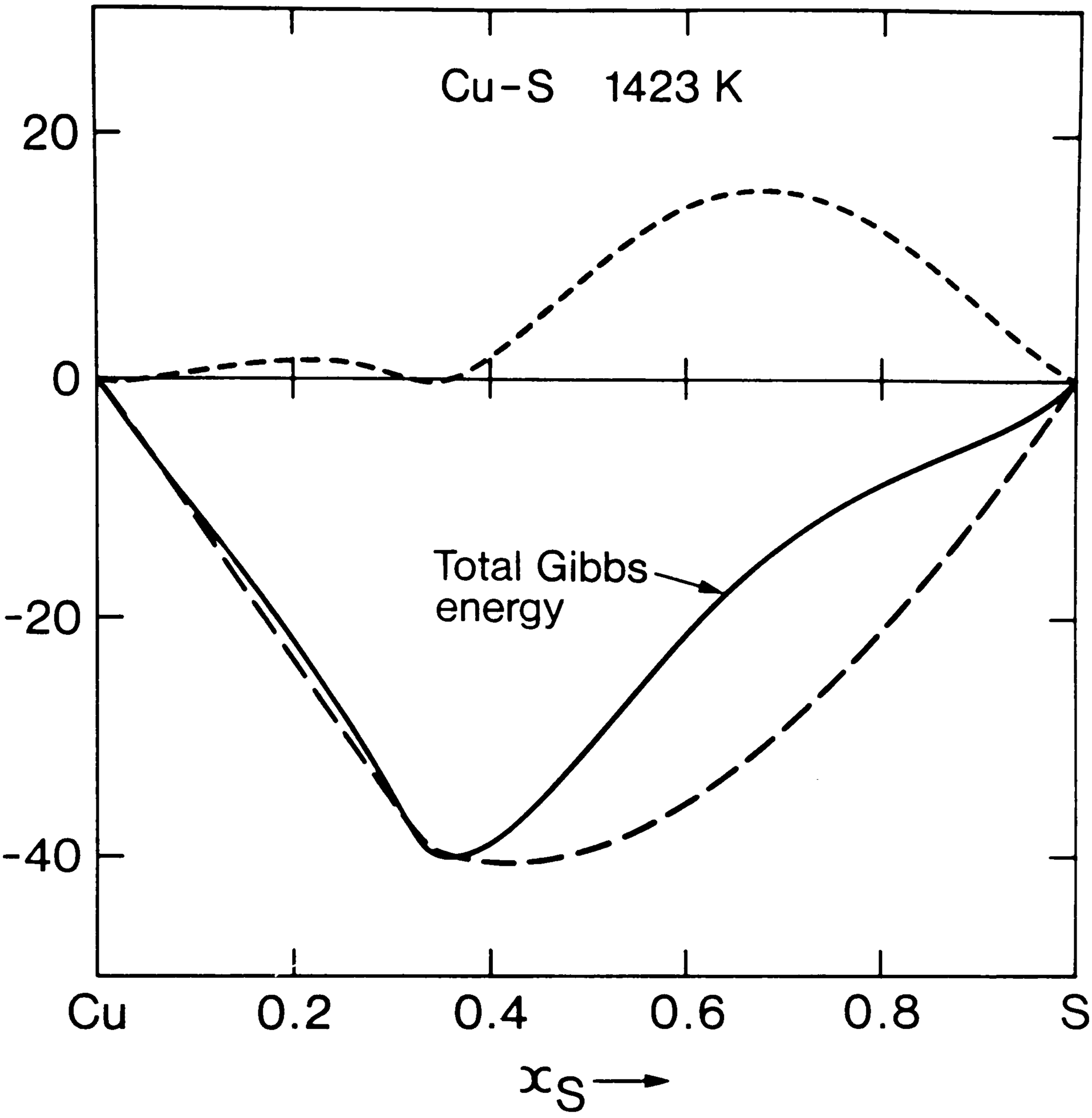

Fig 8.8 Contributions to the Gibbs energy of formation of the Cu-S liquid phase at 1423 K as a function of composition. The solid curve represents the total Gibbs energy of formation, the upper dashed curve the contribution arising from mixing of atoms and vacancies and the lower dashed curve the contribution from the formation of Cu_2S when mixing is disregarded.

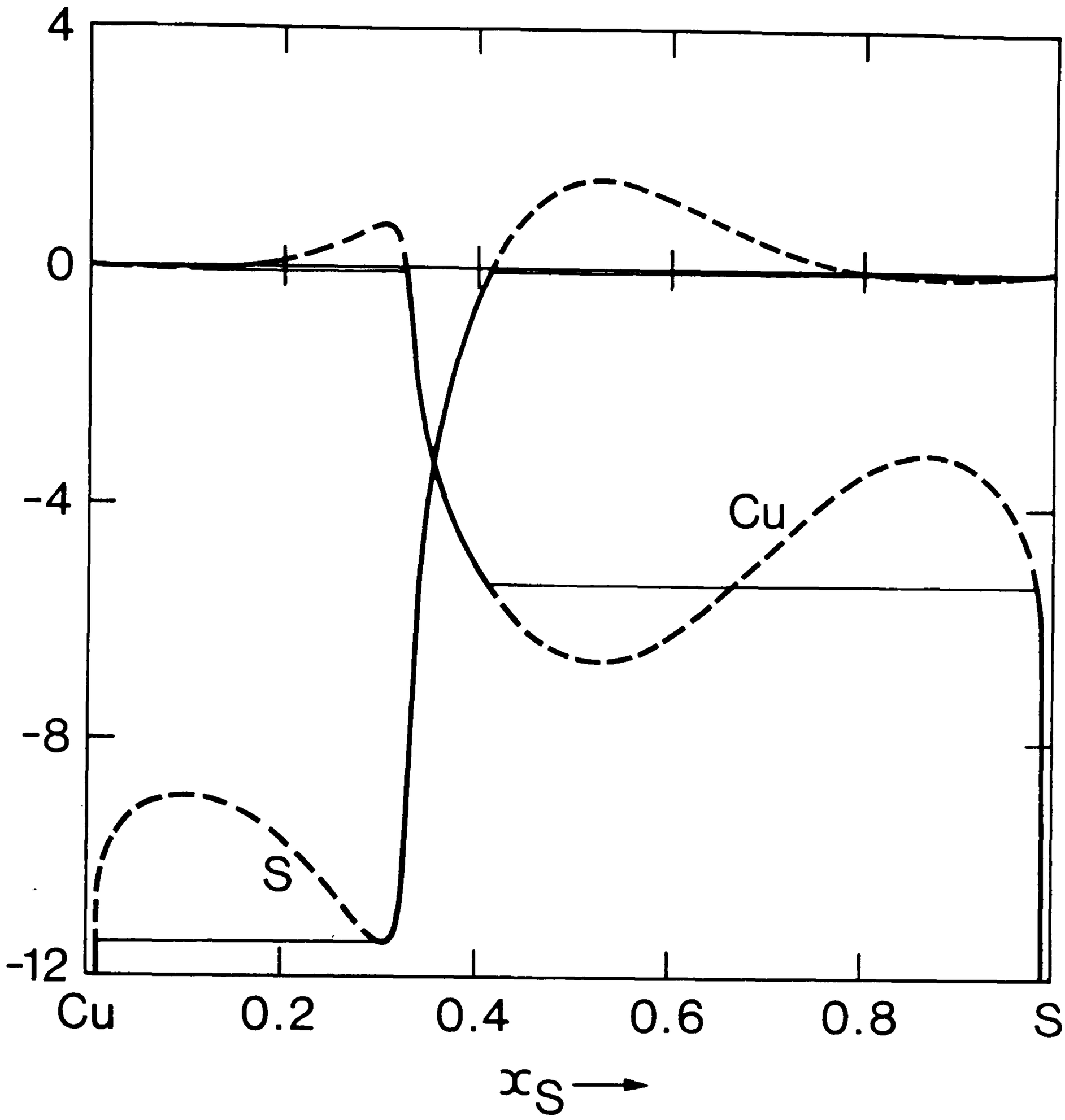

Fig 8.9 The activities of Cu and S at 1423 K in the liquid phase of the Cu-S system. The dashed line refers to the region where the homogeneous liquid phase is metastable with respect to immiscibility.

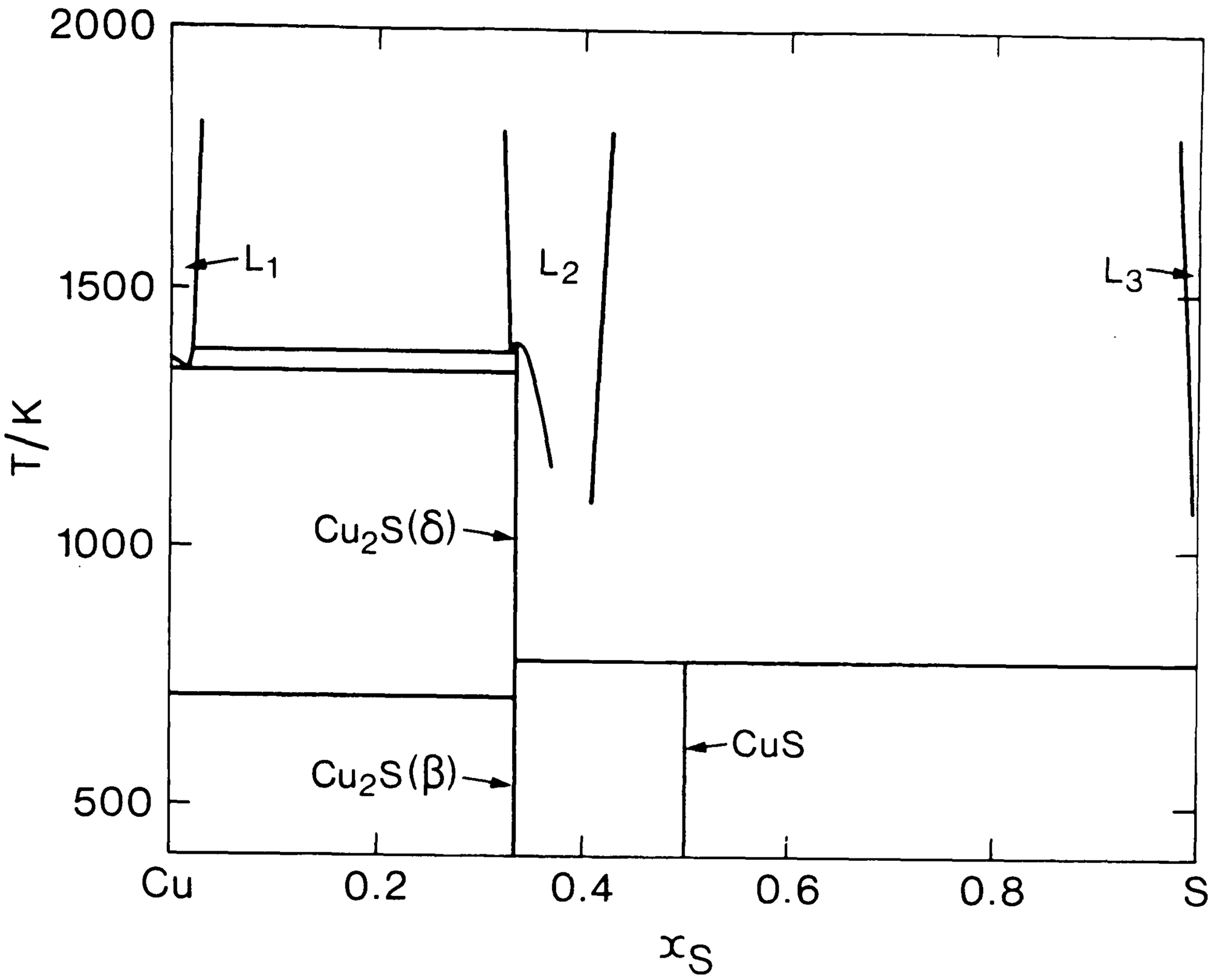

Fig 8.10 Calculated phase diagram for the Cu-S system. The assumption that digenite has no range of homogeneity leads to slight discrepancies with Fig 8.6 on the sulphur rich side of Cu_2S.

Consequently the liquidus curve to the sulphur rich side of digenite and the eutectic at 1085 K have not been reproduced accurately. The calculations in the metal rich part of the diagram indicate excellent agreement with experimental information.

The Ni-S system

The Nickel-Sulphur system has been the subject of much experimental study both from the point of view of the thermodynamic data and the phase diagram.

The phase diagrams reported in Hansen and Anderko (53), Elliott (54), Shunk (55) and the Metals Handbook (63) have been superseded by one given by Craig and Scott (402). The metal rich part of the phase diagram is dominated by a deep eutectic formed by the three phase equilibrium:

Liq = fcc + beta

where the fcc is basically Ni with a very small dissolved concentration of S and beta is the solid solution phase based around the composition Ni_3S_2. The structure of this beta phase is not at all well known being apparently unquenchable and transforming on cooling to the low temperature stoichiometric phase heazlewoodite (Ni_3S_2). There is some evidence (383,386) to suggest that the beta phase consists of two distinct phases of very similar thermodynamic properties. The other high temperature phase in the metal rich part of the system is the monosulphide $Ni_{1-x}S$ phase based upon the NiAs structure ($B8_1$). At low temperatures, various stoichiometric phases appear. In addition to Heazlewoodite there are: Ni_7S_6 (godlevskite), a low temperature form of NiS (Millerite), Ni_3S_4 (Polydymite) and NiS_2 (Vaesite). At high temperatures the sulphur rich side of the system is dominated by a

liquid-liquid miscibility gap. The selected phase diagram shown in Fig 8.11 is based upon that of Craig and Scott (402) but incorporating additional information (378,421-430).

The thermodynamic properties of the liquid phase have been determined by a number of workers (378,379,421,422,431-437). The data from Meyer et al. (378,379) are the most extensive and are to be preferred. Extensive studies have also been carried out on the Beta phase or phases (383,386,438-440) while Rau has also studied the monosulphide solid solution (428). The low temperature stoichiometric phases have also been studied (441-444). Data for the dilute solution of sulphur in nickel have been derived by Brigham et al. (426).

Various authors have attempted to correlate the thermodynamic and phase diagram data. Larrain (217) modelled the liquid phase using species of Ni, Ni_3S_2 and NiS and obtained good agreement with the liquidus at high Ni concentrations above 1000 K. However no other phases were considered. Sharma and Chang (223) have, however, modelled all the phases in the system and obtained excellent agreement between the experimental and calculated phase diagram. For the liquid phase they assumed an associated solution model with associate species of NiS. The beta phases were modelled using an empirical power series for the excess Gibbs energy while the $Ni_{1-x}S$ phase was modelled according to a statistical thermodynamic model similar to that used for pyrrhotite (221). The solubility of sulphur in pure Nickel was neglected.

For this assessment a two sublattice model, as described earlier, was adopted for the liquid phase. The experimental data show a dramatic change in the thermodynamic properties at about $x_S = 0.4$ which led to the adoption by Larrain of associated species of Ni_3S_2. However here it was assumed that the most reliable description of the data using a two sublattice model would be obtained by assuming that Ni had the same valency as Sulphur ie. treating Ni-S liquid in the same way as Fe-S

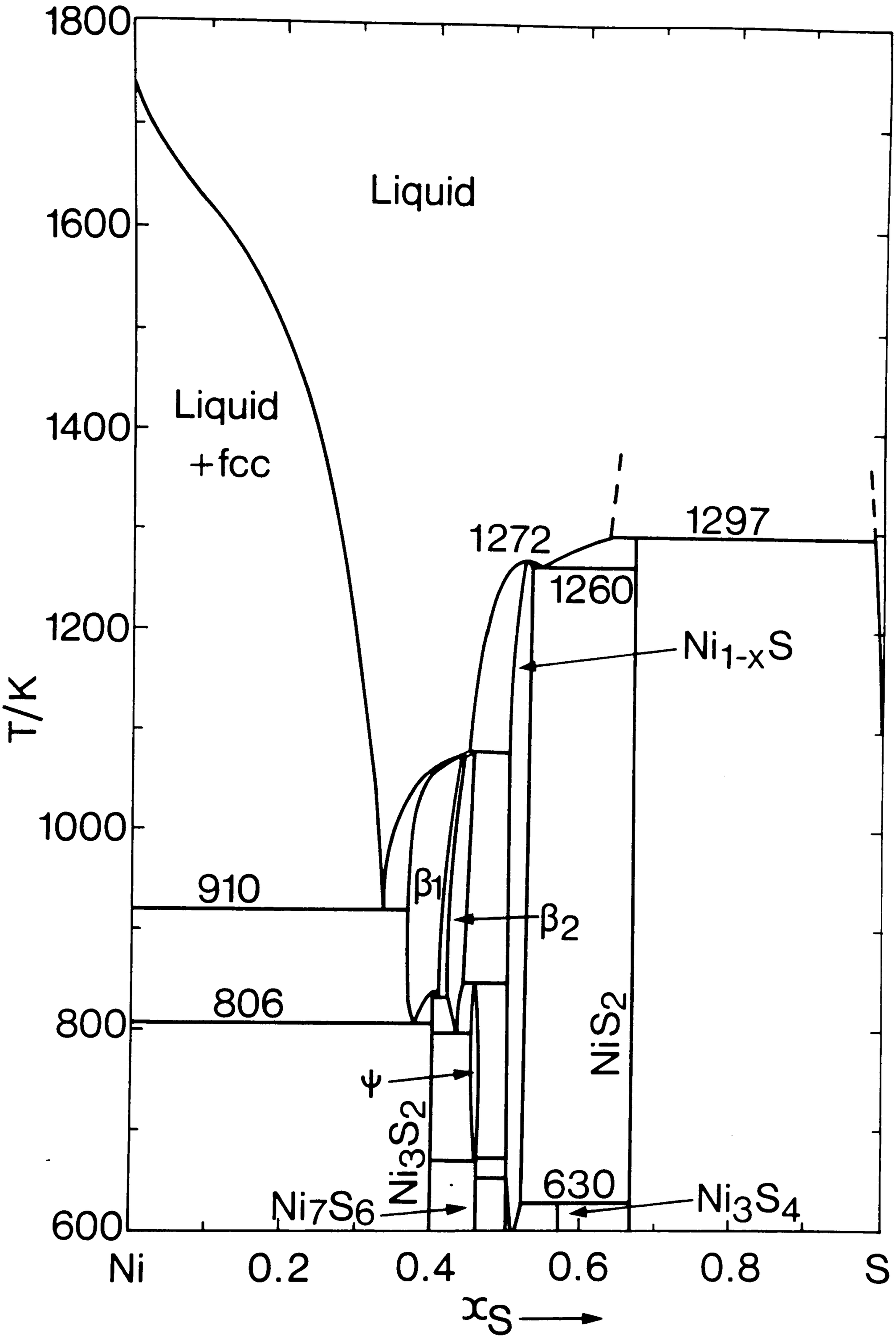

Fig 8.11 Selected phase diagram for the Ni-S system.

liquid. As with previous assessments, liquid phase thermodynamic data for various temperatures were fitted to the sublattice model. The final agreement between the calculated and experimental partial pressures of sulphur, compared in Fig 8.12, is excellent.

For reasons given earlier the solution of sulphur in solid nickel, which at maximum is 0.001 in terms of mole fraction, was neglected. Similarly the monosulphide phase $Ni_{1-x}S$ which has a range of homogeneity from x_S = 0.5 to 0.52, has been treated as stoichiometric NiS.

The high temperature solid solution phase 'beta' based around Ni_3S_2 presented some problems. As mentioned earlier there is evidence which indicates that the phase field consists of two distinct but similar phases separated by a narrow two phase region. For simplicity this phase field was treated as a single phase. The data were represented using a simple Redlich-Kister power series expression as used with success in alloy systems. This model is not really appropriate and the data derived for this phase, although acceptable, must be regarded as provisional. Furthermore the data are applicable only for temperatures below 1150 K. It is recommended that the phase should be reconsidered in terms of a two sublattice description. The other phases in the metal rich part of the system were treated as stoichiometric.

The phase diagram calculated from these data for Ni rich compositions is shown in Fig 8.13.

Calculation of Phase Equilibria in the Cu-Fe-Ni system

Using data tabulated in the appendix, the phase diagram for the Cu-Fe-Ni system was calculated by Chart et al. (169) using the NPL ALLOYDATA system (15,173) between the temperatures 673 K and 1673 K. They critically assessed experimental ternary phase diagram and thermodynamic data for the temperature range 1023 K to 1523 K and

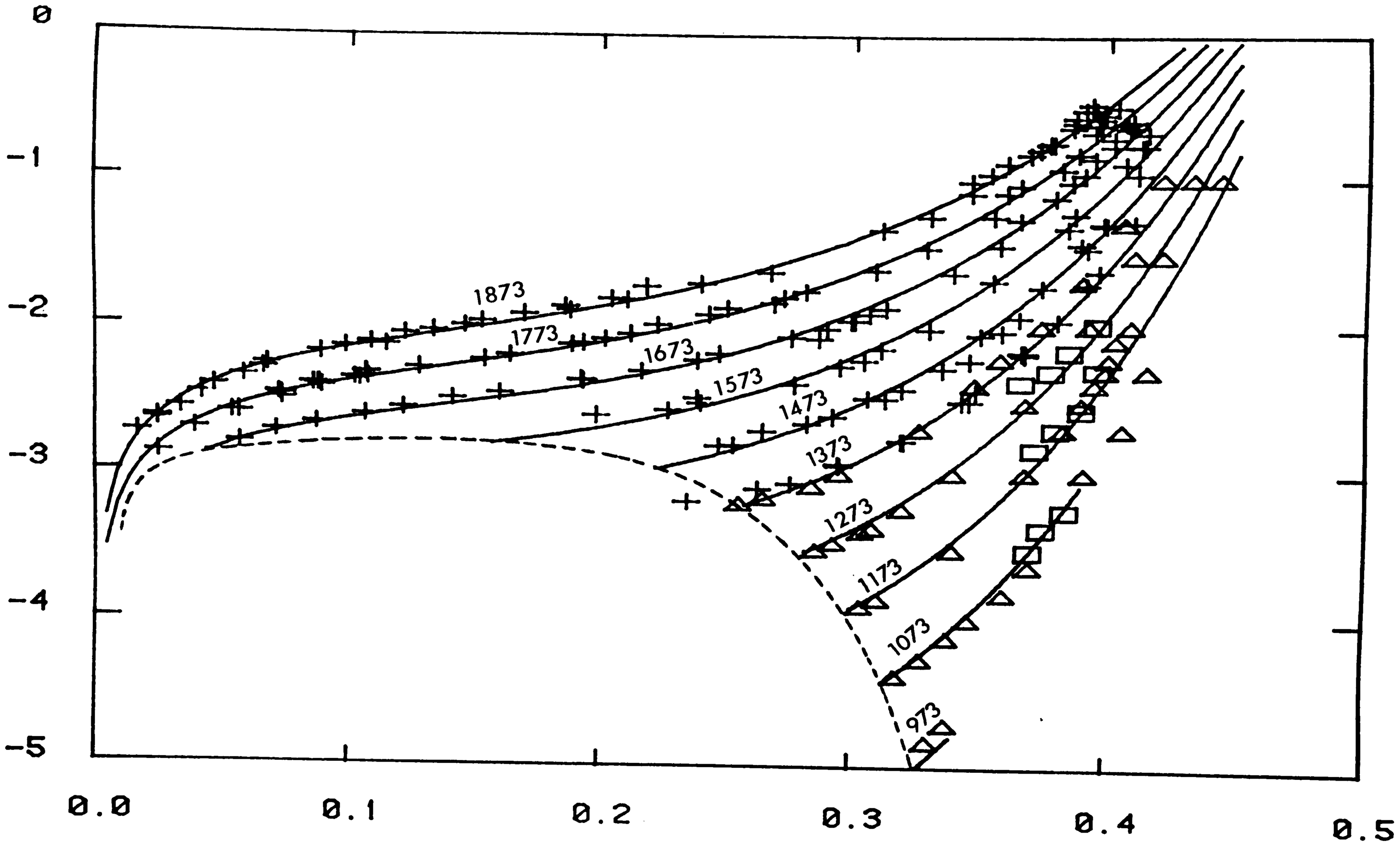

Fig 8.12 Comparison of the calculated and experimental partial pressures of sulphur in the Ni-S system from 1073 K to 1873 K.

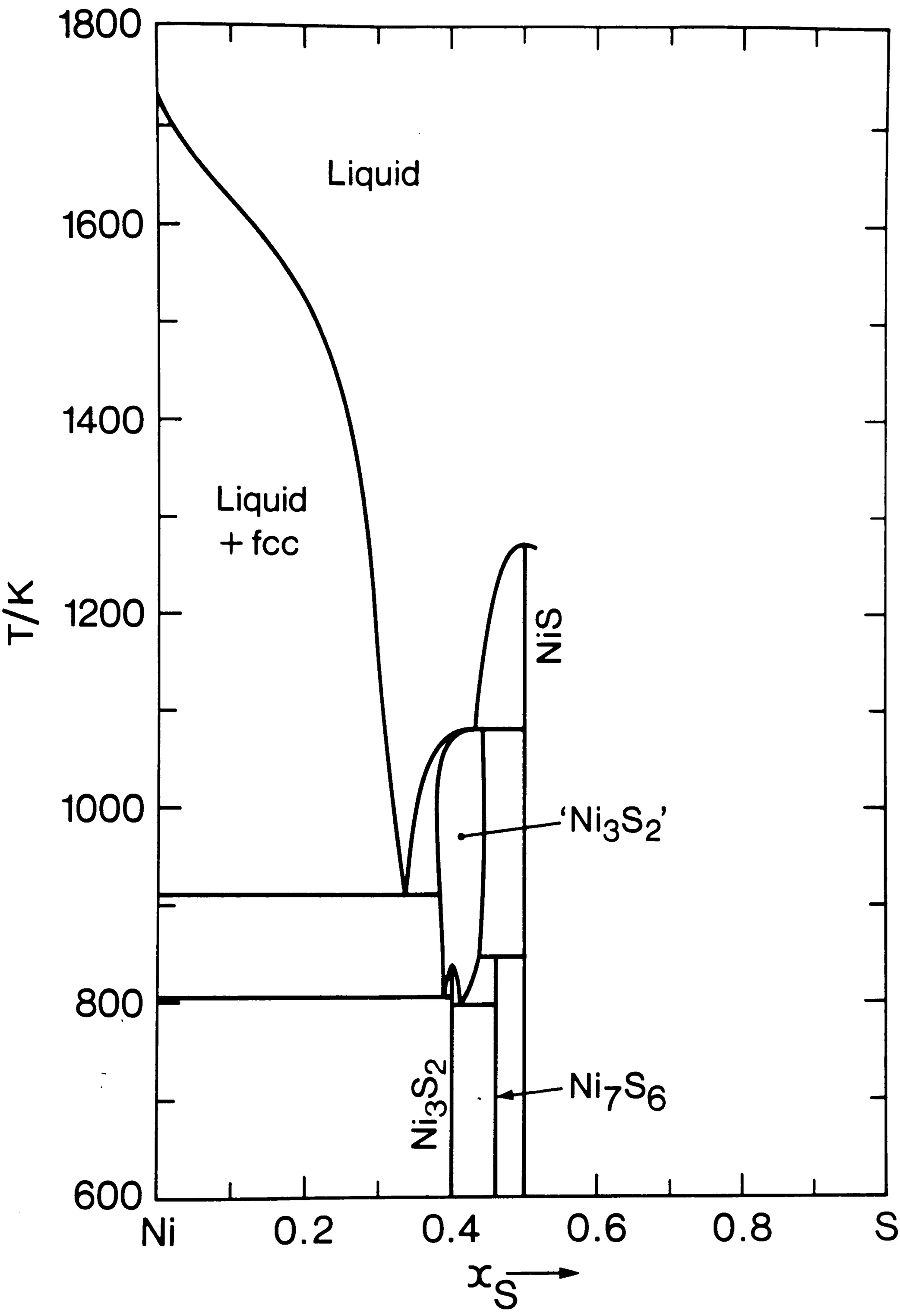

Fig 8.13 The nickel rich part of the Ni-S phase diagram calculated using the critically assessed data.

incorporated them into the data set in the form of a temperature dependent ternary interaction for the fcc phase. It is believed that the need for a ternary interaction term arises from small errors in the data for the Cu-Fe system. The agreement between the calculated and experimental data is good and, it is believed, the optimised data set provides a reliable means of extrapolation and interpolation in both temperature and composition outside the range of experimental data. Furthermore the data provide a reliable base for calculations of equilibria in the Cu-Fe-Ni-S system.

Calculation of phase equilibria in the Fe-Cu-S system

According to Craig and Scott (402) 'more time and effort has been expended in the determination of phase equilibria and minerological relationships among the Cu-Fe sulfides than any other ternary sulfide system'. They go on to say that despite this many aspects of the phase diagram are unknown. This is hardly surprising in view of the large number of ternary phases present in the system. Fortunately as far as this work is concerned most of these ternary phases are stable only at low temperatures and are in any case sulphur rich of the composition line joining Cu_2S and FeS. Fig 8.14 shows the experimental phase diagram for the Fe-Cu-S system at 873 K from Chang et al. (74) based upon the diagram of Cabri (445) and shows how the metal rich part of the phase diagram is separated from the sulphur rich part by the two phase region between Cu_2S and FeS. This situation persists at lower temperatures. Consequently for this work where all the compositions of interest are in the metal rich region, all sulphur rich phases could be ignored.

The experimental work on the phase diagram of the Fe-Cu-S system has been reviewed by Craig and Scott (402) and by Chang et al. (74,446) which incorporate a considerable number of experimental measurements

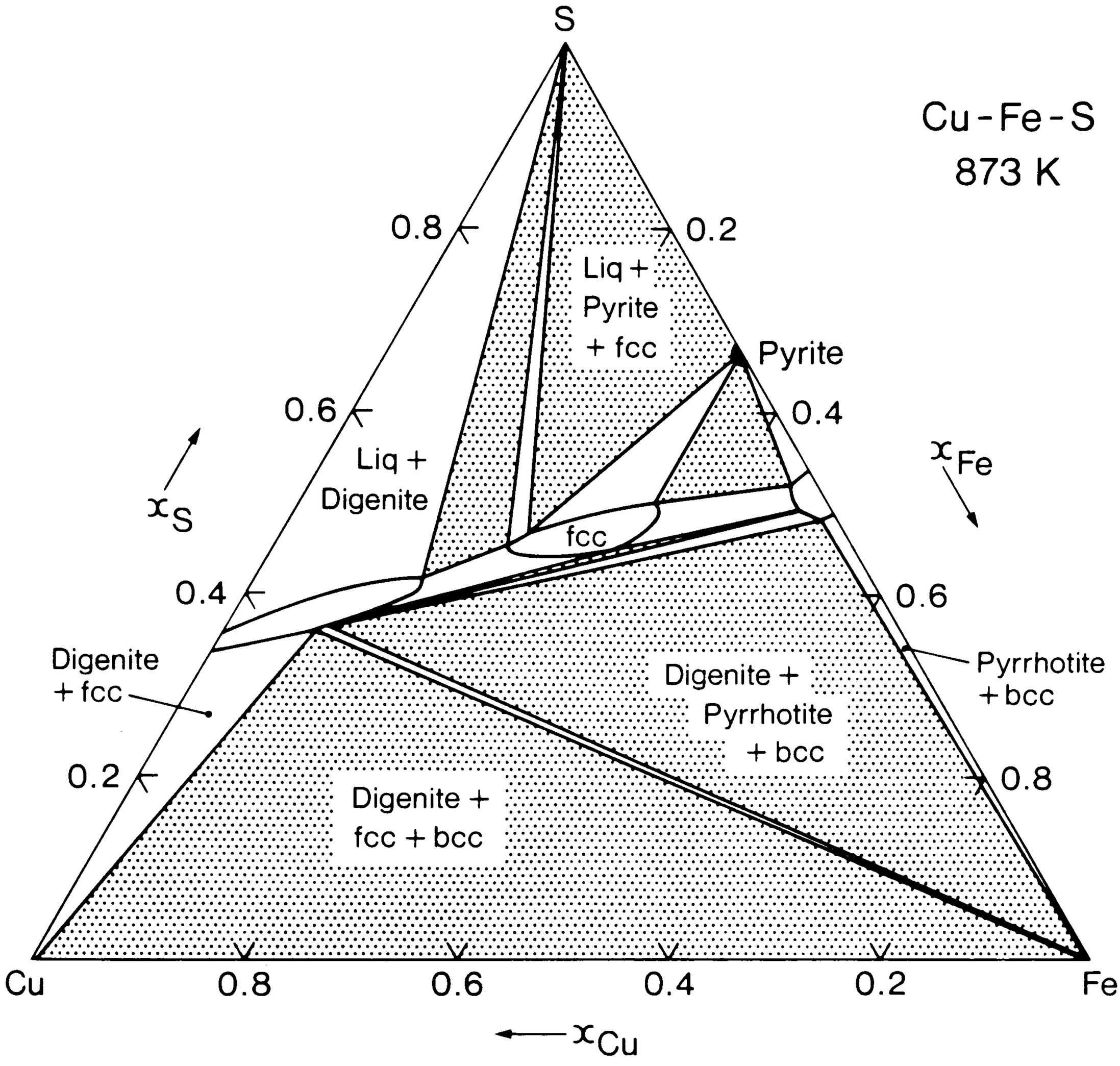

Fig 8.14 Experimental phase diagram for the Fe-Cu-S system for 873 K as assessed by Chang et al. The metal rich part of the phase diagram is separated from the sulphur rich part by the two phase region between digenite and pyrrhotite.

(400,401,445,447-472). The thermodynamic properties of the Fe-Cu-S system have also been reviewed by Chang et al. (74), Craig and Scott (402) and by Barton (401). Data have been derived by a number of groups both for the liquid phase (51,52,400,457,469,473-479) and solid phases (446,480-485).

Lee (380) attempted to model the liquid phase of the Fe-Cu-S using associated species but even using 14 ternary coefficients failed to obtain very good agreement with experimental data. Pelton and Bale (161) used a Fourier cosine series to represent the liquid phase data for the Fe-Cu-S system along pseudo-binary sections. Such a model requires the use of much ternary experimental information and cannot be called predictive.

Fig 8.15 shows the experimentally determined isothermal section for 1473 K from the assessment of Chang et al. (74). This diagram is dominated by the miscibility gaps in the liquid phase and the equilibrium between the liquid phase and the fcc iron based solid solution. The isothermal section for this temperature was also calculated using the data for the binary systems only and this is shown in Fig 8.16. As can be seen the agreement is very good. Also shown in Fig 8.16 is a comparison of the calculated sulphur activity contours and the critically assessed values of Chang et al. Again the agreement is very good. For 1623 K the agreement is not so good. Fig 8.17 shows the experimental phase diagram from Chang et al. which should be compared with the calculated phase diagram in Fig 8.18. Experimentally it is found that the liquid phase intrudes to a much larger extent than predicted but this is almost certainly due to small errors in the thermodynamic data for the Cu-Fe system. Also in Fig 8.18 are contours comparing the calculated and experimental sulphur activities showing very good agreement. Fig 8.19 shows the calculated phase diagram for 1665 K. As can be seen the phase diagram changes rapidly at temperatures

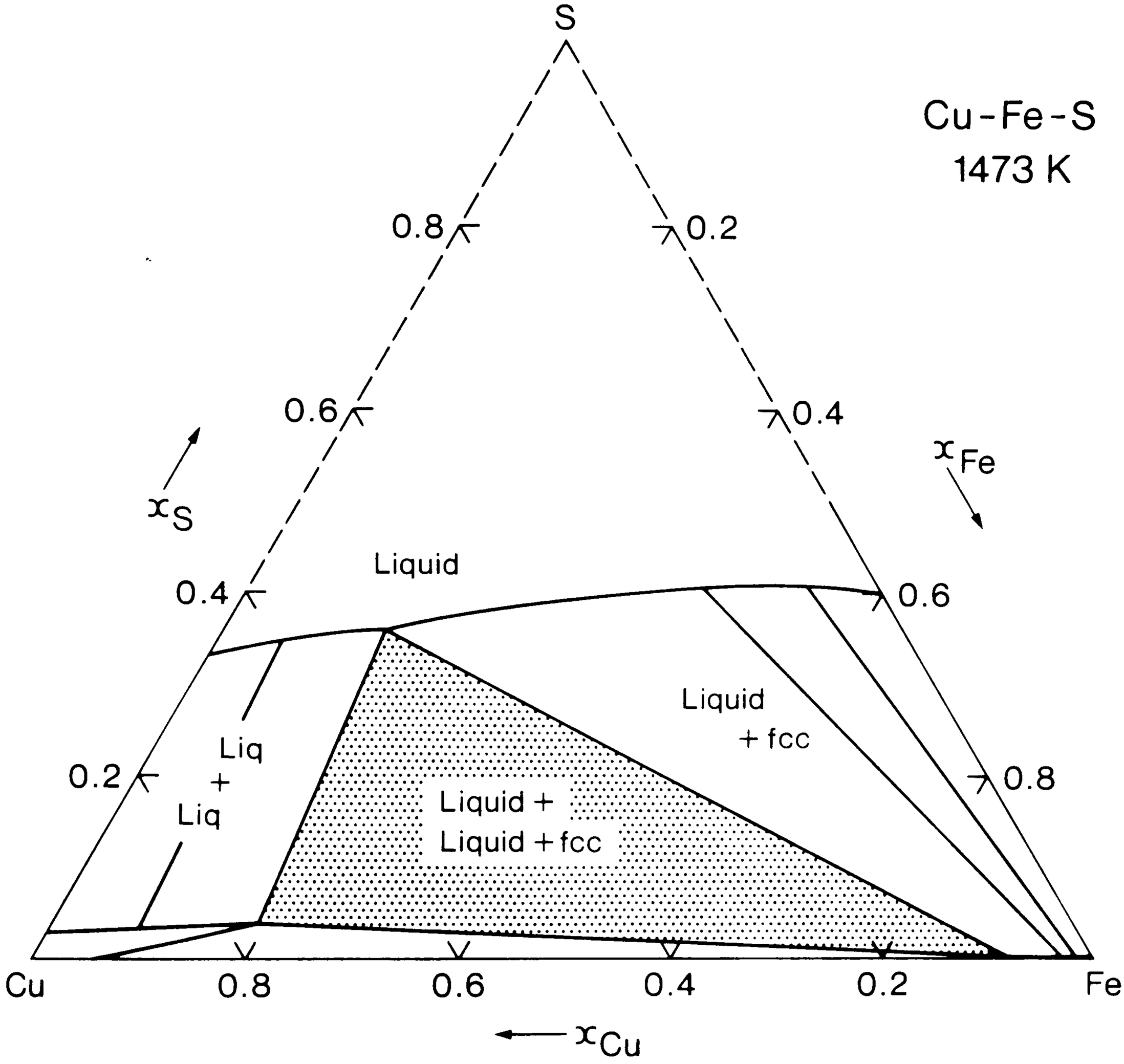

Fig 8.15 Experimental phase diagram for the Fe-Cu-S system for 1473 K as assessed by Chang et al.

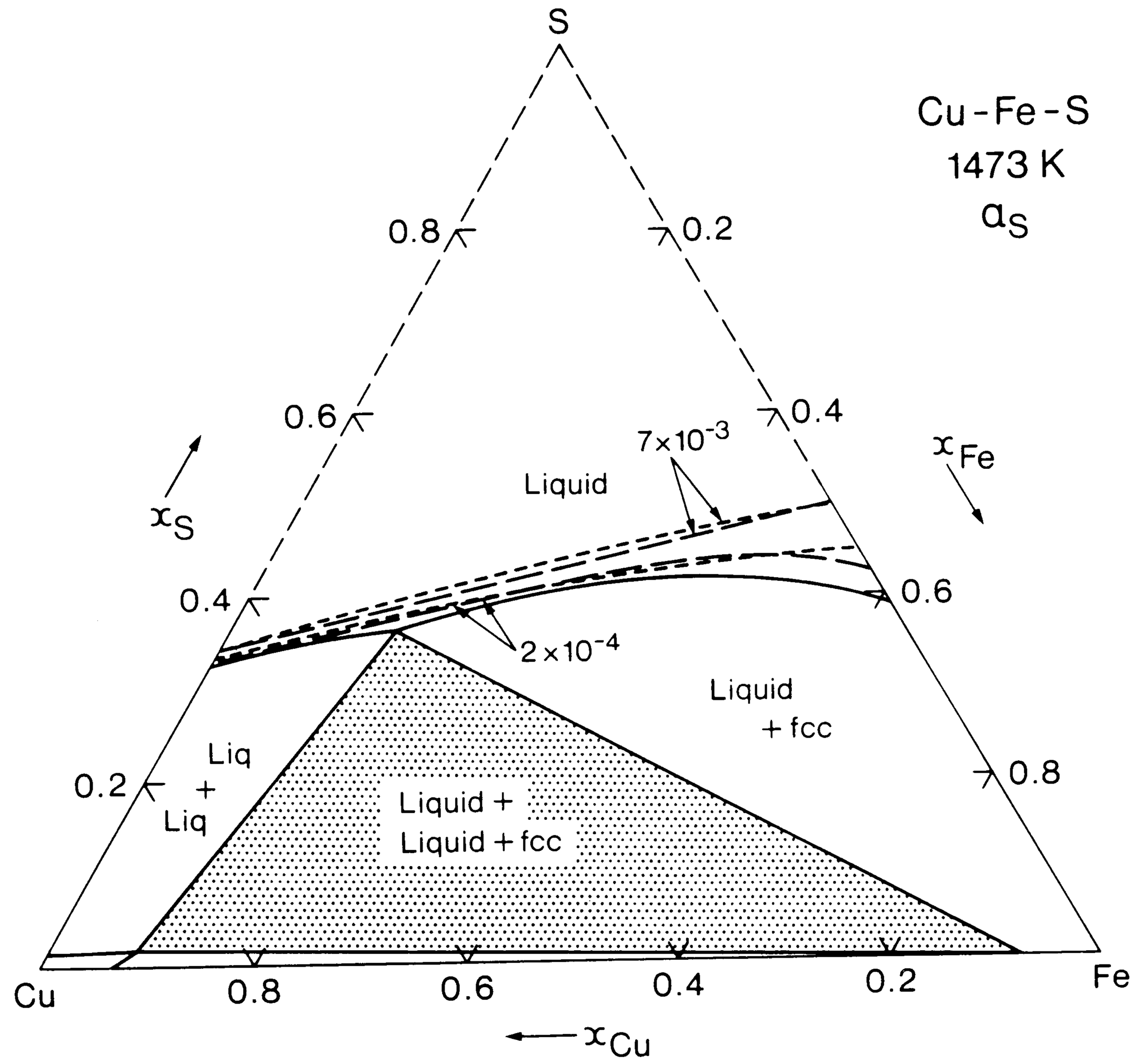

Fig 8.16 Calculated phase diagram for the metal rich part of the Fe-Cu-S for 1473 K. Superimposed are experimental (short dash) and calculated (long dash) sulphur activity contours.

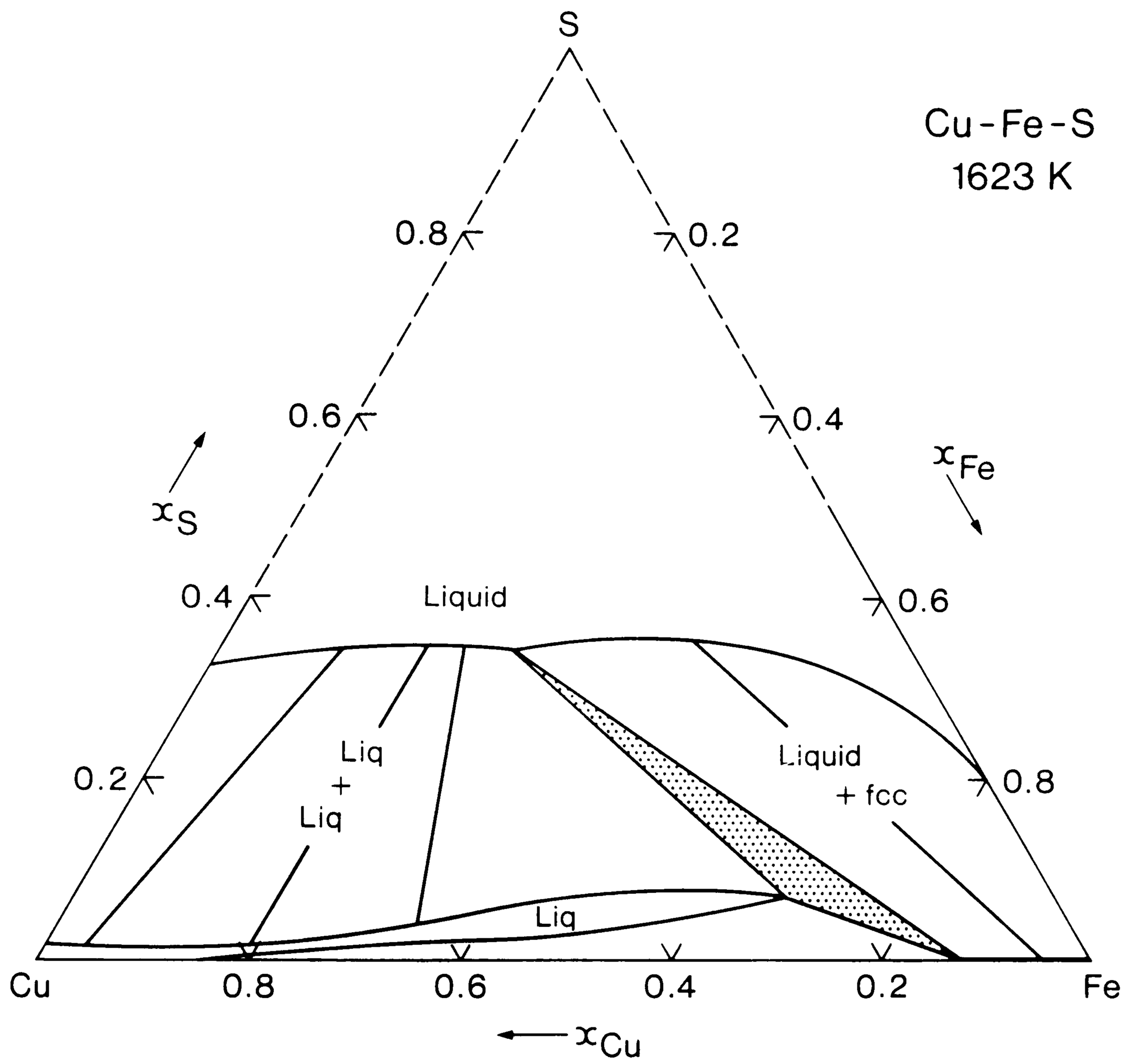

Fig 8.17 Experimental phase diagram for the Fe-Cu-S system for 1623 K as assessed by Chang et al.

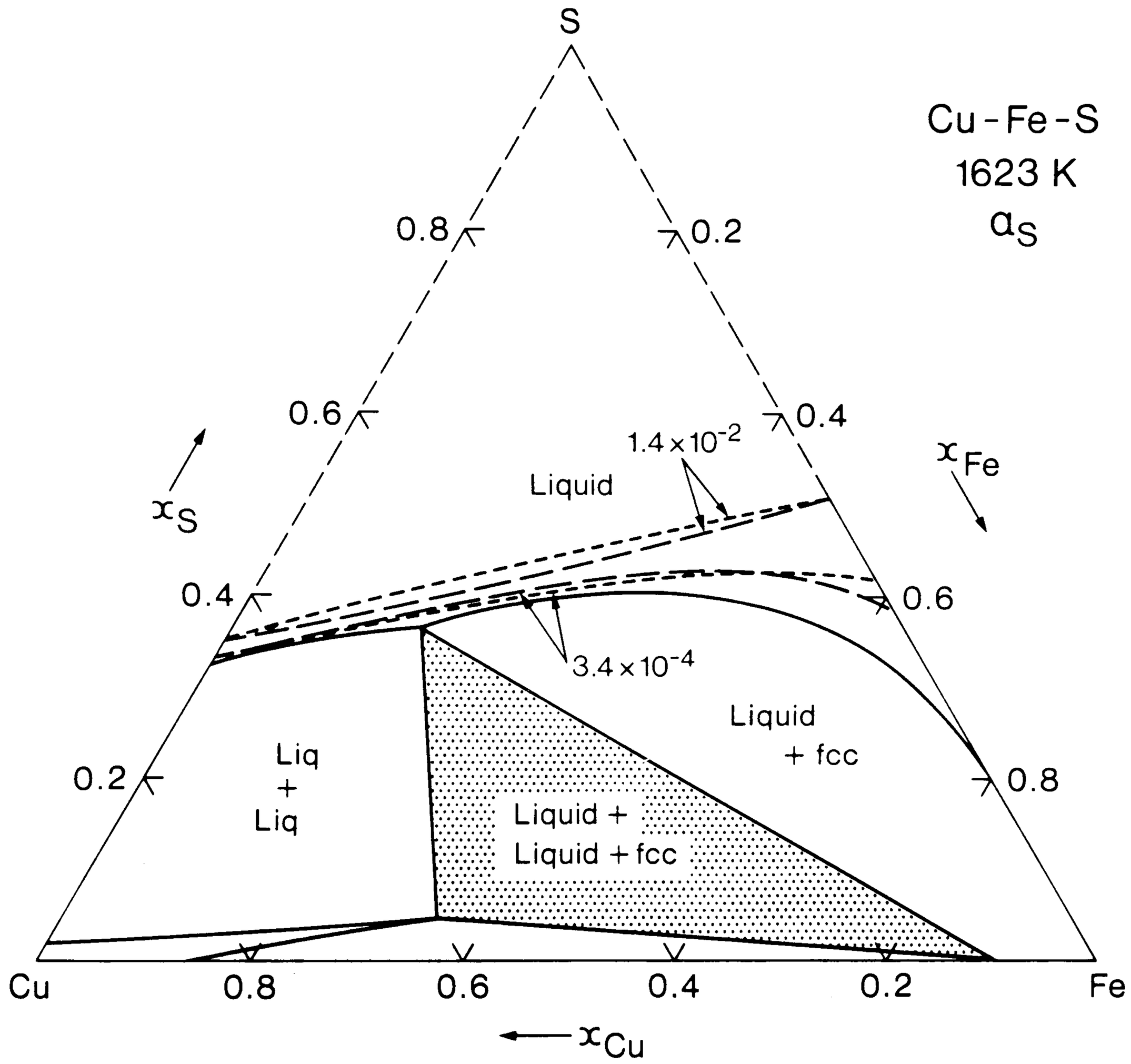

Fig 8.18 Calculated phase diagram for the metal rich part of the Fe-Cu-S for 1623 K. Superimposed are experimental (short dash) and calculated (long dash) sulphur activity contours.

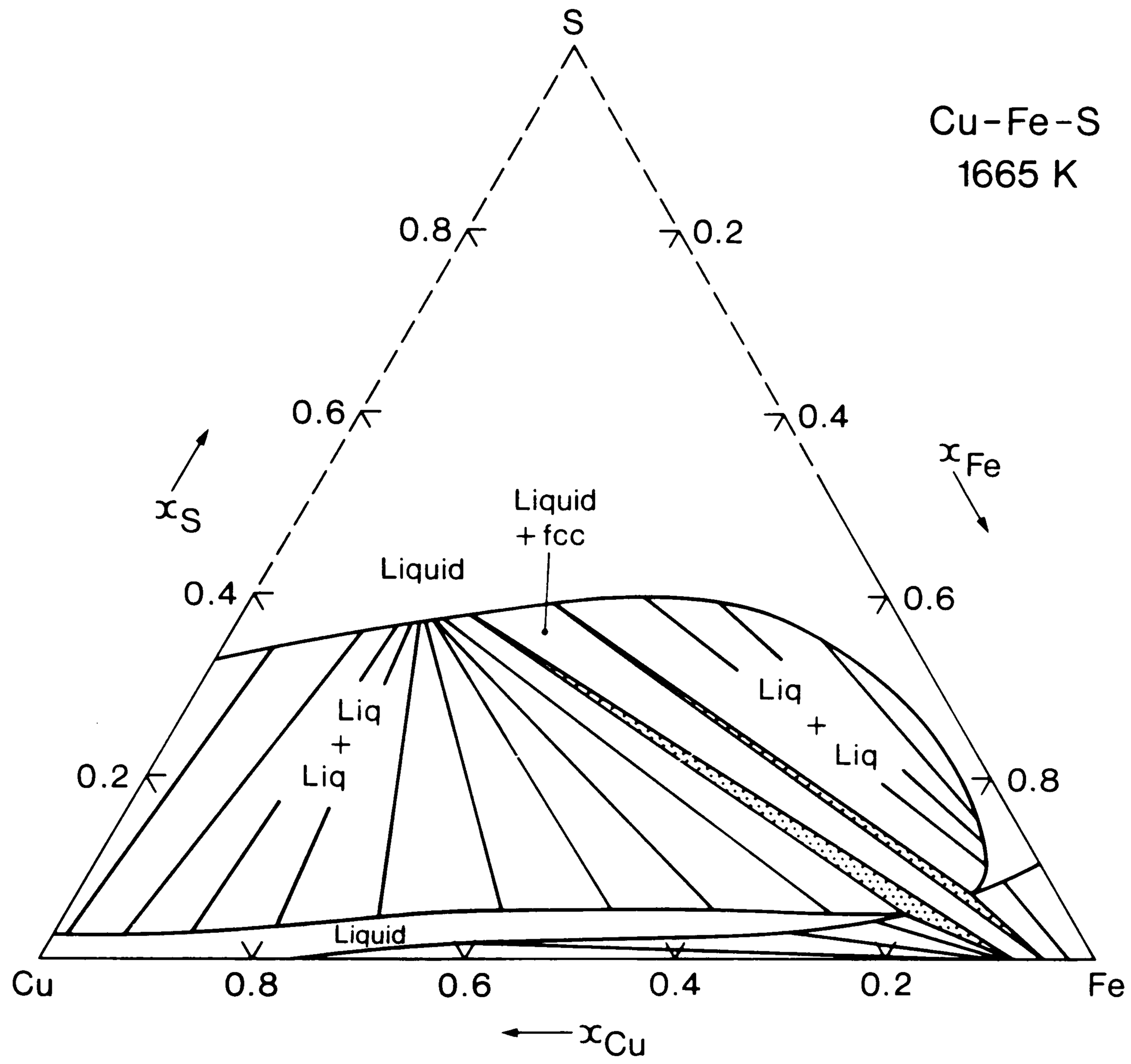

Fig 8.19 Calculated phase diagram for the metal rich part of the Fe-Cu-S system for 1665 K.

above 1600 K and the measured intrusion of the liquid phase for 1623 K is that predicted for about 1650 K.

Figs 8.16, 8.18 and 8.19 were calculated by setting the ternary interaction data to zero in the expression for the Gibbs energy of formation of the liquid phase. It was expected from the experimental work of Krivsky and Schuhmann (457), Bale and Toguri (400), Sinha and Nagamori (478) and Koh and Yazawa (479) that the liquid phase along the join between Cu_2S and FeS was near ideal and this assumption was shown to be correct by the agreement between the calculated and experimental thermodynamic data and phase diagrams.

In their reviews, Chang et al. (74,446) provide a phase diagram for the pseudo-binary section between Cu_2S and FeS. This is reproduced as the bold lines in Fig 8.20. The liquidus curve, the solid line, is fairly well established from experiment down the eutectic at about 1213 K. The other phase boundaries, the dashed lines, are not well known. Data for Cu_2S in the Pyrrhotite phase and FeS in the Digenite phase were then derived to reproduce the liquidus curves and the eutectic temperature. No interaction data were necessary to obtain the excellent agreement shown in Fig 8.20 where the calculated phase boundaries are indicated by the dotted line. At lower temperatures the agreement between the calculated diagram and the diagram of Chang et al. is not so good but it should be remembered that the latter diagram is estimated in this region.

Having derived data for the pyrrhotite and digenite phases, the Fe-Cu-S phase diagram was calculated at a number of temperatures of interest. Figs 8.21 and 8.22 show respectively the experimentally determined diagram as assessed by Chang et al.(74) and the calculated diagram for 1273 K. As can be seen the agreement is again excellent. Below 1200 K the broad features of the phase diagram remain constant being dominated by two three phase regions, the first between digenite,

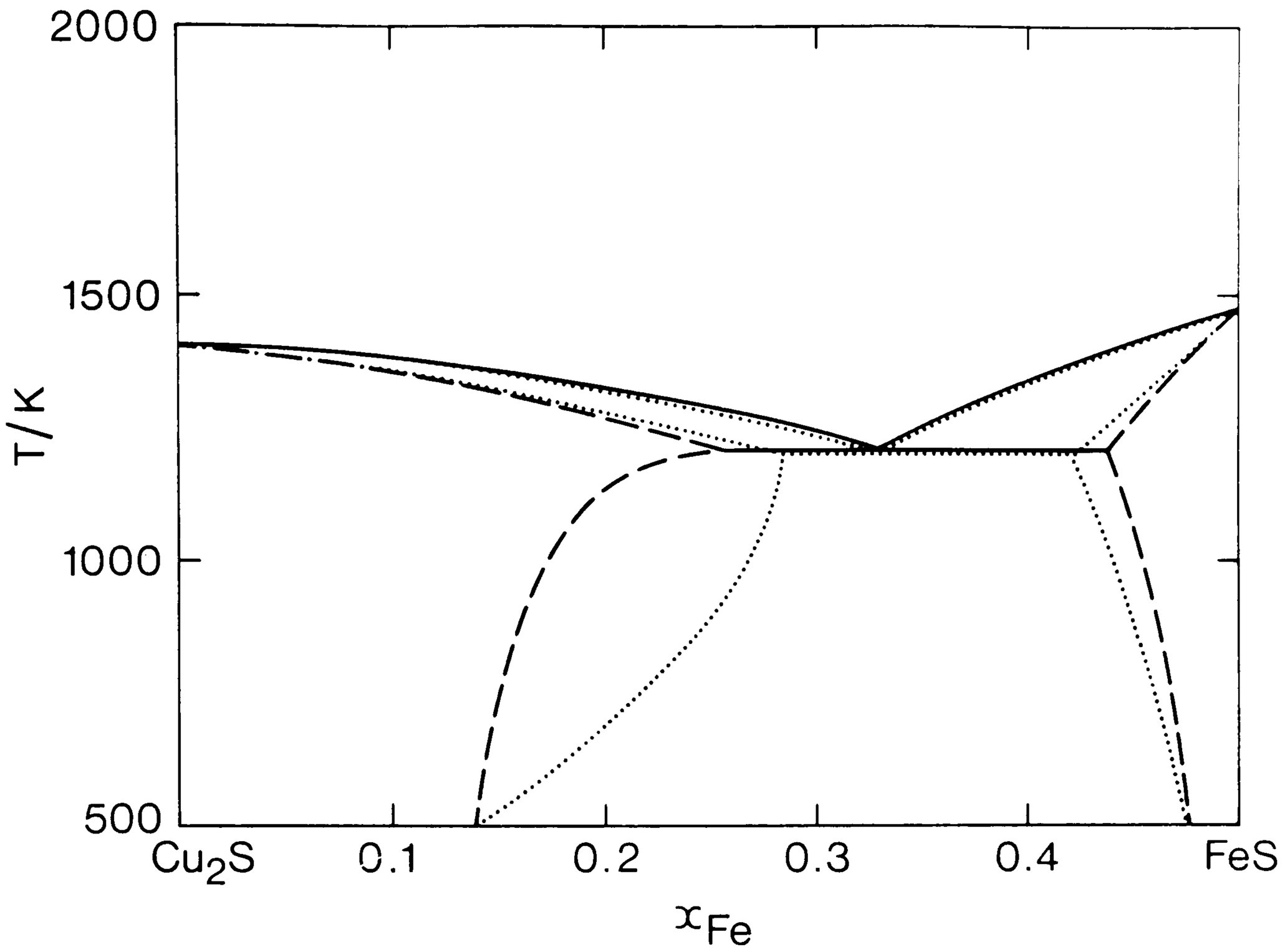

Fig 8.20 Pseudo-binary section between Cu_2S and FeS showing the calculated (dotted line), experimental (solid line) and assessed (dashed line) phase boundaries.

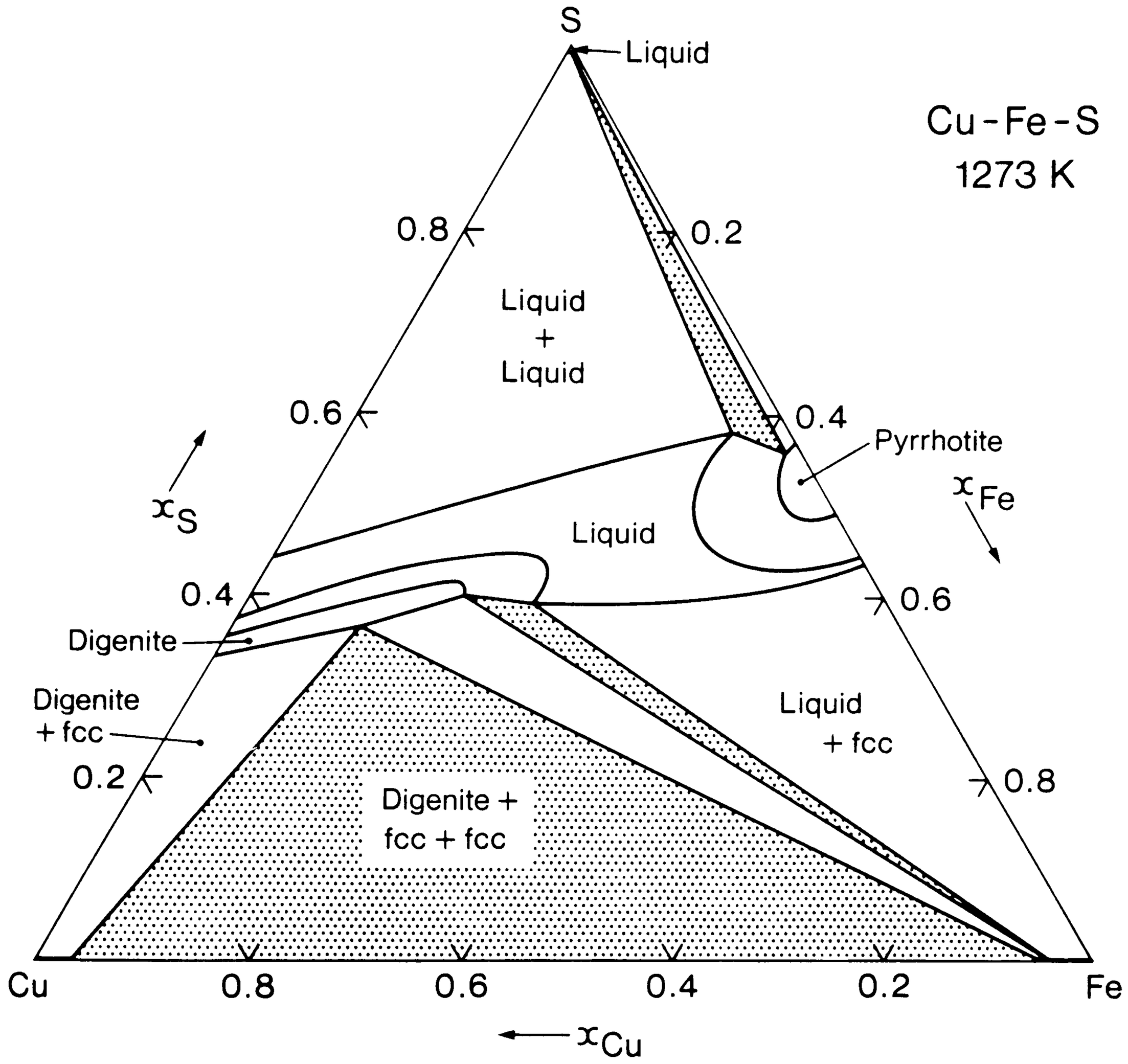

Fig 8.21 Experimental phase diagram for the Fe-Cu-S system for 1273 K as assessed by Chang et al.

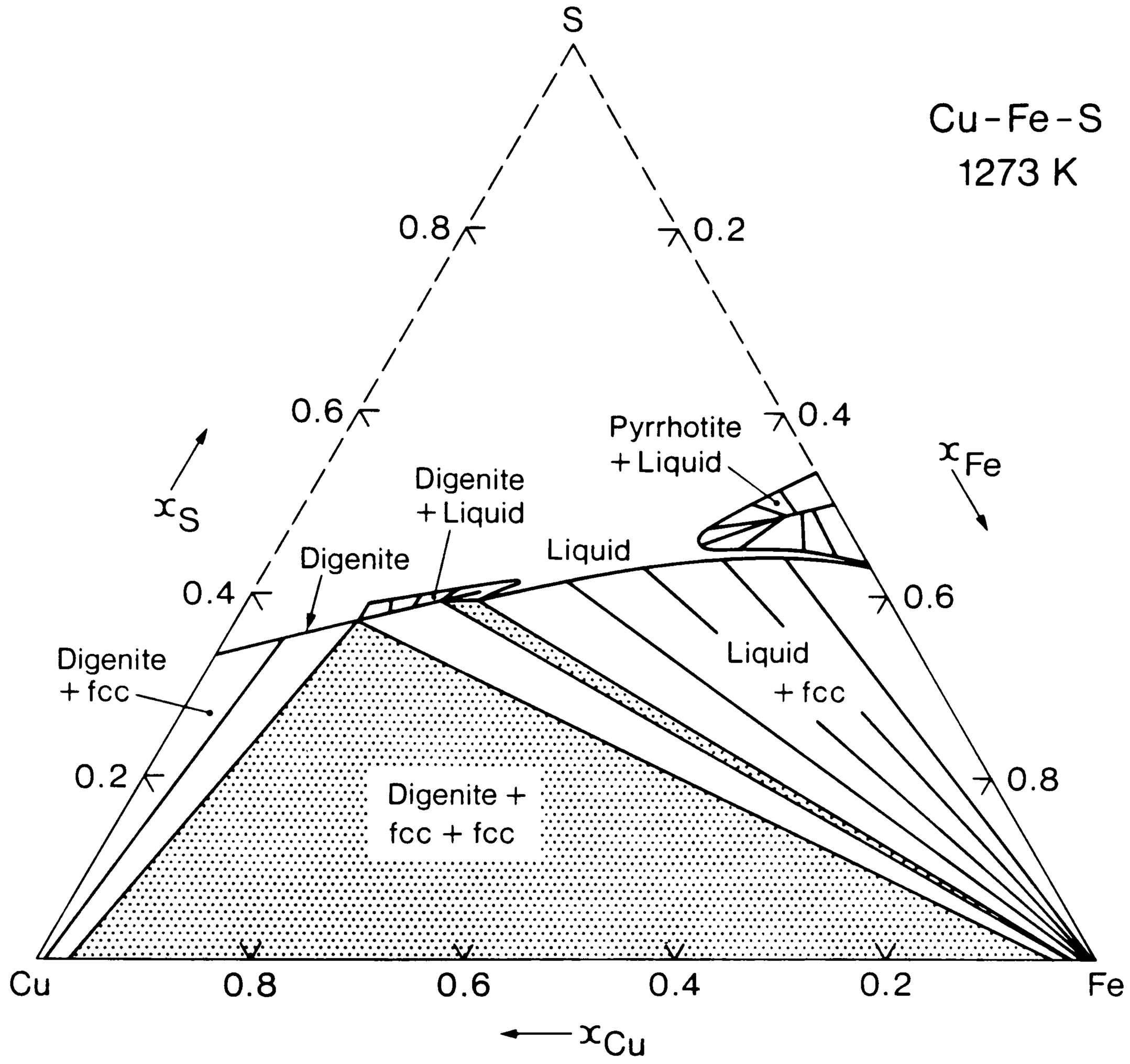

Fig 8.22 Calculated phase diagram for the metal rich part of the Fe-Cu-S system for 1273 K.

fcc and bcc and the second between digenite, pyrrhotite and bcc as shown in Fig 8.23, the phase diagram for 973 K.

Calculation of phase equilibria in the Ni-Cu-S system

The phase diagram of the Ni-Cu-S system has also been the subject of much study and this work has been reviewed by Chang et al. (74). As Kullerud and Moh (486) pointed out, the high temperature phase diagram is dominated by three separate homogeneous liquid regions as in Cu-S binary system. The miscibility gap between the matte phase and the metal rich liquid phase has been studied by a number of groups (380,381,487-490) of which, according to Chang et al. the data of Schlitt et al. (487) and Lee et al. (380,381) are the most reliable. A number of investigations of the phase diagram have been made for lower temperatures (429,466,488,491-496).

Thermodynamic data for dilute solutions of sulphur in liquid copper-nickel alloys have been tabulated by Chang et al. (74). For more concentrated liquids data have been determined by Sryvalin and Esin (497), Matousek and Samis (498) and Lee et al. (380,381).

Two groups have thus far attempted to represent the thermodynamic data for the Ni-Cu-S system and check their assessments for consistency with the phase diagram. Both groups considered only the liquid phase and its equilibrium with the Ni-Cu fcc phase. Larrain and Lee (382) used an associated solution model with species of Cu, Cu_2S, CuS, Ni, Ni_3S_2 and NiS with a large number of ternary interaction parameters to represent the liquid phase and they obtained excellent agreement with all the experimental information. Chuang and Chang (384) also used an associated solution model for the liquid phase with species of Cu, Cu_2S, S, Ni and NiS, and derived the six temperature dependant ternary interactions between the species from the data for the binary system. Their

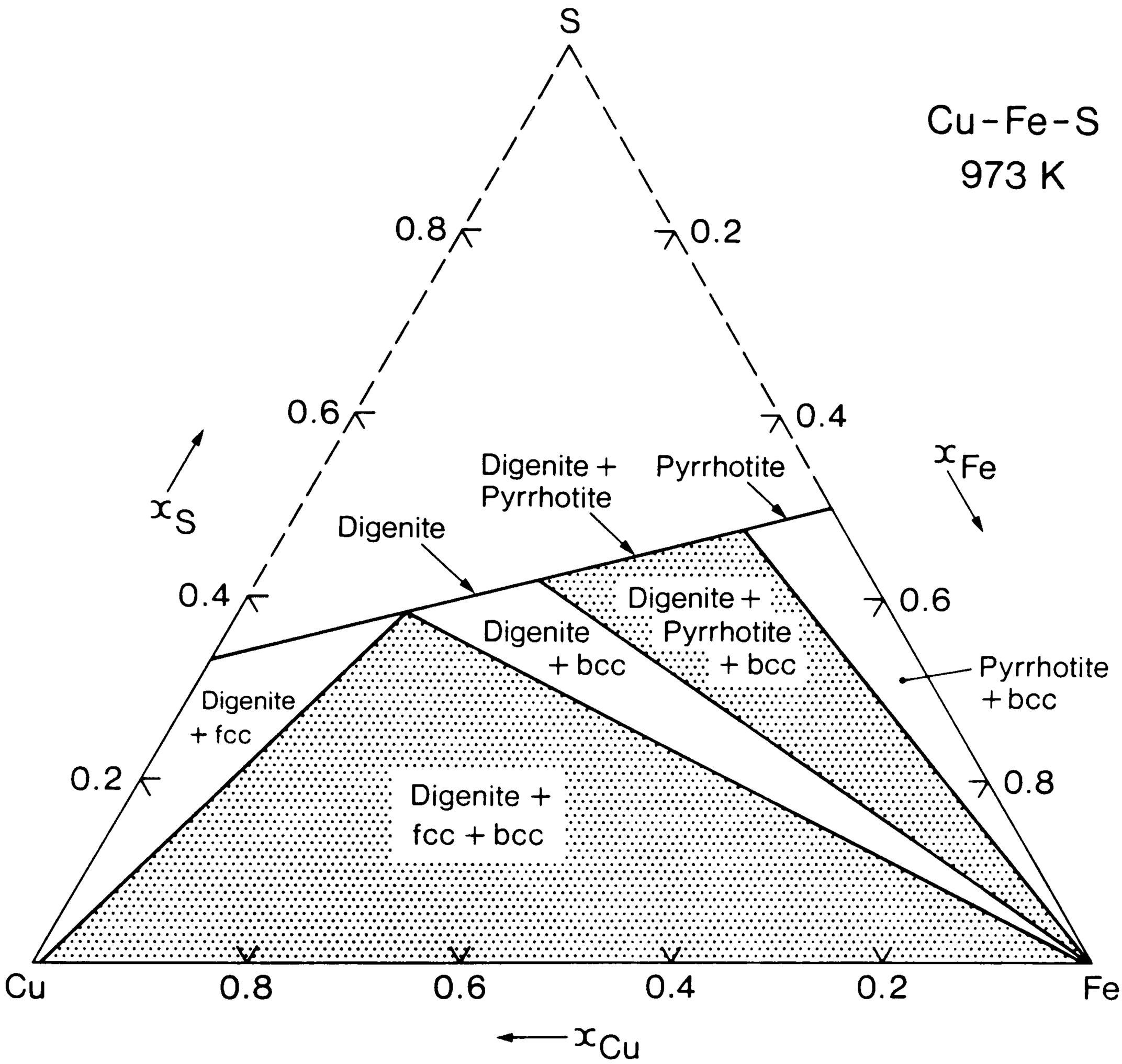

Fig 8.23 Calculated phase diagram for the metal rich part of the Fe-Cu-S system for 973 K.

representation of the available data, while it is very good, is not so good as that of Larrain and Lee but then they used fewer parameters.

As for the calculations of the Fe-Cu-S system, high temperatures were considered first. For the Fe-Cu-S system it was shown that the two sublattice model was able to represent the thermodynamic data for the liquid phase without the need for any ternary interaction data. Tentative phase diagram calculations were made for the miscibility gap in Cu-Ni-S system at 1473 K and 1673 K without any ternary interaction data and it was found that the agreement between calculated and experimental phase diagram was poor. This produced a phase diagram where the miscibility gap in the liquid phase extends much too far into the ternary system from the Cu-S binary compared with the experimental diagram shown in Fig 8.24. Ternary interactions were introduced into the liquid phase data set in order to improve the agreement between the calculated and experimental phase diagrams. Fig 8.25 shows the calculated phase diagram with the experimental phase boundaries superimposed. The agreement is acceptable although it is recommended that more work should be done in the future to improve the agreement. Figs 8.26, 8.27 and 8.28 show the calculated partial pressures of sulphur expressed as $\log(p_{S_2})/2$ for 1473 K and 1673 K for pseudo-binary cuts through the ternary system corresponding to constant $x_{Ni}:x_{Cu}$ ratios of 3, 1 and 0.333 respectively. Superimposed on these curves are the experimental data of Lee et al. (380,381). The agreement is very good for Ni rich compositions. For Cu rich compositions the agreement is not so good and this explains the disagreement between the calculated and experimental miscibility gap phase boundaries which are very sensitive to small changes in the thermodynamic data. Extra terms could have been introduced into the liquid phase data set to obtain better agreement but this would have impaired the predictive power of the model. It is believed that the cause of the discrepancy lies in the choice of the

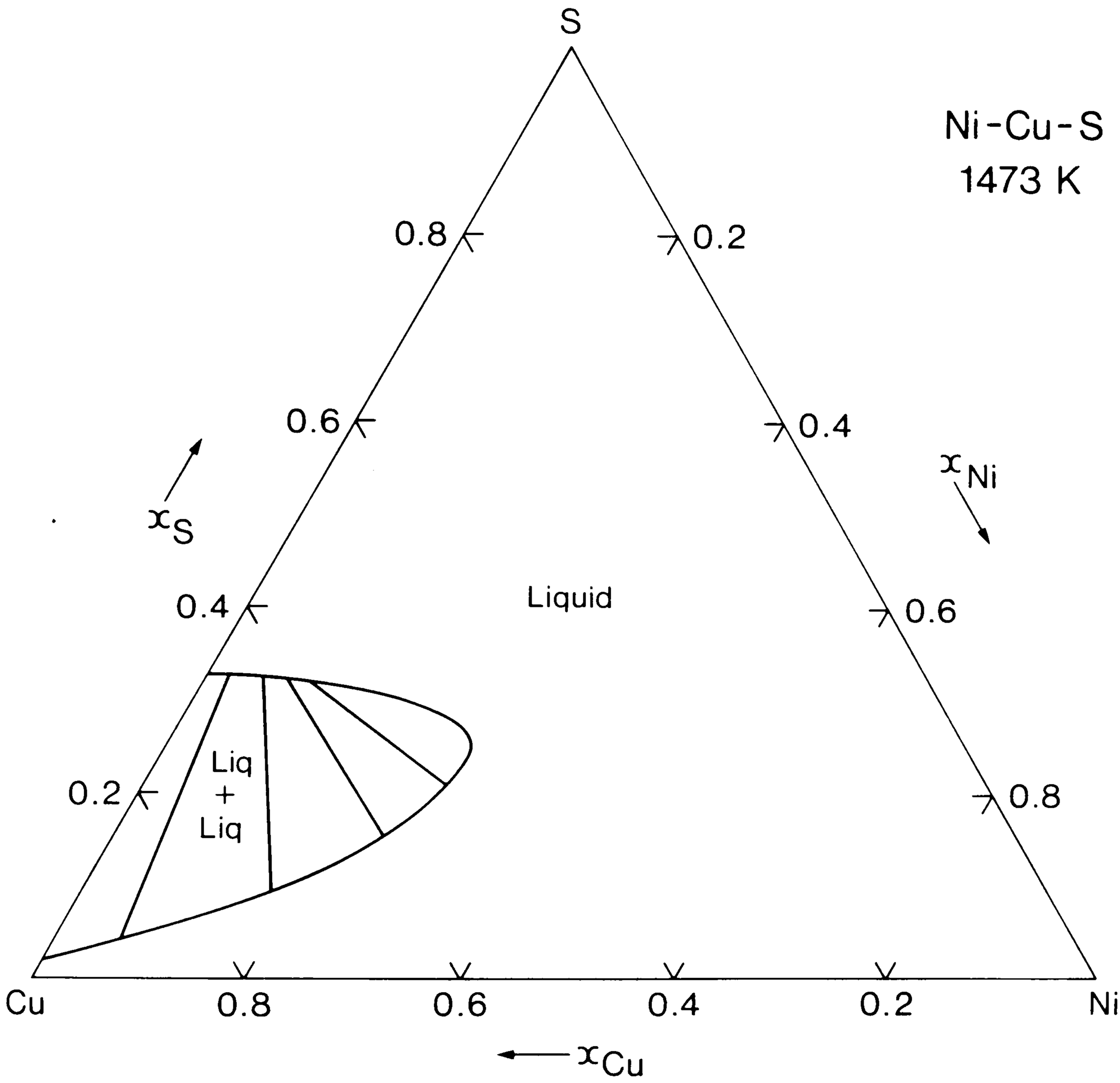

Fig 8.24 Experimental metal-matte miscibility gap in the Ni-Cu-S system for 1473 K as assessed by Chang et al.

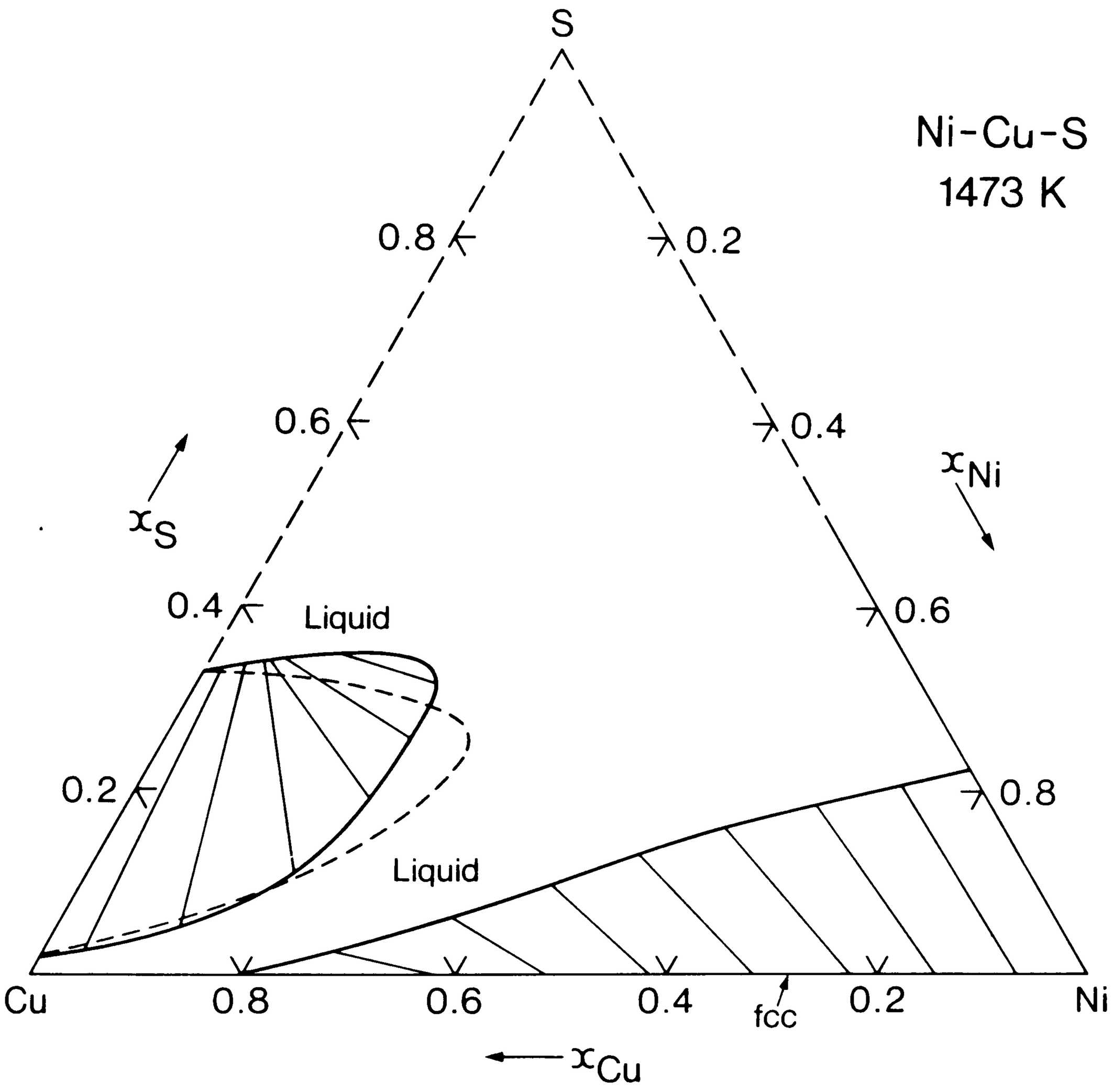

Fig 8.25 Calculated phase diagram for the metal rich part of the Ni-Cu-S system for 1473 K. The experimental metal-matte miscibility gap is superimposed as the dashed line.

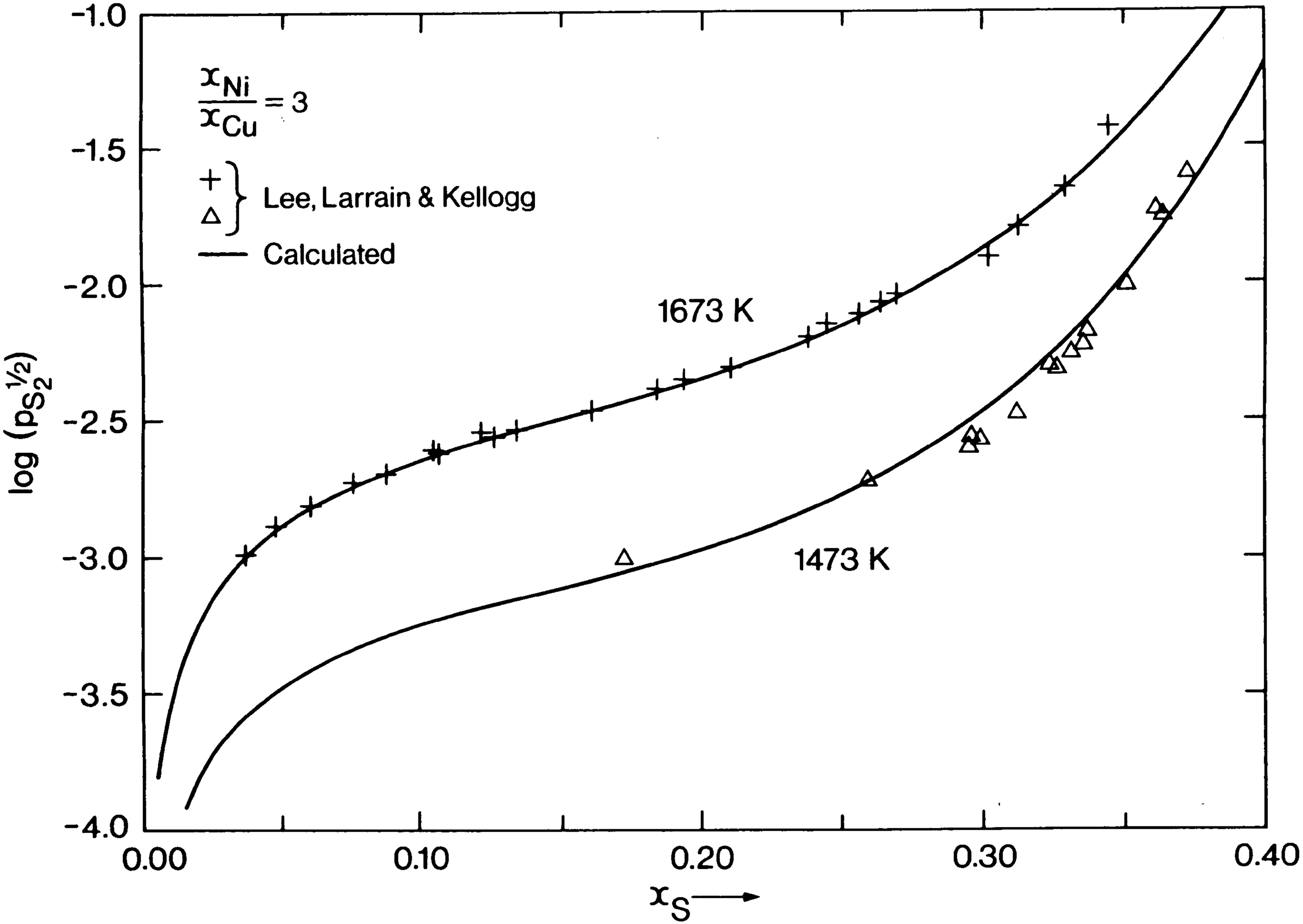

Fig 8.26 Comparison of the calculated and experimental sulphur pressures in the Ni-Cu-S system for the pseudo-binary section where $x_{Ni}:x_{Cu} = 3$.

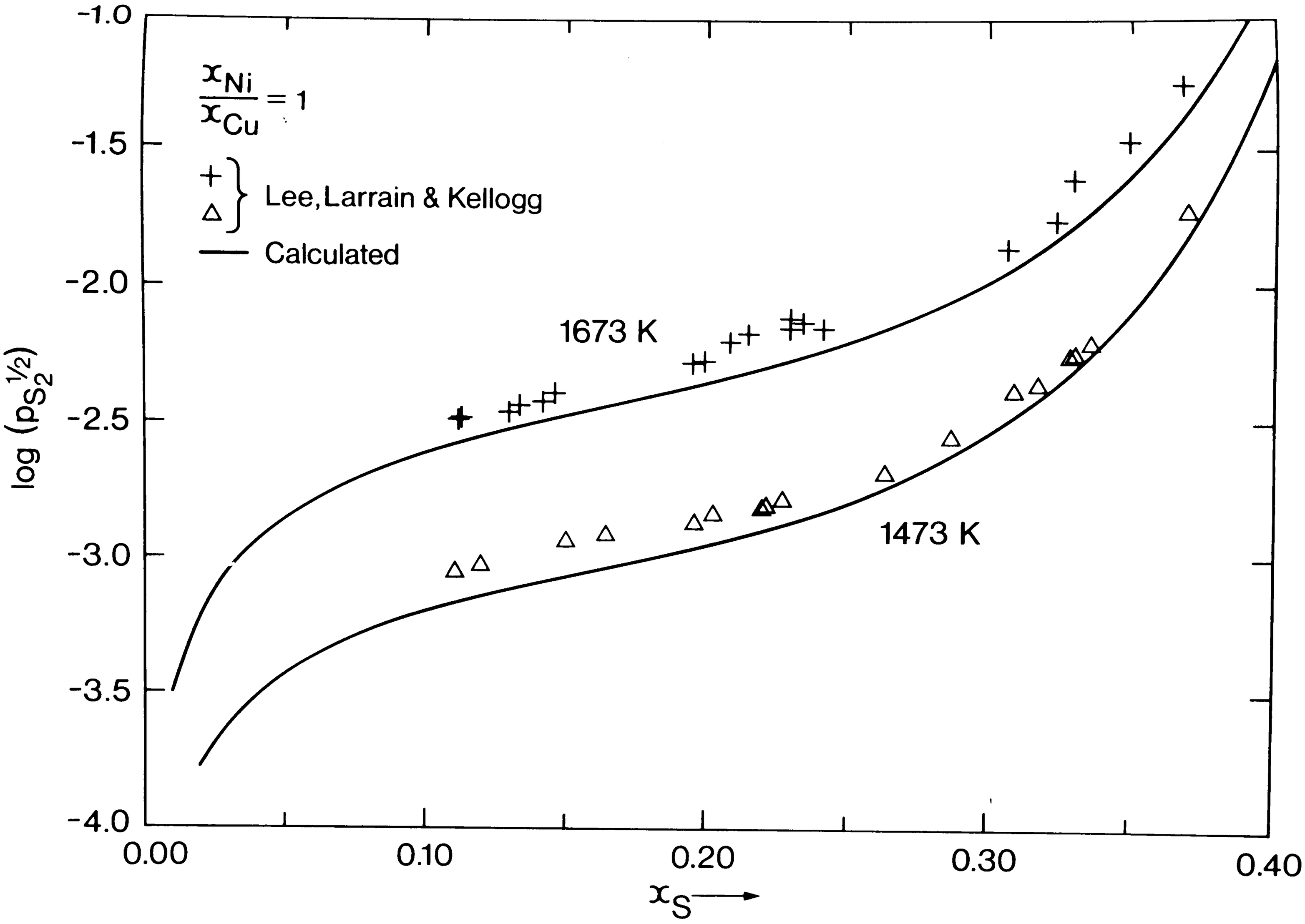

Fig 8.27 Comparison of the calculated and experimental sulphur pressures in the Ni-Cu-S system for the pseudo-binary section where $x_{Ni}:x_{Cu} = 1$.

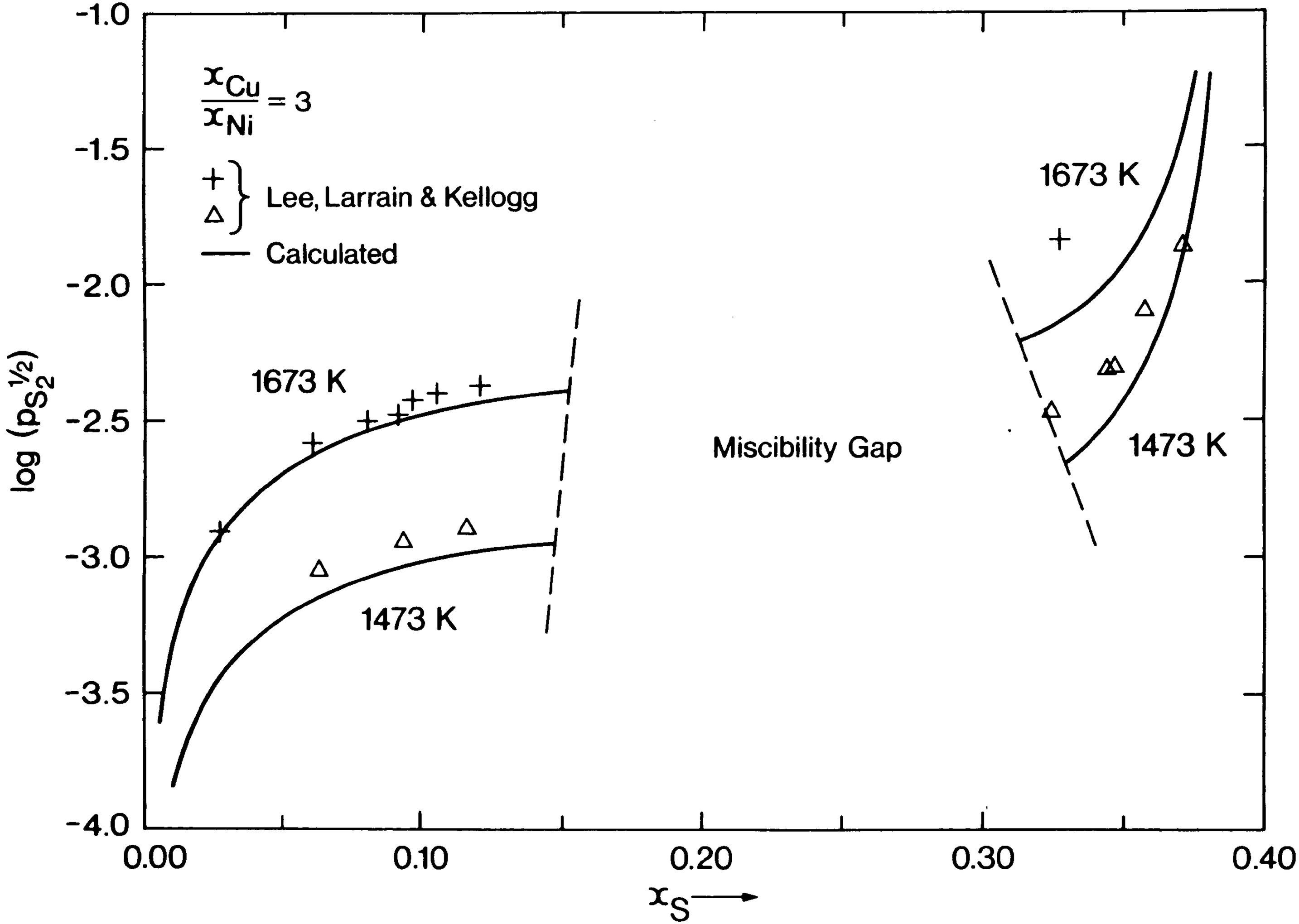

Fig 8.28 Comparison of the calculated and experimental sulphur pressures in the Ni-Cu-S system for the pseudo-binary section where $x_{Cu}:x_{Ni} = 3$.

notional charge for Ni as 2. A value of 1.333, as implied from the thermodynamic data would probably allow better extrapolation into ternary systems. It should however be remembered that the representation of the Ni-S binary thermodynamic data by the present data set is very good as shown in Fig 8.12.

Fig 8.29 again shows the calculated phase diagram for 1473 K but, with superimposed, the contours for constant activity of sulphur. Fig 8.30 shows the experimental diagram for the Ni-Cu-S system at 1673 K which should be compared with Fig 8.31, the calculated diagram. In Fig 8.32, the calculated diagram is shown with contours representing constant sulphur activity expressed as $\log(p_{S_2})/2$. Figs 8.33 and 8.34 show the calculated phase diagram for 1273 K and 1173 K respectively. They show the gradual disappearance of the matte-liquid metal miscibility gap, the formation of the digenite and pyrrhotite phases, the increasing dominance of the three phase region Liq + fcc + Digenite and the formation of the beta phase based around the composition Ni_3S_2. Data for NiS in the digenite phase and interaction parameters for both the digenite and pyrrhotite phases were derived in order to obtain best agreement with the experimental diagram for 1053 K from Chang et al. (74) shown in Fig 8.35. In a similar way data for the Cu-S, Cu-Ni and ternary Cu-Ni-S interactions in the beta phase were derived to be consistent with Fig 8.35. The calculated diagram is shown in Fig 8.36. The results for the sulphur rich part of the system should be ignored for the purposes of comparison. The calculated phase boundaries are in some disagreement with the experimental boundaries, in particular the composition of the fcc phase at the corner of the three phase region with liquid and digenite, and the boundaries of the liquid phase in equilibrium with digenite and fcc. It is felt however that the calculated diagram is likely to be more correct. Fig 8.37 shows the calculated diagram for 973 K close to a predicted eutectic between

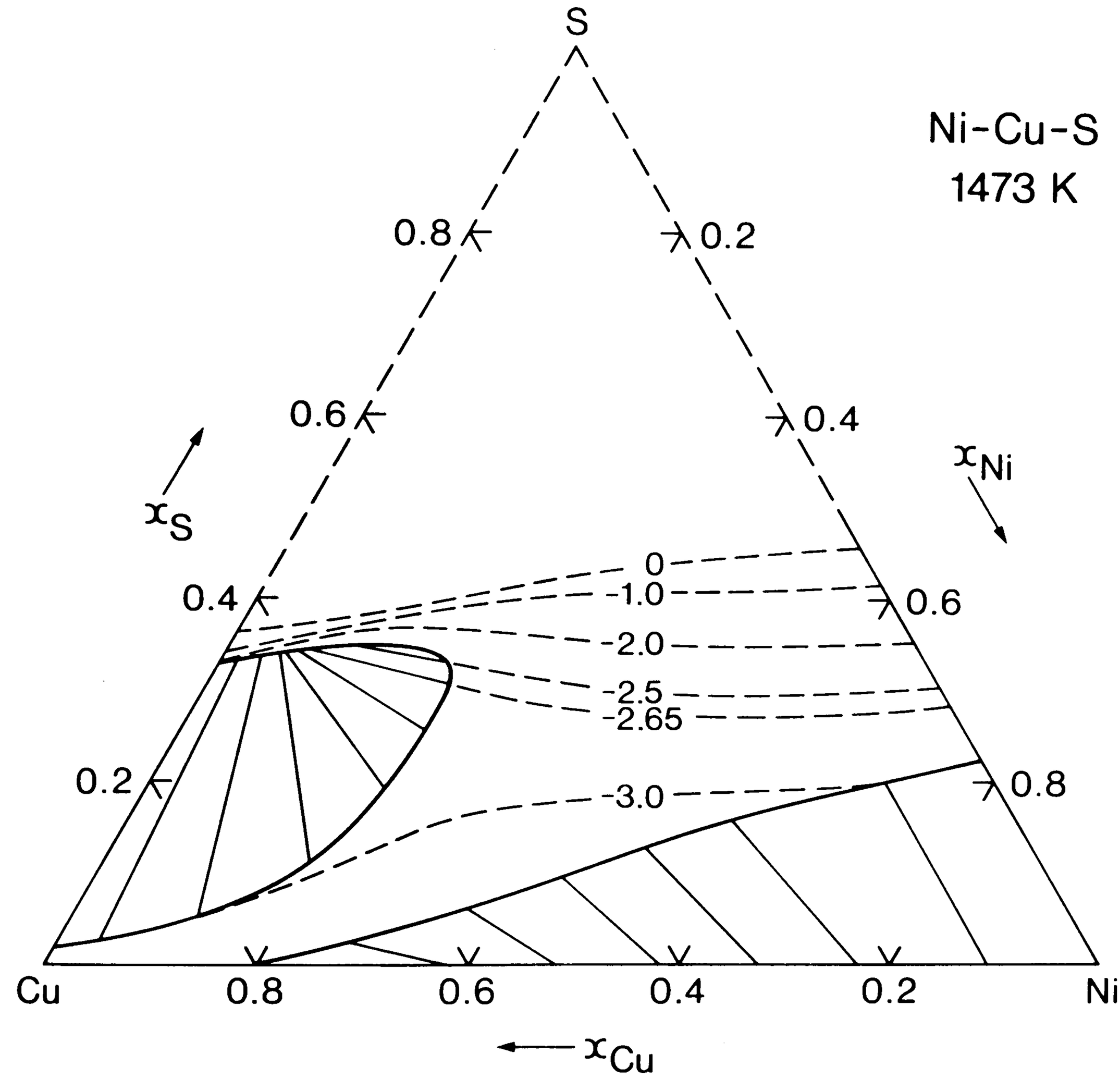

Fig 8.29 Calculated phase diagram for the metal rich part of the Ni-Cu-S system for 1473 K with contours for constant sulphur activity expressed as $\log(p_{S_2})/2$.

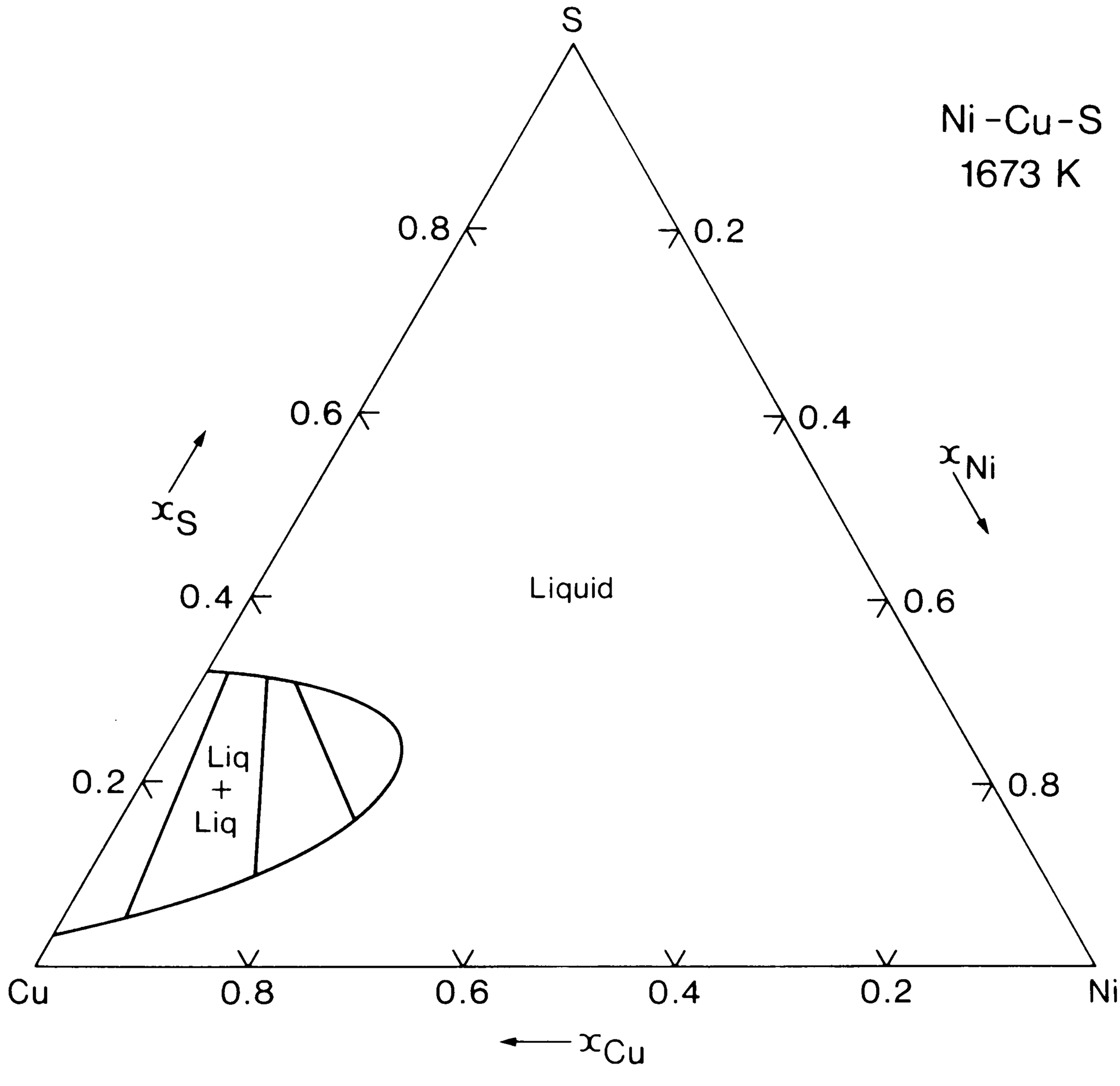

Fig 8.30 Experimental metal-matte miscibility gap in the Ni-Cu-S system for 1673 K as assessed by Chang et al.

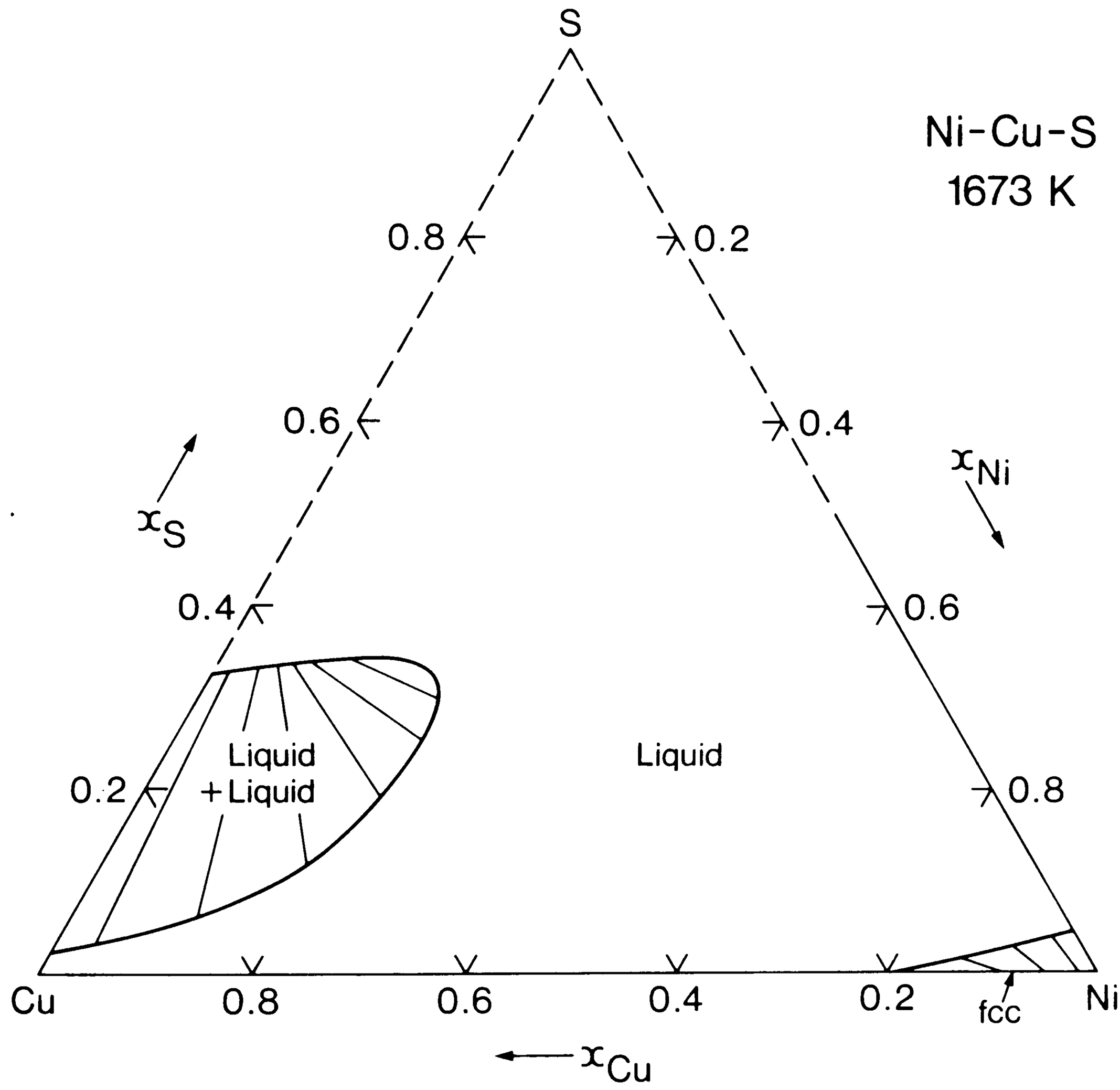

Fig 8.31 Calculated phase diagram for the metal rich part of the Ni-Cu-S system for 1673 K.

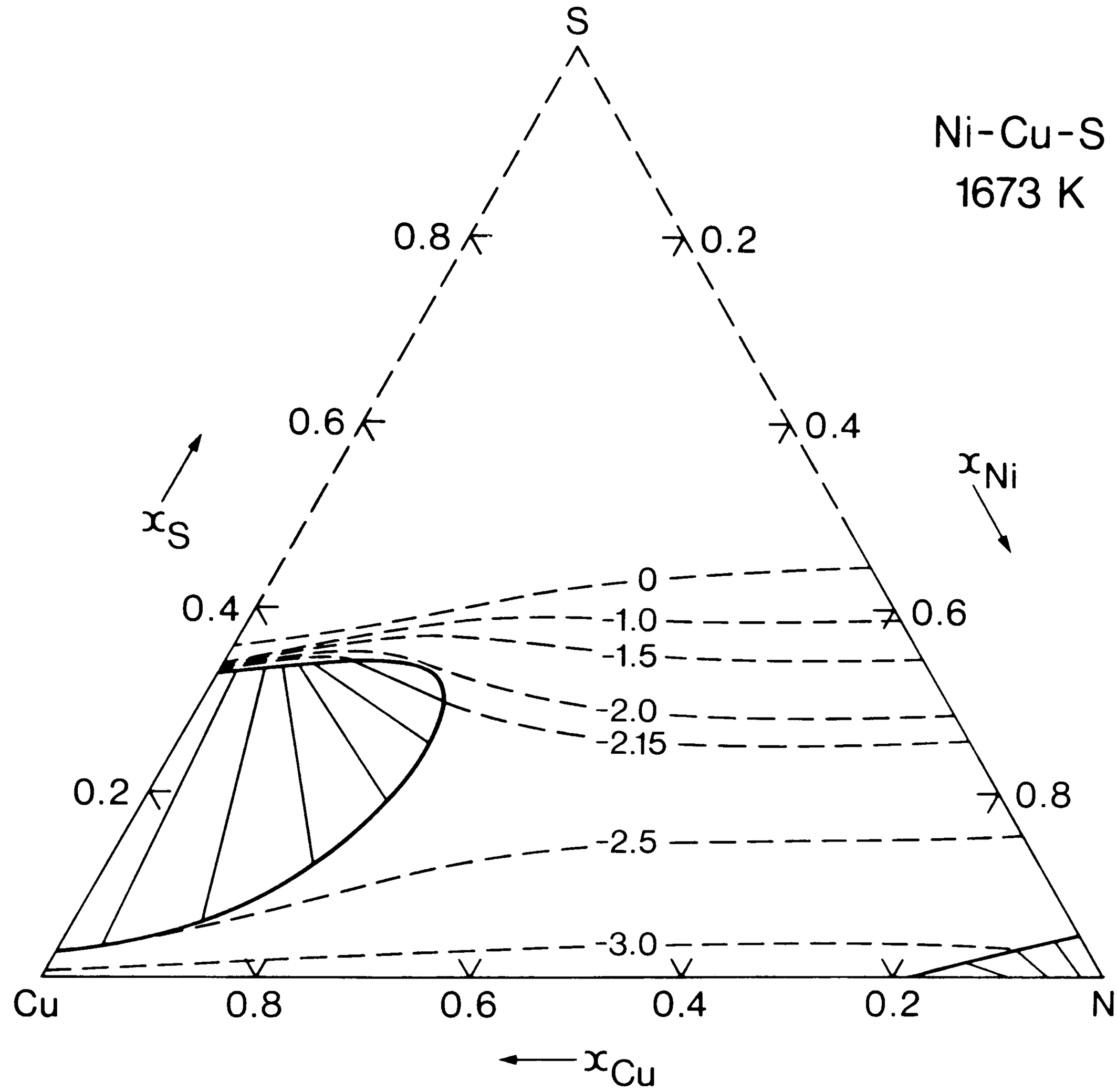

Fig 8.32 Calculated phase diagram for the metal rich part of the Ni-Cu-S system for 1673 K with contours for constant sulphur activity expressed as $\log(p_{S_2})/2$.

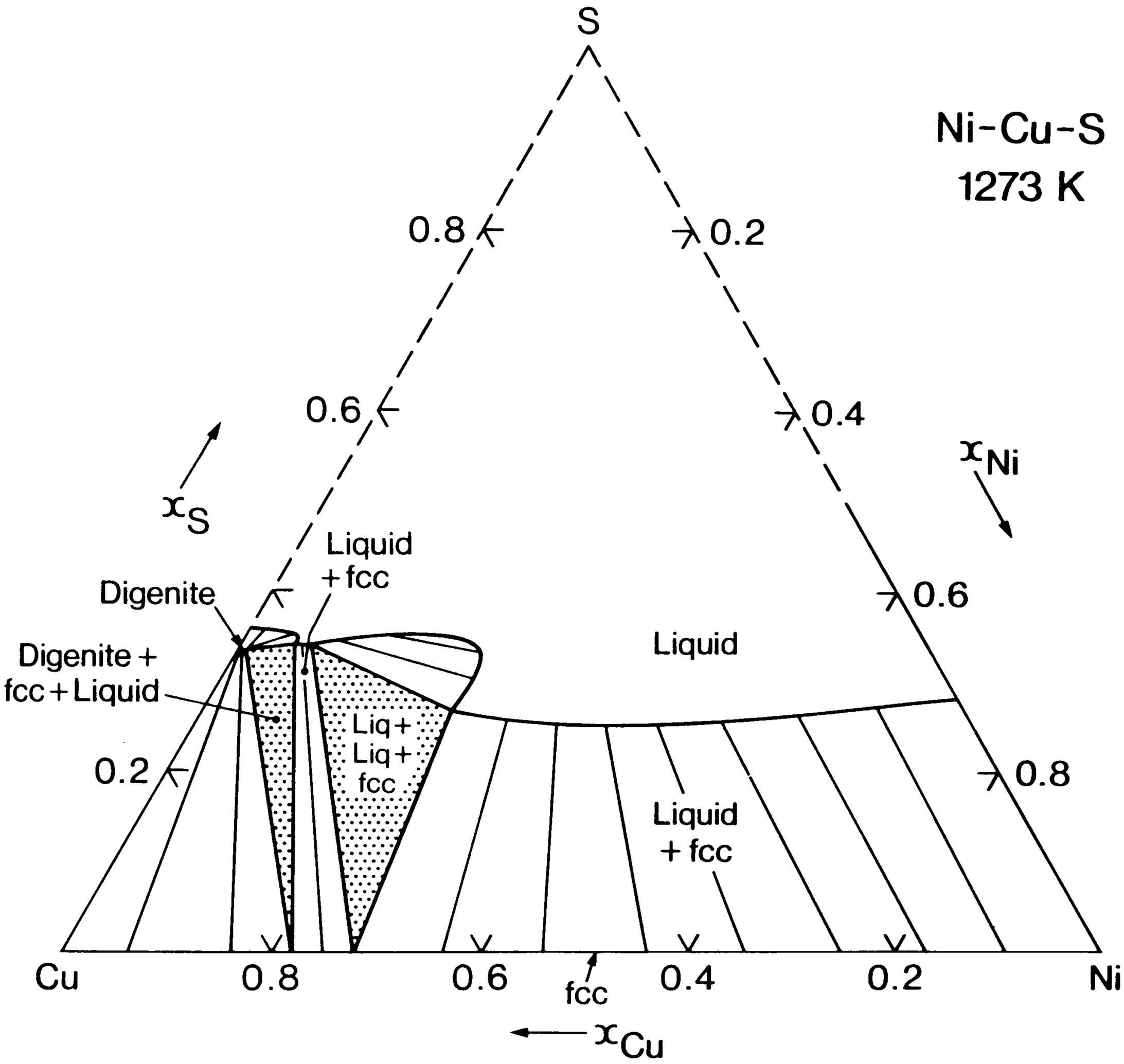

Fig 8.33 Calculated phase diagram for the metal rich part of the Ni-Cu-S system for 1273 K.

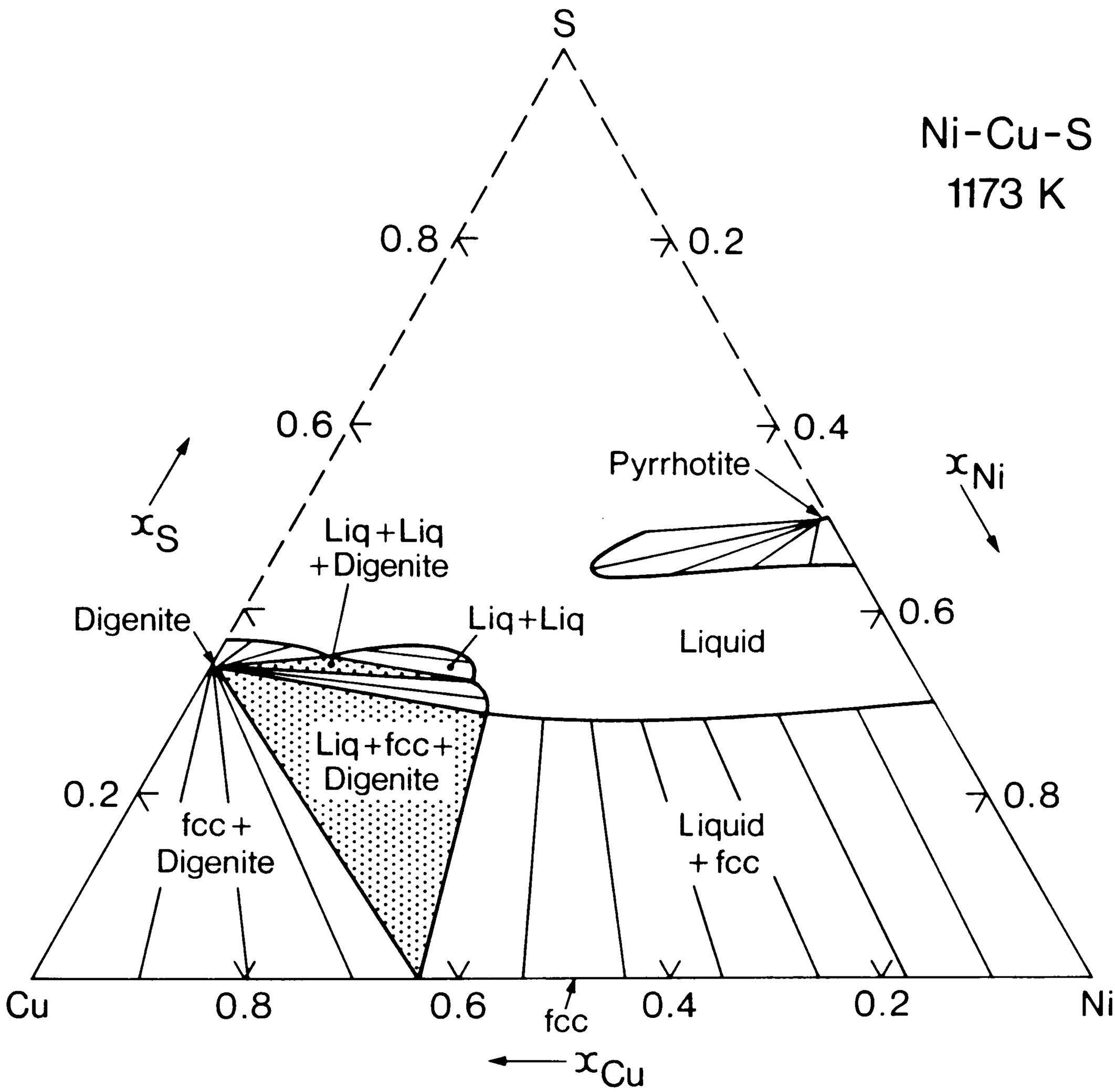

Fig 8.34 Calculated phase diagram for the metal rich part of the Ni-Cu-S system for 1173 K.

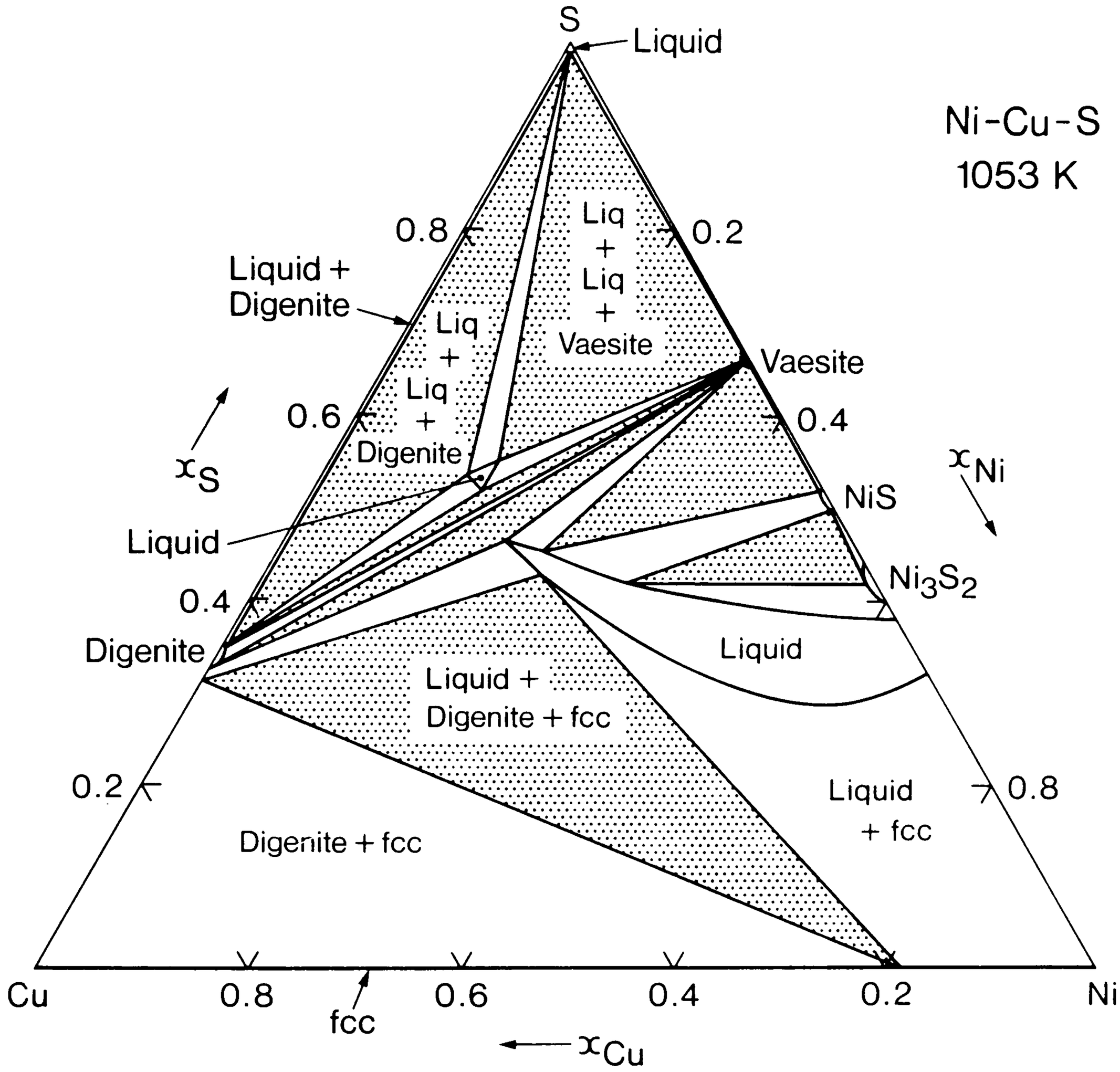

Fig 8.35 Experimental phase diagram for the Ni-Cu-S system for 1053 K as assessed by Chang et al.

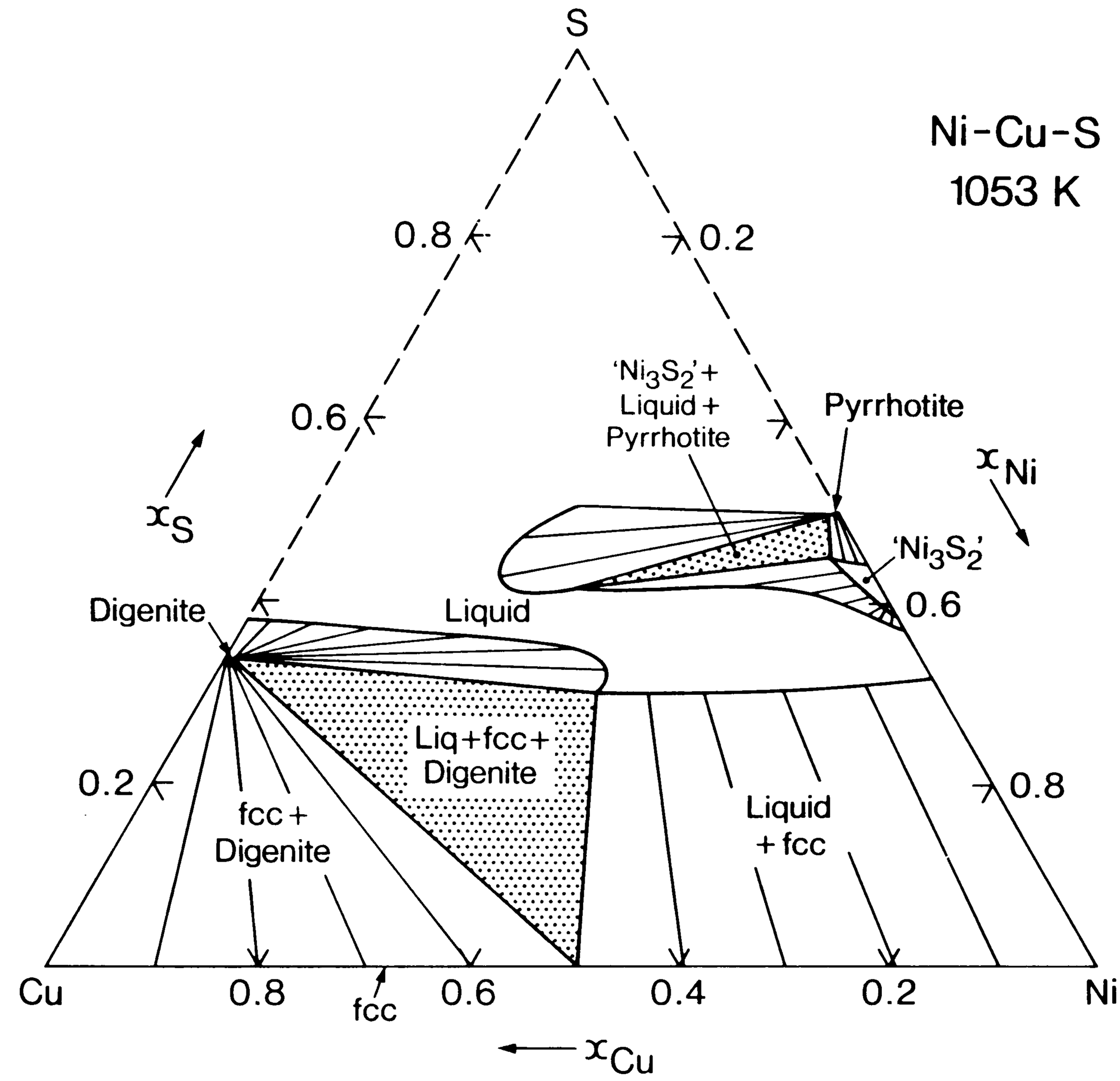

Fig 8.36 Calculated phase diagram for the metal rich part of the Ni-Cu-S system for 1053 K.

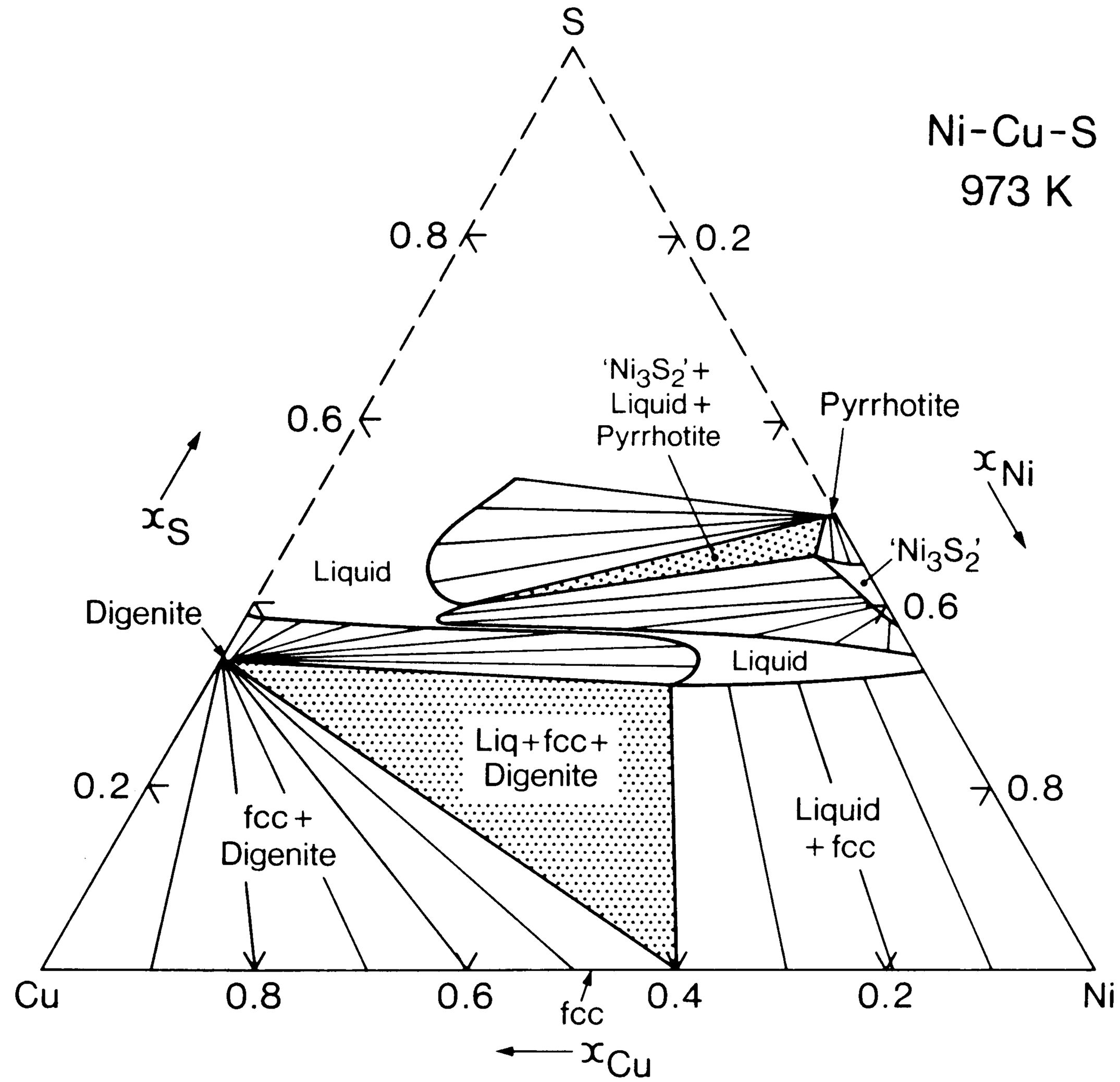

Fig 8.37 Calculated phase diagram for the metal rich part of the Ni-Cu-S system for 973 K.

digenite and the beta phase. This is in excellent agreement with the experimental eutectic temperature of 978 K (74,488). Fig 8.38 shows the calculated phase diagram for 873 K and this should be compared with the experimental phase diagram in Fig 8.39. A ternary eutectic is predicted from the calculations and this has been observed experimentally. The overall agreement between Figs 8.38 and 8.39 is very good.

Calculation of phase equilibria in the Ni-Fe-S system

The Ni-Fe-S system is of great general interest since phases based in this system are found in many ores. The experimental data for the Ni-Fe-S system has been reviewed by Hsieh et al. (499) and Craig and Scott (402) incorporating the large number of studies of the phase diagram (466,500-520).

There have been few experimental studies to derive thermodynamic data for the Ni-Fe-S system. Naldrett and Craig (506) and Kao (517) have studied the partial pressure of sulphur above the monosulphide solid solution (pyrrhotite). Kao, who also studied the two phase region between pyrrhotite and the beta phase, paid particular attention to the phase relationships and the representation of the thermodynamic data. Scott et al. (521,522) investigated the activity of FeS in the pyrrhotite phase at 1203 K and found that NiS and FeS mix ideally for a given mole fraction of sulphur. Studies have been carried out on dilute solutions of sulphur in the liquid phase (432-434,523,524). Concentrated liquids have been studied by Vaisburd et al. (525) who measured the activities of Fe in concentrated liquids at 1573 K while Byerley and Takebe (437), Meyer (379) and Bale (526) have studied the partial pressures of sulphur above the liquid phase at high temperatures.

Thermodynamic data were predicted for the liquid phase from the data

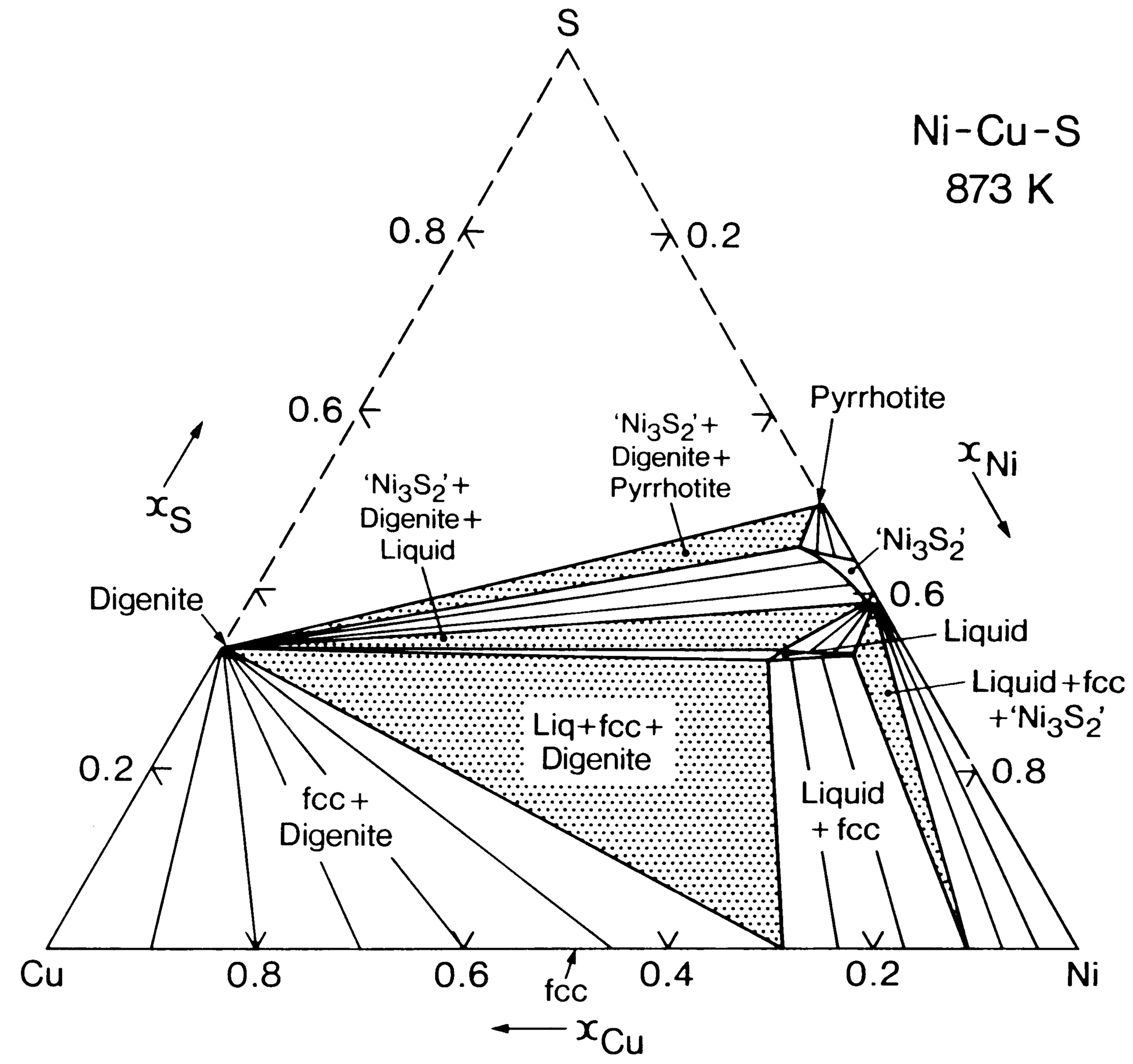

Fig 8.38 Calculated phase diagram for the metal rich part of the Ni-Cu-S system for 873 K.

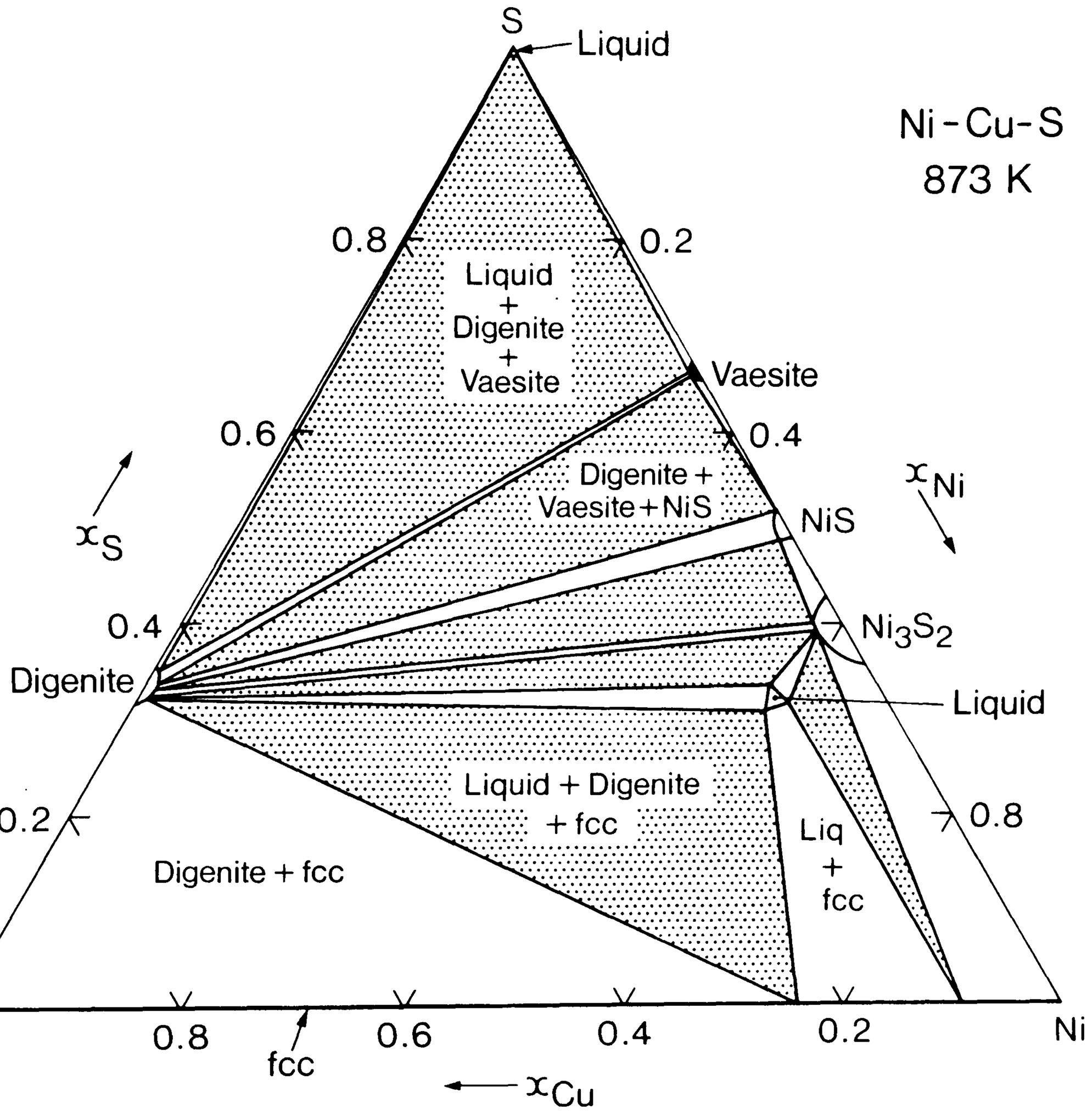

Fig 8.39 Experimental phase diagram for the Ni-Cu-S system for 873 K as assessed by Chang et al.

of the component binary systems only. As was found for the Cu-Ni-S system these predicted data were not in good agreement with the available experimental data and it was necessary to introduce ternary parameters. The data of Byerley and Takebe are thought to be less reliable than those of Meyer and Bale and have not been considered in detail. Some reliable phase diagram data are also available for the equilibrium between the liquid phase and fcc metallic phase (516).

Close agreement between predicted and experimental thermodynamic and phase diagram data was obtained by optimising the ternary parameters with a specially developed computer program. Figs 8.40, 8.41 and 8.42 show the calculated partial pressures of sulphur and, superimposed, the experimental values determined by Meyer (379) for 1473 K, 1573 K and 1673 K and various relative proportions of Fe and Ni. Fig 8.43 shows the calculated partial pressures of sulphur for various relative proportions of Fe and Ni at 1473 K with the experimental data of Bale (526) superimposed. As shown the agreement between calculated and experimental data is very good. There does however seem to be some disagreement particularly for high relative ratios of iron to nickel.

Figs 8.44 and 8.45 shows the calculated phase diagram for 1573 K and 1473 K in good agreement with the experimental work of Lenz et al. (516). The calculated phase diagram for 1473 K is also shown in Fig 8.46 with contours representing constant activities of sulphur expressed as $\log(p_{S_2})/2$.

Below 1464 K the pyrrhotite phase becomes stable first for the composition FeS and at lower temperatures extending completely across the system to NiS. According to Scott et al. (521,522) who measured the variation of the activity of FeS in the monosulphide solid solution, FeS and NiS mix ideally at 1203 K. Furthermore Misra and Fleet (513-515) and Craig (512) found that at temperatures below 573 K a miscibility gap develops either side of a composition corresponding to $FeNiS_2$. These two

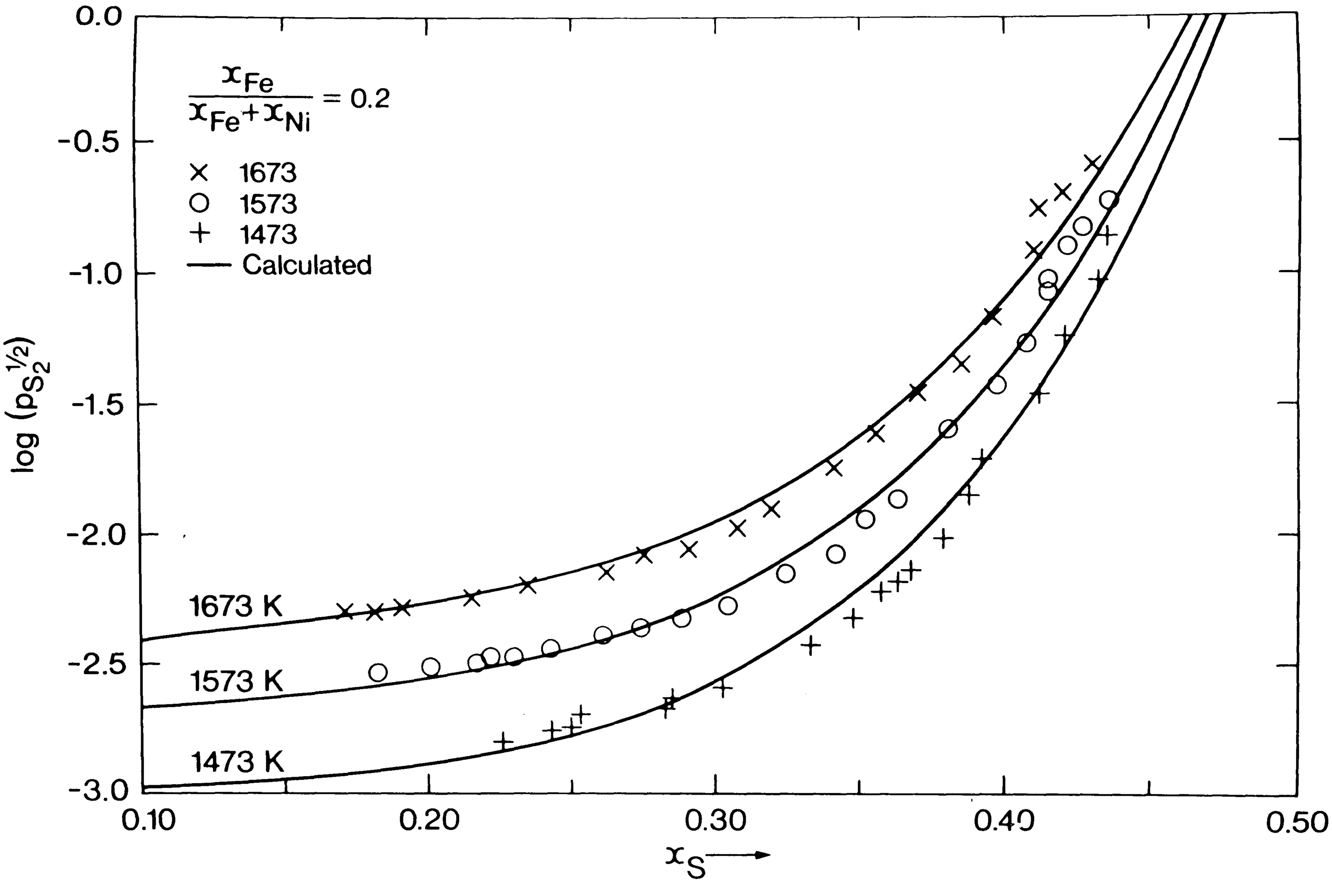

Fig 8.40 Comparison between calculated and experimental sulphur pressures in the Ni-Fe-S system for a pseudo-binary section where $x_{Fe}/(x_{Fe}+x_{Ni}) = 0.2$. Experimental data from Meyer.

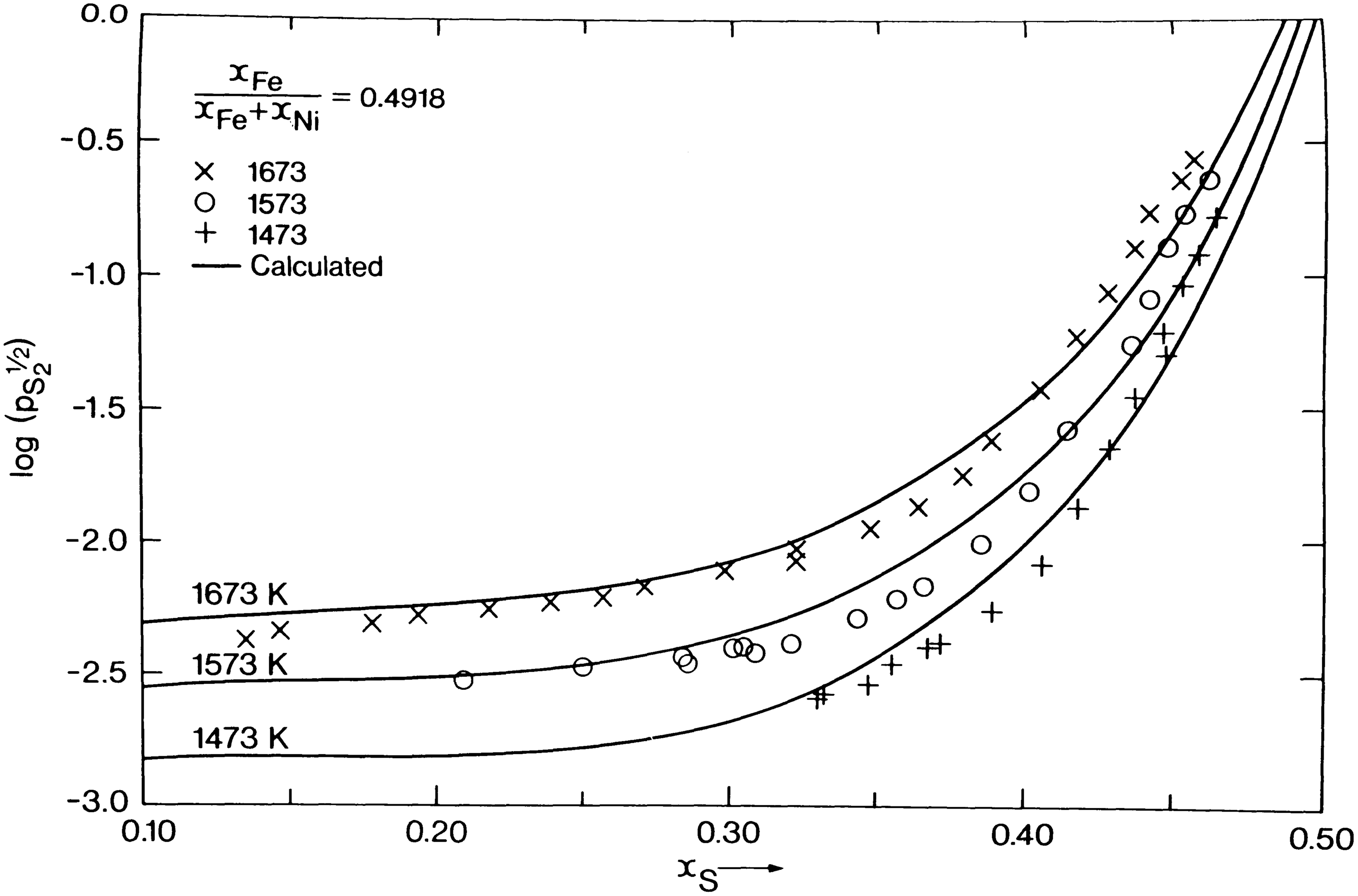

Fig 8.41 Comparison between calculated and experimental sulphur pressures in the Ni-Fe-S system for a pseudo-binary section where $x_{Fe}/(x_{Fe}+x_{Ni})$ = 0.4918. Experimental data from Meyer.

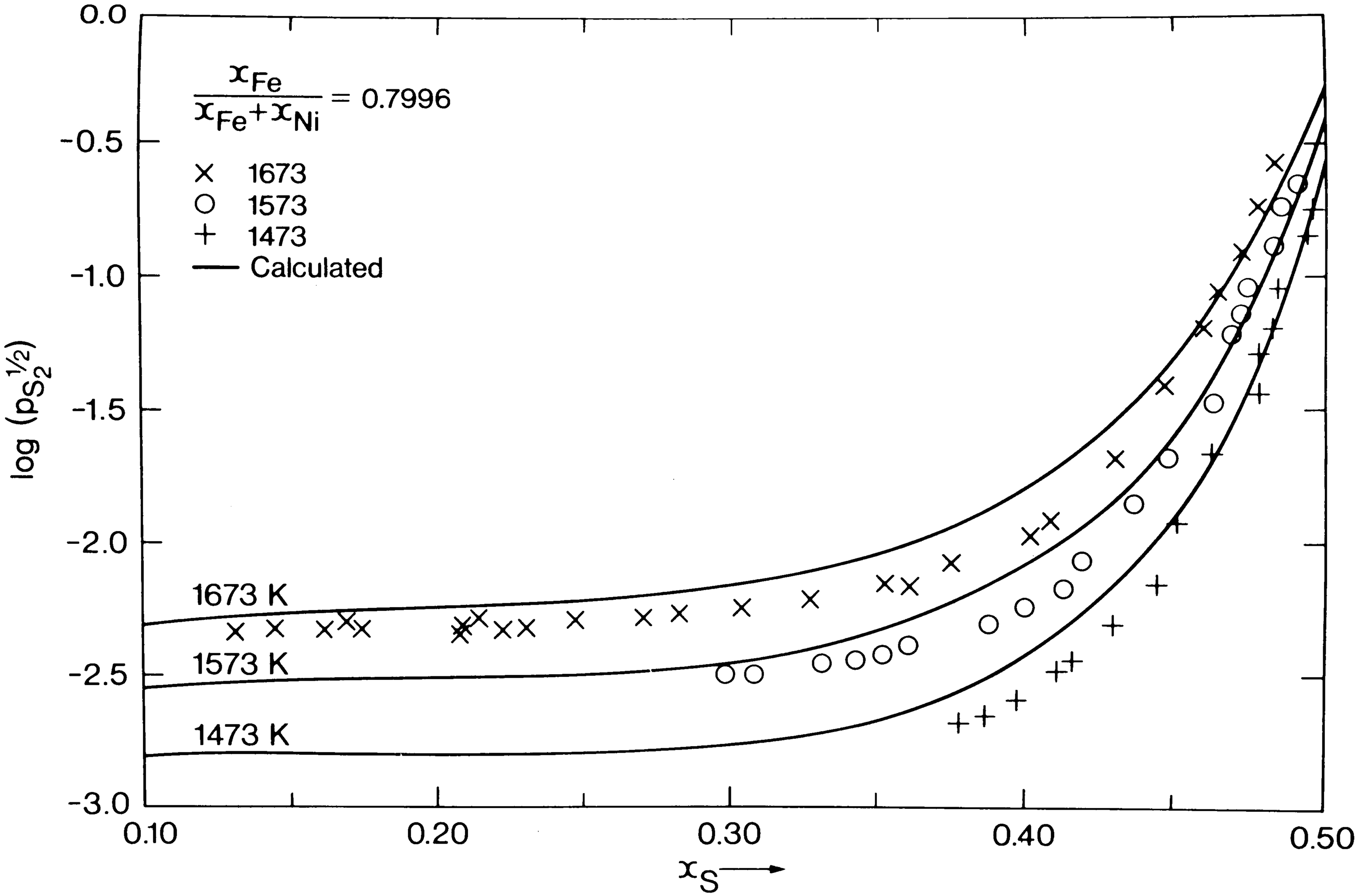

Fig 8.42 Comparison between calculated and experimental sulphur pressures in the Ni-Fe-S system for a pseudo-binary section where $x_{Fe}/(x_{Fe}+x_{Ni})$ = 0.7996. Experimental data from Meyer.

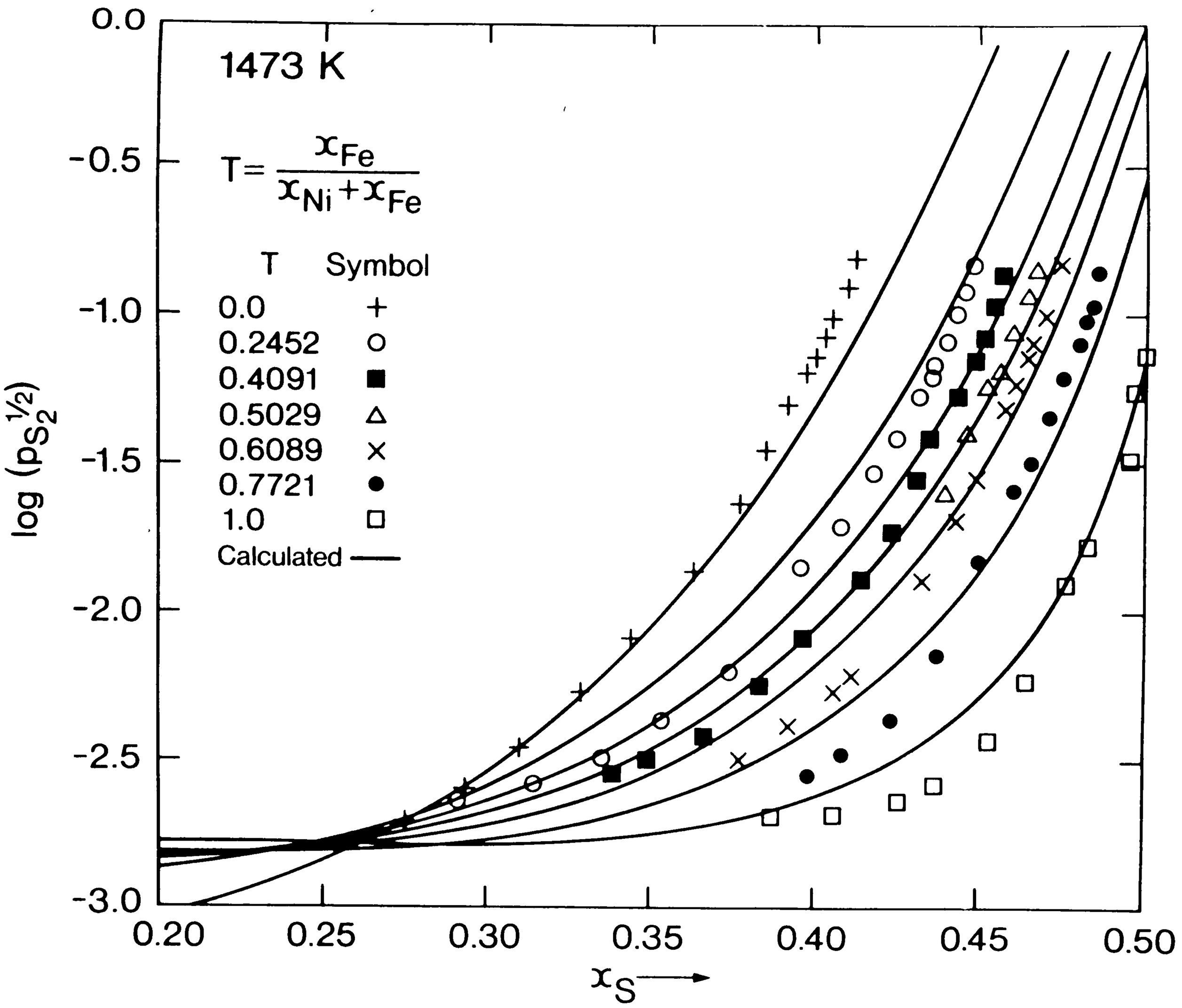

Fig 8.43 Comparison between calculated and experimental sulphur pressures in the Ni-Fe-S system for various pseudo-binary sections. Experimental data from Bale.

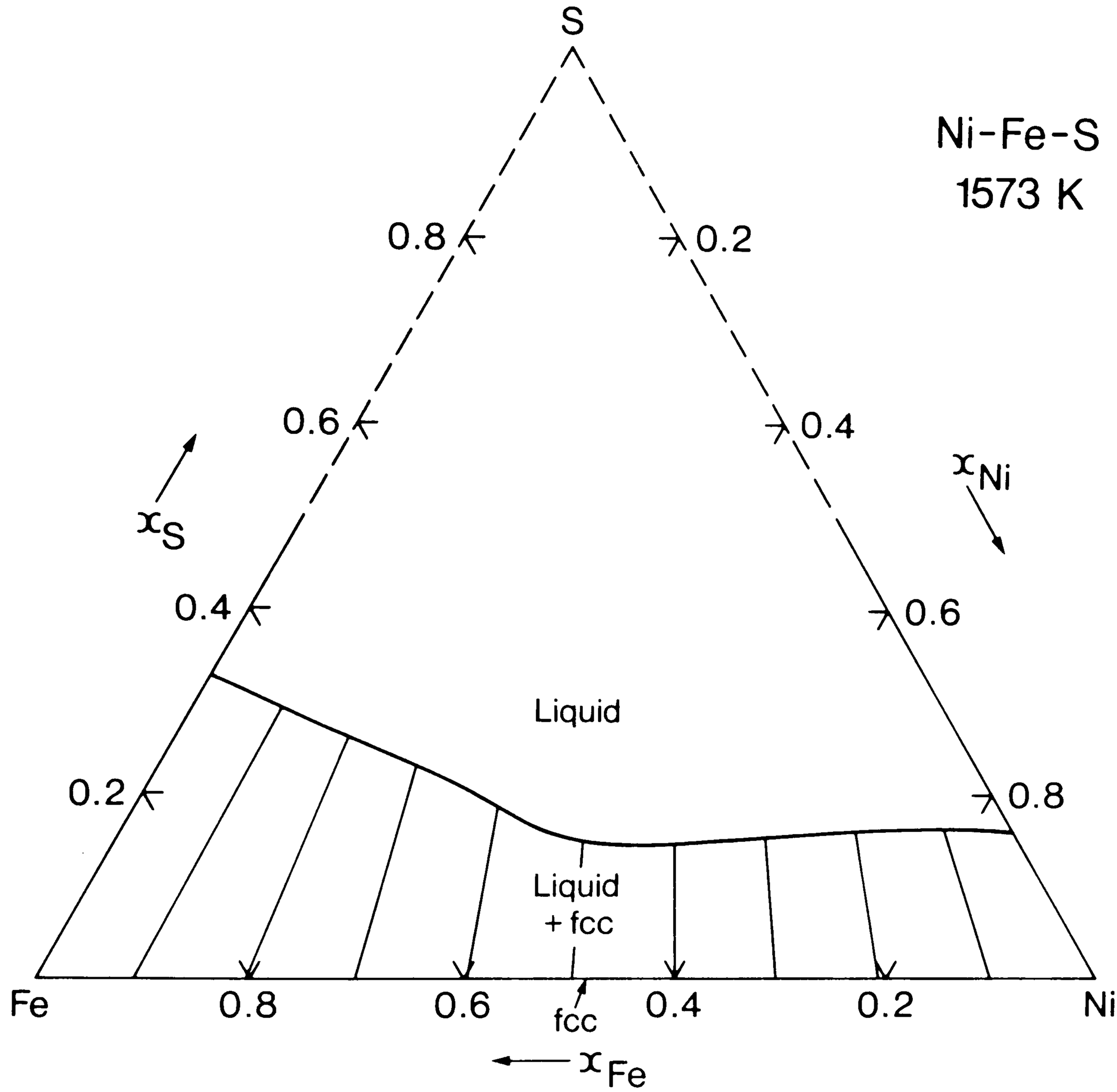

Fig 8.44 Calculated phase diagram for the metal rich part of the Ni-Fe-S system for 1573 K.

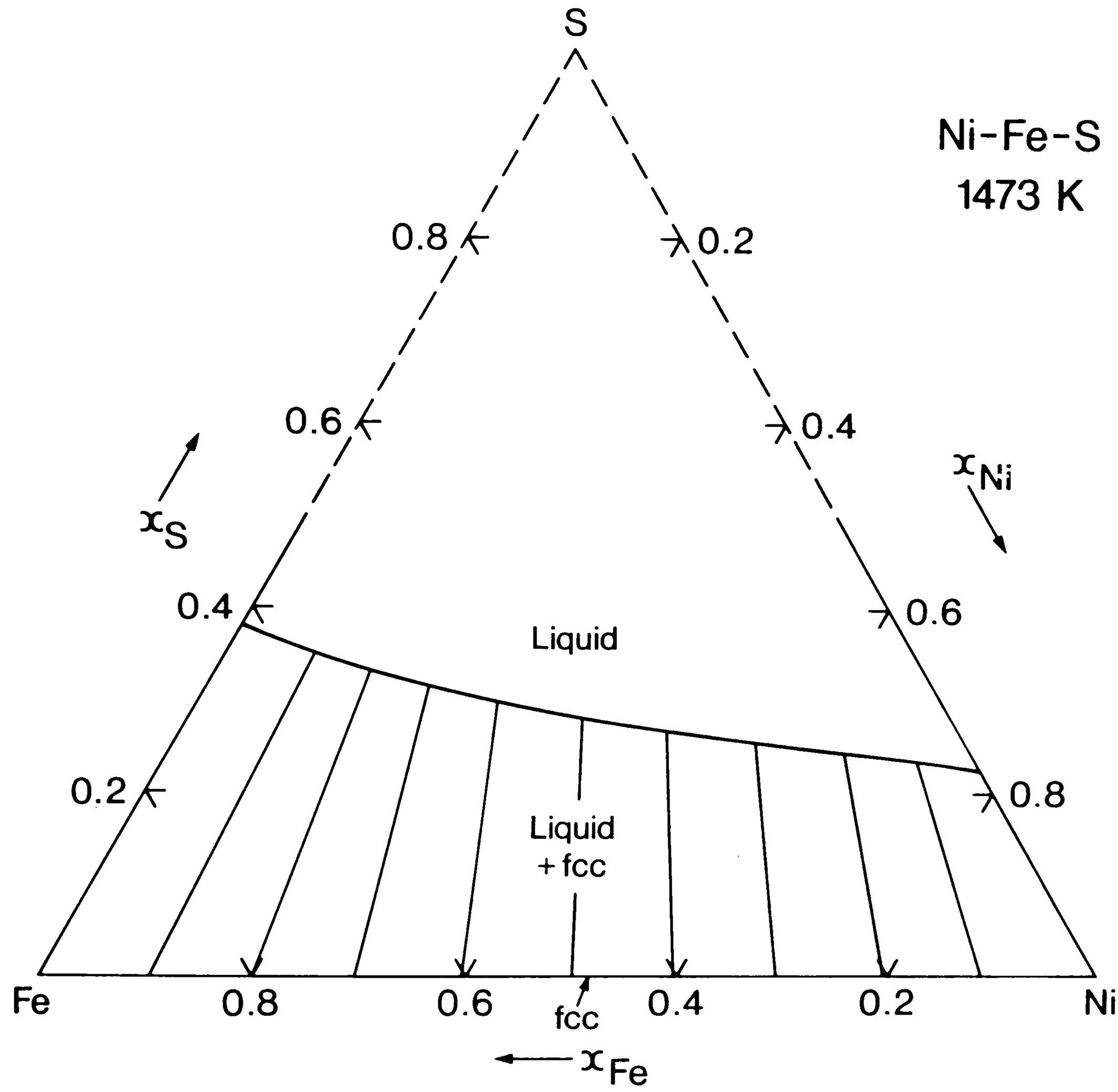

Fig 8.45 Calculated phase diagram for the metal rich part of the Ni-Fe-S system for 1473 K.

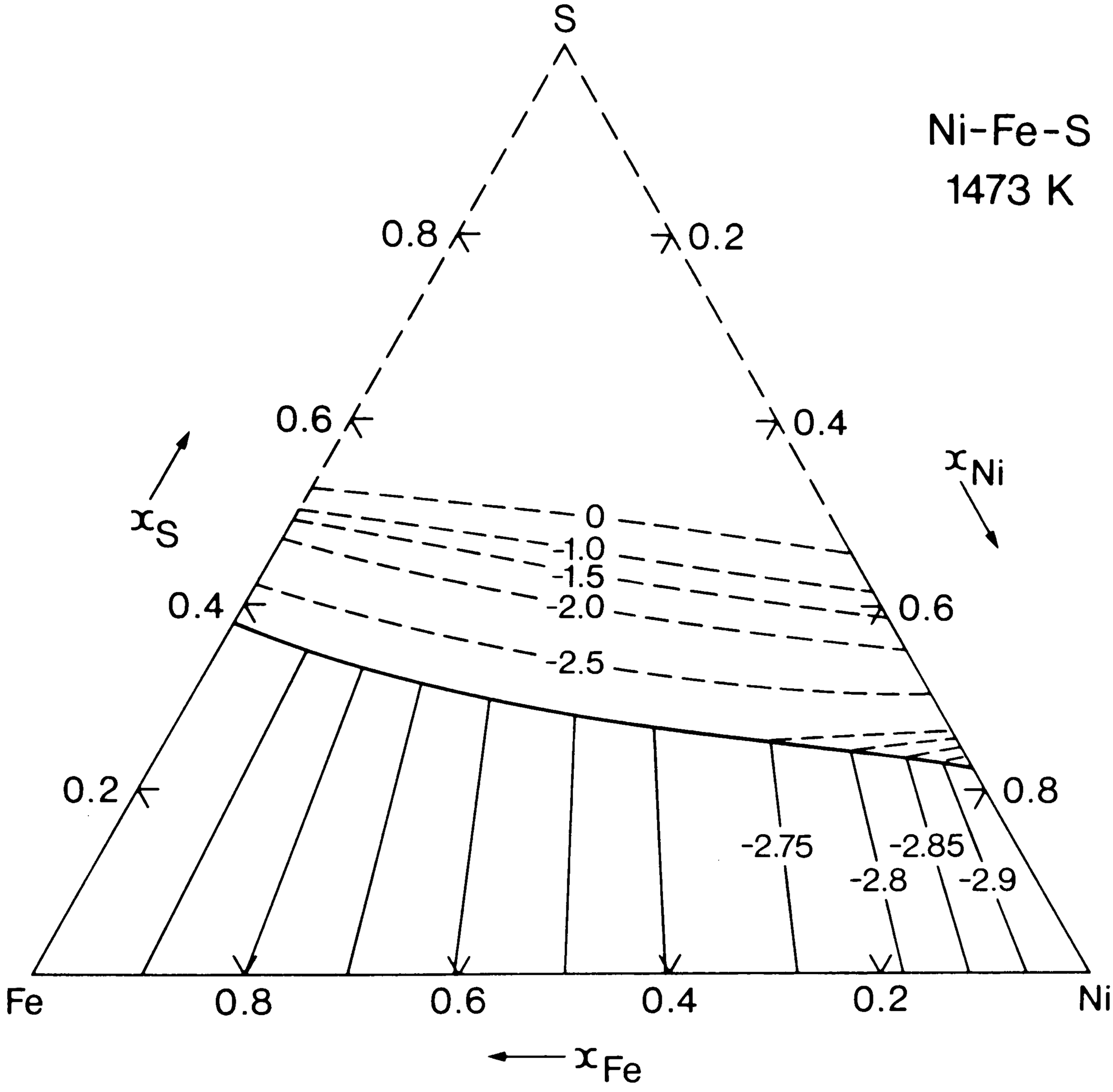

Fig 8.46 Calculated phase diagram for the metal rich part of the Ni-Fe-S system for 1473 K with contours for constant sulphur activity expressed as $\log(p_{S_2})/2$.

pieces of information were sufficient to define the thermodynamic data for the monosulphide solid solution phase over the temperature range of interest. The solid solution in the monsulphide has also been studied by Kao (517) for 973 K. The calculated phase diagram for 1273 K and 1173 K are shown in Figures 8.47 and 8.48.

In the Ni-S binary system the beta phase is stable only below 1073 K. According to Hsieh et al. (499) the beta phase is stable in the ternary system at 1123 K with the mole fraction of Fe of about 0.2. These results were not available when this work was carried out and therefore they have not been considered. Data were developed to represent the intrusion of the Ni_3S_2 solid solution phase into the ternary system based upon the experimental diagram in Craig and Scott (402).

The other phase of interest in this system is the pentlandite phase $(Fe,Ni)_9S_8$ which, according to Kullerud (502) is stable below 883 K. Data were derived for this phase to be consistent with this observation and to reproduce the extent of stability of this phase at 673 K shown by Craig et al. (507). Figures 8.49 and 8.50 shows the region of stability of pentlandite and its predicted phase relationships for 850 K and 673 K respectively.

Calculations in the Ni-Fe-Cu-S system

In the quaternary system experimental data are available for the partial pressure of sulphur above the matte as a function of sulphur concentration for certain relative proportions of Cu, Fe and Ni (380,526). Calculations were made using the data derived for the binary and ternary systems to compare the experimental and predicted thermodynamic thermodynamic data for the liquid phase. As is shown in Figures 8.51-8.53 the agreement is excellent even although no new data

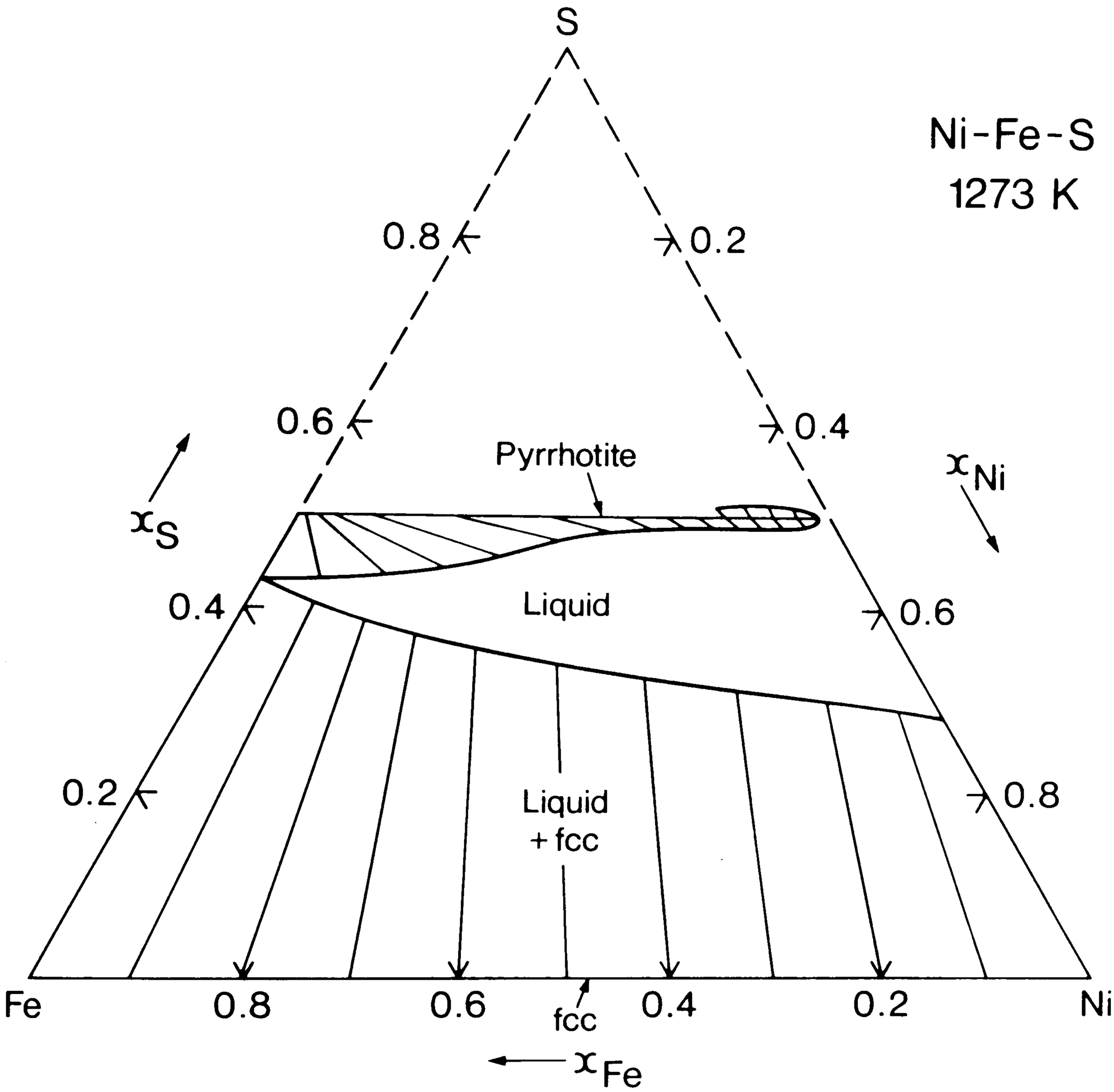

Fig 8.47 Calculated phase diagram for the metal rich part of the Ni-Fe-S system for 1273 K.

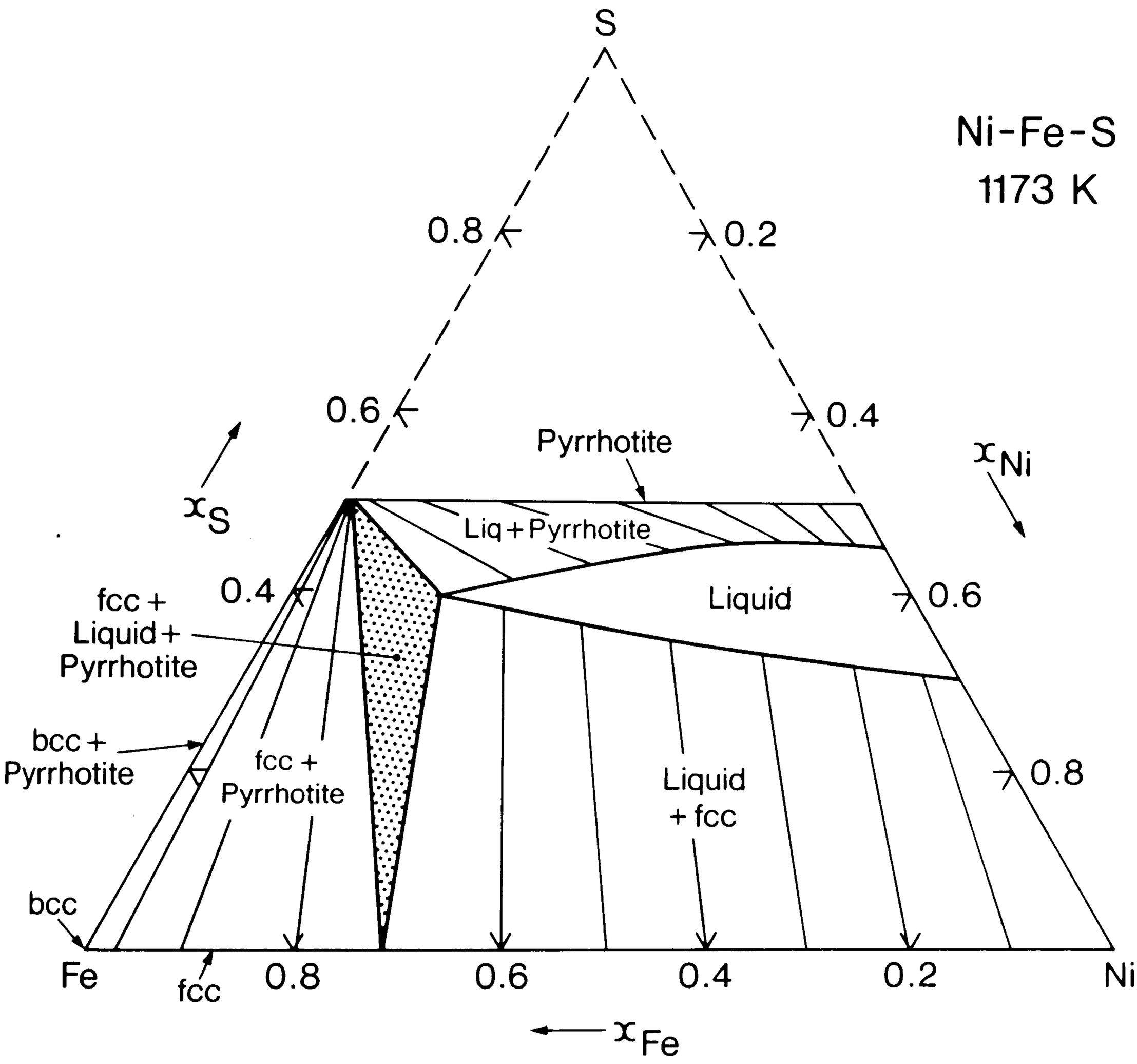

Fig 8.48 Calculated phase diagram for the metal rich part of the Ni-Fe-S system for 1173 K.

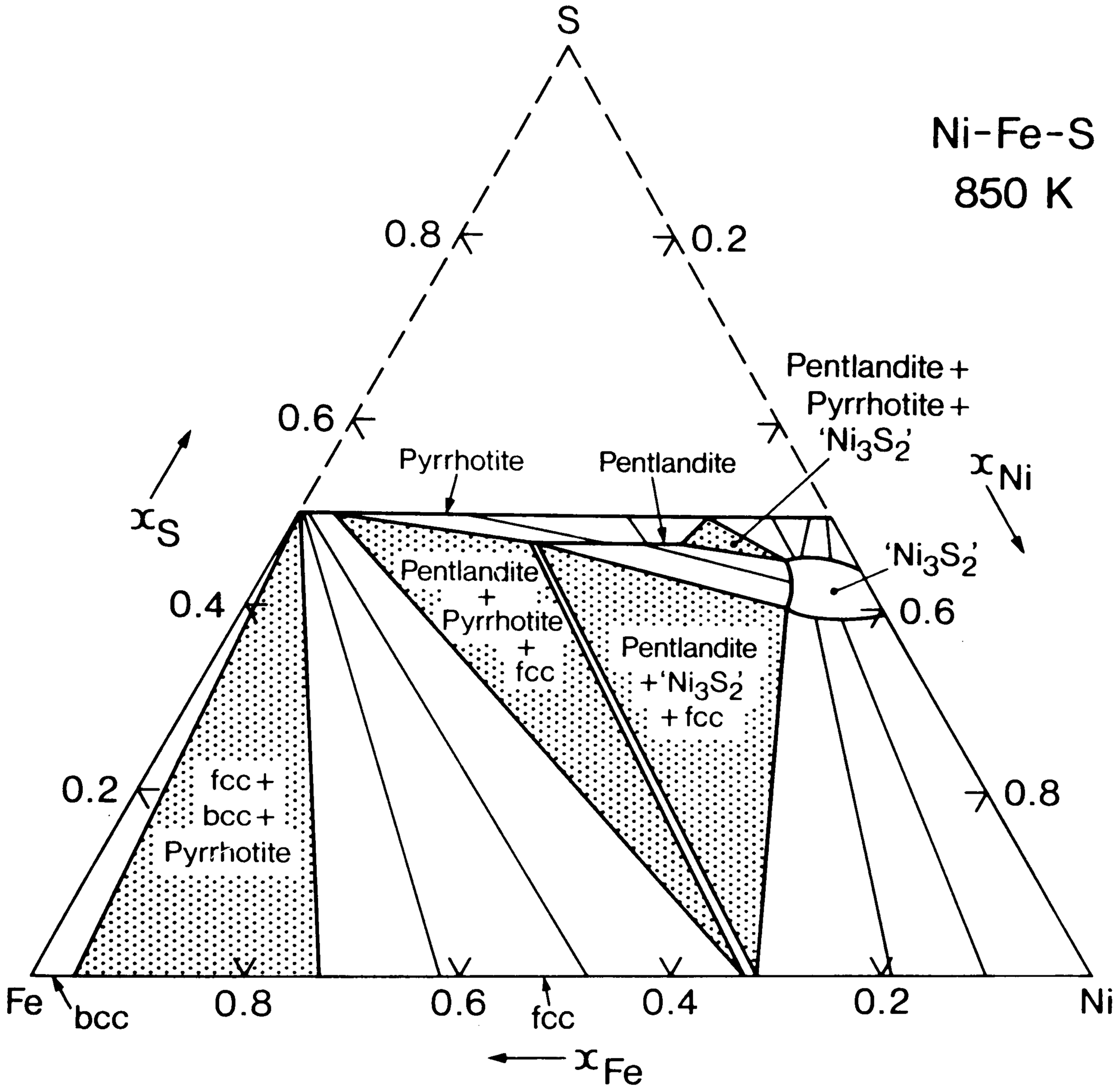

Fig 8.49 Calculated phase diagram for the metal rich part of the Ni-Fe-S system for 850 K.

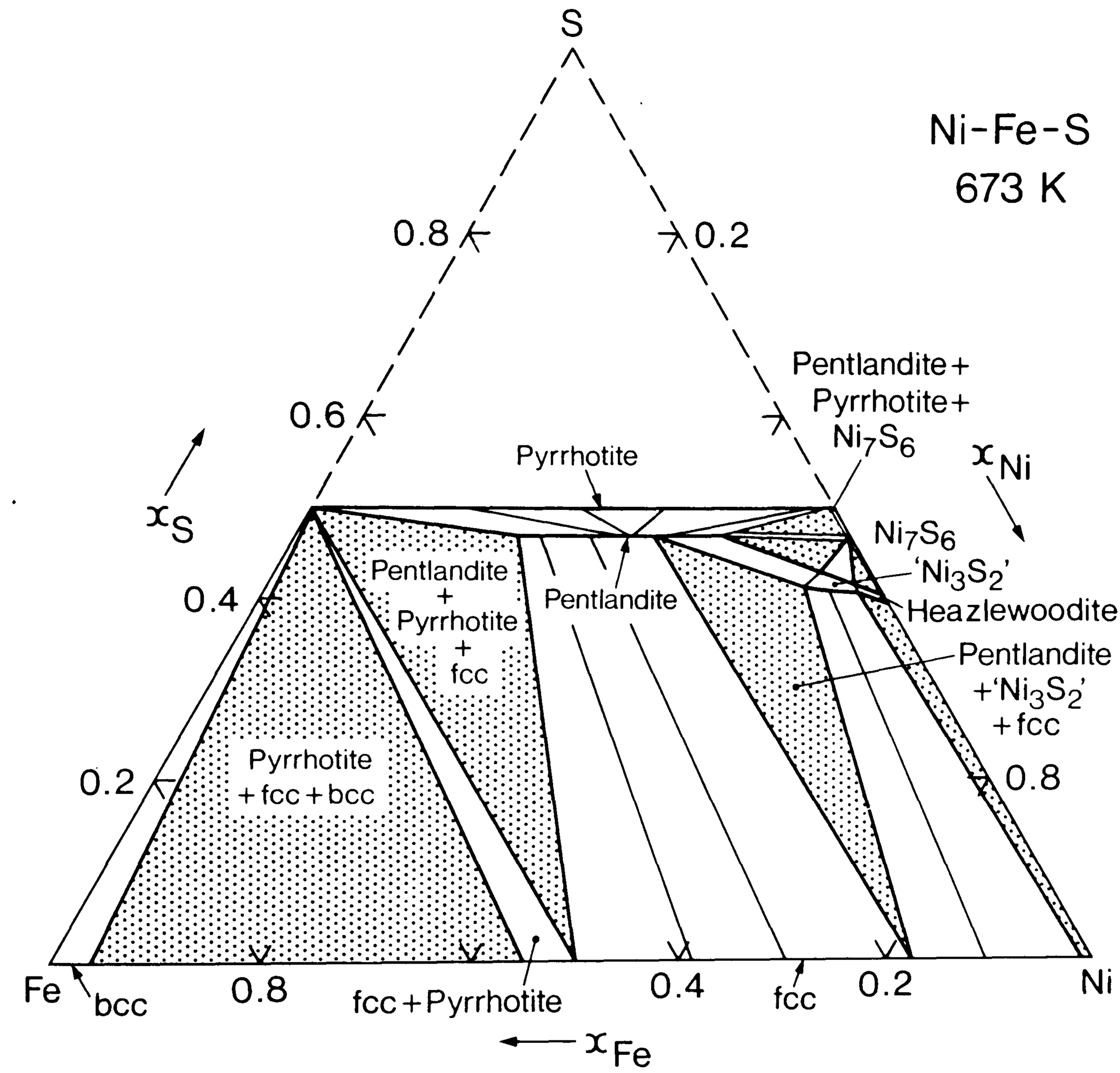

Fig 8.50 Calculated phase diagram for the metal rich part of the Ni-Fe-S system for 673 K.

were included specifically for the quaternary system.

Fig 8.51 compares the calculated properties with the measured properties of Bale (526) for 1473 K for different relative proportions of iron and nickel but with a constant ratio of nickel to copper mole fractions. Figs 8.52-8.53 compares the calculated properties with those from Lee (380) for various temperatures and relative mole fraction ratios of Fe, Ni and Cu.

Conclusions

A new model has been developed for representing the thermodynamic data for the liquid phase in sulphide systems based upon a two sublattice model. The model has been tested out and shown to give results in very good agreement with experimental information.

Data have been derived for all the phases of importance for the metal rich part of the Cu-Fe-Ni-S system. These are of importance in understanding and improving processes for the extraction of metals from ores based on this system. Binary data sets for the Cu-S and Ni-S systems were critically assessed and combined with data for the Fe-S system from Fernandez Guillermet et al. and the Cu-Fe-Ni system of Chart et al. to predict phase equilibria in the ternary and quaternary systems. Ternary interaction data were derived where appropriate from any experimental ternary information available. The agreement between calculated and the experimental phase diagrams and thermodynamic data is very good especially at lower temperatures. At higher temperatures the agreement could be improved through a reassessment of the data for a) the Cu-Fe system taking available ternary data into account, b)the beta phase with a two sublattice model incorporating the most recent experimental data and c) the liquid phase with a different notional charge for nickel ions.

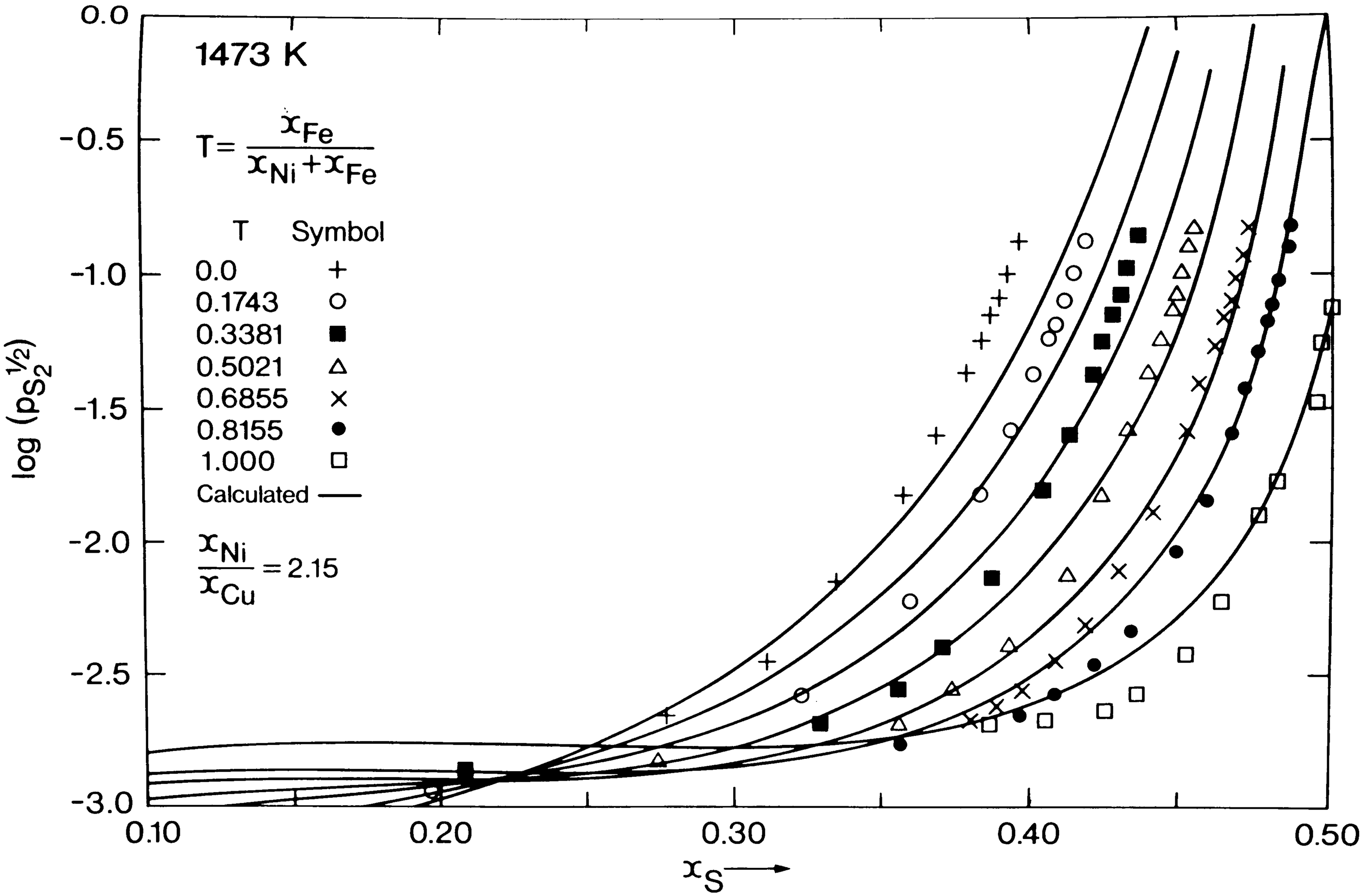

Fig 8.51 Comparison between calculated and experimental sulphur pressures in the Ni-Fe-Cu-S system for various pseudo-binary sections for 1473 K. Experimental data from Bale.

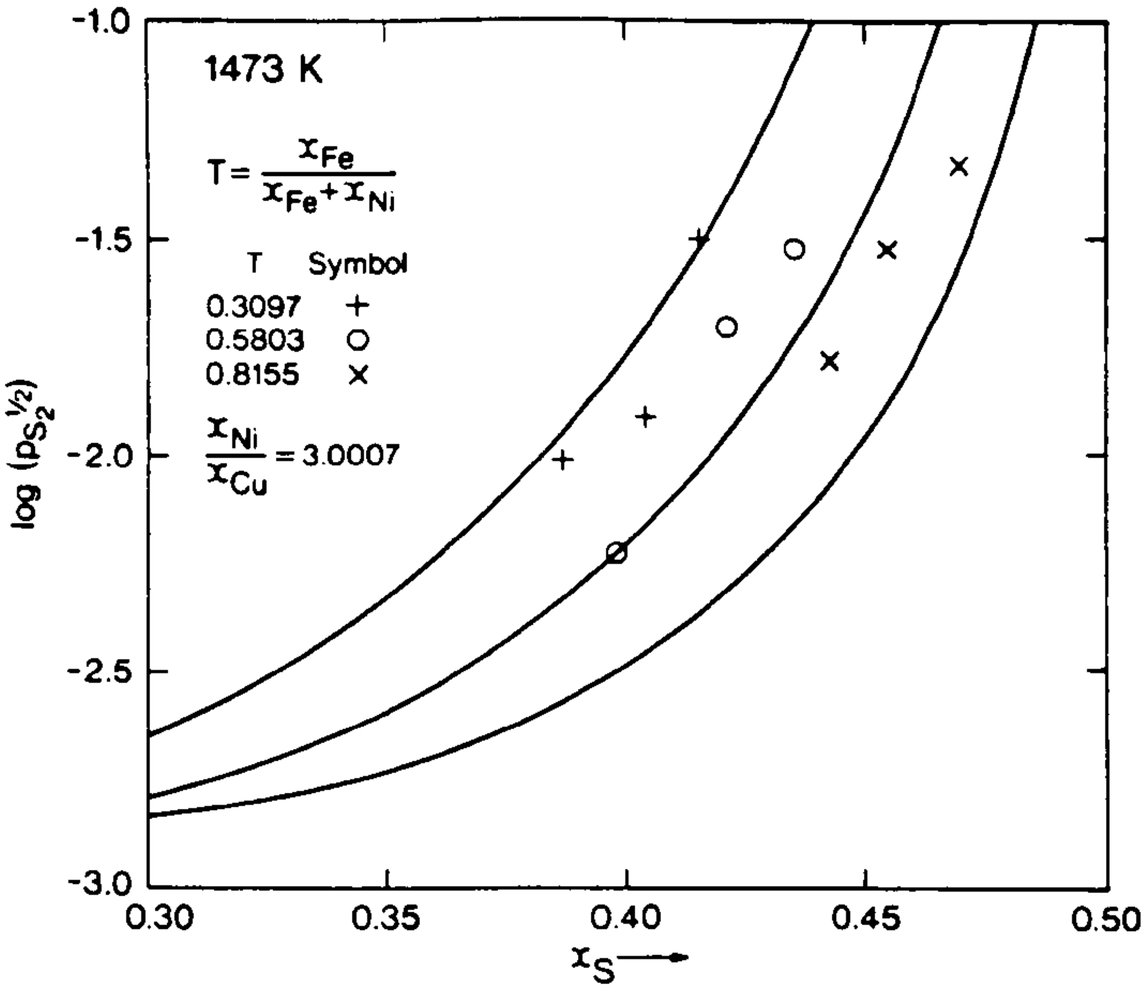

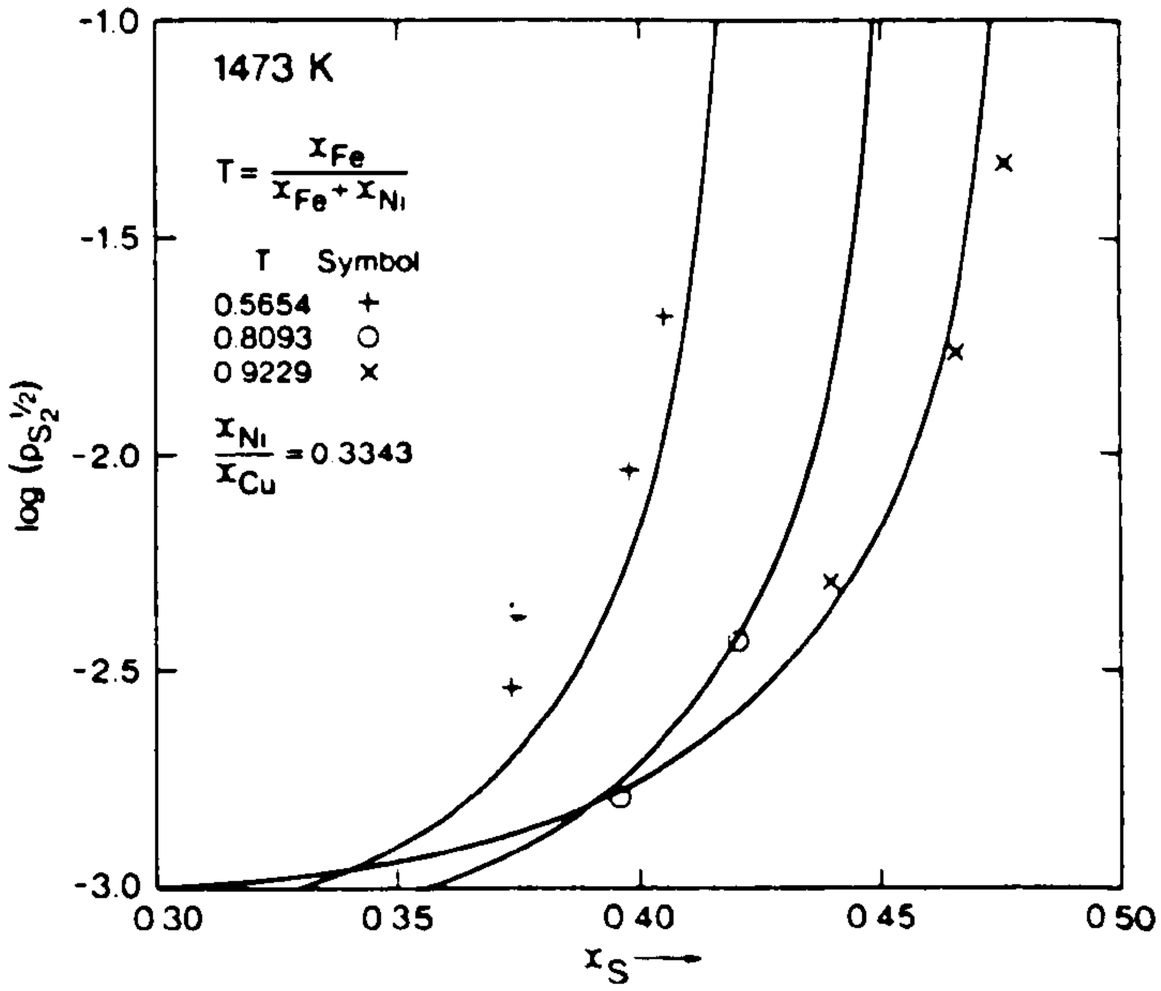

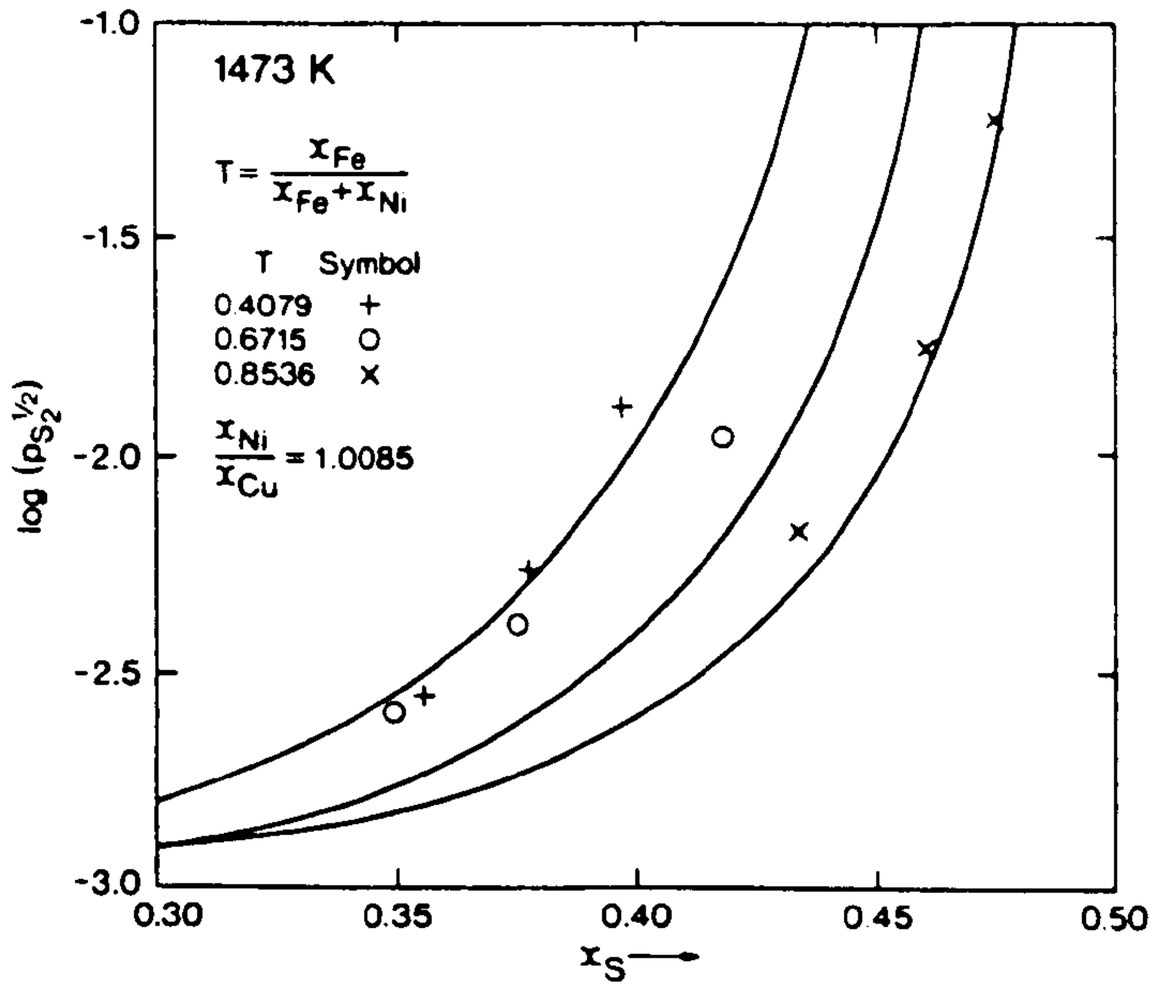

Fig 8.52 Comparison between calculated and experimental sulphur pressures in the Ni-Fe-Cu-S system for various pseudo-binary sections for 1673 K and 1706 K. Experimental data from Lee.

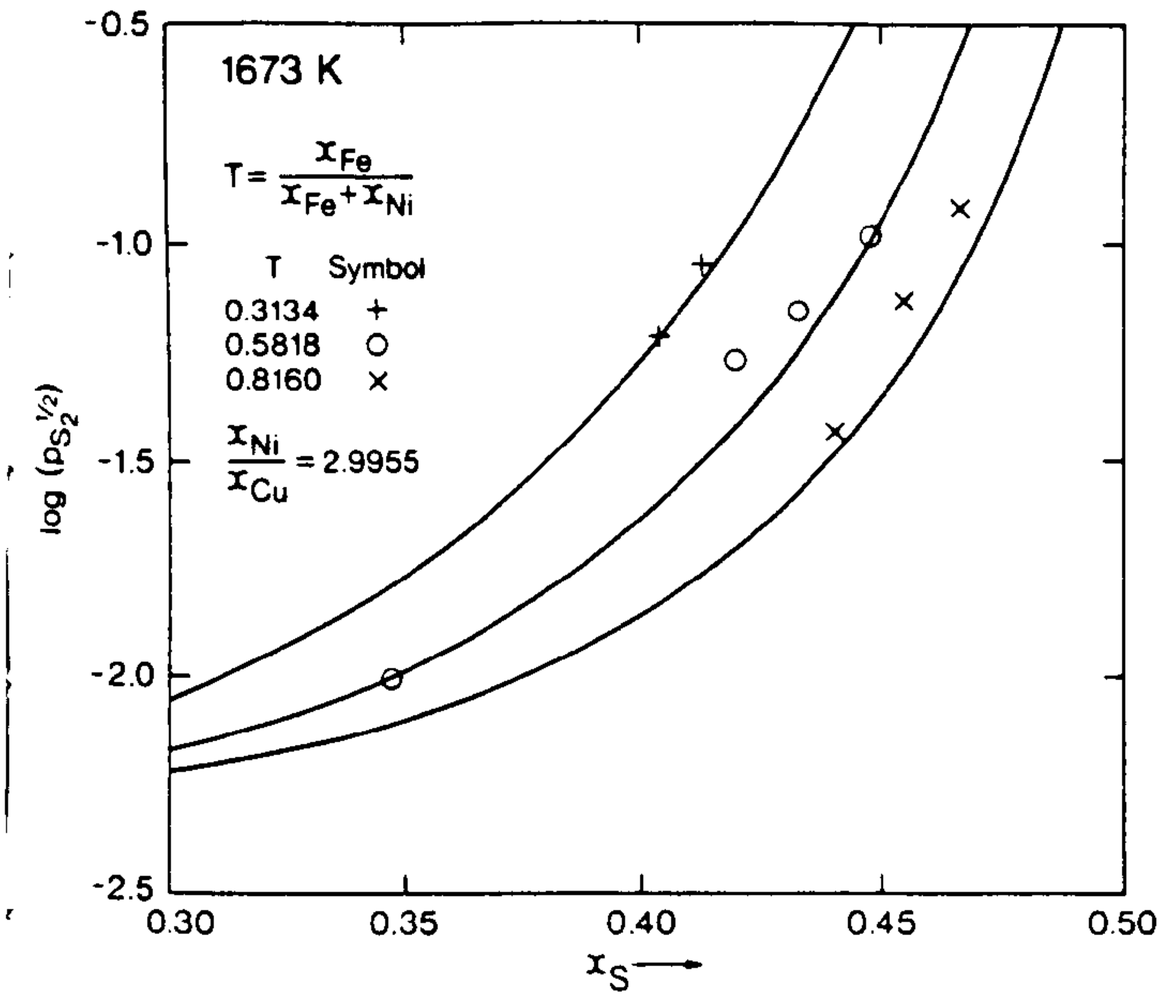

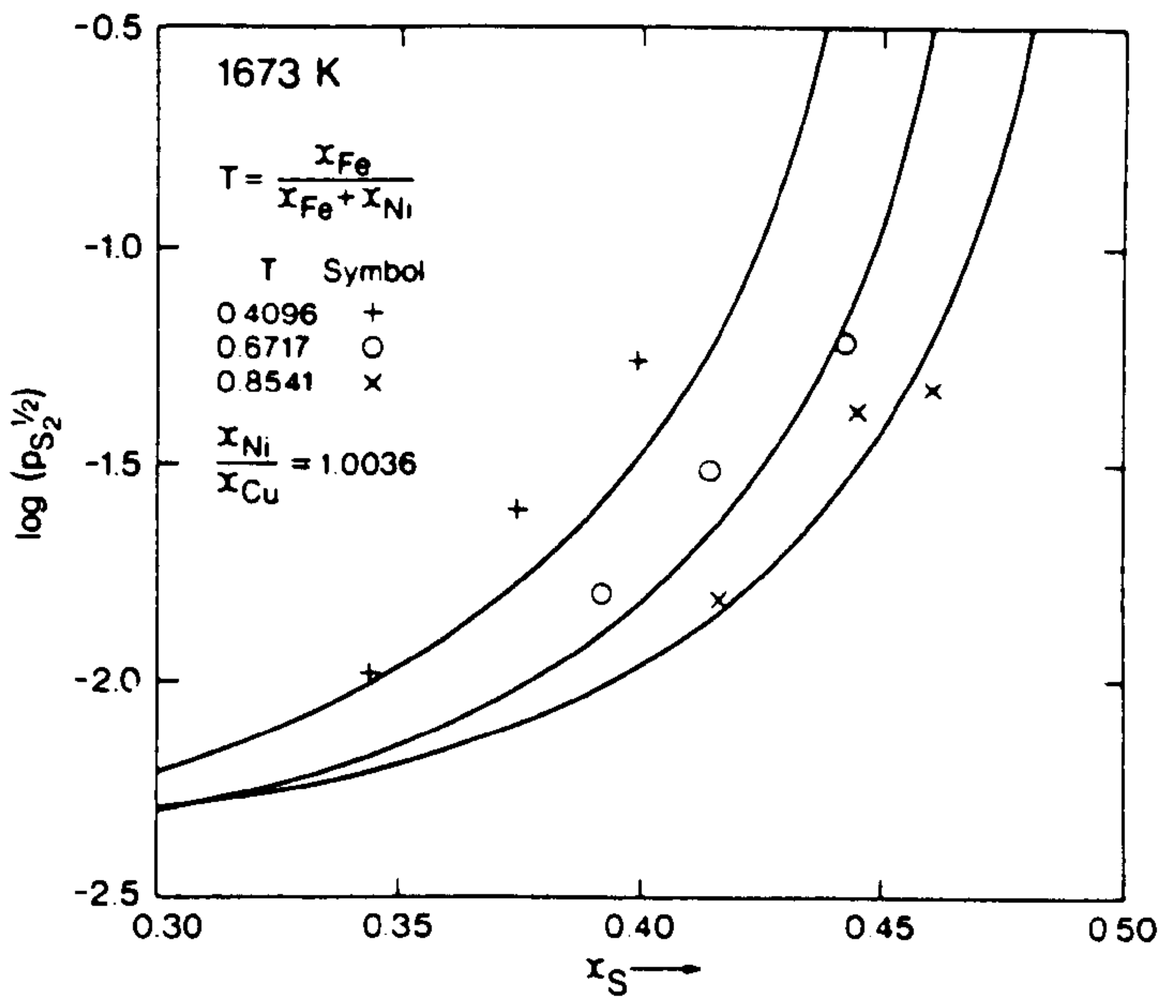

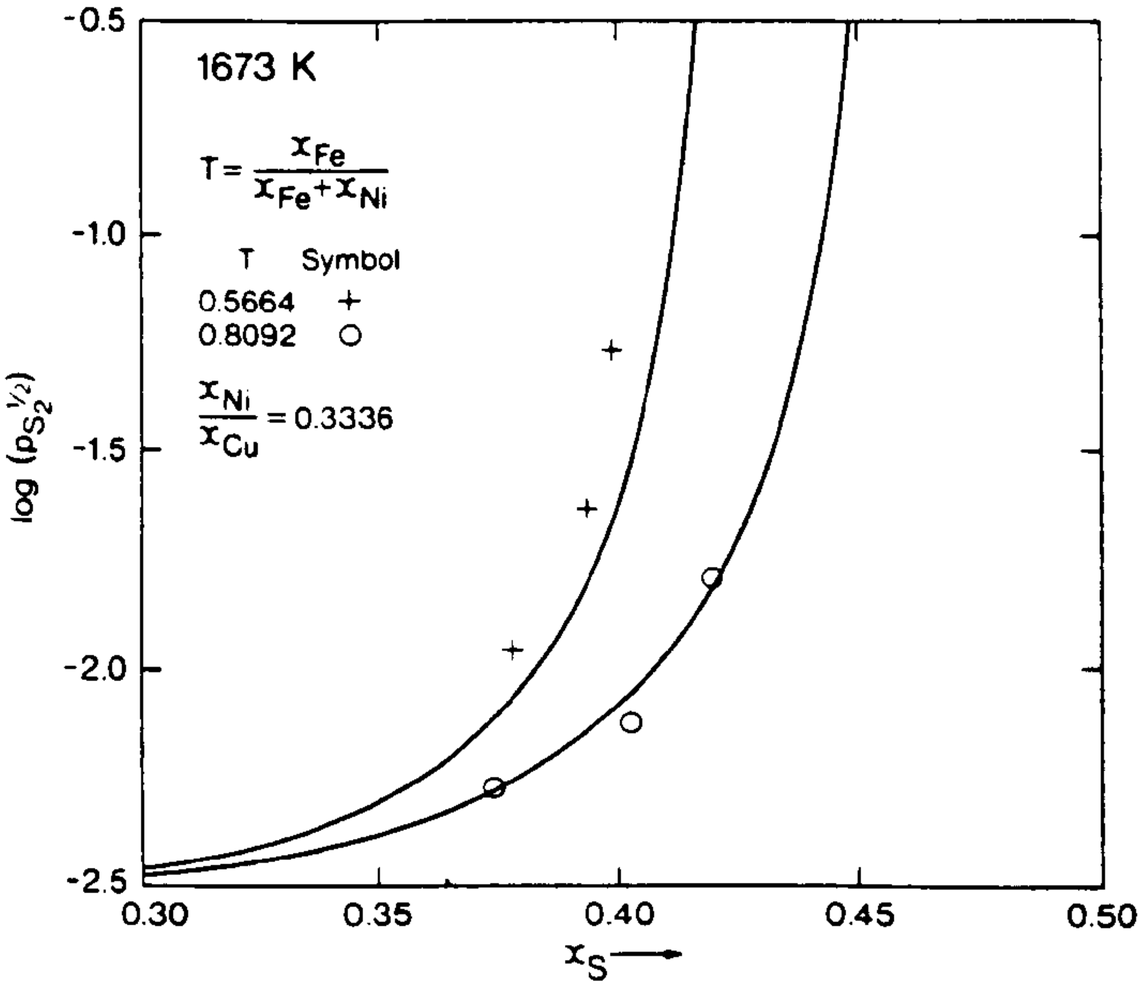

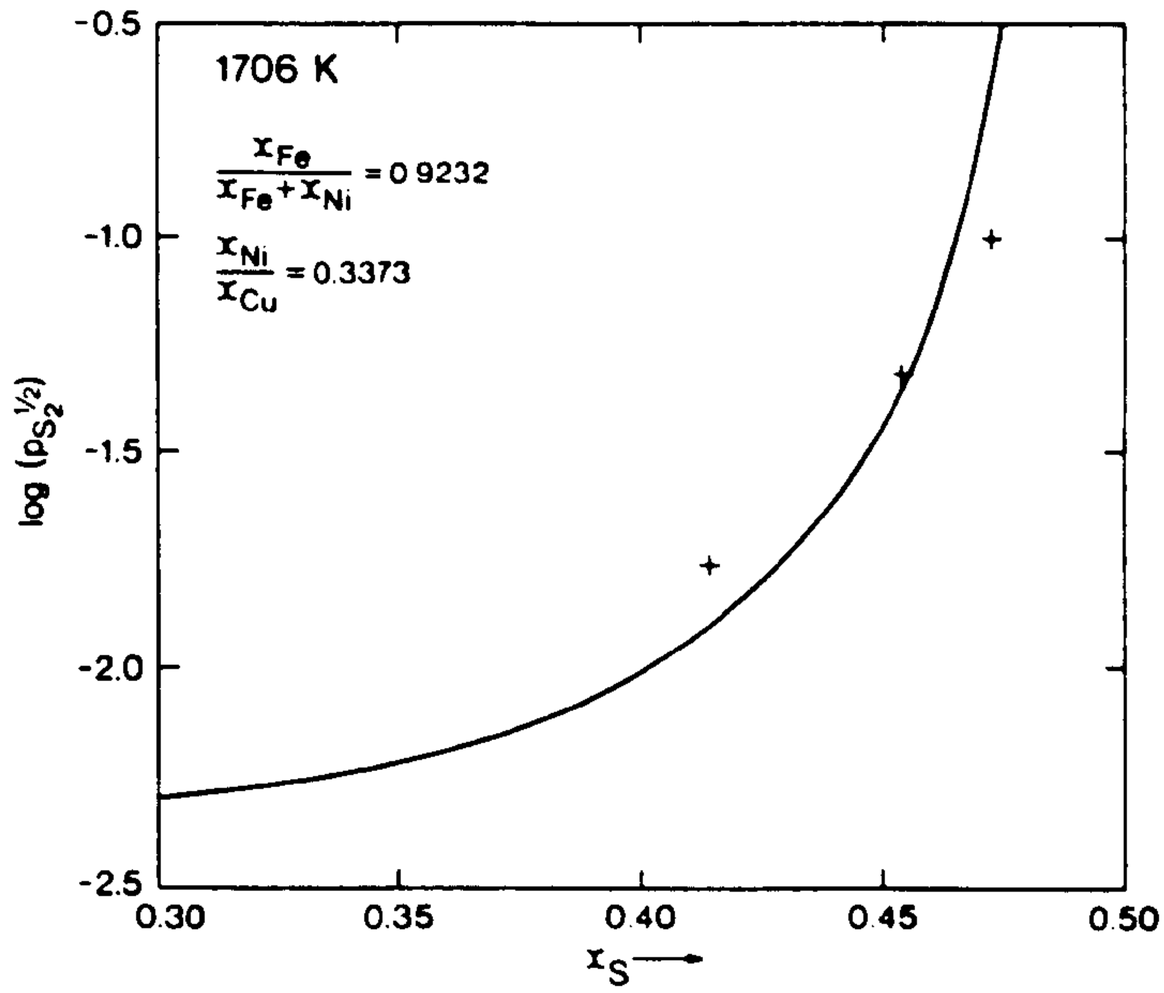

Fig 8.53 Comparison between calculated and experimental sulphur pressures in the Ni-Fe-Cu-S system for various pseudo-binary sections for 1473 K. Experimental data from Lee.

CHAPTER 9

Conclusions and Suggestions for Future Work

A wide range of topics have been dealt with in this thesis ranging from the measurement of the enthalpies of formation for selected alloys in the Fe-Ti system, the critical assessment of data, development of models and expressions to represent data, development of procedures for the calculation of phase diagrams and their use in the calculation of equilibria for steel and sulphide systems.

A fair degree of success has been achieved in this work although it must be admitted that in each of these areas more work needs to be done as has been referred to many times within the text. In particular this thesis has highlighted the need for more theoretical work to understand and represent the various contributions which comprise thermodynamic data. For elements the liquid phase is not well understood and in particular the structural changes leading to the glass transition which occurs as a liquid is cooled down usually below its freezing point. For phase diagram calculations data are also required for elements in unstable phase structures. Theoretical work to provide such data would be most welcome.

For binary systems many reliable models are now available to represent the data for solid phases. Unfortunately the correct choice of models will depend particularly on the structural characteristics of the material and how these change as the composition or temperature is varied. In this thesis two solid 'compound' phases were of particular importance - the Laves phase compound Fe_2Ti and the phase or phases based about Ni_3S_2. The former exists over a wide range of homogeneity in the binary system and although its structure (C14) is known, the way the occupation of lattice sites changes with composition is not. The

situation is worse for Ni_3S_2 since it seems to be virtually unquenchable and its structure is not known at all. Furthermore not only does it exist over a wide range of homogeneity in the Ni-S binary system but it also dissolves significant quantities of Cu and Fe. To complete the gloomy picture there is evidence to suggest that the phase is not just one phase but two phases. In this thesis data for Ni_3S_2 and Fe_2Ti were represented by a Redlich-Kister power series expression which was a convenient although not necessarily physically correct description. Both these phases should be reconsidered using structural models once the required experimental structural information is available.

For multicomponent systems much work still need to be done to develop and test out models to represent thermodynamic data. The work reported here on sulphide systems and in particular the liquid phase was very successful although improvements could be made in the representation of the data for the Cu-Ni-S system. In particular the use of a different notional valency for nickel would be of great interest. This would require a reassessment of the Ni-S binary system which could be carried out in conjunction with a revised treatment of Ni_3S_2.

More recently Hillert et al. have suggested a new model for liquid phases based upon a sublattice description. This model seems more general and versatile than that used in the present work and it is hoped that it will soon be tested out on sulphide systems. Also of great importance is the development of reliable but versatile models for oxide systems and in particular slags.

In more general terms there needs to be continued development of systems for the calculation of phase equilibria linked to databases for the use of industry. This requires a long term programme of data assessment work, backed up by basic experimental work, to create a self consistent database and the development of sophisticated software to simulate industrial processes. Effort must also be made to encourage

industry to use such facilities.

The work reported in this thesis is only a small part in a worldwide effort in thermodynamics but it is to be hoped that it has made some contribution to the generation and application of chemical and metallurgical thermodynamic data.

ACKNOWLEDGEMENTS

There are many people who have helped me in this work over the last few years but I would like to mention a few to whom I owe special thanks:

- Prof. C. Bodsworth for his advice and great patience throughout this project,
- Dr T.G. Chart for his continuous support, interest and valuable contributions,
- My colleagues within MTDS, Dr T.I. Barry, Mrs F.H. Putland, R.H. Davies, Dr M.H. Rand, D.D. Gohil, Mrs S. Hodson and M. Dunlop for many lively discussions, assistance and suggestions for improving my work,
- Dr C.W. Bale for making available his experimental work on sulphide systems,
- Dr J.R. Taylor and Johnson Matthey Limited for their permission to include my work on sulphide systems within this thesis,
- My family and especially my wife, Alison, who have been a constant source of inspiration. Alison in particular has shown great strength and patience over the last two years through various trials and while our house and garden were neglected in the interests of metallurgical thermodynamics.

Alan Dinsdale 20 August 1984

APPENDIX

The liquid phase is chosen as the reference phase for each of the elements. T parameters for the Gibbs energies of formation for the various phases interest in J mol^{-1} are:

Liquid

$$^{o}G_{Ni} = 0$$

$$^{o}G_{Fe} = 0$$

$$^{o}G_{Cu} = 0$$

$$^{o}G_{S} = 0$$

$$^{o}G_{NiS} = -71390.17 - 7.45917\ T$$

$$^{o}G_{FeS} = -80947 - 129.155\ T - 0.0041755\ T^2 + 16.291\ T\ ln(T)$$

$$^{o}G_{Cu_2S} = -86094 - 22.291\ T$$

$$G[Ni:S,Vc] = (-67995.65 + 21.1647\ T) + (-51984.49 + 17.0106\ T)\ (Z_S-Z_{Vc}) + (-1193.338 + 3.55053\ T)\ (Z_S-Z_{Vc})^2$$

$$G[Fe:S,Vc] = (31761 - 9.202\ T) + (-10761 - 0.477\ T)\ (Z_S-Z_{Vc})$$

$$G[Cu:S,Vc] = (19385 + 17.076\ T) + (-3718 - 0.879\ T)\ (Z_S - Z_{Vc})$$

$$G[Va:S,Vc] = 100\ T$$

$$G[Ni,Fe:S] = -10035.03$$

$$G[Ni,Cu:S] = 15000 + 10000\ (Z_{Ni} - Z_{Cu})$$

$$G[Ni,Va:S] = (23228.52 - 2.8569\ T) + (-10168.80 - 9.5614\ T)\ (Z_{Ni}-Z_{Va})$$

$$G[Fe,Cu:S] = 0$$

$$G[Fe,Va:S] = (79779 - 45.139\ T) + (-57510 + 17.082\ T)\ (Z_{Fe}-Z_{Va})$$

$$G[Cu,Va:S] = (107706 + 21.338\ T) + (-6011 - 3.514\ T)(Z_{Cu}-Z_{Va}) + (-39812 - 5.424\ T)(Z_{Cu}-Z_{Va})^2$$

$$G[Ni,Fe:Vc] = (-20292.4 + 5.9622\ T) + (-11924.4 + 3.2426\ T)(Z_{Ni}-Z_{Fe})$$

$$G[Ni,Cu:Vc] = (10460 + 2.0878\ T) + (1451.8 - 0.3933\ T)(Z_{Ni}-Z_{Cu})$$

$$G[Ni,Va:Vc] = 100\ T$$

$$G[Fe,Cu:Vc] = (34321.3 - 1.8577\ T) + (1811.6 - 1.6401\ T)(Z_{Fe}-Z_{Cu}) + (7564.6 - 2.5857\ T)(Z_{Fe}-Z_{Cu})^2 + (2418.3 - 2.3472\ T)(Z_{Fe}-Z_{Cu})^3$$

$$G[Fe,Va:Vc] = 100\ T$$

$$G[Cu,Va:Vc] = 100\ T$$

$$G[Ni,Fe:S,Vc] = 20136.96 + 9913.78\ (Z_{Ni} - Z_{Fe}) - 13519.09\ (Z_S - Z_{Vc})$$

$$G[Ni,Cu:S,Vc] = -25000 + 20000\ (Z_S - Z_{Vc})$$

$$G[Fe,Cu:S,Vc] = 0$$

<u>fcc</u>

$${}^oG_{Ni} = -17614.6 + 10.209\ T$$

$${}^oG_{Fe} = 11274 - 163.878\ T - 0.0041756\ T^2 + 22.03\ T\ \ln(T)$$

$${}^oG_{Cu} = -13054.1 + 9.6232\ T$$

$$G[Ni,Fe] = (-16359.4 + 1.02872E\text{-}2\ T^2 - 4.384E\text{-}6\ T^3) + (-18451.4 + 1.41177E\text{-}2\ T^2 - 6.017E\text{-}6\ T^3)(x_{Ni}-x_{Fe})$$

$$G[Ni,Cu] = (8137.8 + 3.0083\ T) + (2535.5 - 0.8284\ T)(x_{Ni}-x_{Cu})$$

$$G[Fe,Cu] = (48208.0 - 8.4475\ T) + (5916.1 - 5.0166\ T)(x_{Fe}-x_{Cu})$$

$$G[Ni,Fe,Cu] = -62760 + 20.5\ T$$

bcc

$$^{o}G_{Ni} = -31106.99 + 102.0017\,T - 9.9718E\text{-}3\,T^{2} + 3.192592E\text{-}6\,T^{3} - 10.06475\,T\ln(T) + 2693466.3\,T^{-1}$$

$$^{o}G_{Fe} = -268257.4 + 2388.3802\,T + 0.1867633\,T^{2} - 18.2649E\text{-}6\,T^{3} - 337.18251\,T\ln(T) + 35590150\,T^{-1}$$

$$^{o}G_{Cu} = -6778.0 + 6.276\,T$$

$$G[Ni,Fe] = (-7468.4 + 1.83699E\text{-}2\,T^{2} - 7.3894E\text{-}6\,T^{3}) + (-8807.3 + 1.70423E\text{-}2\,T^{2} - 5.8024E\text{-}6\,T^{3})\,(x_{Ni}-x_{Fe})$$

$$G[Ni,Cu] = (8137.8 + 3.0083\,T) + (2535.5 - 0.8284\,T)\,(x_{Ni}-x_{Cu})$$

$$G[Fe,Cu] = (10890.9 + 88.1276\,T - 6.15885E\text{-}2\,T^{2} + 1.2857E\text{-}5\,T^{3}) + (2071.0 - 10.6357\,T)\,(x_{Fe}-x_{Cu})$$

$$G[Ni,Fe,Cu] = 0$$

$L1_2$

$$^{o}G_{Ni} = -17614.6 + 10.209\,T$$

$$^{o}G_{Fe} = 11274 - 163.878\,T - 0.0041756\,T^{2} + 22.03\,T\ln(T)$$

$$G[Ni,Fe] = (-30965.7 + 29.6604\,T) + (-26087.2)\,(x_{Ni}-x_{Fe}) + (297.0)\,(x_{Ni}-x_{Fe})^{2} + (18468.1)\,(x_{Ni}-x_{Fe})^{3}$$

Beta

$^{o}G_{Ni}$ = 290443.6412 - 167.5003 T

$^{o}G_{Fe}$ = 290443.6412 - 167.5003 T

$^{o}G_{Cu}$ = 290443.6412 - 167.5003 T

$^{o}G_{S}$ = 65357 - 165.396 T + 13.513 T ln(T)

G[Ni,Fe] = 0

G[Ni,Cu] = 0

G[Ni,S] = (-896377.028 + 515.2259 T)

+ (-560488.942 + 206.182 T) $(x_{Ni}-x_{S})$

G[Fe,Cu] = 0

G[Fe,S] = -551900 + 300 T

G[Cu,S] = -902000 + 666.7 T

G[Ni,Fe,Cu] = 0

G[Ni,Fe,S] = -1655700 + 900 T

G[Ni,Cu,S] = -600000

G[Fe,Cu,S] = 0

Gas

$^{o}G[\frac{1}{2}S_{2}]$ = 65357 - 165.396 T + 13.513 T ln(T)

Pyrrhotite

$^{o}G_{NiS}$ = -157743.33 + 375.2205 T - 44.372 T ln(T)

$^{o}G_{FeS}$ = -93486 - 127.434 T + 16.358 T ln(T)

$^{o}G_{Cu_2S}$ = -75000 - 120.321 + 13.513 T

G[Ni,Fe:S] = 18192.03 - 15.12 T

G[Ni,Cu:S] = 30000

G[Fe,Cu:S] = 0

Digenite

$^{o}G_{NiS}$ = -60000 - 130 T + 16.358 T ln(T)

$^{o}G_{FeS}$ = -84400 - 130 T + 16.358 T ln(T)

$^{o}G_{Cu_2S}$ = -86136 - 120.321 T + 13.513 T ln(T)

G[Ni,Fe:S] = 0

G[Ni,Cu:S] = 50000

G[Cu,Fe:S] = 0

Chalcocite

$^{o}G_{Cu_2S}$ = -87969 - 117.732 T + 13.513 T ln(T)

Covellite

$^{o}G_{CuS}$ = -44220 - 103.674 T + 13.513 T ln(T)

Millerite

$^{o}G_{NiS}$ = -125300.00 - 49.64 T + 13.513 T ln(T)

Heazlewoodite

$^{o}G_{Ni_3S_2}$ = -235901.51 + 21.5438 T

~~Ni_7S_6~~

$^{o}G_{Ni_7S_6}$ = 1559472.551 - 23670.842 T + 3133.897 T ln(T)

Pentlandite

$$^{o}G_{Ni_9S_8} = -937626.3 + 195.48\ T$$

$$^{o}G_{Fe_9S_8} = -655929.018 - 1352.3247\ T + 178.3323\ T\ \ln(T)$$

$$G[Ni,Fe:S] = (-918799.002 + 809.523\ T) + (-326892.6 + 485.7138\ T)\ (Z_{Ni} - Z_{Fe})$$

References

1. Gibbs J.W., Trans. Conn. Acad. Sci., 1876, 3, 228

2. Clausius R.J.E., "The Mechanical Theory of Heat", transl. Hirst, 1867

3. Planck M., Ann. Physik, 1901, 4, 553

4. Planck M., "Treatise of Thermodynamics", transl. Ogg, 1927

5. Boltzmann L., "Vorlesungen uber Gastheorie", Johann Ambrosius Barth Verlag, Leipzig, 1912

6. Nernst W., Nachr. kgl. Ges. Wiss. Gottingen Math.-physik. kl., 1906, 1

7. "The Physical Chemistry of Metallic Solutions and Intermetallic Compounds", National Physical Laboratory Symposium No 9, HMSO, 1959

8. "Metallurgical Thermochemistry", Proc. Symp. Brunel Univ. and National Physical Laboratory, HMSO, 1972, ed. O.Kubaschewski

9. "Fluids and Fluid Mixtures", Proc. Conf., National Physical Laboratory, Publ. IPC Science and Technology Press, 1978

10. "The Industrial Use of Thermochemical Data", Proc. Conf., ed. T.I.Barry, Publ. The Chemical Society, Sept 11-13, 1979

11. Potter P.E., Rand M.H., ibid, p149

12. Edwards J., Potter P.E., ibid, p160

13. Carlson O.N., Chiotti P., Shiers L., ibid, p169

14. Kaufman L., ibid, p215

15. Chart T.G., Dinsdale A.T., Putland F.H., ibid, p235

16. Burkin A.R., ibid, p180

17. Teyssandier F., Ducarrior M., Bernard C., ibid, p301

18. Glasson D.R., O'Neill P., ibid, p118

19. Hoch M., Chen Y.S., ibid, p312

    Franz-Stern R., Stern I., Bogdanic G., ibid, p325

21. Olette M., Steiler J.M., ibid, p368

22. Steiler J.M., Capelani R., ibid, p391

23. Kyle J., ibid, p403

24. Work D.E., ibid, p128

25. Mottram D.A.J., ibid, p139

26. Dench W.A., Trans. Faraday Soc., 1963, 59, 1279

27. Stull D.R., Prophet H., "JANAF Thermochemical Tables", US Department of Commerce, Washington, 1971

28. Chase M.W., et al., J. Phys. Chem. Ref. Dat., 1974, 3, 311

29. Chase M.W., et al., ibid, 1975, 4, 1

30. Chase M.W., et al., ibid, 1978, 7, 793

31. Chase M.W., et al., ibid, 1982, 11, 695

32. Barin I., Knacke O., "Thermochemical Properties of Inorganic Substances", Springer-Verlag, Berlin 1973

33. Barin I., Knacke O., Kubaschewski O., Supplement to Ref. 32, 1977

34. Gurvich L.V., Veits I.V., Medved'ev V.A., Khachkuruzov G.A., Yungman V.S., Bergman G.A., ed. V.P.Glushko, "Thermodynamic Properties of Individual Substances", Vol 1, Izd. Nauka, Moscow, 1978

35. Gurvich L.V., Veits I.V., Medved'ev V.A., Khachkuruzov G.A., Yungman V.S., Bergman G.A., ed. V.P.Glushko, "Thermodynamic Properties of Individual Substances", Vol 2, Izd. Nauka, Moscow, 1979

36. Gurvich L.V., Veits I.V., Medved'ev V.A., Khachkuruzov G.A., Yungman V.S., Bergman G.A., ed. V.P.Glushko, "Thermodynamic Properties of Individual Substances", Vol 3, Izd. Nauka, Moscow, 1981

37. Gurvich L.V., Veits I.V., Medved'ev V.A., Khachkuruzov G.A., Yungman V.S., Bergman G.A., ed. V.P.Glushko, "Thermodynamic Properties of Individual Substances", Vol 4, Izd. Nauka, Moscow,

1982

38. Wagman D.D., et al., "Selected Values of Chemical Thermodynamic Properties", NBS Technical Notes 270/1-8, US Department of Commerce, Washington, 1965-1981

39. Wagman D.D., Evans W.H., Parker V.B., Schumm R.H., Halow I., Bailey S.M., Churney K.L., Nuttall R.L., "The NBS Tables of Chemical Thermodynamic Properties", J. Phys. Chem. Ref. Dat., 1982, 11, Suppl 2

40. Medved'ev V.A., Bergman G.A., Gurvich L.V., Yungman V.S., Vorob'ev A.F., Kolesov V.P., et al., ed. V.P.Glushko, "Thermochemical Constants of Substances", Parts 1 to 10, Academy of Sciences, USSR, 1965-1981

41. CODATA Task Group on Key Values for Thermodynamics, J.D.Cox, Chairman, "CODATA Recommended Key Values for Thermodynamics 1977", CODATA Bulletin No 28, April 1978

42. CODATA Task Group on Key Values for Thermodynamics, J.D.Cox, Chairman, "Tentative set of Key Values for Thermodynamics. Part VIII", CODATA Special Report No. 8, April 1980

43. Hultgren R., Desai P.D., Hawkins D.T., Gleiser M., Kelley K.K., Wagman D.D., "Selected Values of the Thermodynamic Properties of the Elements", ASM, Metals Park, Ohio, 1973

44. Hultgren R., Desai P.D., Hawkins D.T., Gleiser M., Kelley K.K., "Selected Values of Thermodynamic Properties of Binary Alloys", ASM, Metals Park, Ohio, 1973

45. Kubaschewski O., Alcock C.B., "Metallurgical Thermochemistry", 5th Edition, Pergamon Press, Oxford, 1979

46. Kaufman L., Bernstein H., "Computer Calculations of Phase Diagrams", Academic Press, New York and London, 1970

47. CALPHAD, Computer Coupling of Phase Diagrams and Thermochemistry, ed. L.Kaufman, Pergamon Press, Oxford, New York and Frankfurt

48. Chipman J., J. Iron Steel Inst., 1955, 180, 97

49. Elliott J.F., Gleiser M., Ramakrishna V., "Thermodynamics for Steelmaking II", p491, 1963, Reading, Mass., USA, (Addison-Wesley)

50. Schenck H., Steinmetz E., Supplemental Edition of Stahleisen - Sonderberichte, 1968, 7, 1

51. Sigworth G.K., Elliott J.F., Can. Met. Quart., 1974, 13, 455

52. Sigworth G.K., Elliott J.F., Metal Sci., 1974, 8, 298

53. Hansen M., Anderko K., "Constitution of Binary Alloys", McGraw-Hill, New York, 1958

54. Elliott R.P., "Constitution of Binary Alloys", First Supplement, McGraw-Hill, New York, 1965

55. Shunk F.A., "Constitution of Binary Alloys", Second Supplement, McGraw-Hill, New York, 1969

56. Moffatt W.G., "Handbook of Binary Phase Diagrams", General Electric, New York, Vols 1-3 and supplements, 1976

57. Prince A., "Multicomponent Alloy Constitution Bibliography 1955-1973", The Metals Society, London, 1978

58. Prince A., "Multicomponent Alloy Constitution Bibliography 1974-1977", The Metals Society, London, 1981

59. Ageev N.V., "Diagrammy Sostoyaniya Metallichestikh Sistem", Nos. 1-26, Viniti, Moscow, 1959-1982

60. Wisniak J., "Phase Diagrams", Parts A and B, Elsevier, Amsterdam, Oxford and New York, 1981

61. Pourbaix M., "Atlas of Electrochemical Equilibria in Aqueous Solutions", Pergammon Press, Oxford, 1966

62. Levin E.M., Robbins C.R., McMurdie H.F., "Phase Diagrams for Ceramicists", Amer. Ceramic Soc., Columbus, 1964, Supplements 1969 and 1975

63. "Metals Handbook", 8th Ed., Vol. 8, Metallography, Structure and Phase Diagrams, American Society for Metals, Metals Park, Ohio,

1973

64. Bulletin of Alloy Phase Diagrams, ed. Bennett L.H., ASM

65. Hillert M., "Prediction of Iron-Base Phase Diagram", Report TRITA-MAC-0132, Stockholm, 1977

66. Henig E.-Th, Lukas H.L., Petzow G., Contemporary Inorganic Materials, 1978, S1

67. Pelton A.D., Thompson W.T., Progress Solid State Chem., 1975, 10, 119

68. Rivlin V.G., Raynor G.V., Int. Metall. Rev., 1980, 25, 21; 79; 139; 1981, 26, 133

69. Raynor G.V., Rivlin V.G., Int. Metall. Rev., 1981, 26, 213

70. Rivlin V.G., Int. Metall. Rev., 1981, 26, 269

71. Raynor G.V., Rivlin V.G., Int. Metall. Rev., 1982, 27, 169; 289; 1983, 28, 23; 122; 211; 251

72. Rivlin V.G., Int. Metall. Rev., 1983, 28, 309; 1984, 29, 96

73. Chang Y.A., Neumann J.P., Mikula A., Goldberg D., "Phase Diagrams and Thermodynamic Properties of Ternary Copper-Metal Systems", INCRA Monograph VI, The Metallurgy of Copper, 1979

74. Chang Y.A., Neumann J.P., Choudary U.V., "Phase Diagrams and Thermodynamic Properties of Ternary Copper-Sulfur-Metal Systems", INCRA Monograph VII, The Metallurgy of Copper, 1979

75. Inden G., Proceedings CALPHAD Conference, Dusseldorf, 1976, III, 4-1.

76. Inden G., Physica, 1981, 103B, 82.

77. Hillert M., Jarl M., CALPHAD, 1978, 2, 227.

78. Oriani R.A., Alcock C.B., Trans. Metall. Soc. AIME., 1962, 224, 1104.

79. Ansara I., Int. Metall. Rev., 1979, 24, 20.

80. Ansara I., in 'Metallurgical Chemistry', Proc. Symp. Brunel Univ.-NPL, 1971.

81. Kapoor M.L., Int. Metall. Rev., 1975, 20, 150.

82. Hildebrand J.H., Proc. Nat. Acad. Sci., 1927, 13, 267.

83. Hildebrand J.H., J. Amer. Chem. Soc., 1929, 51, 66.

84. Hildebrand J.H., Scott R.L., "The Solubility of Non-Electrolytes", 3rd ed (New York, Rheinhold, 1950).

85. Heitler W., Ann. Physik, 1926, 80, 629

86. Herzfeld K.F., Heitler W., Zeit. fur Electrochem., 1925, 31, 536.

87. Bragg W.L., Williams E.J., Proc. Roy. Soc., 1934, A145, 699.

88. Meijering J.L., Acta Met., 1957, 5, 527.

89. Hurle, D.T.J., Pike E.R., J. Mater. Sci, 1966, 1, 399.

90. Lehovec K, Slobodskoy A, J. Electrochem. Soc., 1964, 111, 65.

91. Guggenheim E.A., Proc. Roy. Soc. (London), 1935, A148, 304.

92. Rushbrooke G.S., Proc. Roy. Soc. (London), 1938, A166, 296.

93. Guggenheim E.A., 'Mixtures', 1952, Oxford University Press.

94. Fowler R.H., Proc. Camb. Phil. Soc., 1938, 34, 382.

95. Fowler R.H., Guggenheim E.A., 'Statistical thermodynamics', 1960, Cambridge University Press.

96. Bethe H., Proc. Roy. Soc., 1935, A150, 552.

97. Bonnier E., Durand F., Laurent P-J., C.R. Hebd. Seances Acad. Sci., 1962, 254, 107.

98. Jena A.K., Metall. Trans., 1970, 1, 1260.

99. Stringfellow G.B., Greene P.E., J. Phys. Chem. Solids, 1969, 30, 1779.

100. Stringfellow G.B., Greene P.E., J. Electrochem. Soc., Solid State Sci., 1970, 117, 1075.

101. Kleppa O.J., J. Amer. Chem. Soc., 1950, 72, 3346.

102. Hagemark K.I., J. Chem. Phys., 1973, 59, 2344.

103. Hagemark K.I., J. Chem. Phys., 1974, 61, 2596.

104. Wagner C., Acta Metall., 1973, 21, 1297.

105. Li Y.Y., J. Chem. Phys., 1949, 17, 447.

106. Takagi Y., Proc. Phys. Math. Soc. Japan 1941, 23, 44.

107. Kikuchi R., Phys. Rev., 1951, 81, 988.

108. Kurata M., Kikuchi R., J. Chem. Phys., 1953, 21, 434.

109. Kikuchi R., Brush S.G., J. Chem. Phys., 1967, 47, 195.

110. Kikuchi R., J. Chem. Phys., 1974, 60, 1071.

111. Kikuchi R., Acta Metall., 1977, 25, 195.

112. Kikuchi R., de Fontaine D., Murakami M., Nakamura T., Acta Metall., 1977, 25, 207.

113. Kikuchi R., J. de Phys., 1977, 38, C7-307.

114. Kikuchi R., Physica, 1981, 103B, 41.

115. Kikuchi R., CALPHAD, 1982, 6 ,1.

116. van Baal C.M., Physica 1973, 64, 571.

117. Hume-Rothery W., Mabbott G.W., Channel-Evans K.M., Phil. Trans. Roy. Soc. (London), 1934, A233, 1.

118. Buckley R.A., Hume-Rothery W., J. Iron Steel Inst (London), 1963, 201, 227.

119. Hume-Rothery W., "Phase Stability in Metals and Alloys", (P.S. Rudman, J. Stringer, and R.I. Jaffe eds) McGraw Hill, New York 1967.

120. Hardy H.K., Acta Met., 1953, 1, 202.

121. Sharkey R.L., Pool M.J., Hoch M., Metall. Trans., 1971, 2, 3039.

122. Lupis C.H.P., Elliott J.F., Acta Metall., 1967, 15, 265.

123. Mathieu J.C., Durand F., Bonnier E., J. Chim. Phys., 1965, 62, 1289.

124. Mathieu J.C., Durand F., Bonnier E., J. Chim. Phys., 1965, 62, 1297.

125. Hicter P., Mathieu J.C., Durand F., Bonnier E., J. Chim. Phys., 1967, 64, 261.

126. Brion B., Mathieu J.C., Hicter P., Desre P., J. Chim. Phys., 1969, 66, 1238.

127. Brion B., Mathieu J.C., Hicter P., Desre P., J. Chim. Phys., 1970, 67, 1745.

128. Margules M., Akad. Wiss. Wien, Sitzungs., Math.-Naturwiss., 1895, 104, 1243.

129. Zawidzki J. von, Z. Phys. Chem., 1909, 69, 630.

130. Guggenheim E.A., Trans Faraday Soc., 1937, 33, 151.

131. Wohl K., Trans. Amer. Inst. Chem. Eng., 1946, 62, 215.

132. Carlson H.C., Colburn, A.P., Ind. Eng. Chem., 1942, 34, 581.

133. Benedict M., Johnson C.A., Solomon E., Rubin L.C., Trans. Amer. Inst. Chem. Eng., 1945, 41, 371.

134. Bale C.W., Pelton A.D., Can. Met. Quart. 1975, 14, 213.

135. Bale C.W., Pelton A.D., Metall. Trans., 1974, 5, 2323.

136. Krupkowski A., Bull. Acad. Polon. Sci. Lett., Ser. A, 1950, 1, 15.

137. Esdaile J.D., Metall. Trans. B, 1982, 13B, 213.

138. Wilson G.W., J. Am. Chem. Soc., 1964, 86, 127.

139. Redlich O., Kister A.T., Ind. Eng. Chem., 1948, 40, 345.

140. Redlich O., Kister A.T., Turnquist C.E., Chem. Eng. Progr. Symp. Ser., 1952, 48, 49.

141. Bonnier E., Caboz R., C.R. Hebd. Seances Acad. Sci., 1960, 250, 527.

142. Spencer P.J., Hayes F.H., and Kubaschewski O., Revue de Chimie Minerale, 1972 9, 13.

143. Toop G.W., Trans. Metall. Soc. AIME, 1965, 233, 850.

144. Ajersch F., Hayer E., Barbier J-N., Ansara I., Z. Metallkde., 1975, 66, 624.

145. Kohler F., Monatsh. Chem., 1960, 91, 738.

146. Olson N.J., Toop G.W., Trans. AIME., 1966, 236, 590.

147. Kehiaian H., Bull. Acad. Pol. Sci., 1966, 14, 153.

148. Kaufman L., Nesor H., Metall. Trans., 1974, 5, 1617.

149. Kaufman L., Nesor H., Metall. Trans., 1974, 5, 1623.

150. Kaufman L., Nesor H., Metall. Trans., 1975, 6A, 2115.

151. Kaufman L., Nesor H., Metall. Trans., 1975, 6A, 2123.

152. Kaufman L., Nesor H., CALPHAD 1978, 2, 35.

153. Kaufman L., Tanner L.E., CALPHAD, 1979, 3, 91.

154. Dew-Hughes D., Kaufman L., CALPHAD, 1979, 3, 175.

155. Kaufman L., CALPHAD, 1979, 3, 27.

156. Kaufman L., CALPHAD, 1979, 3, 275.

157. Kaufman L., Hayes F., Birnie D., CALPHAD, 1981, 5, 163.

158. Kaufman L., Nell J., Taylor K., Hayes F., CALPHAD, 1981, 5, 185.

159. Kaufman L., Agren J., Nell J., Hayes F., CALPHAD, 1983, 7, 71.

160. Ansara I., Gambino M., Bros J.P., J. Cryst. Growth 1976, 32, 101.

161. Pelton A.D., Bale C.W., CALPHAD 1977, 1, 253.

162. Darken L.S., J. Amer. Chem. Soc., 1950, 72, 2909.

163. Colinet C., D.E.S., Fac. Sci. Univ. Grenoble, France, 1967.

164. Muggianu Y.M., Gambino M., Bros J.P., J. Chim. Phys., 1975, 72, 83.

165. Jacobs K.J., Fitzner K., Thermochimica Acta, 1977, 18, 197.

166. Hillert M., CALPHAD, 1980, 4, 1.

167. Chart T.G., Putland F.H., Dinsdale A.T., CALPHAD, 1980, 4, 27.

168. Putland F.H., Chart T.G., Dinsdale A.T., CALPHAD, 1980, 4, 133.

169. Chart T.G., Gohil D.D., Xing Zhong shu, NPL Report DMA (A) 54, August 1982.

170. Ansara I., Bernard C., Kaufman L., Spencer P.J., CALPHAD, 1978, 2, 1.

171. Ansara I., Bonnier E., Monatshefte fur Chemie 1971, 102, 1855.

172. Dinsdale A.T., National Physical Laboratory Internal Report, DCS 1/78, February 1978.

173. Dinsdale A.T., National Physical Laboratory Report, Chem 90, July 1978.

174. Throop G.J., Rogl P., Rudy E., High Temperatures - High Pressures,

1978, 10, 553.

175. Sundman B., Agren J., J. Phys. Chem. Solids, 1981, 42, 297.

176. Hillert M., Staffansson L.I., Acta Chem. Scand., 1970, 24, 3618.

177. Harvig H., Acta Chem. Scand., 1971, 25, 3199.

178. Wagner C., Schottky W., Z. Physik. Chem., 1931, B11, 163.

179. Libowitz G.G., Lightstone J.B., J. Phys. Chem. Solids, 1967, 28, 1145.

180. Libowitz G.G., J. Solid State Chem., 1969, 1, 50.

181. Brebrick R.F., J. Solid State Chem., 1969, 1, 88.

182. Hertzman S., Sundman B., Royal Institute of Technology Report TRITA-MAC-0180, Stockholm, Jan 1981.

183. Hertzman S., Sundman B., CALPHAD, 1982, 6, 67.

184. Temkin M., Acta Phys. Chim. USSR, 1945, 20, 411.

185. Flood H., Forland T., Grjotheim K., Z. Anorg. Chem., 1954, 276, 289

186. Forland T., Norg. Tek. Vitenskapsakad, 1957, ser 2, no 4

187. Chart T.G., Unpublished work.

188. Oonk H.A.J., Blok K., van de Koot B., Brouwer N., CALPHAD, 1981, 5, 55

189. Bouwstra J.A., Oonk H.A.J., CALPHAD, 1982, 6, 11

190. Oonk H.A.J., Blok G.J., Bouwstra J.A., CALPHAD, 1983, 7, 211

191. Saboungi M.-L., Blander M., J. Am. Ceram. Soc., 1974, 58, 1

192. Saboungi M.-L., Blander M., J. Chem. Phys., 1975, 63, 212

193. Saboungi M.-L., J. Chem. Phys., 1980, 73, 5800

194. Bale C.W., Pelton A.D., CALPHAD, 1982, 6, 255

195. Pelton A.D., Lin P.L., CALPHAD, 1983, 7, 295

196. Hillert M., Jansson B., Sundman B., Agren J., Royal Institute of Technology Report TRITA-MAC-0218 (Revised), Feb 1984.

197. Eliezer N., Howald R.A., Marinkovic M., Eliezer I., J. Phys. Chem., 1978, 82, 1021.

198. Eliezer I., Eliezer N., Howald R.A., Verwolf M.C., CALPHAD 1979, 3, 1.

199. Byker H.J., Craig R.E.R., Eliezer I., Eliezer N., Howald R.A., Viswanadham P., CALPHAD 1981, 5, 217.

200. Chang D.R., Howald R.A., Roy B.N., CALPHAD 1982, 6, 83.

201. Eliezer I., Eliezer N., Howald R.A., Viswanadham P., J. Phys. Chem., 1981, 85, 2835.

202. Kaestle G., Koch K., Proc. CALPHAD Conference, Stuttgart 1978, p6.

203. Lumsden in "Physical Chemistry of Process Metallurgy", G.R. St Pierre ed., pp165-205, Interscience, New York, 1961.

204. Sharma, R.C., Chang Y.A., Metall. Trans., 1980, 11B, 575.

205. Dolezalek F., Z. Phys. Chem., 1908, 64, 727.

206. Lacmann R., Z. Phys. Chem. Neue Folge, 1960, 23, 313.

207. Lacmann R., Z. Phys. Chem. Neue Folge, 1960, 23, 324.

208. Lacmann R., Z. Phys. Chem. Neue Folge, 1962, 35, 86.

209. Jordan A.S., Zupp R.R., J. Electrochem. Soc., 1969, 116, 1264.

210. Jordan A.S., Metall. Trans., 1970, 1, 239.

211. Jordan A.S., Metall. Trans., 1976, 7B, 191.

212. Gerling U., Pool M.J., Predel B., Z. Metallkde., 1983, 74, 616.

213. Kellogg H.H., Can. Metall. Quart., 1969, 8, 3.

214. Kellogg H.H., in 'Physical Chemistry in Metallurgy', 1976, eds. R.M.Fisher, R.A.Oriani, E.T.Turkdogan (Monroeville, PA: US Steel Research), 49.

215. Predel B., Oehme G., Z. Metallkde., 1976, 67, 826.

216. Chang Y.A., Sharma R.C., in 'Calculation of Phase Diagrams and Thermochemistry of Alloy Phases', eds. Y.A.Chang, J.F.Smith, 1979, (Metals Park, OH: American Society for Metals), 145.

217. Larrain J.M., CALPHAD, 1979, 3, 139.

218. Larrain J.M., CALPHAD, 1980, 4, 155.

219. Larrain J.M., Kellogg H.H., in 'Calculation of Phase Diagrams and

Thermochemistry of Alloy Phases', eds. Y.A.Chang, J.F.Smith, 1979, (Metals Park, OH: American Society for Metals), 130.

220. Larrain J.M., Lee S.L., Kellogg H.H., Can. Metall. Quart., 1979, 18, 395.

221. Sharma R.C., Chang Y.A., Metall. Trans., 1979, 10B, 103.

222. Sharma R.C., Chang Y.A., Z. Metallkde., 1979, 70, 104.

223. Sharma R.C., Chang Y.A., Metall. Trans., 1980, 11B, 139.

224. Fosnacht D.R., Goel R.P., Larrain J.M., Metall. Trans., 1980, 11B, 69.

225. Bhatia A.B., Hargrove W.H., Phys. Rev. B, 1974, 10, 3186.

226. Osamura K., Nakajima K., Murakami Y., J. Electrochem. Soc., 1979, 126, 1992.

227. Sommer F., Predel B., Eschenweck D., Oehme G., Berichte der Bunsen-Gesellschaft, 1977, 81, 997.

228. Goel R.P., Kellogg H.H., Larrain J.M., Metall. Trans., 1980, 11B, 107.

229. Hillert M., Staffansson L.I., Metall. Trans., 1975, 6B, 37.

230. Staffansson L.I., Metall. Trans., 1976, 7B, 131.

231. Hillert M., Staffansson L.I., Metall. Trans., 1976, 7B, 203.

232. Fernandez Guillermet A., Hillert M., Jansson B., Sundman B., Report TRITA-MAC-0169, 1980.

233. Fernandez Guillermet A., Hillert M., Jansson B., Sundman B., Metall. Trans., 1981, 12B, 745.

234. Brebrick R.F., Metall. Trans. A, 1982, 13A, 1107.

235. Dinsdale A.T., Chart T.G., Barry T.I., Taylor R.J., High Temperatures - High Pressures, 1982, 14, 633.

236. Bottinga Y., Richet P., Earth Planet Sci. Lett., 1978, 40, 382

237. Flood H., Knapp W.J., J. Am. Ceramic Soc., 1963, 46, 61.

238. Fincham C.J.B., Richardson F.J., Proc. Roy. Soc., 1954, 223, 40.

239. Bjorkman B., Thesis "Quantitative Equilibrium Calculations on

Systems of Relevance to Copper Smelting and Converting", University of Umea, 1984.

240. Bjorkman B., Eriksson G., Rosen E., Metall. Trans. B, In print.

241. Gaskell D.R., Can. Met. Quart., 1981, 20, 3.

242. Bottinga Y., Weill D.F., Richet P., Advances in Physical Geochemistry, 1981, 1, 207

243. Toop G.W., Samis C.S., Trans. TMS-AIME, 1962, 224, 878.

244. Masson C.R., Proc. Roy. Soc., 1965, A287, 201.

245. Whiteway S.G., Smith I.B., Masson C.R., Can. J. Chem., 1970, 48, 33.

246. Whiteway S.G., Smith I.B., Masson C.R., Can. J. Chem., 1970, 48, 1456.

247. Kapoor, M.L., Mehrotra G.M., Frohberg M.G., Achiv. Eisenhuttenw, 1974, 45, 213.

248. Kapoor, M.L., Mehrotra G.M., Frohberg M.G., Achiv. Eisenhuttenw, 1974, 45, 663.

249. Kapoor, M.L., Mehrotra G.M., Frohberg M.G., Proc. Aust. Inst. Mining Metall., 1975, 254, 11.

250. Yokokawa T., Niwa K., Trans. Jap. Inst. Metals, 1969, 10, 3.

251. Borgianni C., Granati P., Metall. Trans., 1977, 8B, 147.

252. Borgianni C., Granati P., Metall. Trans., 1979, 10B, 21.

253. Lin P.L., Pelton A.D., Metall. Trans., 1979, 10B, 667.

254. Blander M., Pelton A.D., Report ANL/FE-83-19, Argonne National Laboratory.

255. Chart T.G., Counsell J.F., Jones G.P., Slough W., Spencer P.J., Int. Metall. Rev., 1975, 20, 57

256. Barry T.I., Dinsdale A.T., Ellender J.M., NPL Internal Report DCS 3/79, September 1979

257. Barry T.I., Dinsdale A.T., NPL Report DMA(B)12, October 1980

258. Barry T.I., Dinsdale A.T., Jones G.P., NPL Report DMA(B)11,

October 1980

259. Turnbull A.G., Chemistry in Australia, 1977, 44, 334

260. Kaufman L., Nesor H., Proc. "Conference on Computer Simulation for Materials Applications", NBS, Gaithersburg, Maryland, USA, 1976

261. Jones P.A., Unpublished work, September 1983

262. Bale C.W., Pelton A.D., Thompson W.T., "Facility for the Analysis of Chemical Thermodynamics", F*A*C*T User's Guide, Ed. 1, McGill University/ Ecole Polytechnique, 1979

263. Thompson W.T., Pelton A.D., Bale C.W., Engineering Educ., Nov. 1979, 201

264. Alcock C.B., Goetze E., Proc. Conf. "Industrial Use of Thermochemical Data" ed. T.I.Barry, 1979, p35

265. Nolang B.I., Richardson M.W., Report UUIC-B18-76

266. Thermodata, "Guide d'Utilisation du Systeme Thermodata a partir d'un Terminal", 1983

267. Spencer P.J., Barin I., Mater. Eng. Appl., 1979, 1, 167

268. Barin, I., Gallagher R., Lemperle M., Proc. Conf. "Industrial Use of Thermochemical Data", ed. T.I.Barry, 1979, p44

269. Gallagher R., Spencer P.J., CALPHAD, 1983, 7, 157

270. Barry T.I., Proc. Symp. "Thermodynamics of Aqueous Systems with Industrial Applications", AICE, Washington, Oct 1979

271. Barry T.I., Xing Zhong shu, NPL Report DMA(C)16, June 1982

272. Smith W.R., Theoretical Chemistry: Advances and Perspectives, 1980, 5, 185

273. Smith W.R., Ind. Eng. Chem. Fundam., 1980, 19, 1

274. van Zeggeren F., Storey S.H., "The Computation of Chemical Equilibria", Cambridge University Press, New York, 1970

275. Eriksson G., Rosen E., Chem. Scr., 1973, 4, 193

276. Eriksson G., Acta Chem. Scand., 1971, 25, 2651

277. Eriksson G., Chem. Scr., 1975, 8, 100

278. Turnbull A.G., CALPHAD, 1983, 7, 137

279. Thompson W.T., Pelton A.D., Bale C.W., CALPHAD, 1983, 7, 113

280. Eriksson G., Anal. Chim. Acta, 1979, 112, 375

281. Eriksson G., Johansson T., Scand. J. Metall., 1978, 7, 264

282. Nolang B., Thesis, Uppsala University, 1983

283. Nolang B., Richardson M.W., Proc. Conf. "Industrial Use of Thermochemical Data", ed. T.I.Barry, 1979, p75

284. Nolang B.I., Report UUIC-B18-98

285. Nolang B.I., Richardson M.W., J. Cryst. Growth, 1976, 34, 198

286. Nolang B.I., Richardson M.W., J. Cryst. Growth, 1976, 34, 205

287. Depeneier W., Schmid H., Nolang B.I., Richardson M.W., J. Cryst. Growth, 1979, 46, 718

288. Chenavas J.C., Valignat N., Ansara I., Bonnier E., Chim. Ind. Genie China, 1971, 104, 1907

289. Counsell J.F., Lees E.B., Spencer P.J., Metall. Sci., 1971, 5, 210

290. Lukas H.L., Weiss J., Henig E.-Th., CALPHAD, 1982, 6, 229

291. Sundman B., Report series D, No 54, Div. of Physical Metallurgy, Royal Institute of Technology, Feb 1984

292. Jansson B., Report series D, No 55, Div. of Physical Metallurgy, Royal Institute of Technology, Feb 1984

293. Agren J., Report TRITA-MAC-0184, Royal Institute of Technology, Stockholm, April 1981

294. Agren J., Report TRITA-MAC-0185, Royal Institute of Technology, Stockholm, April 1981

295. Agren J., Report TRITA-MAC-0193, Royal Institute of Technology, Stockholm, October 1981

296. Eriksson G., Hack K., CALPHAD, 1984, 8, 15

297. Saxena S.K., Eriksson G., Earth Planet. Sci. Lett., 1983, 65, 7

298. Saxena S.K., Eriksson G., Geochim. Cosmochim. Acta, 1983, 47, 1865

299. Jansson B., Report TRITA-MAC-0233, Royal Institute of Technology,

Stockholm, April 1984

300. Jansson B., Report series D, No 56, Div. of Physical Metallurgy, Royal Institute of Technology, Stockholm, Feb 1984

301. Hillert M., Physica, 1981, 103B, 31

302. Hillert M., Proc. Conf. "Industrial Use of Thermochemical Data", ed. T.I.Barry, 1979, p1

303. Hodson S.M., Proc. Conf., 30th SIAM Anniversary Meeting, July 1982, Stanford University, California, USA, "Optimisation Techniques Applied to Chemical and Metallurgical Equilibrium Calculations"

304. Marshall E.M., Pedley J.B., Proc. Conf. "Industrial Use of Thermochemical Data", ed. T.I.Barry, 1979, p83

305. Hiskes R., Tiller W.A., Mater. Sci. Eng., 1967/68, 2, 320

306. Hiskes B., Tiller W.A., Mater. Sci. Eng., 1969, 4, 163

307. Hiskes B., Tiller W.A., Mater. Sci. Eng., 1969, 4, 173

308. Rao M.V., Hiskes B., Tiller W.A., Acta Metall., 1973, 21, 733

309. Chiotti P., Simmons M.F., Kateley J.A., Nuclear Metallurgy, 1969, 15, 659

310. Lukas H.L., Henig E-Th., Zimmerman B., CALPHAD, 1977, 1, 225

311. Zimmerman B., Thesis, University of Stuttgart, 1976

312. Lukas H.L., Weiss J., Kattner U., Henig E.Th., "Manual of the Computer programs BINGSS, TERGSS, QUAGSS, BINFKT, TERFKT, QUAFKT and PMLFKT", 1984

313. Boyle M.L., van Tyne C.J., Tarby S.K., Nucl. Metall., 1976, 20, 187

314. Jansson B., Report series D, No 57, Div. of Physical Metallurgy, Royal Institute of Technology, Feb 1984

315. Jansson B., Report TRITA-MAC-0234, Royal Institute of Technology, Stockholm, April 1984

316. Sundman B., Report Series D, No 28, Div. of Physical Metallurgy,

Royal Institute of Technology, Jan 1981

317. Bale C.W., Pelton A.D., Metall. Trans B., 1983, 14B, 77

318. Oonk H.A.J., "Phase Theory: The Thermodynamics of Heterogeneous Equilibria", 1981, Elsevier

319. Bouwstra J.A., Brouwer N., van Genderen A.C.G., Oonk H.A.J., Thermochimica Acta, 1980, 38, 97

320. Brouwer N., Oonk H.A.J., Z. fur Phys. Chem. Neue Folge, 1977, 105, 113

321. Brouwer N., Oonk H.A.J., Z. fur Phys. Chem. Neue Folge, 1979, 117, 55

322. "A program for advanced information technology", The Report of the Alvey Committee, HMSO, 1982

323. Hillert, M., 'Calculation of Phase Equilibria', ASM Symposium, Phase Transformations, Cleveland, Ohio, 1968, p 181.

324. Hillert, M., 'Methods of calculating phase diagrams', Report TRITA-MAC-0153, 1979. Materials Centre, Royal Inst. Technology, Stockholm.

325. Oonk H.A.J., J. Chem. Educ., 1970, 47, 227

326. Gale, B., Davis, J.M., Metal Sci. J., 1971, 5, 25.

327. Gaye, H., Lupis, C.H.P., Scripta Met., 1970, 4, 685.

328. Gaye, H., Lupis, C.H.P., Metall. Trans. A, 1975, 6A, 1049.

329. Tomiska, J., Erdelyi, L., Neckel, A., Nowotny, H., Z. Metallkunde, 1977, 68, 734

330. Henig E-Th., Lukas H.L., Petzow G., Proc. CALPHAD Conf., Stuttgart, 1978, p235.

331. Pelton, A.D., Bale, C.W., Rigaud, M., Z. Metallkunde, 1977, 68, 135.

332. Nussler H.D., D. Ing. Thesis, RWTH Aachen, 1979.

333. Nelder, J.A., Mead, R., Computer J., 1965, 7, 308.

334. Chart T.G., Putland F.H., Dinsdale A.T., National Physical

Laboratory Report, Chem 91 (1978).

335. Spencer P.J., Putland F.H., J. Chem. Therm., 1975, 7, 531.

336. Spencer P.J., Putland F.H., J. Chem. Therm., 1976, 8, 551.

337. Abrahamson II E.P., Lopata S.L., Trans. Metall. Soc. AIME, 1966, 236, 76.

338. Raub E., Raub Ch.J., Roschel E., Compton V.B., Geballe T.H., Matthias B.T., J. Less-Common Met., 1967, 12, 36.

339. Nasu S., Gonser U., Blasius A., Fujita F.E., J. de Phys. (Colloq), 1979, 40, C2-619.

340. Matyka J., Faudot F., Bigot J., Scripta Metall., 1979, 13, 645.

341. Ko M., Nishizawa T., J. Japan Inst. Met., 1979, 43, 118

342. Kubaschewski O., Dench W.A., Acta Metall., 1955, 3, 339.

343. Gachon J.C., Giner J., Hertz J., Scripta Metall., 1981, 15, 981.

344. Gachon J.C., Notin M., Hertz J., Thermochim. Acta, 1981, 48, 155.

345. Gachon J.C., Hertz J., CALPHAD, 1983, 7, 1.

346. Miedema A.R., Niessen A.K., Private Communication referred to in reference 345.

347. Watson R.E., Bennett L.H., CALPHAD, 1981, 5, 25.

348. Palma R.J., Schroder K., J. Less-Common Met., 1973, 31, 249.

349. Robinson D., Argent B.B., Met. Sci. J., 1976, 10, 219.

350. Wagner S., St. Pierre G.R., Metall. Trans., 1974, 5, 887.

351. Furukawa T., Kato E., Trans. Iron and Steel Inst. Japan, 1976, 16, 382.

352. Chipman J., Trans. Metall. Soc. AIME, 1960, 218, 767.

353. Hadley R.L., Derge G., Trans. Metall. Soc. AIME, 1955, 203, 55.

354. Chino H., Nakamura Y., Tsunetomi E., Segawa K., Trans. Iron and Steel Inst. Japan, 1966, 6, 167.

355. Suzuki K., Sanbongi K., Tetsu-to-Hagane, 1972, 58, 1594.

356. Fruehan R.J., Metall. Trans., 1970, 1, 3403.

357. Smellie A.M., Bell H.B., Canadian Met. Quart., 1972, 11, 351.

358. Dyubanov V.G., Stomackhin A.Ya., Filippov A.F., Izv. Vuz. Chern. Met., 1975, 3, 5.

359. Kaufman L., Nesor H., CALPHAD, 1978, 2, 55.

360. Murray J.L., Bulletin of Alloy Phase Diagrams, 1981, 2, 320.

361. Chart T.G., Putland F.H., CALPHAD, 1979, 3, 9.

362. Muller F., Kubaschewski O., High Temp. - High Pressures, 1969, 1, 543.

363. Berezin B. Ya., Katz S.A., Kenisarin M.M., Teplofiz Vys. Temp., 1974, 12, 524.

364. Kaufman L., CALPHAD, 1977, 1, 7.

365. Chart T.G., High Temp. - High Pressures, 1973, 5, 241.

366. Roe W.P., Fishel W.P., Trans. ASM, 1952, 44, 1030.

367. Wada T., Trans. Nat. Res. Inst. Met., 1964, 6, 43.

368. Moll S.H., Ogilvie R.E., Trans. Metall. Soc. AIME., 1959, 215, 613

369. Hellawell A., Hume-Rothery W., Phil. Trans. Roy. Soc. London, 1957, A249, 417.

370. Fischer W.A., Lorenz K., Fabritius H., Hoffmann A., Kalwa G., Arch. Eisenhuttenw., 1966, 37, 79.

371. Watkin J.S., Gittus J.H., Standring J., in "Proceedings of International Conference on Radiation Effects", Scottsdale, Arizona, 1977

372. Kaufman L., Watkin J.S., Gittus J.H., Miodownik A.P., CALPHAD, 1977, 1, 281

373. Watkin J.S., in "Proceedings of the 8th International Conference on Irradiation Effects on the Microstructure and Properties of Metals", ASTM Special Publication 611, ASTM, Philadelphia, 1976, p270

374. Kaufman L., Nesor H., Z. Metallkde., 1973, 64, 249

375. Thomas G.B., Hondros E.D., Proc. 28th Colloque de Metallurgie, Saclay, France, 24-25 June 1982, p15

376. Lea C., Hondros E.D., Proc. Roy. Soc. (London), 1981, A377, 477

377. Seah M.P., Spencer P.J., Hondros E.D., Met. Sci., 1979, 13, 307

378. Meyer G.A., Warner J.S., Rao Y.K., Kellogg H.H., Metall. Trans. B, 1975, 6B, 229-235

379. Meyer G.A., D. Eng. Sci. Thesis, Columbia University, New York, 1972. "A Thermodynamic study of the Systems Ni-S and Ni-Fe-S"

380. Lee S.L., D.Eng.Sci. Thesis, 1975, Columbia University, New York.

381. Lee S.L., Larrain J.M., Kellogg H.H., Metall. Trans. B., 1980, 11B, 251.

382. Larrain J.M., Lee S.L., Can. Met. Quarterly, 1980, 19, 183.

383. Lin, R.Y., Hu, D.C., Chang, Y.A., Metall. Trans. B., 1978, 9B, 531-538

384. Chuang Y-Y., Chang Y.A., Metall. Trans. B., 1982, 13B, 379.

385. Hillert, M., Private Communication

386. Rau, H., J. Phys. Chem. Solids, 1976, 37, 929-930

387. Hasebe, M., Nishizawa, T., CALPHAD, 1980, 4, 83

388. Hasebe, M., Nishizawa, T., CALPHAD, 1981, 5, 105.

389. Lindqvist, P.-A., Uhrenius, B., CALPHAD, 1980, 4, 193

390. Kubaschewski, O., Smith, J.F., Bailey, D.M., Z. Metallkd., 1977, 68, 495.

391. Harvig, H., Kirchner, G., Hillert, M., Metall. Trans., 1972, 3, 329.

392. Hasebe, M., Nishizawa, T., NBS Special Publication 496, Vol.2., "Applications of Phase Diagrams in Metallurgy and Ceramics", ed. Carter, G.C., National Bureau of Standards, Washington D.C., p911.

393. Elford, L., Muller, F., Kubaschewski, O., Ber. Bunsenges. Phys. Chem., 1969, 73, 601.

394. Kaufman, L., CALPHAD, 1978, 2, 117.

395. Larrain, J.M., Canad. Metall., Quart., 1979, 18, 401.

396. Chamberod, A., Laugier, J., Penisson, J.M., Journal of Magnetism

and Magnetic Materials, 1979, 10, 139.

397. Gruzin, P.L., Rodionov, Yu. L., Pryakhin, V.A., Dokl. Akad. Nauk SSSR., 1980, 251, 1384.

398. Albertsen, J.F., Knudsen, J.M., Roy-Poulson, N.O., Vistisen, L., Phys. Scr., 1980, 22, 171.

399. Xing, Z.S., Chart, T.G., National Physical Laboratory Report, To be published.

400. Bale C.W., Toguri J.M., Can. Met. Quart., 1976, 15, 305-318

401. Barton P.B., Econ. Geol., 1973, 68, 455-465

402. Craig J.R., Scott S.D., "Sulphide Mineralogy" ed. P H Ribbe (Washington DC: Mineral. Soc. Amer.), 1974, CS-1

403. Burylev B.P., Fedorova N.N., Tsemekhan L.Sh., Russ. J. Inorg. Chem., 1974, 19, 1249-1250

404. Johannsen F., Vollmer H., Z. Erzbergbau Metallhuttenwes, 1960, 13, 313-322

405. Judin V.P., Eerola M., Scand. J. Metall., 1979, 8, 128-132

406. Nagamori M., Metall. Trans., 1976, 7B, 67-80

407. Rau H., J. Phys. Chem. Solids, 1967, 28, 903-916

408. Rau H., J. Phys. Chem. Solids, 1974, 35, 1415-1424

409. Roseboom E.H., Econ. Geol., 1966, 61, 641-672

410. Vanyukov A.V., Bystrov V.P., Snurnikova V.A., Sov. J. Non-Ferrous Met., 1971, 12, 11-14

411. Sudo K., Sci. Rep. Res. Inst. Tohuku Univ., 1950, A2, 513-530

412. Schuhmann Jr. R., Moles O.W., Trans. AIME., 1951, 191, 235-241

413. Yagihashi T., Nippon Kinzoku Gakkai-Si., 1953, 17, 483-487

414. Alcock C.B., Int. J. Appl. Radiat. Isotopes, 1958, 3, 135-140

415. Bale C.W., Toguri J.M., J. Thermal Anal., 1971, 3, 153-167

416. Nesmayanov A.N., Samal G.I., Pavlynchenko M.M., Russ. J. Inorg. Chem., 1967, 12, 1713-1715

417. Peronne R., Balesdent D., Rilling J., Bull. Soc. Chim. Fr., 1972,

457-463

418. Bjorkman B., Fredriksson M., Scand. J. Metall., 1982, 11.

419. Ferrante M.J., Stuve J.M., Pankratz L.B., High Temp. Sci., 1981, 14, 77.

420. Sharma R.C., Chang Y.A., Chinese J. Mats. Sci., 1979, 11, 58-62

421. Nagamori M., Ingraham T.R., Metall. Trans., 1970, 1, 1821-5

422. Rosenqvist, T., J. Iron Steel Inst., 1954, 176, 37-57

423. Bornemann, K. von, Metallurgie, 1908, 5, 13

424. Bornemann, K. von, Metallurgie, 1910, 7, 667

425. Barbouth N., Oudar J., C.R. Acad. Sci., 1969, C269, 1618-21

426. Brigham R.J., Neumayer H., Kirkaldy J.S., Can. Met. Quart., 1971, 9, 525-9

427. Lafitte, M., Bull. Soc. Chim. France, 1959, 1211

428. Rau, H., J. Phys. Chem. Solids, 1975, 36, 1199-1204

429. Kullerud, G., Yund., R.A., J. Petrol., 1962, 3, 126-75

430. Arnold R.G., Malik, O.P., Econ. Geol., 1975, 70, 176

431. Venal M.V., Geiger G.H., Metall. Trans., 1973, 4, 2567

432. Baren M.R., PhD Dissertation, University of Pennsylvania 1966

433. Alcock C.B., Cheng L.L., J. Iron Steel Inst., 1960, 195, 169-73

434. Cordier J.A., Chipman J., Trans. AIME, 1955, 203, 905-907

435. Dashevskii V.Ya., Polyakov A.Yu., Izv. Akad. Nauk SSSR, Metal, 1966, 5, 34-41

436. Remen T.F., Kheifets V.L., Vaisburd S.E., Zh. Prik. Khim., 1963, 36, 218-20

437. Byerley J.J., Takebe N., Metall. Trans., 1972, 3, 559-64

438. Line G., Lafitte M., C.R. Acad. Sci. Paris, 1963, 256, 3306

439. Schenck R., Forst P. v.d., Z. Anorg. Allg. Chem., 1939, 241, 145

440. Delmaire J.P., Le Brusq H., Marion F., C.R. Acad. Sci. Paris 1970, 271, 1449

441. Biltz, W., Voigt, A., Meisel, K., Z. Anorg. Allg. Chem., 1936,

228, 275

442. Mah, A.D., Pankratz, L.B., US. Bureau of Mines Bulletin 668. US Government Printing Office 1976

443. Conard, B.R., Sridhar, R., Warner, J.S., Paper Presented at the 106th AIME Annual Meeting at Atlanta, Georgia, March 7-11, 1977

444. Leegaard, T., Rosenqvist, T., Z. Anorg. Chem., 1964, 238, 294-98

445. Cabri L.J., Econ. Geol., 1973, 68, 443

446. Chang Y.A., Lee Y.E., Neumann J.P., "Extractive Metallurgy of Copper" (ed. J.C. Yannopoulos and J.C. Agarwal) Vol 1 Chapter 2, The Metallurgical Society AIME, New York, 1976.

447. Carpenter C.B., Hayward C.R., Eng. Min. J.-Press, 1923, 115, 1055.

448. Bogitch B., Compt. rend., 1926, 182, 468.

449. Guertler W., Metall u. Erz, 1927, 24, 97.

450. Reuleaux O., Metall u. Erz, 1927, 24, 99, 129

451. Merwin H.E., Lombard R.H., Econ. Geol., 1937, 32, 203.

452. Peyronel G., Pacilli E., Mem. R. Accad. Ital., Cl. Sci. Fis. Mat. Nat., 1943, 14, 203.

453. Schlegel H., Schuller A., Z. Metallk., 1952, 43, 421.

454. Schlegel H., Schuller A., Freiberg. Forschungsh. B, 1952, 2, 3.

455. Oelsen E., Schurmann E., Maetz H., Erzmetall, 1953, 6, 128.

456. Hiller J.E., Probsthain K., Z. Kristallgeom., Kristallphys., Kristallchem., 1956, 108, 108.

457. Krivsky W.A., Schuhmann R.,Jr., Trans. AIME, 1957, 209, 981.

458. Roseboom E.H.,Jr., Kullerud G., Carnegie Inst. Washington Year Book, 1958, 57, 222.

459. Yund R.A., Kullerud G., Carnegie Inst. Washington Year Book, 1960, 59, 111.

460. Brett P.R., Carnegie Inst. Washington Year Book, 1963, 62, 193.

461. Kullerud G., Carnegie Inst. Washington Year Book, 1964, 63, 200.

462. Yund R.A., Kullerud G., J. Petrol., 1966, 7, 454.

463. Takenouchi S., Fujiki Y., J. Fac. Eng., Univ. Tojkyo, Ser. A., 1968, No. 6, 50.

464. Kullerud G., Carnegie Inst. Washington Year Book, 1968, 66, 404

465. Josey G.A., Floridis T.P., Trans. Metall. Soc. AIME, 1968, 242, 161.

466. Kullerud G., Yund R.A., Moh G.H., "Magmatic Ore Deposits" ed. H.D.B. Wilson, Economic Geology Publishing Co., Monograph, 1969, 4, 323.

467. Mukaiyama H., Izawa E., "Volcanism and Ore Genesis", ed. T. Tatsumi p339, Univ. Tokyo Press, Tokyo, 1970

468. Sugaki A., Shima H., Kitakaze A., Harada H., Econ. Geol., 1975, 70, 806.

469. Lakernik M.M., Shabalina R.I., Rusakova T.V., Mel'nikova T.P., Sagitaev K.S., Tsvetn. Met., 1975, 16, 14. (Sov. J. Non Ferrous Met., 1975, 16, 16.)

470. Taloi D., Rev. Chim. (Bucharest), 1976, 27, 1045.

471. Vorob'ev Yu.K., Nov. Mineral. Issled, (Mater. Nauchn. Konf. Mosk. Otd. Vses. Mineral. O-va.) 1st, 1974, 165-8.

472. Shemilt J.M., Steele B.C.H., Weston J.E., Solid State Ionics 1981, 2, 73.

473. Alcock C.B., Richardson F.D., Acta Met., 1958, 6, 385.

474. Remen T.F., Kheifets V.L., Vaisburd S.E., Izv. Vyssh. Ucheb. Zaved., Tsvet. Met., 1962, 5, No.6, 57.

475. Shabalina R.I., Lakernik M.M., Yur'eva G.M., Tsvet. Metally, 1966, 39, No.10, 32.

476. Mazanek C., Baranowska-Buzek A., Zesz. Nauk. Poltech. Slask., Hutn., 1973, 3, 143.

477. Eric H., Timucin M., Metall. Trans., 1981, 12B, 493.

478. Sinha S.N., Nagamori M., Metall. Trans., 1982, 13B, 461.

479. Koh J., Yazawa A., Tohoku Daigaku Senko Seiren Kenkyusho Iho,

1982, 38, (2), 107.

480. King E.G., Mah A.D., Pankratz L.B., INCRA Monograph II, "Thermodynamic Properties of Copper and its Inorganic Compounds", The International Copper Research Association, Inc., New York, 1973.

481. Young P.A., Aust. Miner. Devel. Lab. (AMDEL) Bull., 1967, 3, 1.

482. Ospanov Kh.K., Isv. Akad. Nauk Kaz. SSR, Ser. Khim., 1970, 20, 30.

483. Schneeberg E.P., Econ. Geol., 1973, 68, 507.

484. Barton P.B.,Jr., Toulmin P.,III, Econ. Geol., 1964, 59, 747.

485. Pemsler J.P., Wagner C., Metall. Trans., 1975, 6B, 311.

486. Kullerud G., Moh G.H., Carnegie Inst. Washington Year Book, 1968, 66, 409.

487. Schlitt W.J., Craig R.H., Richards K.J., Metall. Trans., 1973, 4, 1994.

488. Koster W., Mulfinger W., Z. Elektrochem., 1940, 46, 135.

489. Asano N., Ichio T., Suiyokwai-Shi, 1962, 14, 467.

490. Lipin B.V., Sov. J. Non-Ferrous Met., 1960, No.1, 57.

491. Moh G.H., Kullerud G., Carnegie Inst. Washington Year Book, 1963, 62, 189.

492. Moh G.H., Kullerud G., Carnegie Inst. Washington Year Book, 1964, 63, 209.

493. Chizhikov D.M., Gulyanitskaya Z.F., Belyanina N.V., Blokhina L.I., Russ. Metall., 1974, No.3, 42.

494. Friedrich K., Metall u. Erz, 1914, 11, 160.

495. Hayward C.R., Trans. AIME, 1914, 48, 141.

496. Stansfield A., Faith W.V., Trans. R. Soc. Can., 1924, 18, 325.

497. Sryvalin I.T., Esin O.A., Zh. Fiz. Khim., 1952, 26, 371.

498. Matousek J.W., Samis C.S., Trans. Metall. Soc. AIME, 1963, 227, 980.

499. Hsieh K C, Chang Y.A., Zhong T., Bull. Alloy Phase Diagrams, 1982,

3, 165.

500. Lundqvist D., Ark. Kemi. Mineral. Geol., 1947, 24A, no. 22.

501. Kullerud G., Carnegie Inst. Wash. Year Book, 1963, 62, 175.

502. Kullerud G., Can. Mineral., 1963, 7, 353.

503. Clark L.A., Kullerud G., Econ. Geol., 1963, 58, 853.

504. Naldrett A.J., Craig J.R., Kullerud G., Econ. Geol., 1967, 62, 826.

505. Craig J.R., Carnegie Inst. Wash. Year Book, 1967, 66, 434.

506. Naldrett A.J., Craig J.R., Carnegie Inst. Wash. Year Book, 1968, 66, 436.

507. Craig J.R., Naldrett A.J., Kullerud G., Carnegie Inst. Wash. Year Book, 1968, 66, 440.

508. Shewman R.W., Clark L.A., Can. J. Earth Sci., 1970, 7, 67.

509. Craig J.R., Naldrett A.J., Geol. Assoc. Can. - Mineral. Assoc. Can. Sudbury, 1971, 16.

510. Malik O.P., Arnold R.A., Geol. Assoc. Can. - Mineral. Assoc. Can., Sudbury, 1971, 40.

511. Craig J.R., Am. Mineral., 1971, 56, 1303.

512. Craig J.R., Am. J. Sci., 1973, 273A, 496.

513. Misra K.C., Fleet M.E., Econ. Geol., 1973, 68, 518.

514. Misra K.C., and Fleet, M.E., Mat. Res. Bull. 1973, 8, 669-678.

515. Misra K.C., Fleet M.E., Econ. Geol., 1974, 69, 391.

516. Lenz J.G., Conard B.R., Sridhar R., Warner J.S., Metall. Trans. B., 1978, 9B, 531.

517. Kao M., M.S. Thesis, University of Wisconsin-Milwaukee, Milwaukee, WI, USA, 1980, "A Thermodynamic Study of the Fe-Ni-S System at 973 K"

518. Vogel R., Tonn W., Arch. Eisenhuttenw., 1930, 3, 769.

519. Urazov G.G., Filin N.A., Metallurg., 1938, 13, 3.

[illegible] Tsvetyne Metally,

1955, 28, 23.

521. Scott J.R., Naldrett A.J., Gasparrini E., Econ. Geol., 1972, 67, 1010.

522. Scott S.D., Naldrett A.J., Gasparrini E., Int. Mineral. Assoc. Ninth Gen. Meet., Berlin 1974, "Regular solution model in the Fe_{1-x}-$Ni_{1-x}S$ (mss) solid solution"

523. Zellars G.R., Payne S.L., Morris J.P., Kipp R.L., Trans. Met. Soc. AIME, 1959, 215, 181.

524. Speiser R., Jacobs A.J., Spretnak J.W., Trans. Met. Soc. AIME, 1959, 215, 185.

525. Vaisburd S.E., Remen T.F., Sheinin A.B., Zhur. Fiz. Khim., (Russ. J. Phys. Chem.) 1969, 43, 1780.

526. Bale C.W., Unpublished Work.